Development of a satellite-based dynamic regional vegetation model for the Drâa catchment

Dissertation
zur
Erlangung des Doktorgrades (Dr. rer. nat.)
der
Mathematisch-Naturwissenschaftlichen Fakultät
der
Rheinischen Friedrich-Wilhelms-Universität Bonn

vorgelegt
von
Pierre Fritzsche
aus
Hoyerswerda

Bonn 2010

Angefertigt mit Genehmigung der Mathematisch-Naturwissenschaftlichen Fakultät der Rheinischen Friedrich-Wilhelms-Universität Bonn

Gutachter: Prof. Dr. Gunter Menz

Gutachter: Prof. Dr. Sebastian Schmidtlein

Tag der Promotion: 17.12.2010

Erscheinungsjahr: 2011

Follow the white rabbit....

Acknowledgements

Many people had helped to make this dissertation possible and supported me along the windy road to its end. First of all I wish to thank Professor G. Menz for his continuous support, ideas and inspiration. I would also thanks Prof. Schmidtlein for his generosity of offering a helping hand. I am also very thankful to Prof. Reichard and Prof. Goldbach for their support and their kindness during the IMPETUS project and for being a great help during the last phase of this work.

I heartily thank Gisela Baumann for her generosity of ideas, her critical questions (which drive me mad sometimes) and motivation. Your intellectual support open some doors I would never think of before. Thank you for you close friendship.

This work would never come to an end without the help and support of many colleagues. And most of all I am very thankful to call most of them friends. I thank Dr. Anja Lindstädter and the former B3 Workgroup for their support, their motivation and help. A great personal thanks go to Ingo Elbertzhagen for his active support during this PHD, his friendship and ideas. I thank Anna and Stephan Klose, Gero Steup for the fruitfully discussions and professional advices, Henning Busche for his support and help on Hydrologic Issues. A special thanks go to Oliver Schulz for his advices and helping hand on all meteorological measurement and data preparation. A great thanks go to Manfred Finck for his introduction into the area, support and helping hand.

I great thank goes to the RSRG group, namely Henryk, Roland, Kerstin, Julia and Bärbel for their support and help. Special thanks go to Rainer for his patient and the inspiring discussions about IDL and statistics. Music is around you. And by the way: I herby resign as Printing commissioner. I also thanks Frauke, Emelie,Thorsten M. Und W., Pamela und all other staff members I had the honour to meet.

Significant parts of this thesis was done in Morocco, and I appreciate this opportunity. A foreign Islamic country with 2 official languages is a challenge of its own. So I am very thankful for all the help I got. Special thanks goes to Aziz Labdi. Thanks to you I had the best time of my life there. Wunderbar! Together with Hamid I got an intensive view on living in southern Morocco. I also thanks all families which I had the honour to be their guest. Especially Mohammed Ait Lahsen and his family for letting me join family life. I also thank Mohammed Ait Richa for his hospitality and help.

The field work of this thesis would never succeed without the help of Jamal Ait El Hadj and his team Abdelsalam, Nour-Eddine und Achmed. “My” Hillux always runs and runs and runs... And if he doesn’t, you and your team are always their with a helping hand.

Last but not least I want to thank my family for all their support. Robert and Kathleen I thank you both for always having an open ear, open mind and solutions for all problems. I can’t thank you both enough. A great potion of thanks go to my grandmother Erika, which guide me through dark times and making all this possible. I thank my parents for giving me all the freedom I need to evolve myself. A special thank go to my nieces Linda and Aimée for their grounding questions and always reminding me that there are more important things in life than work and knowledge.

Index of Content

Index of Tables

Index of Figures

Abbreviations

ABH	Agence de bassin hydraulique Souss Massa
AMSU	Advanced Microwave Sounding Unit
ANOVA	Analysis of variance
ANPP	above Ground Net Primary Productivity
APAR	Absorbierte Photosynthetisch Aktive Strahlung
Aqua	EOS PM Payload satellite
ARG	Arg Guin
ASR	Asrir
AVHRR	Advanced Very High Resolution Radiometer
BSK	Bou Skour
CDP	Constant Data Product
CD-ROM	Compact Disk - Read Only Memory
C-Fix	Net Primary Productivity model
C-Fixing	Carbon fixing in Plants
DEM	Digital elevation model
DM	Dry Matter
DMP	Dry Matter Productivity
DN	Digital Number
DOY	Day of the Year
DTM	Digital terrain model
ECMWF	European Centre for Medium-Range Weather Forecasts
EET	Effective Evapotranspiration
EMY	El Myuit
ENVI	Environment to visualize images
EOS-1	Earth Observing System-1 (TERRA)
EROS	Earth Resources Observation Systems
ET	Evapotranspiration
FAO	Food and Agriculture Organization of the United Nations
FPAR	Fraction of absorbed Photosynthetically Active Radiation
GCM	Global Circulation Model
GCP	Ground Control Point
GDD	Growing degree days
GLM	General linear model
GPS	Global Positioning System
GT	Ground Truth
GUI	Graphical User Interface
HDF	Hierarchical Data format
HDF	Hierarchical Data Format
HRBM	High Resolution Biosphere Model
HRVIR	High Resolution Visible - Infrared-Sensor
IBP	International Biological Program
IDL	Interactive Data Language
IFOV	Instantaneous Field of View
IMS	Imskar
IPCC	Intergovernmental Panel on Climate Change
IRK	Lac Irique
ISIN	Intergerized Sinusodial Projection
ITC	Inner Tropical Convergence
JHB	Jbel Bani
LAI	Leaf Area Index

LCC	Land Cover Change
LP DAAC	Land Processes Distributed Active Archive Center
LUC	Land Use Change
LUCC	Land Use and Cover Change
LUE	Light Use Efficency
MD	MOVEG Drâa („*Modèle pour l´acquisition de la dynamique de la végétation dans la vallée du Drâa*“)
MGN	M'goun Station
MGN_f	Mgoun Ground Truth Testsite
MODIS	Moderate-resolution Imaging Spectroradiometer
MRT	MODIS Reprojection Tool
MSG	Meteosat Second Generation
MVC	Most Value Composite
NASA	National Aeronautics and Space Administration
NDVI	Normalized Differenced Vegetation Index
NEP	Net Ecosystem Productivity
NOAA	National Oceanic and Atmospheric Administration
NPP	Net Primary Productivity
ODD	Overview, Design concepts and Details protocol
ORNL	Oak Ridge National Laboratory
PAR	Photosynthetic Active Radiation
PET	Potential evapotranspiration
PFT	Plant Function Types
RBM	Regionales Biomasse-Modell
RCM	Regional climate modelling
RCN	Runoff Curve Number
RMS	Root Mean Square Error
ROI	Region of Interest
RSRG	Remote Sensing Research Group
SDS	Scientific Data Set
SE	Service Eau
SPI	Standard Precipitation Index
SRTM	Shuttle Radar Topography Mission
TAO	Toujgalt
Terra	EOS AM payload satellite (EOS 1)
TIC	Tichki
TRL	Trab Labied
TZT	Tizi Tounza
USGS	US Geological Survey
UTM	Universal Transverse Mercator-Projektion
VCF	Vegetation Continuous Field
VGT	VEGETATION
VITO	Flemish Institute for Technological Research
WGS84	World Geodetic System 1984
WMO	World Meteorological Organisation
YDP	Yearly Data Product

Abstract

Analysing and modelling land cover dynamic of the vegetation under a changing hydrological cycle inside the semi-arid area resulting from the global climate change are a difficult task. It is important to be able to understand and predict the characteristics and availability of vegetation as result of the global climate. This study was carried out inside the upper and middle Drâa catchment in south Morocco, focusing on the natural vegetation outside rural and agricultural areas. Development of a dynamic regional land cover model is traditionally driven by site specific plant growing parameters or by spatial information from remote sensing (e.g. NDVI). By scaling both approaches to a regional level plant activity can be analysed with the MODIS sensor and interpreted by local measurements. By using signal processing techniques, a double regression approach was developed and tested under the conditions of temporal trends and performance parameters. Completed by a regional adopted vegetation model, important productivity parameters could be extracted. This semi-automatic approach is realized in the conceptual model MOVEG Drâa, bringing together remote sensing, meteorological and other data and techniques. An extensive phenological database was built up by integrating Terra MODIS NDVI time series (2000 until 2008), a vegetation monitoring network and 10 years of meteorological measurements. In order to validate the method a comprehensive field measurement along a North-South transect was established. The results show that a robust point conclusion on vegetation trends and parameters on a statistical significant level is possible. Based on these findings a spatial explicit output was realized by a spatial extrapolation technique considering the annual and intra-annual vegetation trends. Based on the IPCC Scenarios (A1B and B1) a forecast of vegetation activity and productivity was implemented until 2050.

MOVEG DRAA is an improvement to the hitherto state of unknown atmospheric-vegetation-relationship for the semi-arid area of southern Morocco. The study reveals that the semi automatic modular model approach is capable of handling the highly variable vegetation signal and projecting further scenarios of environmental changes. The model output will help to refine all models using land cover information (e.g. pastoral modelling), hydrological modelling (e.g. SWAT) and meteorological parameterisations (e.g. FOOD3DK). The output of the MOVEG DRAA model can also built a valuable information source for all kind of land users.

1 Vegetation monitoring in semi arid areas

Vegetative productivity is the source of all food, fibre and fuel available for human consumption and therefore defines the habitability of the earth. (NASA, 2006).

Arid and semiarid ecosystems (often called “dry lands”) cover more than 40 % of the global land surface. Nearly one quarter of this drylands is used by humans, mostly as farm (Dregne 1983) or pastoral land. The impact of environmental change is likely to be most serious in drylands. Changing Biomass productivity, as a key factor of ecosystem service (Lobell et al., 2002), impacts land users daily life. Land-cover change – or modifications- hereby affected the character of the land cover, without changing its landscape classification. The changing or transformation inside these drylands is defined as changing in biological productivity due to human impact (Diouf & Lambin, 2001).

The biological productivity of arid rangelands at different time scales is governed by biophysical driving factors (e.g. rainfall variability, ENSO effects) (Lambin *et al.*, 2001b;Potter & Brooks, 1998). Actual Land-cover changes in arid areas are driven by the annual and interannual vegetation growth which are mainly steered by the amount of precipitation and the annual temperature distribution (Bonan, 2002) and human activity. Arid and semi arid areas are embossed by small, intermittent and extreme precipitation events (Pachauri *et al.*, 2007;Born *et al.*, 2008a). High temperatures and aligned high evaporation rates (Oke, 2003) assist a high drying out of the surface and the soil (Berndtsson *et al.*, 1989;Fisher *et al.*, 2005). This necessitates a high adaptation of species and formation to natural conditions. The historical, actual and future vegetation composite and land cover is a consequence of the development of the vegetation diversity (Le Houérou, 2001). The observed rainfall mean annual rainfall of NW Africa, during the 1951-2000 period, shows a series of wet and dry periods (Born *et al.*, 2009;Le Houérou, 1980;Paeth *et al.*, 2005a;Le Houérou, 2004;Le Houérou, 2001) and a corresponding expansion and shrinking of more or less permanent arid to semi-arid flora along the tropic cancer. “Mediterranean and temperate species were in existence in the northern Sahara and the highlands of Morocco throughout the Pleistocene and Holocene, with periods of expansion during the wet phases and retreat during the dry periods.” (Le Houerou, 1997). Moisture shortfalls control efficiency of plant photosynthesis (Seaquist *et al.*, 2003). Landscape structure and functions are crucial for prediction of landscape changes (O'Neill *et al.*, 1991).

The present Saharian flora inherits almost 3000 species of vascular plants, although some species - of economic value or not - are endangered through man-made destruction of their habitat (Le Houerou, 1997). The composition of these species has emerged since the

Quaternary epoch (1·7 Ma) and is subject to changes over a decades period(Finckh & Staudinger, 2003). Land use is embossed by urbanisation, extensive pastoralism as well as irrigated and rain fed agriculture. Since agricultural use is tightly delineated on rivers, the pastoral land use is extensive. Excessive pasturing has therefore been identified of having increasingly led to land degradation in these regions over the last decades (Guevara *et al.*, 1997;Le Houérou, 2001;Hegarat-Mascle, 2006;Culmsee, 2004). The IPCC forecast an increase of total averaged land use 5 to 8% by 2080 in arid and semi-arid land in Africa under a range of climate scenarios. By 2020, between 75 and 250 million of people are projected to be exposed to increased water stress due to climate change (Strengers *et al.*, 2001;Watson *et al.*, 2000).

Rising emission of CO_2, CH_4 and N_2O leading to an average global surface temperature increase of approximately 0.6°C ± 0.2°C over the last century, with a 95% probability of rising to 0.4 and 0.8°C (IPCC, 2003;IPCC Working Group1, 2001a). The carbon cycle reacts to the rising CO_2 levels in a variety of responses and feedback mechanisms. Looking at the terrestrial uptake of CO_2 it is known that NPP (Net primary productivity) increases with atmospheric CO_2 concentration, due to a fertilisation effect which occurs directly through enhanced photosynthesis, and indirectly through effects such as increased water use efficiency. The effectiveness of the terrestrial uptake as a carbon sink depends on the transfer of carbon to forms with long retention time (wood or modified soil organic matter) (IPCC, 2003;IPCC Working Group1, 2001a;IPCC Working Group1, 2001b). It is known that warming increases the rate of heterotrophic respiration on land but the magnitude over longer time scales is not clear yet. Anthropogenic N deposition is increasing terrestrial NPP in some regions; excess troposphere ozone (O_3) is likely to be reducing NPP (Watson et al., 2000). Climate changes not only influence the growth of plants but also the composition of species (Le Houerou, 1997;le Houerou, 1980). “Smallholder and subsistence farmers, pastoralists [...] will experience negative effects on yields of low-latitude crops, combined with a high vulnerability to extreme weather events” (Easterling, 2007). For most dry land regions, climate models predict higher temperatures, decreased precipitation, and an increase in intensity and frequency of extreme weather events such as droughts and heavy rainfall (IPCC Working Group2, 2001b;Pachauri *et al.*, 2008;Strengers *et al.*, 2001;Watson *et al.*, 2000;Brown & Funk, 2008), although when, where and how is often unknown (Menz *et al.*, 2005;Pickup, 1995). All this may impact people and the dry land ecosystems through:

- Increased land degradation/ desertification,
- Reduced carbon sequestration services,
- Vegetation shifts from semi-arid towards arid vegetation,
- Decreased water availability and quality,
- Shortening of the vegetation period,
- Reduction of rain-fed areas,

- Diminished agricultural productivity and crop yields,
- Productivity decline in grasslands.

Climate change will potentially increase poverty and undermine sustainable development, and developing countries with vast dry land areas are particularly vulnerable (comp. (Gruber, 2008;Rosegrant *et al.*, 2002). The adaptive capacity of pastoralists, smallholder and subsistence farmers, highly dependent on natural resources, may be overstretched and economic alternatives and safety nets are mostly lacking (Kamotho *et al.*, 2008). For the northern part of the Drâa area the nomads of the Ait Tourmert live under the strategy of economic adaption (Scholz, 1995;Kemmerling, 2008). This strategy includes the having access to water. Shortage of fresh water is expected to be the dominant water problem of the 21st Century and that, along with water quality, may well jeopardise all other efforts to secure sustainable development, and even in some cases may lead to social and political instability (Impetus, 2006).

Land use is a driving factor of land cover changes (Le Houérou, 1980) and impacts the regional climate (Le Houérou, 1995;Le Houérou, 1996;Paeth *et al.*, 2005b;Born *et al.*, 2008b;Born *et al.*, 2009). Understanding this dynamics will improve our knowledge about the causes of changes and is effects (Lambin & Geist, 2006). The land cover inside the Drâa can be described as unique combination of geology, topography, vegetation and human influence. This semi- arid ecosystem is an actively used area, which is in a stress situation between production of biomass and the use as fodder for animals (Baumann, 2009). The conflict between a sustainable land use and the degrading ecosystem due to overexploitation is the challenge inside an area that is affected by global change and a rising population. Understanding the mechanism between environmental factors and its reaction in natural vegetation growth is the key to answer the usability and sustainability land cover inside the Drâa Valley.

By using the approach of analyzing vegetation activity in response of selected climatic parameters, it is possible to model the vegetation response in a appropriated complexity and variability across space and time. By using a common structure for analysing and a hypothesized causal mechanism (Lambin & Geist, 2006) it is possible to identify the risks of environmental change (Kasperson *et al.*, 1995) and the relationship between vegetation activity and rainfall (Potter & Brooks, 1998). Local factors s of Land use change can be monitored by a global operating system and analysed in a regional context, since it is possible to accurately track seasonal variations of vegetation (Lambin *et al.*, 2001b).

The problem for forecasting is the fact that regional precipitation patterns are among the least consistent and reliable aspects of current climate models (Hulme & Dessai, 2007).

Human activity is a functional part of this climatically determinate “semi-natural” ecosystem (Lambin *et al.*, 2001a). Tropical and temperate rangelands are both highly dynamic and also resilient. Eliminating the human influence will trigger significant changes (Bork *et al.*, 1998;Lambin *et al.*, 2001a). Those rangelands, defined by presence of grass and trees used by grazers, are the main land cover. Vegetation indices have been used in varies studies to examine the LUC and LCC (comp.: (Gottschalk *et al.*, 2005)). Besides their prime importance as a research tool in autecology, predictive geographical modelling recently gained importance as a tool to assess the impact of accelerated land use and other environmental changes (Guisan & Zimmermann, 2000). It can also be used to test biogeographic hypotheses (e.g. Mourell and Ezcurra, 1996; Leathwick, 1998), the distribution of organisms (Lischke et al., 1998; Kienast et al., 1995, 1996, 1998; Guisan and Theurillat, 2000); to improve floristic and faunistic atlases (e.g. Hausser, 1995) or to set up conservation priorities (Margules and Austin, 1994). Land cover and land use changes are always bound to changes in the atmosphere - Earth surface energy exchange (Lambin & Geist, 2006;Oke, 2003).

The carrying capacity as intrinsic variability of rangeland ecology makes it difficult to distinguish the direction of fluctuations, especially interpretations of “degradation” or “desertification” (Sandford, 1983). Rangelands in arid regions are therefore discussed as non equilibrium ecosystems (comp. (Bollig & Göbel, 1997;Ellis, 1994;Gillson & Hoffman, 2007;Powell, 1998)). The influence of stock on the rangelands is still discussed under multiple points of view (Behnke, 1995;Behnke & Abel, 1996;Bester *et al.*, 2003;Todd, 2006;Weber *et al.*, 2000). The resulting management strategy must include aspects and patterns of pastoral land use, including water points and long-term exposure (Ellis & Swift, 1988). This management strategy needs a monitoring system that is able to monitor and forecast vegetation parameters. Satellite observations are able to support this mission, by using there spatial and temporal coverage, and may serve as independent observer.

Since 1972, when satellite imagery became available, extensive research and use of satellite imagery, supported by the development of GIS systems, has been conducted (Gottschalk et al., 2005). Ever since Tucker (1979) introduced the Normalized Difference Vegetation Index(NDVI) as Vegetation Index (VI), vegetation monitoring has become an important part of investigating vegetation as natural resource and ecosystem services (Scholes *et al.*, 2005). The continuous study of the earth’s surface started with the launch of the continuous space born observation in the late 60s. The consistency of the programs, especially the LANDSAT program, allows long term observations and trend analysis. Since that time radiometric calibration and geometric corrections have been greatly improved and developed (Xiong, 2005;2006;2008;Kobayashi *et al.*, 2007;Moran *et al.*, 1995;Scanlon *et al.*, 2002). With

the start of SeaWiFS and SPOT Vegetation in 1997 and 1998, advanced with MODIS in 2000, a generation of well calibrated sensors provided a high spectral and temporal resolution for earth observation (Colditz, 2007).

MODIS is a passive imaging spectroradiometer that are sampled across the visible and infrared spectrum (Xiong, 2005). Fensholt & Sandholt (2005) investigate for Senegal, that. “a comparison of in situ MODIS indices with the MODIS 16-day constrained view angle Most Value Composite (MVC) product showed that the satellite MODIS NDVI and EVI satisfactorily capture seasonal dynamics (R2 from 0.55 to 0.97)”. In situ MODIS EVI is more sensitive to dense vegetation than MODIS NDVI ((Diouf & Lambin, 2001).By adding that land use and land cover changes in the world’s dry lands are mostly human-induced by various forms of land degradation. Temporal satellite measurement provides a comprehensive picture of the patterns of inter- and intraannual variation and trends of the vegetation activity (Anyamba & Tucker, 2005). Remote sensing of vegetation is a proven and still promising tool for spatiotemporal monitoring at low cost and “near” real time for large areas. The phenological dynamic of terrestrial ecosystems reflects the response of the earth’s surface climate and hydrological systems (Zhang *et al.*, 2003;Myneni, 1997;White *et al.*, 1997c).

The scaling of this system is vital for addressing the processes and their impact. “Scale” is used to refer both, the magnitude of an study (e.g. geographical extent) and the degree of detail (e.g. its level of geographic resolution) (Quattrochi & Goodchild, 1997).

Scale is the spatial, temporal, quantitative, or analytic dimension that is used to measure and study objects and processes (Gibson *et al.*, 2000). Especially GIS offers a new perspective on scale in the context of space. Scale can be a ratio between distances (cartography), but might be also the representation of species habitat. Mostly scale is linear dimension, which applies in geography often in the maps scale (e.g., 1:20000). The ability to change the scale is the possibility to disaggregate or aggregate data in a logical, rigorous and well grounded way. The discussion of data aggregation is essentially a discussion of scaling. (Quattrochi & Goodchild, 1997) defined the four connotations of scale in remote sensing:

- Map scale
- Geographic scale (extent or domain in ecology)
- Resolution
- Operational scale

For this thesis the scaling concept is bounded to resolution. Resolution is the definition of the pixel length on the earth’s surface and is explicitly linked to real units. There are different definitions in other disciplines.

The scale of this thesis can be classified as a choric dimension according to landscape ecology (Leser & Mosimann, 1997). That means an area with heterogeneous content, classified by areal context and actual-dynamic attributes. As an example, one choric must inherit the same mesoclimate and watershed. From a remote sensing point of view the same area has often been discussed as part of issues of observed variance in different resolutions (Delcourt *et al.*, 1982;Woodcook C. & Strahler, 1987). The spatial resolution of high local variance changes is a function of this environment.

The capability of performing analyses at multiple layers (e.g. time and space, comp. numerical prediction) is rare (Lambin & Geist, 2006). The scale concept use in this thesis is a linked synthesis from land use/cover change approaches and temporal dimensions. According the classification of (Coleman, 2000), this thesis uses a micro-level land use change decision approach (see Figure 1).

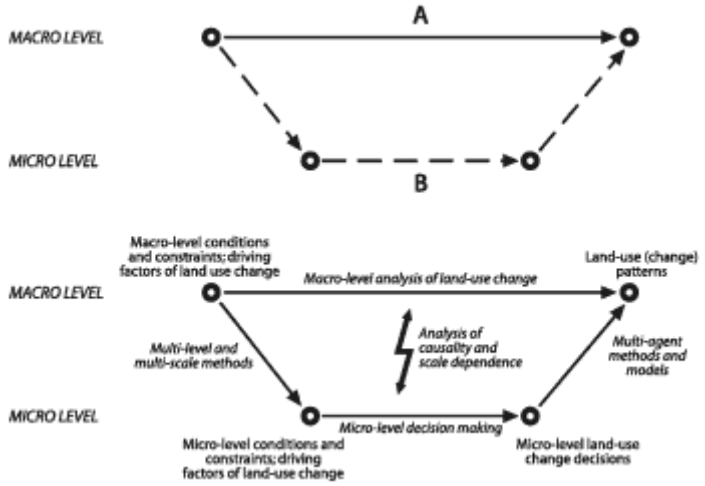

Figure 1 Representation of Scale (Source: Lambin &Geist(2007)). Micro and Macro level symbolize the upper and lower limits for this sketch.

The geographical scale can be defined as a regional scale (Upper Drâa Valley) with tendencies to the local scale (point analyses at meteorological stations). It also uses a mesoscale in the challenging task of using daily and half-monthly (16 day) data. The approach of the out coming model can be classified as a multi-scale approach (path B in Figure 1) regarding spatial and temporal scale in the quantification of driving factors. The resolution of the input satellite data is set to be a 250 m x 250 m ground resolution. This is the finest (i.e. smallest) resolution of MODIS NDVI available. (Bian & Walsh, 1993) has demonstrated that a spatial aggregation leads to an integrated radiance of all location which in turn leads to a smoothing effect under the assumption of positively related covariance and a inversely related variance. This effect is considered in chapter 5 during the extraction and preparation of the satellite images.

1.1 Scientific Goals

Former vegetation models are mostly based on calculating the statistic biomass production from past vegetation situations (Brown, 1999;Franklin, 1995), mostly on a global scale. The aim of this work is to analyze the productivity of the natural dynamic vegetation, inherit the past vegetation activity, and predicting the future NDVI. By using meteorological forecast models, the situation of the lower atmosphere is set. The goal of this study is to set up an empirical statistical model. By using remote sensing techniques together with analysing techniques from hydrology and biology a multidisciplinary approach is generated. This work is embedded in the actual climate change debate and should answer the questions:

- Is it possible to combine multiscale information from different sources like Hydrology, Biology and Geography related of vegetation activity, measured by remote sensing.
- Is it possible to analyze vegetation activity on the base of meteorological measurement?
- How to improve the quantification of the phenological cycle? Which methods are available, usable and improvable or to generate?
- It is possible to forecast vegetation activity and derivate parameters?

One method to investigate vegetation activity is to use time series analysis (Armstrong, 1985b;Wagenseil & Samimi, 2006;Zhang *et al.*, 2006;Zhang *et al.*, 2003). Time series analysis is used in stochastic approaches and able to transfer functions for forecasting (Armstrong, 1985a;Jeltsch *et al.*, 2008). In particular the state of the phenological cycle is an important information for environmental and atmospheric modelling (Potter & Klooster, 1999). Those needed a standardized, but flexible, consistent long term time series analysis and added the flexibility of possible expansion and ability to scale temporally and spatially. Operationally acquired and automatically processed datasets are a vault for regular updates.

Summarizing, this study focuses on the following goals:

- Development of a robust[1] semi-automatic approach to analyze time series of vegetation activity and their dependency on meteorological data,
- Calculating natural vegetation activity and the related useable productivity output,
- Analyse the phenological cycle inside the investigation area,
- Prediction of further vegetation status on the base of IPCC Scenarios

The overall goal of this work is to model and predict biomass as a product of the processes of the lower atmosphere and pedosphere, summarized into vegetation reaction. Figure 2 introduces all steps of this work as a graphical overview.

[1] Robust here means: The statistical proved, significantly, result.

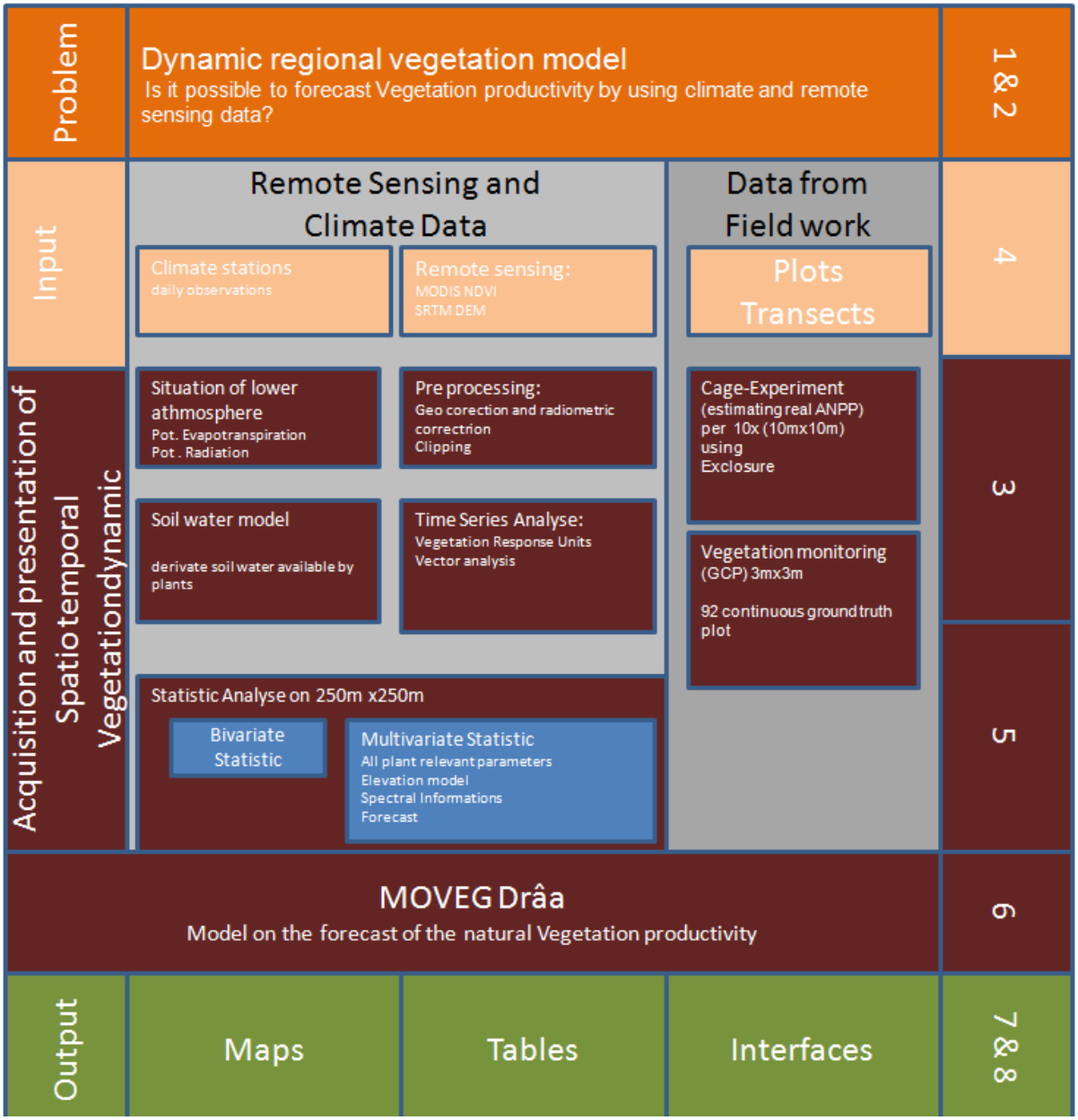

Figure 2 Graphical Overview including all work packets of this Thesis including a short description and included Data/Sub-Packets with number of corresponding chapter on the right side

This study is embedded into the interdisciplinary research project IMPETUS. IMPETUS has investigated the key aspects of the hydrological cycle in two river basins in Morocco and Benin since 2000. The goal of the project is the implementation of a sustained management of the scare resource water. The approach of current and future problems should be augmented by an interdisciplinary and holistic approach. The availability of water is controlled by the atmosphere, the continental hydrosphere and biosphere. Those key aspects are subject of the investigation of IMPETUS through networking of different science aspects, bundling the research of different disciplines.

1.2 Outline

Each chapter contains a first section with an introduction and an in-depth discussion, necessary to understand the subsequent methods, datasets or results. First chapter is a short outline and description of the goals of this work. The second chapter gives an introduction to the investigation area and what natural conditions occur in the area. Together with a short introduction of the climatic and meteorological situation, it prepares for chapter three, which introduces the theory and the derivated design of MOVEG Drâa (MD). The fourth chapter gives a detailed view on a field measurement. Chapter five describes every calculation in depth, together with necessary assumptions and programming techniques. The results are presented in chapter six. Final discussion prospects and limits of this thesis are described in chapter seven, which contours an outlook of possible future developments and improvements.

2 The Drâa Valley in southern Morocco

The Drâa Catchment (Figure 3) is located south of the central High Atlas Mountain chain between 31.5° north to 29° south and 6.5° to 5.5° west, reaching from the top of the Atlas mountain chain to the Hamada Desert of Lac Irique. It contains an area of 34.000 km².

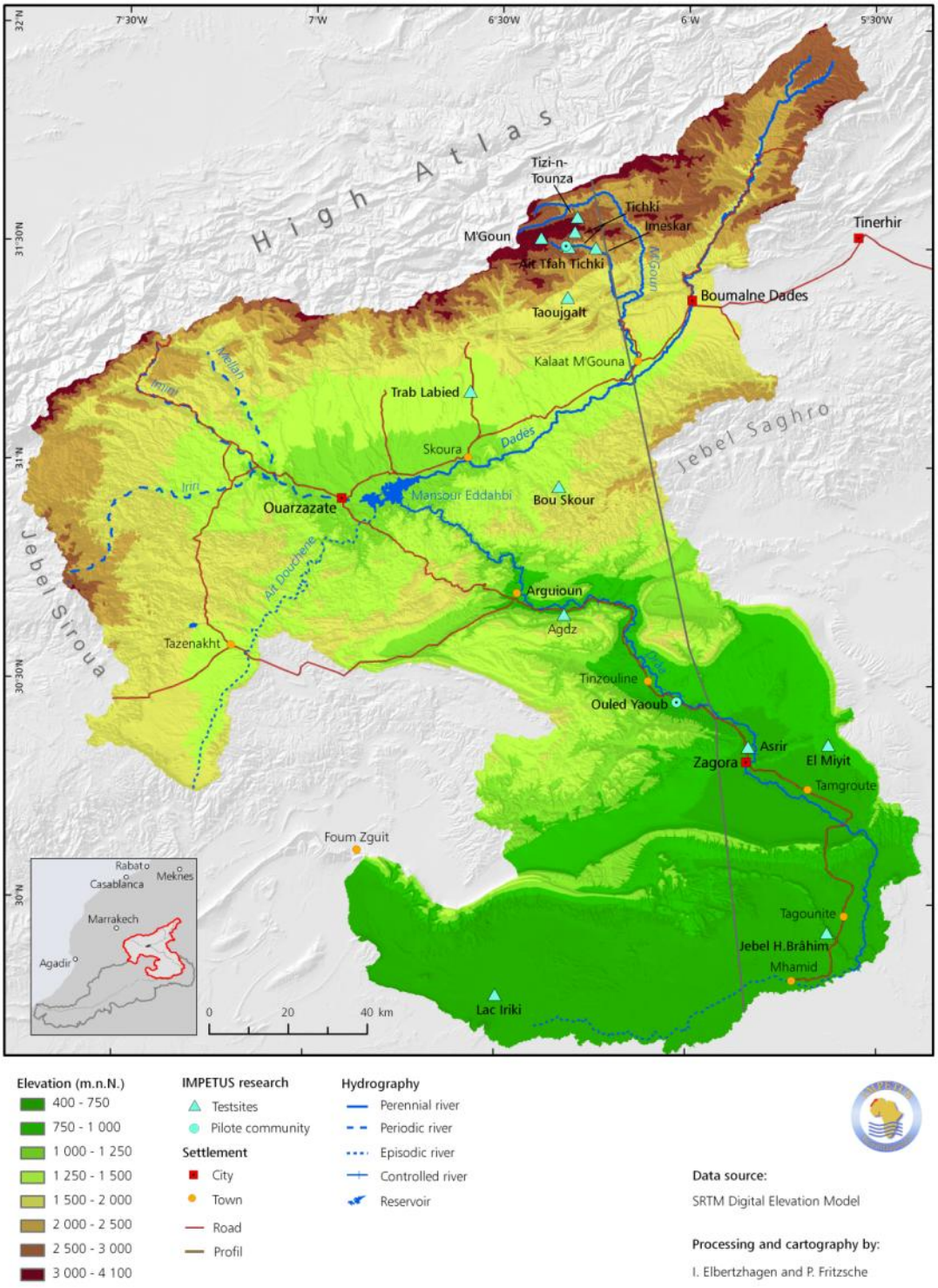

Figure 3 Upper Catchment of the Drâa, the research areas of the IMPETUS Project in Morocco. The map includes all Test sites and the N-S Profile for investigation (Source: IMPETUS Atlas, 2009)

The landscape is rich on details, from High Mountain areas of the central High Atlas Mountain chain, over the modest mountain ranges of the Anti Atlas of Jbel Saghro and Jbel Bani into the Hamada Desert of Lac Iriki on the Boarder to Algeria. The most dominant landscape feature is the river Qued MGoun which goes south as Qued Drâa and is the most important source of scare water within the area.

2.1 Natural Formations

The High Atlas mountain chain directs WSW to ENE trough Morocco. On its western Part the highest peaks goes from Jebel Toubkal (4.165 m) to the central Jebel M'Goun (4072m). The volcanic massive of Jebel Siroua (up to 3300m) combined the western part of the Basin of Ouarzazate and is the north western part of the Drâa valley. Following the south slopes of the Atlas Mountain lies the Tertiary and Quaternary Basin of Ouarzazate (1400 until 1000m). All rivers north of the Jebel Saghro and Anti Atlas united into the 1972 build El Mansour Eddahbi Reservoir (RISER 1973). South of the basin follows the Anti Atlas Mountain range, which is characterized by a large Protozoic fold belt. The area of the Anti Atlas is dominated by moderate highs and a rough orography. From north to south lies the Anti Atlas (up to 1500m) as well as Jbel Siroua (3300m) in the east the Jebel Saghro (2500) in the south the Jbel Bani (up to 1300m). The transverse valley of Jebel Bani begins near of M'hamid and marks the beginning of the lower Drâa valley. The Jbel Bani is the southern border to the dead end sea Lac Iriki (450m). This area is characterized by large barren land, with hard and rocky plateaus and very little sand. In Arabic, it is called Hamada and means dry rocky area. The *Hamada du Drâa* presents one of the world larges rock deserts (Griffiths & Soliman.KH, 1972).

The southern Morocco is located between the Mediterranean climate (ITC high pressure belt) and the Sahara Desert Climate. The arid regions are marked by weak seasonal variations with episodic rainfall, whereas in the Mediterranean and Atlantic regions moderate, wet winters and hot, dry summers prevail (Griffiths, 1972;Griffiths & Soliman.KH, 1972). One characteristic is the transition zone marked by cyclonal winter Rain (Born *et al.*, 2008a;Born *et al.*, 2009) (Schulz *et al.*, 2008a) and hot and dry Summers marked by sub-tropical high pressures systems of the tropical trade wind system. The climate of Northwest Africa has changed dramatically since the late Pleistocene, including the expansion of the Sahara (with all effects of desertification) (Le Houerou, 1997;Nicholson *et al.*, 1998;Nicholson, 2000;Prince *et al.*, 2007;IPCC, 2001).Together with a large land cover change from Savannas into desert, the change is most recognised in the sub Saharian Sahel Zone. The major fluctuation of rainfall, with a strong inter-annual persistence of rainfall anomalies in semi-arid regions of the northern hemisphere Africa (Nicholson, 2000), leads to a larger recurrence times of dry

Standard Precipitation Index (SPI) values (years with below average Rainfall)(Born *et al.*, 2008a).

2.2 Climate and Meteorological Monitoring

The climate within the catchment is characterized by its thermal and hygric gradient along a altitude and aridity gradient between the High Atlas Mountain chain and the *Hamada du Drâa* with transition to saharian climate. The investigation area is globally classified by Bwk and BWh climate (Köppen, 1931), which stands for hot desert climate (BWh) and cold desert climate (Bwk). (Müller-Hohenstein, 1990) classified it as semi-arid to arid with semi arid in the highest elevations on Atlas Mountain range. In the traditional Köppen climate classification (based on observational data) Morocco has a broad variety of climate classifications from moderate (C), tropical (A), steps (B) to desert (B) climates. The High Atlas Mountain Range is a climate boarder inside Morocco. North of the Atlas more temperate climates can be found (C and B), south more high temperature climates (B). The Atlas Mountain Ridge itself reflects that in a profile gradient.

Climate monitoring provides important environmental data for analysis, evaluation and modelling of environmental processes. In order to specify and enhance climate trends supplied by literature and Moroccan long term measurement the Impetus Project setting up and operate 13 IMPETUS climate stations inside the catchment along an altitude and aridity gradient (Schulz *et al.*, 2008b) and Figure 3). The sites within the catchment were selected to cover the variety of main topographic and geological units, following a temperature and aridity gradient (Impetus, 2003) from north to south. A denser cluster was installed inside the Jebel M'Goun area to investigate hydrological, meteorology, plant ecology and social and agriculture topics on a greater regional scale.

Figure 4 Automated Climate station as operated by IMPETUS (TZT Station ~3000m asl.)

The climate of the Atlas is characterized by cool humid winters (-7 to -1°C) and dry hot summers (up to 40°C), which underscore the Mediterranean character altered by altitude gradient. The precipitation inside the investigation area ranges from 363 mm at a High mountain station (e.g. Tizi'n'Tounza) to 59 mm inside Lac Iriki. The mean temperature decrease with altitude, with minima lower than -20°C inside the High Mountain Atlas range above 3000 m (Joly, 1954;Rauh, 1952). The southern parts of the Drâa valley, especially the south Hamada, expecting night frost at ground during long high pressure period in winter (Weischet & Endlicher, 2000). Depending on elevation, the mean precipitation and temperature values change significantly. The precipitation lowers from north to south (see Figure 5), without disturbances of the Anti Atlas elevation which are not capable of reduction the pre Sahara influence up to the southern slopes of the Atlas Mountain range (Joly, 1954).

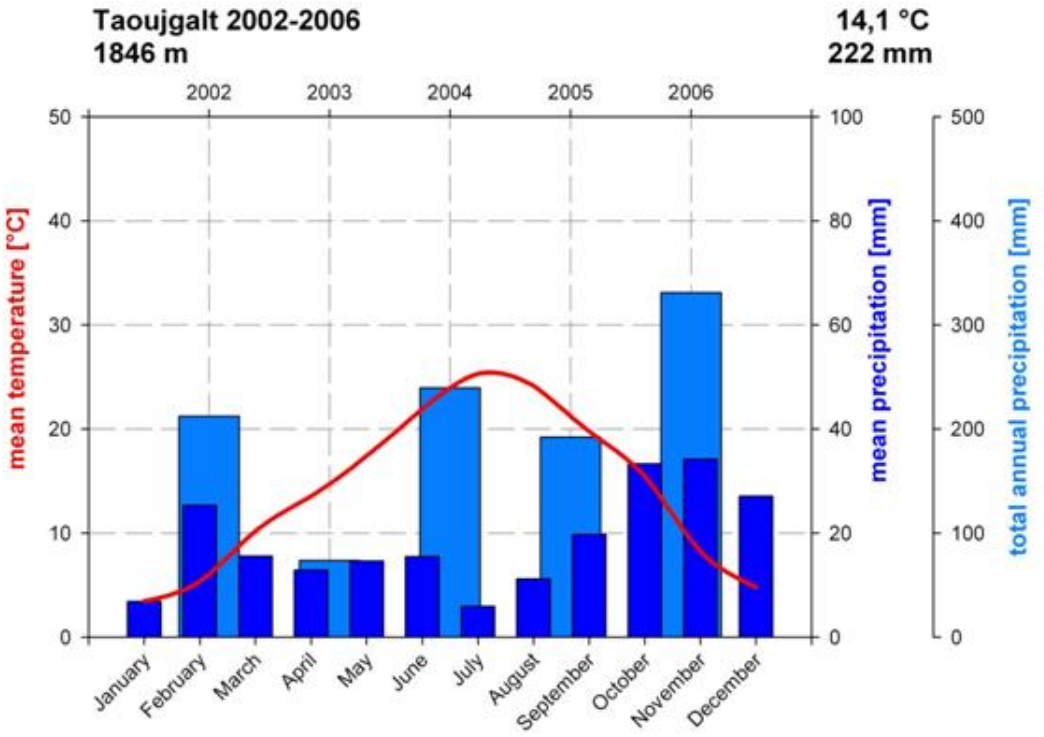

Figure 5 Climate diagram of Station Toujgalt (~1846m asl) showing the annual mean temperature and precipitation together with total annual precipitation for every month for the period 2002 to 2006.

The precipitation results mainly from the movement of the North Atlantic Oscillation (NAO) to the south during the north hemisphere winter influencing the area with low pressure cyclones (Knippertz *et al.*, 2003). The precipitation inside the catchment depends on atmospheric circulation over the subtropical and extra tropical North Atlantic and the Mediterranean Sea, where main precipitation sums occur during the winter from November to March. The winter precipitation inside the High Atlas Mountain range is discontinued by clear, precipitation free weather, especially in January (Rauh, 1952). As Klose (2009) explained the rain days vary from 74 to 325 mm, as well as precipitation/rain day ratio.

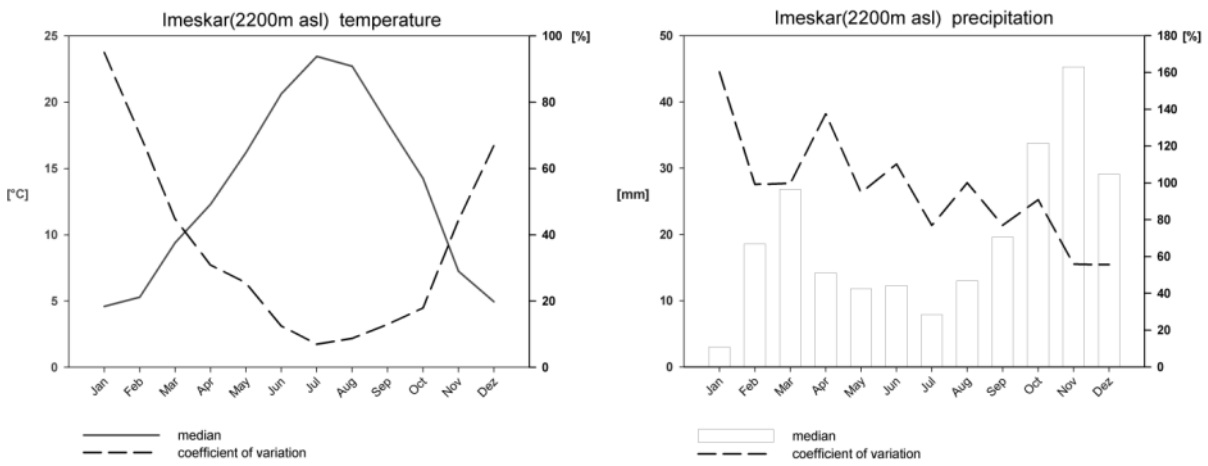

Figure 6 Measured median and coefficient of variation for monthly temperature and precipitation for station IMS (~2000m asl.)

A look at the climate data (e.g. station IMS in Figure 6) reveals that the investigation area inherits a heterogeneous meteorological situation throughout the year. The precipitation for IMS generally varies most in fall/winter, as temperature varies most in July/August. The temperature peaks on late July, begin August. A more interesting fact is the very high temperature variation during the winter months. This first information about the area and its special intraanual situation raise the scientific question of the landscape composition of this area and all inherit factors regarding vegetation.

2.3 Geology and Soil

2.3.1 Geology

The Geology of Westafrica is a geological record of 3 Ga (Pique,2001). The North Western Africa is dominated by the WAC Craton (Kennedy, 1962), representing a stable and spacious unit which extends over an area of 4,500,000 km² (Klose, 2011). The ancient Precambrian basement builds the West African Schield. The IMPETUS investigation zone is embossed by Precambrian and the Pan-African orogeny. It is part of the Western African craton. The ancient Precambrian shield consist of two major orogenies, the Archean and Eburnean (Pique, 2001), with granitoids, gneisses and metamorphic rocks, 3 to 2 Ga old. This surrounded by the Pan African belts (760 to 560 Ma) in its northern (e.g. the Moroccan Anti Atlas) and southern edge (e.g. the Dahomeyides in Togo, Ghana and Benin) (Michard, 2008).

The Morocco geology is dominated by rugged topography and an active plate collision zone (the alpine belt system). Morocco on the northern edge of WAC exhibits a complex geodynamic evolution of alternating phases of continental building and break up, whereas the southern part remained more or less stable for at least 1.7 to 1.0 Ga (Michard, 2008)

2.3.1.1 Atlas Mountain

The Moroccan Atlas mountain chain extends from Agadir in his western to Algeria eastward. It is composed of two secondary ranges, the Middle Atlas and High Atlas. In his western part, including the investigation area, it is dominated by mesetan blocks, wich remaind more or less stable during Mesozoic and Cainozoic(Pique, 2001).

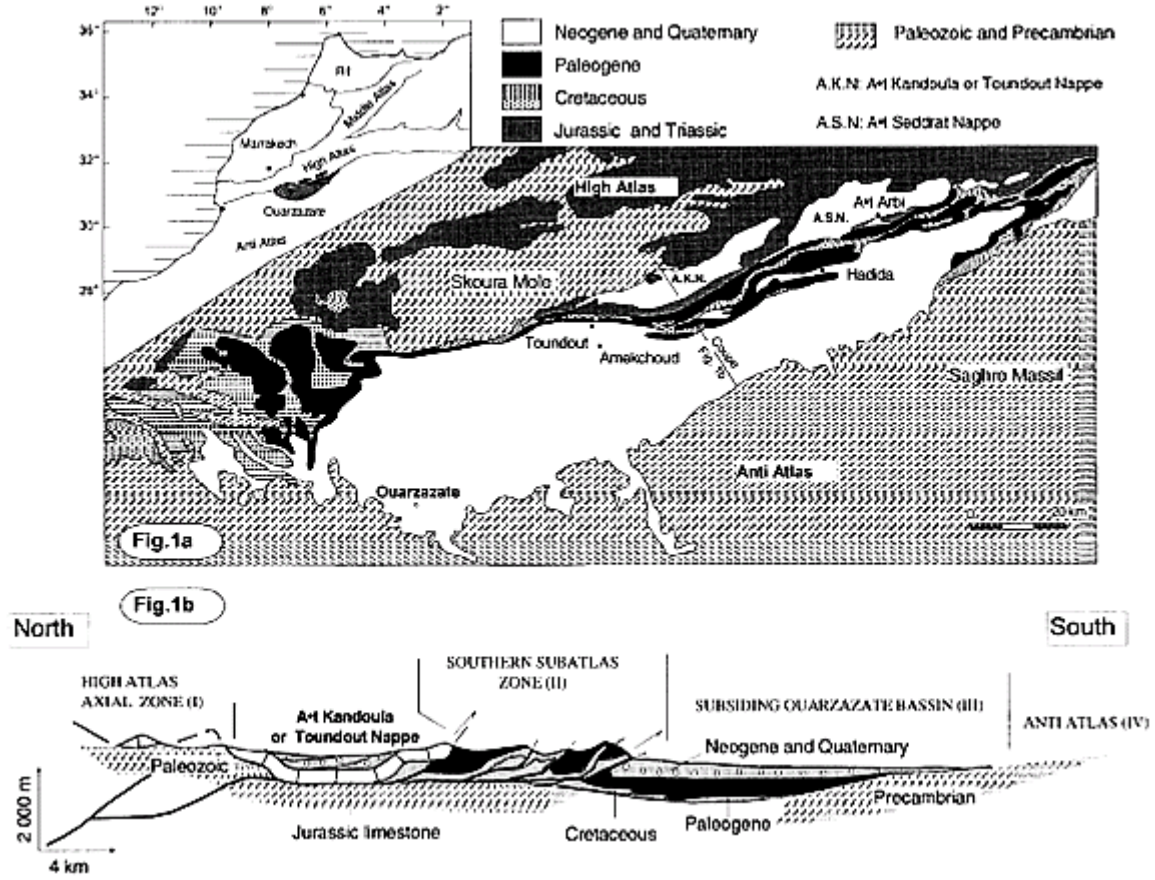

Figure 7 Geology of the basin of Ouarzazate (El *et al.*, 2001)

The western part of the investigation area High mountain atlas range is a well developed Crateceous-Eocene series (Laville et. al. 1977; Fraissinet et al., 1988, Görler et al. 1988, Zuykla, 1988). Inside the western and central part, (Sous and Ouarzazate) is a major thrust fault caring allochtonous units onto the foreland basins (Michard, 2008). The Atlas Mountain range is a fold-belt developed over a continental basement. It is compared to the rift system and the alpine system, a intracontinental, autochtononous system, developed over a continental crust which is slightly thinned during its pre-orogenic evolution (Michard, 2008). Seismic data show a lack of Triassic beds below the Ouarzazate Basin (de Lammote, 2001).The transition between Atlas and its foreland East of Ouarzazate is described with no flexural basin, low tectonic load, probably Sahara Platform which is not weekend by Triassic rifting.

The Anti-Atlas is part of the Zenaga and Kerdous series (Schoubert, 1963). The Anti Atlas Mountain range is a large Paleozoic fold belt, characterized by inliers of Precambrian basement (e.g. so called “Boutonniés”) (Michard, 2008), which shifted toward the northern border of the fold belt. Each inlier correspond to a more or less faulted anti-form with Precambrian rocks that are exposed due to post-variscan erosion.

It is part of the Pre-Panafrican series of the Eburnean orogeny. Eburnean ages found in granits of Azguemerzi and Tazenakht, dated 1850±50MA and 1744±32 MA (Bilal & Derre 1989). Similar ages found farther west in anticlinal inlinier of lower Draa (ait Malek, 1998). In the lower Draa inliers Ikenne (1997) describe a weakly metamorphosed metasedimentary unit, in central rocks injected with small aplite veins and grade into micaschists containing 110 m sized syntectonic graitoids. Tamousift granodiorites 1965±32Ma (Charlot, 1982). Several anticlinal of the the Anti Atlas Zenga Series unit consists of Augen Gneisses, metadolorites and metamorphic rocks with RB/Sr isochron of 1988±41Ma (Charlot, 1978 1982). The syntectonic pluton at Tahala could result from mixing mantlederived magma and magma arising from fusion of a granodioritic crust at 2000 MA.

The quarzite Series (precambrium II) is a 2000 to 3000 m thick on the north of Kerdous, but lateral variations are significant (Pique, 1981;Pique, 2001). It consists of detrital unit with siltstone, politic sandstone, conglomerates and especially thick quartzite layers. Limestones, often stromatolitic, are intercalated in the central Anti Atlas. The Intrusions of dolerites and tholeitic gabbros emplaced in into quarzites as sills and laccoliths are more or less concordant with sedimentary bedding. The Jebel Siroua towards Bou Azzer inhabits a abundance of limestone and quartzite and developed of black shales containing levels of siltstone and jasper, and acid and basic volcanic flows.

In Bou-Azzer inlier itself the Quarzit series replaced by ophiolitic complex (Leblanc, 1976) 4000 to 5000 m thick, disturbed during Panafrican orogeny. The whole series is a serpentinized mantle peridotites complex over a thickness of 2k of ultrabasic and basic cumulates, at top containing microgabbros ad quartzite diorites recut by basic dykes. These dolorites and spilitized pillow lavas are a volcano-sedimentary succession passing up into limstones and quarziote intercalations with facies identical to the platform. A comparable situation can be noted in Jbel Siroua (Schermerhorn et al., 1986) with a distinguish pre-arc ophiolit. Geochemical patterns indicate mid-oceanic ridge and intra-oceanic island environments (El Boukhari et al., 1991). Dolerits and lavas of boninitic affinity assdigned to an intra-oceanic island arc setting (Chabane et al. 1991; Amou, 2000). Marini & Ouguir (1990) show that turbidic facie correspond to continental margin clastic supply from north. The hercynian structure is classically for the Anti Atlas, with a largly free of shortening during the herynian orogeny. Metamorphism inside the area is extremely weak, often nonexistent, with no in situ hercynian granites.

2.3.1.2 Lower Draa Zone

The Lower Draa is characterized by crystalline basement of the anticlinal inlier, herzynian deformation (Mezeas & Puit, 1968; Belfoul, 1991; Souilaimani, 1998) represented by only some compressive faults. On the other side are folds of kilometric which crop out to south east of the crystalline axis. The asymmetry suggest a strong dextral component of deformation (Janette & Pique, 1981). Recent studies show, however, that the major component corresponds mainly to overthrusting fold towards the south (Soulaimani, 1997). On both sides the deformation is concentrated at the base of the cover, particulary in the volcanic and detrial rocks of the end-Proterozoic. Cleavage trajectories show that the fold is parallel to boundaries of the anticlinal inlier and that the basemant, behaved like an indenter, overthrusting its cover towards the SE.

2.3.1.3 Hamada du Draa

The Draa Hamada is the larges one of the “Grandes Hamadas” incl. Guir Hamada and smaller Daoura Hamada (Pique, 2001). It is a crataceos tertiary plateau which escaped from main effects of Triassic rifting and Alpine shorting (Zouhri, 2008; in (Michard, 2008)). The surface is covered by Mio-Pliocene sandstones and conglomerates with silicified woods which are quaternary deposits of Morocco (Plaziat in (Michard, 2008)). The Base of the area is build by quaternary material aged 1,8 Ma to be placed until 2.6 MA.

2.3.2 Soil

2.3.2.1 Overview on Nutrient and Influence on Vegetation

The following paragraph is prepared as short overview on the soils characteristics inside the investigation area. For more detailed information see (Klose, 2009). The availability of soil information in the Drâa catchment is restricted to oasis areas under irrigation agriculture, making up approximately 2 % of the catchments surface (Brancic, 1968; Radanovic, 1968a, 1968b, 1968c and Zivcovic, 1968). Inside the Impetus Project various asses spatial soil information. (Klose, 2009) provides spatial soil maps, based on 211 soil profiles with the intention “soils characteristics (e.g. its texture or organic matter content) are more important than its pedogenetic type”. Those maps provide soil properties (which can vary widely within classes) but explicitly not aiming to provide pedogenetic information, but spatially continuous maps of soil properties (Klose, in prep.). Those maps investigate fundamental regional trends and differences in the soil properties, but are not intended to offer detailed information at the local scale. Therefore, the soil information derived from this map on the local are taken as regional trend of soil information, not as ground truth for every pixel investigated.

The soils of arid regions generally raw textured, skeleton rich and are poor on organic substance. As part of the extreme evapotranspiration and the aszendial soil water movement, some soils tend to be salinization and encrustation (Volk & Geyger, 1970, Beven, 2002). The direct infiltration rate (Scheffer & Schachtschabel, 2002) is forced by precipitation, irrigation or flood irrigation. The infiltration rate is marked by the amount of water that can be introduced into the soil per time unit. The infiltration and saturation discharge amount and technique of measurement/calculation will be described in Chapter 5.7 of the Hydrological Model. The spatial infiltration rate is, in difference to that of humid latitudes, not coupled on soil wetness distribution but more on slope gradient, vegetation distribution and soil physics (see below) (Childs, 1969; Yair & Lavee, 1982). Therefore the infiltration is marked by great spatial variability and complexity (Descroix et al., 2002).

2.3.2.2 Soil physical characteristics

(Scheffer *et al.*, 1989)pointed out that short, periodic wetness favours sites with a raw substrates because of a effective infiltration. In consequence Floret et al. (1982) showed for tunesian step soils that under same yearly precipitation 60 % shorter periods of dry soil conditions occurrence then on silt soils. Ceballos et al. (2002) have shown that in dry periods the capillary water transport in sandy soils breakaway, storing residual moisture inside the soil body. On the other hand sandy soils minimize the effective total water capacity by a high discharge rates into the aquifer, making it less reachable and usable depending on the root system. More fine material soil sites are characterized by lower infiltration rate but more

effective Water carrying capacity (Zillbach, 1984; van Wesemael et al., 2000). (Weber, 2004)pointed out that the moistening of arid soils depends on sorption and desorption leading to a different (likly degree) of infiltration capacity, like fingering on texturel instability on sandy soils (Ritsema et al., 1998; Bauters et al., 2000) because of pre wetness irregular and digit form into the soil body (Nguyen et al., 1999). The soil pre wetness plays a subdominant role for infiltration and discharge (Fritzjohn, 1998) because of the high evaporation loss (potential Evaporation around 2000-3000 mm, depending on altitude and time of the year).

2.3.2.3 Soil types & characteristics

Inside the High Atlas soils typical for sub-humid (Luvisol) and steppic (Kastanozem, Chrenozem) climates are mapped Klose(2009). On jurassic limestones furthermore Calcisols can be found. Inside the sedimentary basins of Tazenakth and Ouarzazate Kastanozems, Chernozems and Regosols are mapped. Surprisingly the former two soil types are not expected because their development demands steppe climate and relatively dense vegetation to form the topsoil rich in organic matter, conditions which are currently not given (Klose, in prep.). The Anti Atlas region Leptosol are listed as typical mountainous soils. The Saharan Foreland soils are mapped as typical Aridisols alluding for arid conditions. More intensive work has been done on the soils of the date palm oases along the Drâa River (Brancic, 1968; Radanovic 1968a, 1968b, 1968c and Zivcovic, 1968). But those soils are out of the natural environmental context and are only mentioned here.

An detailed analyses detailed overview over soil types can be found in Klose (2009)

The analysed soil samples and soil profiles consistently show typically (semi-) arid characteristics. Overall shallow soils featuring high skeleton and high $CaCO_3$ contents and high pH values are found. Furthermore the typically low contents of organic matter (organic carbon and nitrogen) are detected.

On the gateway between Soil and Vegetation hydrological Processes inherits a great spatio-temporal variability (Wierenga, 1987). Like Bergkamp (1998) and Didao (2002) mentioned: there is a significant and effective feedback between vegetation and hydrological characteristics, which is bound to Slope, Soiltype etc.. (Puigdefabregas *et al.*, 1999;Pardo *et al.*, 2000;Beven, 2003) have shown that there is a significant coherence between vegetation cover dominance and infiltration rate. Klose (unpl) prepared their regionalisation /Pedotransfer function by combine soil texture, skeleton content and organic nutrient content to the map of vegetation units by Dr. M. Finkh (botanical

research group of the University of Hamburg). All physical processes, like Infiltration and Discharge, are described in the Runoff Curve Number model (RCN) chapter 5.7.

2.4 Vegetation formations inside the Drâa Catchment

The area is divided into three large floristic regions contributing to the phytodiversity of the Drâa Catchment.

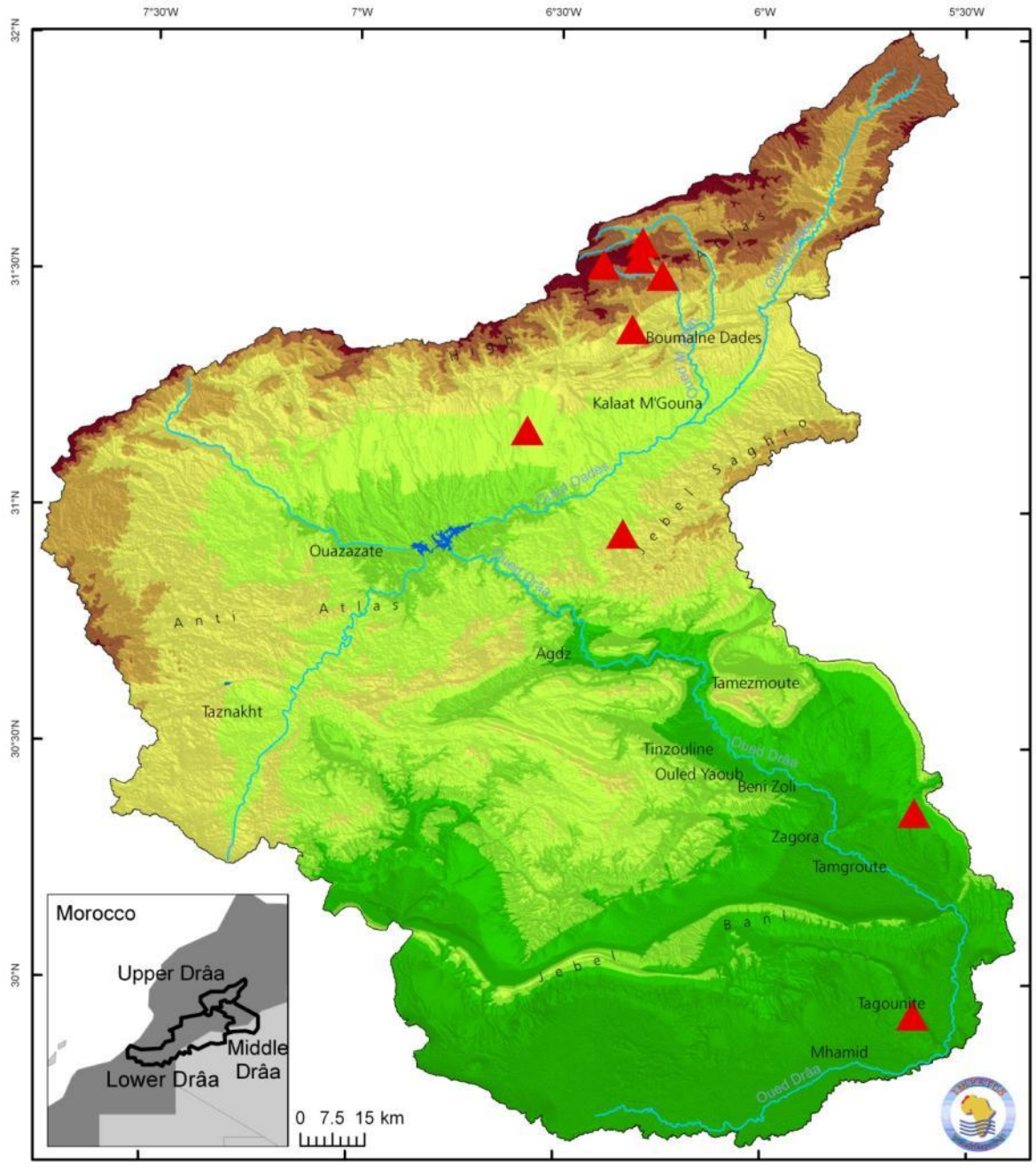

Figure 8 Upper and middle Drâa Catchment orographic overview. Red triangles marking the IMPETUS climate station.

These three formations are separated by altitude, with the High Atlas Mountain, Jbel Siroua and Jebel Saghro (2200 m and up), the south slopes of the Atlas Mountain range (1400 to 2400 m) and the presaharian/Saharan Flora(400 to 1400 m). Beside that there is some azonal vegetation formations inside the catchment like the salt pan of Lake Iriki and extrazonal vegetation along watercourses and agricultural systems.

2.4.1 High Atlas Mountain, Jebel Siroua and Jebel Saghro (2200 m and up)

The higher Mediterranean vegetation are Oromediterranean ecosystems, embossed by principally Mediterranean flora. The semiarid slopes and plateaus of the High Atlas, Jebel Saghro and the western Anti Atlas (including the Jebel Siroua) have few permanent settlements, but constitute important grazing resources. The vegetation gradient, ordered from top altitudes to low, starts with Junipero-thuriferae-Quercion-rotundifoliae steppes with mediterranean cushion-like shrub formation at ~3000 m a.s.l. (Jauffret & Lavorel, 2003), over Artemisia herba-alba steppes at ~1800 m a.s.l. (Finckh & Oldeland, 2006;Muche *et al.*, 2005) to Hammada scoparia-Farsetia occidentalis steppes at ~1380 m a.s.l.. Shrubs (i.e. Hammada scoparia) and periodic occurrences of grass (i.e. Stipa capensis) characterize the vegetation inside the Basin of Ouarzazate.

Figure 9 High Atlas mountain *Junipero-thuriferae* formation

The adaptation of the cushion-like shrub formation is dependent on extensive roots, reduction of transpiration and growing reduction/ recovery phases during heat or hygric stress (Weber, 2004). The *Junipero-thuriferae* formation steppes is the dominating formation between 2200 and 3000 m a.s.l. Three Juniper species (*Juniperus thurifera* L., J. oxycederus ad J. phoenica) with near absence of *Quercus rotundifolia* Lam (as an effect of firewood clearing) and ash (*Fraxiunus xanthoxyloides*) are the tree cover species. Those southern margins of the evergreen Mediterranean forest are now heavily degraded and overused (Fink *et al.*, 2008).

2.4.2 South slopes of the Atlas Mountain range (1400 to 2400 m)

The south slopes of the Atlas Mountain range (1400 to 2400 m), as well as similar altitudes in the Jebel Sirua and Jebel Saghro are characterized by Ibero-Mauretanian sagebrush steps with *Artemisia herba-alba Asso(A. Mesoatlantica Maire, Teurcrium mideltense Humb.* and *perennial grasses including Lygeum spartum L,Stipa spp. A.)* with low roughness length. These perennial grasses have annual emerges in spring and contribute to the floristic

richness if this steppe biome. The adaptation of the cushion-like shrub formation is dependent on extensive roots, reduction of transpiration and growing reduction/recovery phases during heat or hygric stress (Weber, 2004). The identification of the physical plant properties/requirements, density information and identification of vegetation associations is the basic for understanding local vegetation dynamic.

2.4.3 Presaharian/Saharan Flora

The Presaharian and saharian flora is the largest by surface area. The pre-saharan semi-desert and rock steps are embossed by *Convolvulus trabutianus* as well as *Hamma scorpia* (pommel Iljin) which startet to appear in the Ouarzazte Basin and lower belt of the jebel Saghro. The presaharian belt start south of the Jebel Saghro below 1000 m a.s.l.. The wadi vegetation is dominated by trees (e.g. *Acacia raddiana Savi, A. ehrenbergiana Hyne, Maerua crassfolia Forskk.*) and perennial C4 grasses (e.g. *Panicum turgidum, Forss. pennisetum dichotomun Delile*) of Sahelic origin (Finckh & Oldeland, 2005a). *Hammada scorparia* alone dominate pediments and loamy soils (Fink et al., 2008).

2.4.4 Extrazonal vegetation

The vegetation along the watercourses has shown a similar transition from Mediterranean to Saharan ecosystems. The higher altitude watercourses are accompanied by scattered fragments of sub Mediterranean alluvial forests with *Fraxinius angustifolia* (Vahlm) and species of *Populus* and *Salix*, most used for construction. Those habitats are interstratified by walnuts and apple orchards. In lower regions (2000-1200 m) there is a Mediterranean alluvial vegetation with *Nerium oleander* (L.) and different *Tamarix* accompanied with almond, walnuts, croub orchards. Below the Jebel Saghro (1200 m) the river terraces are covered by *Tamarix amplexicaule* (Ehrenb.) and oasis vegetation (Saharan date palm: *Phoenix dactylifera*). Inside the salt plans are some special habitats for ephemeral halophytes (*Frankia pulverulenta L., Mesembryanthum nodiflorum L.*). The sand dunes of M Hamid and Erg Chegagua inhabits some specialists like Aristida pungens Desf., Calligonum polygonides L., Tamarix aphylla L.. Karst and on rural sites may inhabits some naturalised plants like *Calotropis procera* and Echium *Aiton fil*..

2.5 Pastoral land use

For better Process understanding of vegetation activity it is fundamental to understand the and use and therefore their influences on plant production and management (comp: (Behnke & Scoones, 1993;Scoones, 1993;Sandford, 1994;Illius & O'Connor, 2000). Pastoralism is the

dominant extensive land use outside the river terraces and urban settlement. It is mostly investigated within the area of the Atlas Mountain down to Jebel Saghro and the Anti Atlas (comp. (Kemmerling, 2008). Secondly it's the resilience of pastoral-land use (Barfield, 1993; Humphrey & Sneath, 1999) and their ability to asset from degradation to sustainable land use (Gillson & Hoffman, 2007). Nomadism can be defined as range management which is based on the economic and natural and ecological needs, adapted to the local active tier of optimum survival (Scholz, 1995). The definition of a sustainable range management is given by Schäfer (1992:211) as "meeting the needs of the present without compromising the ability of future generations to meet their own needs..."[2]. That implies the survival of herdsman and reduction of poverty (Schaefer & Tischler, 1983). ((Snyman, 1998):645f) established 5 principles:

- Protection of natural resources
- Risk minimization
- Persistence or augmentation of biological productivity
- Economical survivability
- Social acceptance

These five factors are postulated as key factors of the land use inside the area.

Persistence or augmentation of biological productivity is a discipline and an art that skillfully applies an organized body of knowledge accumulated by range science and practical experience for two purposes (Heady & Child, 1994). Those are:

- the protection of rangelands
- the sustainable development of the people

Within this definition the herd management (herd size, herd structure, individual or communal herding) is included because practices affect directly natural resources (Niamir, 1989).

The Influence on the vegetation can also be discussed under degradation aspects or population evolution aspects. As an example on vegetation influences the grazing area of the Ait Toumert can be point out. It is a collective land on which the members have exclusively using right on the summer and intermediate pasture sites (Kemmerling, 2008).

[2]UnitedNations(1987):Report of the World Commissionon Environment and Development.

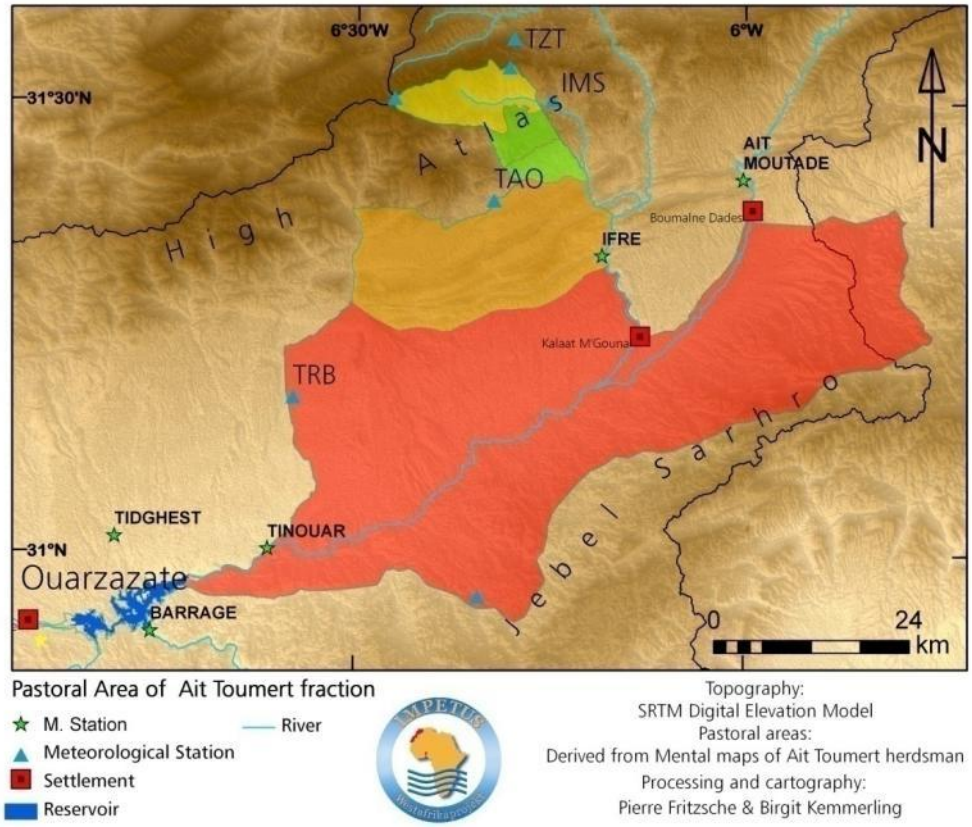

Figure 10 Pastoral Area of the herdsman of the Ait Toumert during the year. The herdsman using their winter ara (red), the intermediate area (oragange) and summer areas (green/yellow) during their yearly pastoral cycle.

A very important factor for a pastoral management system is the traditional *agdal* institution.

"*An agdal is a communal pasture whose opening and closing dates are fixed by the community of users. An agdal is a collective property used by tribal and intertribal groups: customary laws limit its boundaries and fix its closing and opening dates.*" (Ilahiane, 1999)"

The *agdal* here is an instrument to protect forage plants, which needs to be a time for its reproducing cycle and for a regrowth of its phytomass. Closing an important pasture during the plant growth periods guarantees an effective generation of forage and woody species and mountain biodiversity (Ilahiane, 1999):40f).

The livestock of sheep and goats in Morocco exhibits a number of 16.4 Mio sheep and 5.4 Mio goats. Cattles are of minor importance inside the high Atlas Mountain. The typical herd size are between 200 and 400 herbivores (Kemmerling, 2008;Darfaoui, 1998). The traditional herd composition is a high rate of sheep, but tended to a higher goat percentage do to a increasing demand on goat meat (Kemmerling, 2008). The second importance is the transportation of herds from one pastoral area to another.

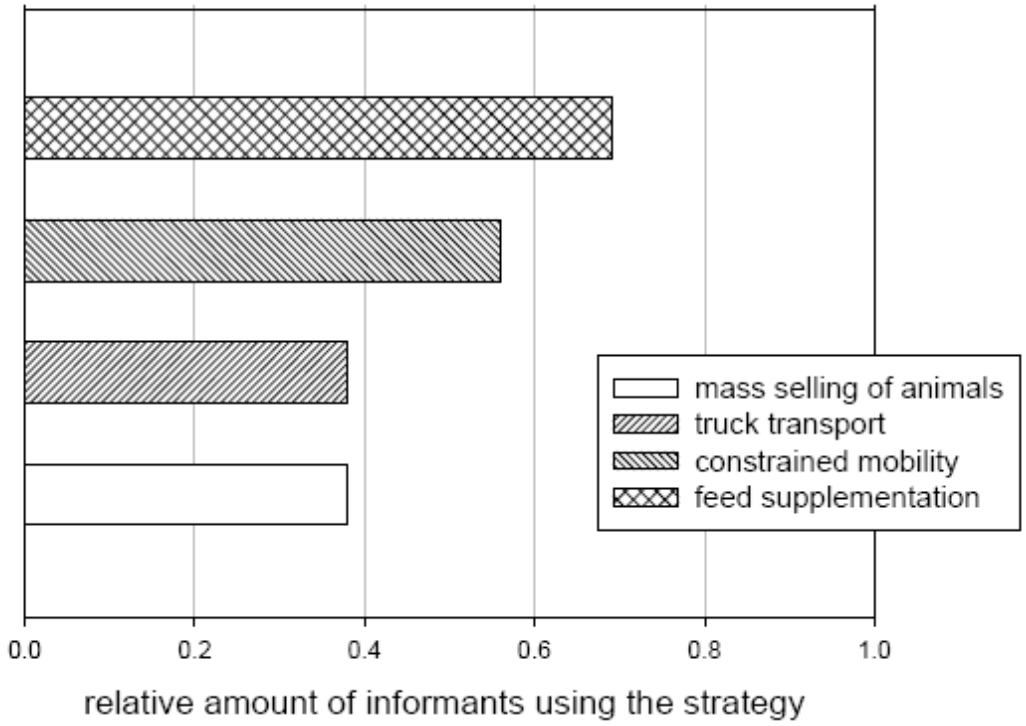

Figure 11 Relative frequency of range management strategies used by pastoral-nomads in 2007 (n=32) Source: Birgit Kemmerling

Pastoral-nomads cherish particularly perennial species that are trees, dwarf shrubs and perennial forbs tighter with cushion xerophytes and perennial bunch grasses (survey by Birgit Kemmerling & Gisela Baumann, 2008). Annual herbaceous species only attain a margin of the used plants[3]. The transhumance circle (see Table 1 and Table 2) is bound to local knowledge and the climatic situation (for further detail see: Kemmerling, 2008).

Table 1 Local Knowledge on forage plants and the transhumance cycle (Source: Birgit Kemmerling (2008))

pasture	main plant occurrence	transhumance
summer pasture	woody and perennial species	May – September
intermediate pasture	woody and perennial species	March – May; September - October
near winter pasture	herbaceous species	October – March
far winter pasture	herbaceous species	October – March

The management startegies can be describted by a matrix, as shown in Table 2. Type C to A meaning a degreasing access to livelihood ressources

[3] Herdsmen mentioned equally woody species (53%) and herbaceous species (47%) (Kemmerling, 2008)

Table 2 Managment strategies in relation to the socio-economic framework (Source: Birgit Kemmerling (2008)

type of year	strategies	management decisions by the three households		
		Type C	Type B	Type A
good year	full transhumance cycle	x	x	
	feed supplementation	x	x	x
	constrained mobility			
	truck transport			
	mass selling of animals			
average year	full transhumance cycle	x	x	
	feed supplementation	x	x	x
	constrained mobility		x	x
	truck transport			
	mass selling of animals			
bad year	full transhumance cycle		x	
	feed supplementation	x	x	x
	constrained mobility		x	x
	truck transport	x		
	mass selling of animals			
very bad year	full transhumance cycle			
	feed supplementation	x	x	x
	constrained mobility			x
	truck transport	x	x	
	mass selling of animals		x	

The management depends on the type of the sensed type of year (for further details see (Kemmerling, 2008)).

3 Spatio Temporal Vegetation Modelling

Introducing the Investigation area highlights several important prerequisites. This chapter will introduce the advanced modelling concept. It will also highlight the NDVI as main source of vegetation monitoring and discuss its theoretical background. Addressing the background of vegetation activity, the carbon cycle will be discussed. This will conclude in a summary of model possibilities and taken choices for model building. There are two important issues, which build up on each other. Firstly the design approaches will be discussed. Secondly, based on the first, the theoretical preparation of MD will be carved out. This chapter will furthermore discuss the theoretical background of the NDVI, as well known vegetation activity measurement. This is completed by a view on the relationship between vegetation activity and productivity.

3.1 Vegetation Modelling conception

Vegetation models are classified as analogical models by the Standford Encyclopaedia4 of Philosophy. A model allows us to investigate and analyse certain relationships between objects, which range between positive, negative and neutral analogies. These relationships can be objects by themselves or the relationship itself, which is essentially the understanding of processes, dependencies and interactions. Ecological model conceptions consist of the identification of five components (Jörgensen, 1988). Firstly the forcing function is the external nature that influences the state of the ecosystem. Secondly state variables describe the states of the ecosystem. Thirdly the biological, chemical and physical processes are represented by mathematical equations. Fourthly the coefficients or parameters used in the model. The calibration phase is an attempt to find the best accordance between computed and observed state variables. Fifthly universal constants were defined that are not part of the calibration. Such constants are gas constants, Energy conservations etc. (Jörgensen, 1988). Models are an approximation of a complex system that enables us to reveal the system´s properties, to survey and to test scientific hypotheses. Various models for analysing land use and land use change have been developed under different assumptions regarding technique or model use (Agarwal *et al.*, 2002). (Levins, 1966) formulated the principle that only any two out of three desirable model properties (generality, reality, precision) can be improved simultaneously (Figure 12), while the third property has to be sacrificed (Guisan & Zimmermann, 2000).

[4] http://plato.stanford.edu/

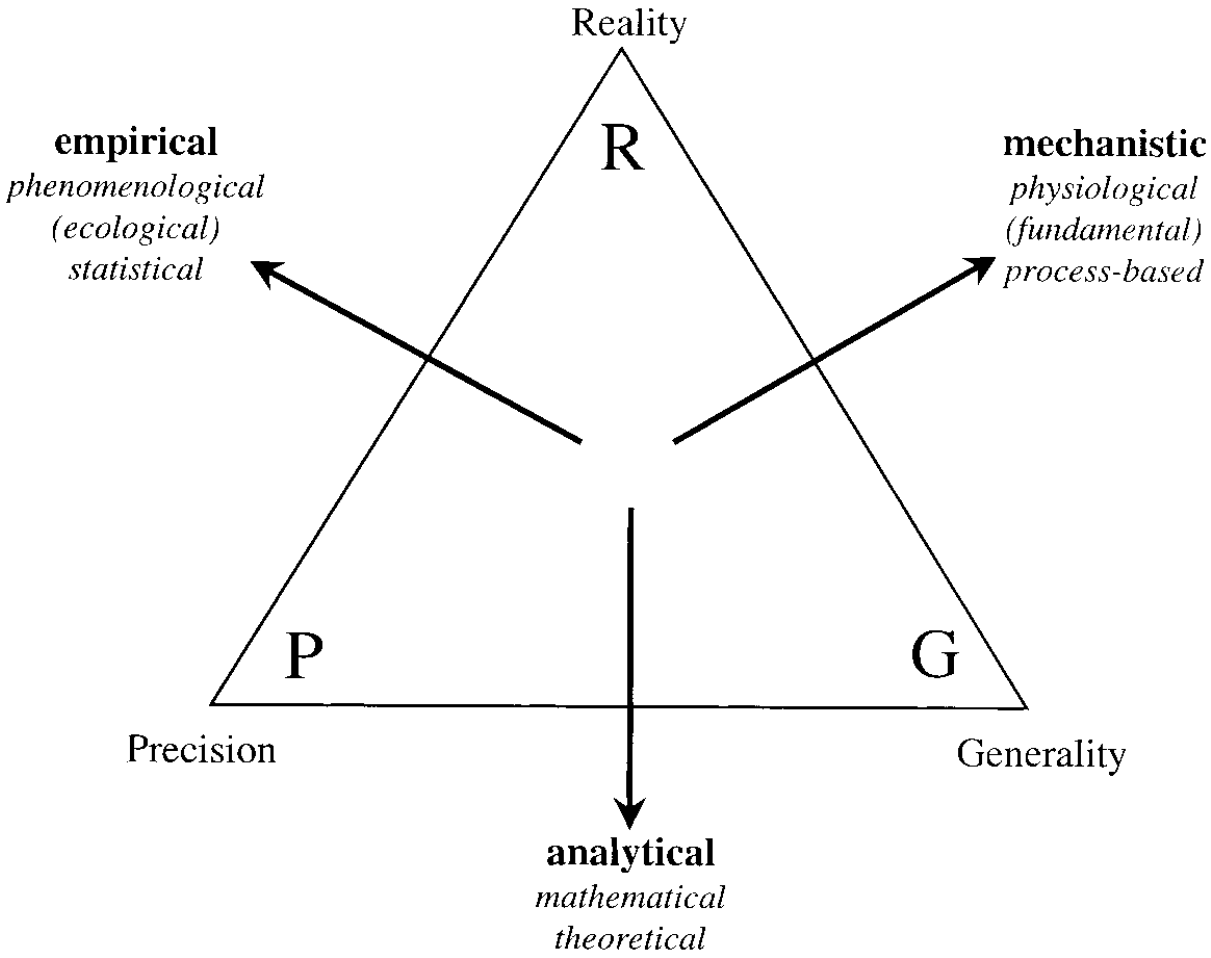

Figure 12 A classification of models based on their intrinsic properties (After Levins (1966), and Sharpe (1990)).

In order to define a model it is necessary to classify the approbated model typ. Using an empirical approach exchange generality for precision and reality (Guisan & Zimmermann, 2000). Therefore such a model insufficiently describes reality in mathematical formulas nor does it inform the underlying ecological functions and mechanisms (Wissel, 1992). This discrepancy is too dissolved. Such a model has to be realistic, but adaptive to satisfy the general criteria. And as (Peters, 1991); p.32) noted: ‘‘there is no necessary conflict between precision and generality’’.

The Model building process is a step by step build up process. From the idea of the concept to the statistical formulation up to the evaluated model (Guisan *et al.*, 1999).

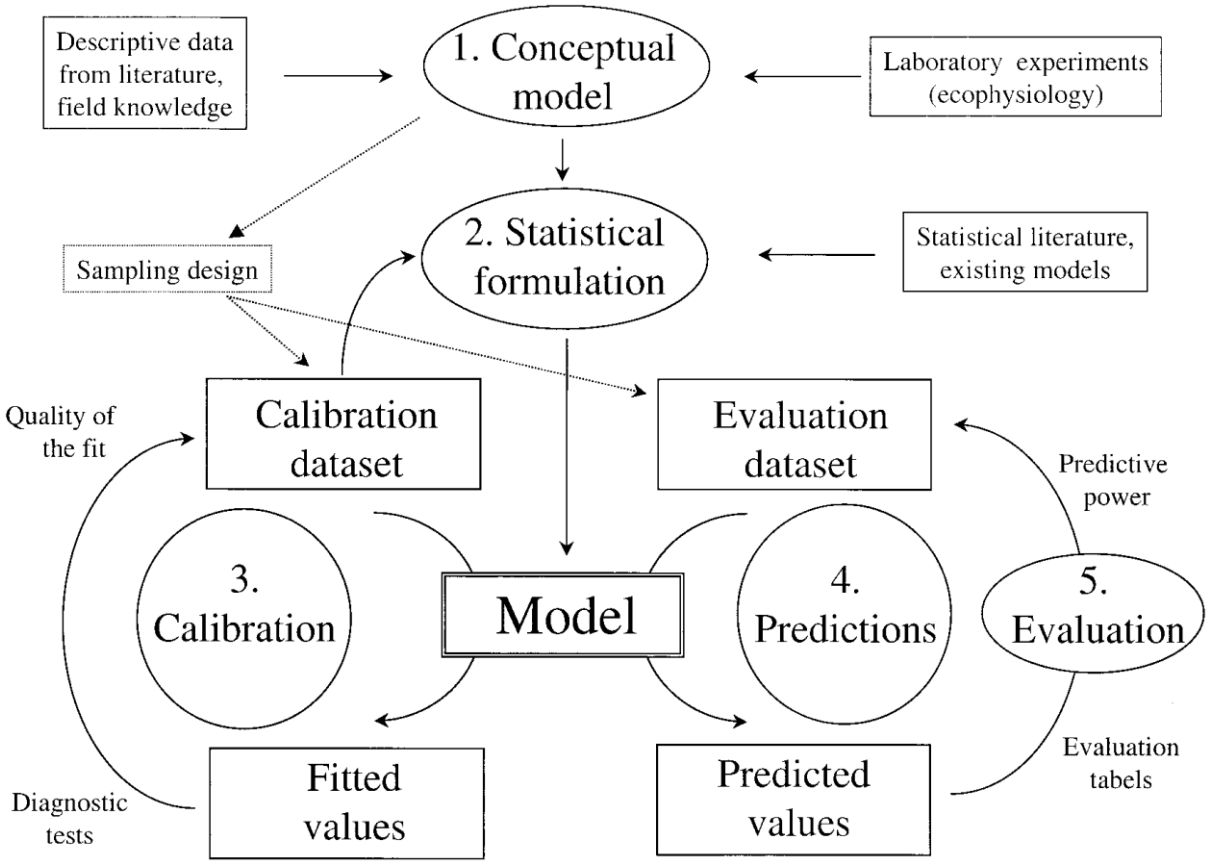

Figure 13 Model building process (Guisan & Zimmermann, 2000)

Figure 13 introduces the concept of dividing Data into a calibration and evaluation dataset. This concept is often used in hydrological modelling (Refsgaard, 1997;Henriksen *et al.*, 2003) and is called split-sample test. In advance, a model to model comparison can be used, especially if there is no ground truth data available (Giertz, 2004).

3.2 MOVEG Drâa, a Dynamic Vegetation model

"The scope of the model is to determine the complexity, which determines the quality and quantity of the Data[..]" (Jorgensen, 1988). This means that the selection and availability of data determinate the complexity of the model. "If good data are not available it is better to go for a simple model than one, which is too complex" (Jorgensen, 1988).

The definition of modelling in the previous chapter left the limits and advantages of modelling. Jörgensen & Bendoricchio (2001) show that solving this scientific question definition is more comprehensively by using other model types. A model must have its specific database, the approval definition of processes and an overview about past development. For ecosystem modelling it is necessary to capture the essential features which should reflect in the model. This leads to questions such as:

- Is it possible to model a system that has only uncertain observations/ data?
- The forcing functions and several ecological processes are stochastic. How to account for that?

Those questions are part of the Data exploration and the retrieval of knowledge about the function inside the investigation area. It is therefore necessary to characterise the parameters of vegetation monitoring , and in which magnitude, the investigation area (and therefore the model) is influenced by: (Potter & Klooster, 1999)

- plant competition for resources of water and light (short time periods of months and seasons)
- long-term patterns (growth-limiting resources such as water and nutrients)

MOVEG Drâa is designed to answer these questions: What kind of data is needed to analyse and predict vegetation inside the Drâa Valley? But furthermore: How is the relationship between NDVI, the atmospheric condition and the soil water availability[5]? Knowing these key factors enables us to describe the dynamic parameters (comp. (Karnieli, 2003;Myneni *et al.*, 1992;Verstraeten *et al.*, 2006). MOVEG Drâa is designed as a structurally dynamic model (Agarwal et al., 2002). Structurally dynamic models are indicated by the ability to account for adaption, its possibility to use knowledge or artificial intelligence to describe changes in parameters and using a goal function to find changes of parameters (Jörgensen, 2008). A precondition of this model approach is the selection of a goal function. The goal function here is the adaptation of the situation of plant growing factors dynamically by using regression approaches which are concluded to a non calibrated ANPP. It is recommended for models that are used on environmental management to make prognoses resulting from major changes into forcing functions (Armstrong, 1985a). Dynamical models require data that can elucidate the dynamics of the process inside the Model (Jörgensen, 1988;Kumar & Maity,

[5] In Terms of a accesable water for plants (eg (Doudill, 1998))

2008). It is necessary to build up a consistent database, covering an as large as possible space of time. MD should also give information about the spatial distribution. MD is therefore considered a individually-based model and at the very least needs information about structure and structural changes (Jörgensen, 2008).

3.3 From Images and Meteorological Stations to Vegetation monitoring

The modelling concept of MD is based on the Overview, Design concepts and Details protocol (ODD) (Grimm *et al.*, 2006). The Purpose of the model is the identification of relevant factors explaining vegetation growth and the dynamical adaptation of the lower atmosphere conditions on the state of the vegetation by defining the plant competition factors, like water and light, as resources ratio of vegetation change. Therefore the fundament for every land cover change analysis is the acquisition, processing and interpretation of remote sensing imagery data (Lambin & Geist, 2006) as state variables and scale. (Schultz & Halpert, 1993;Lambin *et al.*, 2001a) and others have investigated the relationship between temperature, precipitation and NDVI. Their time series found no high correlation between monthly climate data. Often, more than one technique, that may or may not belong to the same statistical approach, can be applied appropriately to the same response variable (Guisan & Zimmermann, 2000). Investigation (Tucker *et al.*, 1986;Nicholson *et al.*, 1990;Shinoda, 1995;Justice *et al.*, 2000) implied that lag times of about one month between rainfall and NDVI are common (with proxies for onset being derivable. Therefore a lag factor is introduced inside the model. Besides the lag discussion (on which is focussed later), it is essential to understand that the response of a terrestrial ecosystem depends upon the contemporary relation between climate and plant production (Potter et al, 1998) and that it must therefore be downscaled to the meso scale. Since vegetation dynamic is strongly dependant on rainfall (Diodato, 2006), the process analysis of robustness and reaction of the vegetation must be multi temporal analysis.

Growth imitating factors, like water and nutrients, are on a long term pattern

Long term patterns are such things as growth imitating factors like water and nutrients. Foley (1996) mentioned that the first models predict vegetation on a global scale as conceived mechanical response to climate and atmospheric conditions. The Miami Model is one of the first models (developed by Leith (1975)). It can be described as a bio-geographical model with implicit plant types. It inherits no mechanism for changing vegetation density and it states that the implicit vegetation will immediately adjust to changes in climate (Adams *et al.*, 2004).

Therefore satellite observation can be used to fill the gap between field studies and enlarge data about vegetation responses to the climate (and may scale up to global assessment (Potter & Brooks, 1998). (Potter & Klooster, 1999) suggests to scale-up the dynamics of the vegetation cover from daily to longer time periods (10 years). By using a six year vegetation cover monitoring, the target is approached.

"An obvious limitation of using NDVI in global change simulations, however, is in application of the model outside the time period of satellite data collection. Therefore, climate-based predictions of the vegetation greenness information represented in NDVI are important for studies of past and future biosphere states" (Potter & Brooks, 1998). Especially for the projection, and therefore the consequences of global change, dynamical models are essential (Cramer *et al.*, 2001;Pachauri *et al.*, 2008). MD inherits a statistical regression approach (Armstrong, 1985b;Draper & Smith, 1981;Foody, 2003;Maselli *et al.*, 1998) (see Chapter 5.14) for future prognosis. This requires a the calculation of a large amount of data, but modern computer systems are extremely helpful to crunch large numbers and have their capability greatly increased as mentioned by Moore´s Law (Moore, 1965). This must be also seen in the context of geographical modelling having gained an important role as a tool to understand plant life and activity processes in arid and semiarid areas (Muhar, 2001). Since plant live depends on the availability of water (comp. (Dina & Klikoff, 1973;IPCC Working Group2, 2001a;Watson *et al.*, 2000) the understanding of its processes and driving factors is not only scientific essential. , but are also very important for the sustainability of human livelihoods.

In summary the design of MOVEG Drâa is a conceptual, modular, statistically dynamic model that extrapolates the situation of vegetation inside the catchment until 2050 on the basis of the IPCC climate scenarios and their underlying calculations. MOVEG Drâa inherits an implicit mechanism for a vegetation density through a NDVI vegetation cover function, and a mechanism for the delayed reaction of vegetation through a max covariance approach. MOVEG Drâa tries to include a more realistic representation of land surface processes (comp (Sellers *et al.*, 1995)). The model includes several sub models, for example the RBM model (Richters, 2005b). MD can be classified as a top-down approach of the dynamic global vegetation model (DGVMs) on a meso scale (Peng, 2000) by providing a interactive representation of the vegetation climate interactions and feedbacks.

3.4 NDVI: Introduction and Relationship to other factors

The Normalized Difference Vegetation Index (**NDVI**) is a simple numerical indicator that can be used to analyze remote sensing measurements to assess to the activity of vegetated land surface. The NDVI is a linear index scaling from -1 to a maximum of 1 for dense green Vegetation and is given by:

Equation 1 NDVI (after Tucker, 1979)

$$\mathrm{NDVI} = \frac{(\mathrm{NIR} - \mathrm{RED})}{(\mathrm{NIR} + \mathrm{RED})}$$

Based on the AVHRR sensor on EOS-A, in Equation 1 Red stands for the measured spectral wavelengths of 0.63-0.69-µm and NIR (Near Infrared Radiation) for the wavelength of 0.75-0.80 µm. The Satellite remote sensing of primary production is measured Rayleigh /Mie Scattering (Iqbal, 1983a) of leaves and their cellular interspace. Figure 12 shows the principle radiation flux on a leave. The reflectance, scattering and absorption in different wavelengths, measured by the instrument (in this case AVHRR), allows a tonal signature. This makes the leave spectral distinguishable from ground and allows, under most conditions, a comparisation/ differentiation from other species.

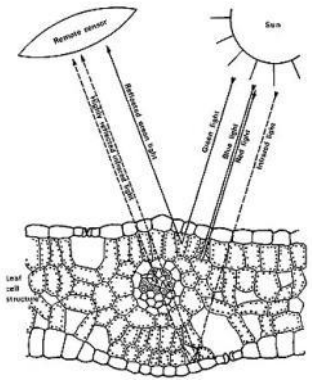

Figure 14 Scattering inside leaves (Source http://www.fas.org/irp/imint/docs/rst/Sect3/leaf_structure.jpg)

Living cells that contain Chlorophyll A or B (See Figure 15) are able to use those spectra for the absorption of photo synthetically active radiation (PAR) due to the process of photosynthesis. They also scatter and transmit solar radiation in the near infrared spectrum (around 550 nm), hence their not sufficient for synthesised of organic material (see Figure 15). (Larcher, 2000) reported that the maximum of the absorbed solar radiation is in the range between 0.35 - 0.45 and 0.6 - 0.75µm.

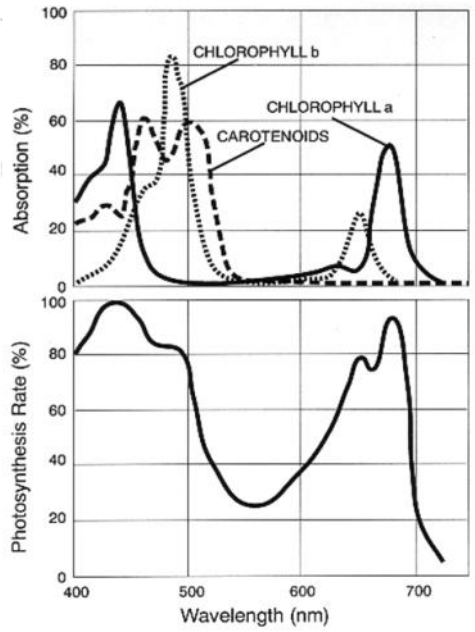

Figure 15 Absorption Spectrum and photosynthesis rate of Chlorophyll

(Tucker, 1979) found out that the IR/red ratio (and the related IR and red linear combinations) are to be preferred to the green/red ratio (and the related green and red linear combinations) for the monitoring of vegetation. The NDVI provides a measure indicating the vigour of vegetation (e.g. Campbell 1987, (Bannari *et al.*, 2002;Xie *et al.*, 2007). It is an ecological surrogate measure of the absorbed photo synthetically active radiation (APAR) and thus photosynthetic activity in the vegetation (e.g. Asrar et al. 1984, Daughtry et al. 1992, (Myneni *et al.*, 1995a).

The strength of the NDVI as universal Index is the high temporal availability of information and the ability of defining important attributes of vegetation phenology (Running, et al. 1995). As described in chapter 5.8 the generation of Time Series empowered the NDVI to a powerful tool to describe the Vegetation activity.

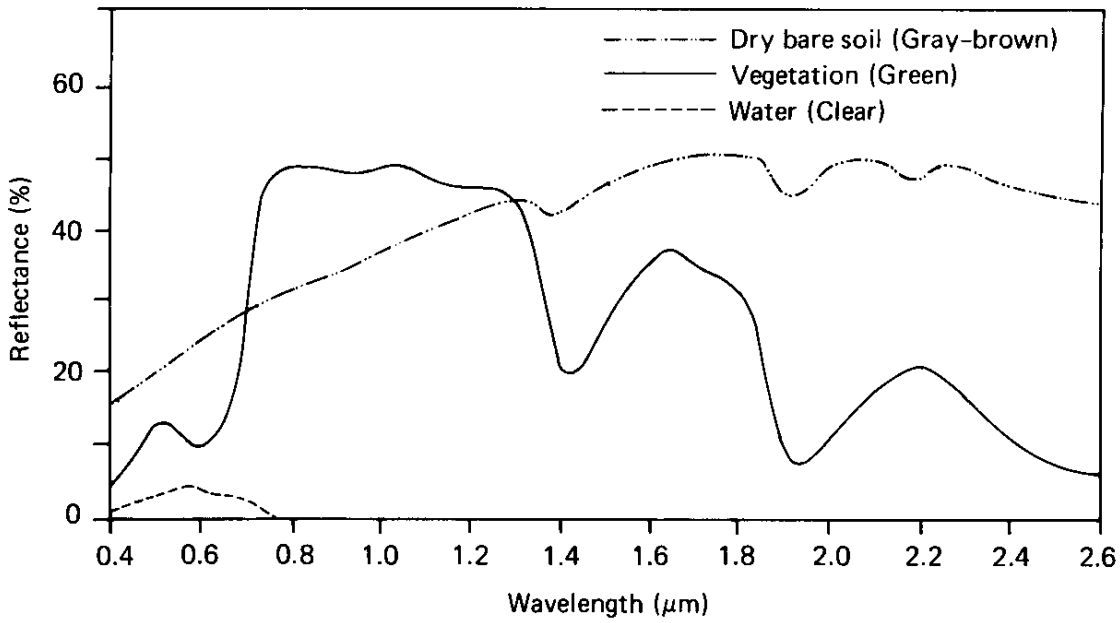

Figure 16 NDVI in relation to Bare Soil and Water (Source: Lillesand &Kiefer, 1994)

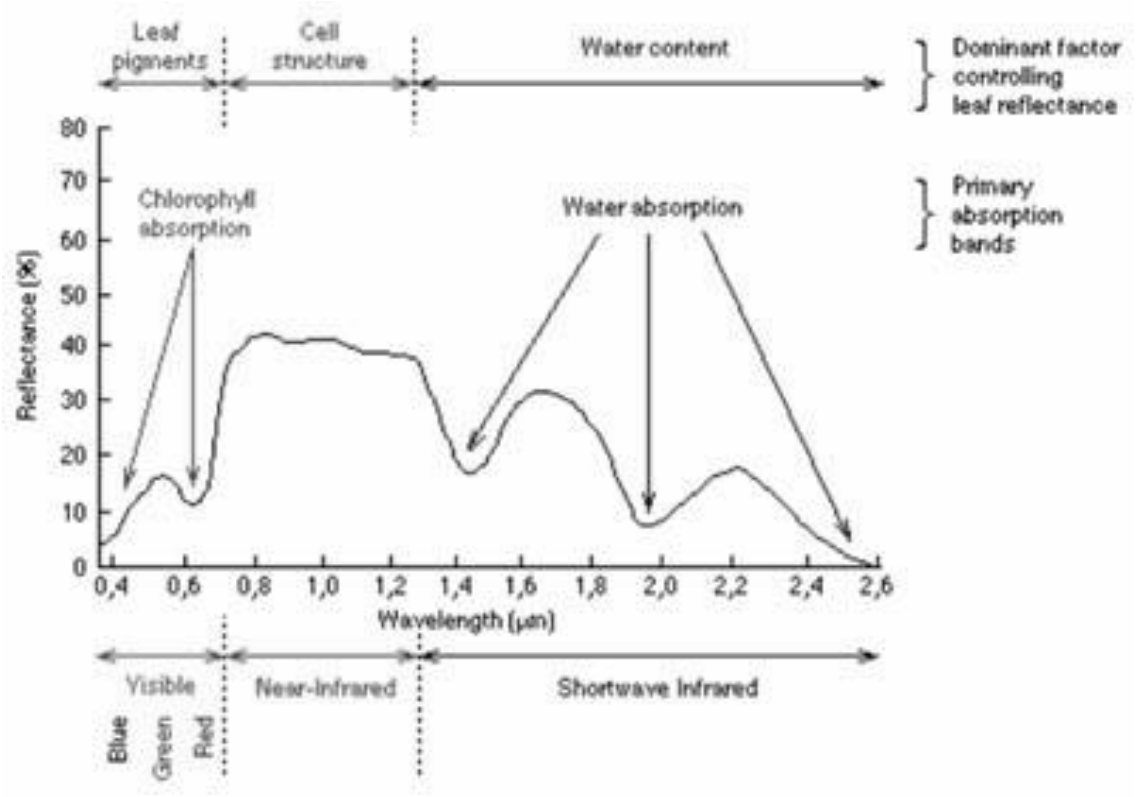

Figure 17 Atmospheric Transmission (Source: http://www.csc.noaa.gov/crs/rs_apps/sensors/specsig.htm)

Also Stress can be a relevant factor on the Vegetation Signal (see Figure 18), but will not discussed in detail since the vegetation is under a continuous stress situation (comp. (Baumann, 2009).

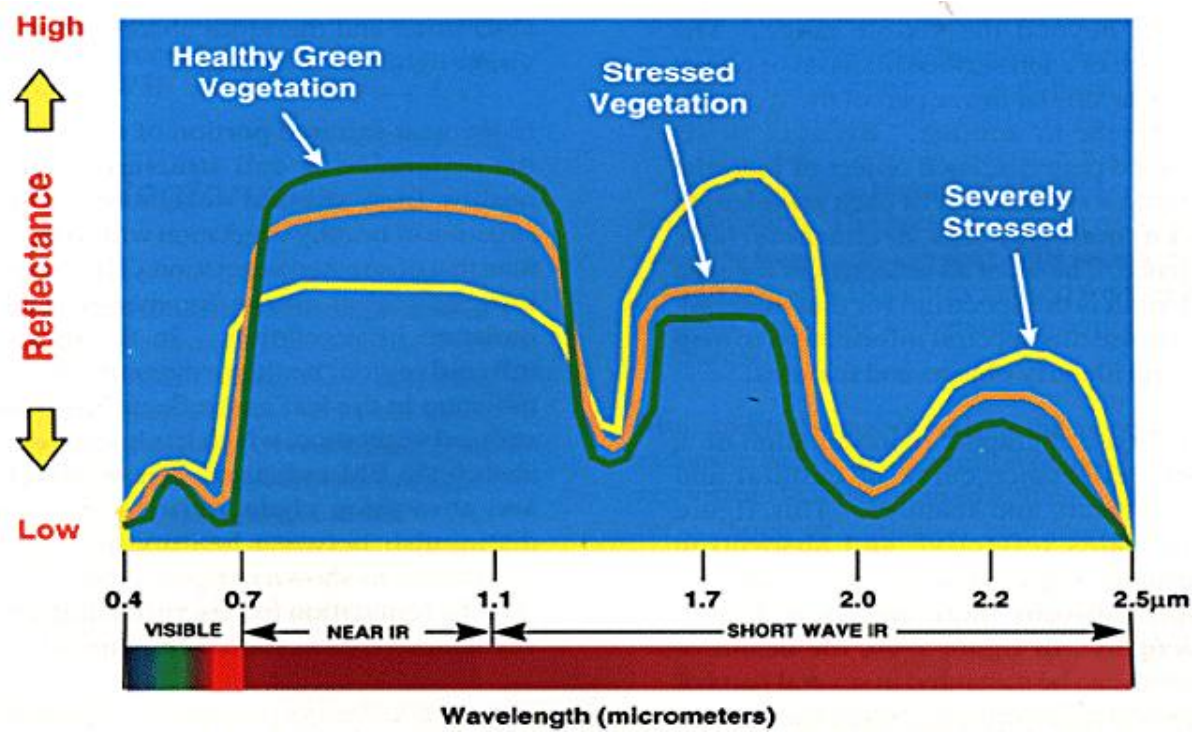

Figure 18 Stress visible on the Vegetation spectral (Source: http://www.csc.noaa.gov/products/gulfmex/html/rsdetail.htm)

The in situ plant-canopy reflectance is altered by different soil backgrounds(Bannari *et al.*, 2002;Huete, 1988). Those influences the relationship between percent vegetation cover and vegetation indices (Purevdorj *et al.*, 1998;Carlson & Ripley, 1997;Myneni *et al.*, 1992;Potter & Klooster, 1999;Scanlon *et al.*, 2002) (see also Figure 19 and Figure 24).

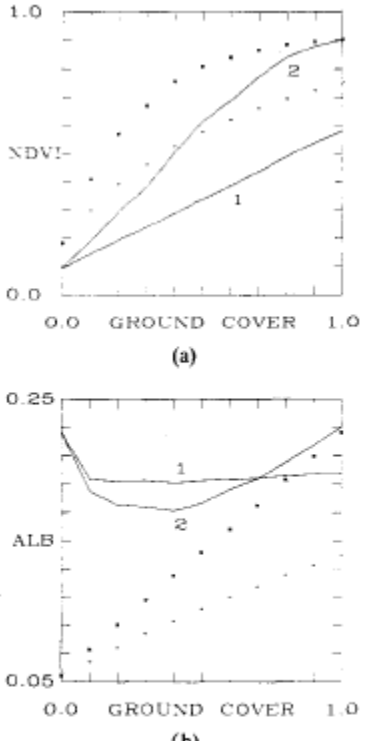

Figure 19 NDVI (a) and Albedo (b) to Ground cover relationship (Source: Myeni, 1992)

Nevertheless the signal of the NDVI on non Tree covered Areas is mostly influenced by soil and the water content in the top soil (Lillesand, 2006). The measured signal depends on the overall albedo, which is the reflection integrated over the solar spectrum (Iqbal, 1983a). (Daughtry *et al.*, 1995)show that the absorption in the Short Wave Infrared Radiation (SWIR) are different for agriculture areas, depending on minerals and soil components. To differentiate soil and vegetation it is useful to have information on the soil albedo, the geometric relationship between sensor and surface and the vegetation cover (see: (Iqbal, 1983b;Lambin & Strahler, 1994;Strahler *et al.*, 1999b). Huete (1998) add that soil also has a temporal dynamic, like organic matter input etc. That makes it necessary to understand soil spectral properties. Especially Myneni, et al (1992) discussed ground cover issues of desert surface and their reflectance. The Sensitivity angle fractions of solar radiation absorbed by the canopy to the NDVI is only between 6-8%, by a Solar zenith between variation 15 to 55%. “Spatial heterogeneity in vegetation canopies was found not to affect the relationship between NDVI and radiation absorption by the canopy and soil.” (Myneni et al., 1992). It is therefore possible to use NDVI as diagnostic of radiation absorption. This is important for calculation of leave and canopy structure related parameters like FAPAR. The Relationship between dark soil is insensitive to all “problem” (Myneni et al., 1992) parameters and not linear.

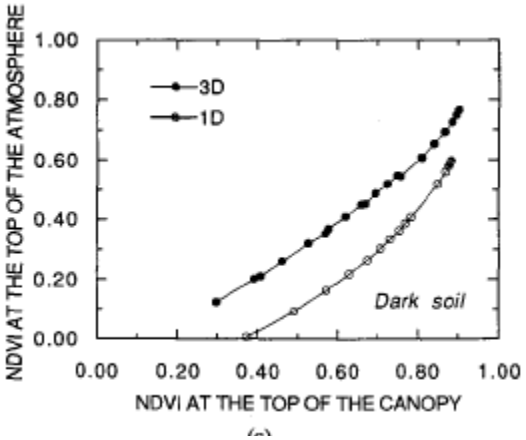

Figure 20 Dark soil NDVI Relationships (Myeni, 1992)

Figure 20 stated that the NDVI Signal is significant increase for dark soils. This is important because large areas inside the Investigation areas covered by Desert Varnish. The atmospheric transmission is untouched by this. By including sensitivity to leaf normal distribution and solar zenith angle the relationship is insensitive to changes in leaf angle distribution and solar zenith angle. The albedo of vegetated surface is therefore darker than the canopy (background absorptive, see Figure 21).

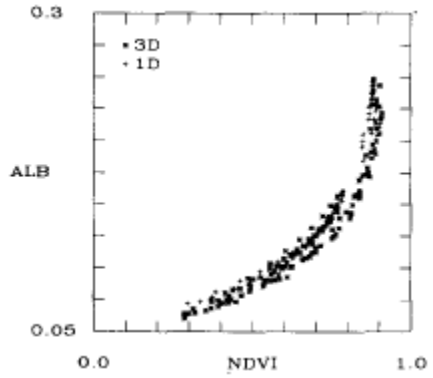

Figure 21 Albedo NDVI Relationship for vegetated surfaces (Myeni, 1992)

“For sparsely vegetated areas and bare soil (low NDVI and high reflectance in both channels), the perturbation [inside the Atmosphere] is weak.”(Myneni et al., 1992).

The NDVI is not the only parameter to described vegetation radiation reflection and absorption. The Leaf Area Index (LAI) and the Fraction of Absorbed Photosynthetically Active Radiation (FAPAR) represent two biophysically complementary ways of describing the earth’s vegetated surface (Fensholt *et al.*, 2004).

The Fraction of Absorbed Photosynthetically Active Radiation (FAPAR, sometimes also noted fAPAR or fPAR) is the fraction of the incoming solar radiation in the photosynthetically active radiation spectral region that is absorbed by Chlorophyll. The FAPAR is defined as the linear scalar relationship between bare surface (lower boundary) and the maximum NDVI as

upper boundary (Goward & Huemmrich, 1992; Potter et al., 1993; Ruimy et al., 1996; Prince et al., 1995(Seaquist *et al.*, 2006;Prince *et al.*, 1995;Prince, 1991b;Runyon *et al.*, 1994)). (Fensholt et al., 2004) gave a good overview over the dependency of NDVI and FAPAR for different Biomes.

The LAI is defined as the one-side green leaf area unit per ground area in broadleaf canopies (Myneni *et al.*, 2006) and is a estimation of the green leaf area of a terrestrial vegetation.

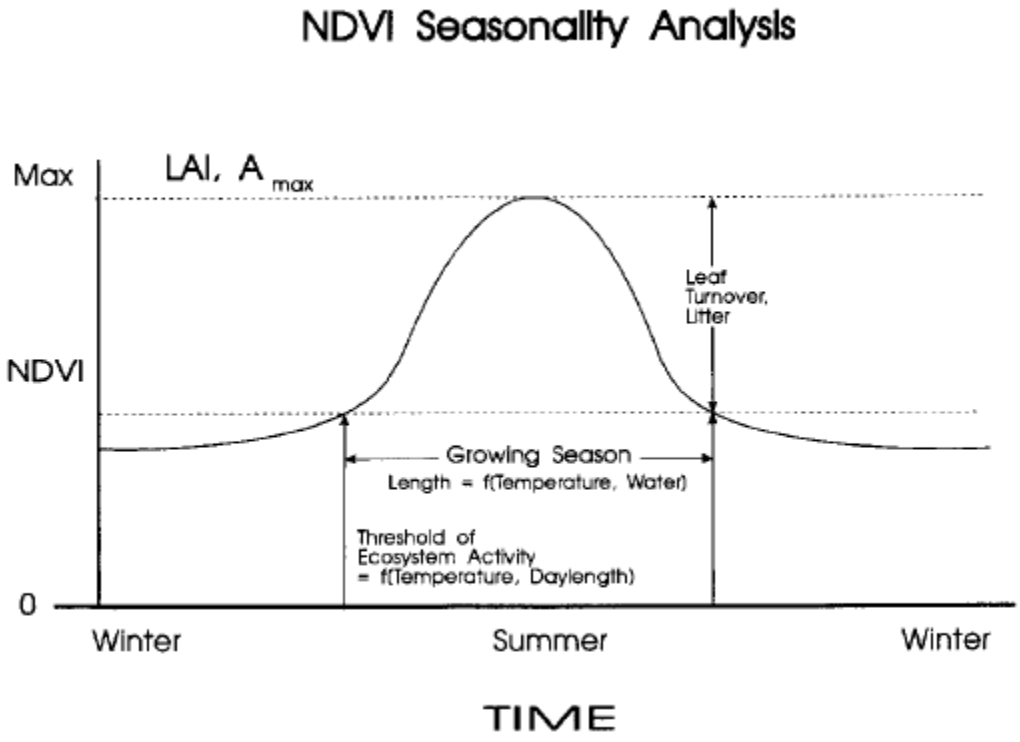

Figure 22 LAI / NDVI Seasonal dependency (Source: Running et al;1995)

Figure 22 shows the Seasonal dependency of the NDVI/LAI relationship. This is important for calculating the LAI from NDVI, as the LAI not only depends on Season, but on the thresholds and activity (See Chapter 6.3.4 for calculating LAI). The NDVI is correlated with biomass when the leaf area index (LAI) is less than 3 (Asrar *et al.*, 1986;Marques da Silva *et al.*, 2008). When collected with ground-based platforms, aircraft, or satellites it offers a non-destructive and minimally invasive method of sampling herbage mass (Flynn *et al.*, 2008). The LAI is one of the key inputs in models describing biosphere processes (Knyazikhin *et al.*, 1999;Running *et al.*, 1999;Chen *et al.*, 2004;Myneni *et al.*, 2006;Davi *et al.*, 2006).

3.5 Primary Productivity and C-fixing with the remote eye

Primary productivity time integrate the positive increments of plant biomass and is well and often modelled in global scale (Field *et al.*, 1995). Net primary productivity is the difference

between CO2 fixed by photosynthesis and CO2 lost to autotrophic respiration and is one of the most important components of the carbon cycle ((IPCC, 2003)). The first model that relates NPP to precipitation and temperatures are the Miami models by Lieth, 1975. These models are based on the law of the minimum, mean annual NPP is a function of the minimum of empirical mean annual precipitation (MAP) and mean annual temperature (MAT) functions. (Delgrosso, 2008). It stands therefore for the effective productivity of a plant community or gross primary productivity minus respiration losses. At this point a difference between the Total Net primary productivity (TNPP) and the Above Ground Netto primary productivity (ANPP) occur. The main difference between both is the subsurface Biomass like roots, root tubers and other storages of carbon (Watson et al., 2000). NEP (Net Ecosystem Productivity) can best be understood within the context of a complete organic C balance for an ecosystem, which can be (simply) written as the Photosynthesis: (Lovett *et al.*, 2006)

$6\ CO_2 + 6\ H_2O + \text{light photons} = C_6H_{12}O_6 + 6O_2$

Almost all primary production is performed by vascular plants. There is a suspicion that some algs or mosses could play a part in the southern region, but that can't be denied or agreed on a scientific base during this work, but the influence of Microphysics already discussed in literature (Karnieli *et al.*, 1996).

The historical survey of investigation can be read at (Lieth, 1973) and enhanced today's knowledge by introducing Energy balancing as universal criteria. It further "leads to the observation that among the forest types, caloric contents are correlated with climate and taxonomic group Caloric" (Lieth, 1973). The knowledge of biomass ("[...]or dry matter – sometimes referred as standing crop- as distinguished from productivity as rate value) is essential for knowledge of nutrient pools in organism as part of nutrient cycling and biogeochemistry" (Lieth, 1973).

Therefore can be defined (Sabbe & Veroustraete, 2000):

- Gross Primary Productivity: $GPP_d = S_{g,d} \cdot fAPAR_d \cdot F_d \cdot C$[6]
- Net Primary Productivity: $NPP_d = GPP_d (1- A_d)$ (2)
- Net Ecosystem Productivity: $NEP_d = NPP_d – R_d$

GPP_d.. uptake of carbon
NPP_d accounts for the autotrophic respiratory losses
NEP_d (Net Ecosystem Productivity)
R_d, soil respiration losses

[6] The relationship of fapar and NDVI will discussed later

The break down from global scale to meso scale is therefore not only a division of the cartographic scale, but also to the inherit parameter composition and their time scale. The change of time scale (as shown in Figure 23) is a change in the processes involved.

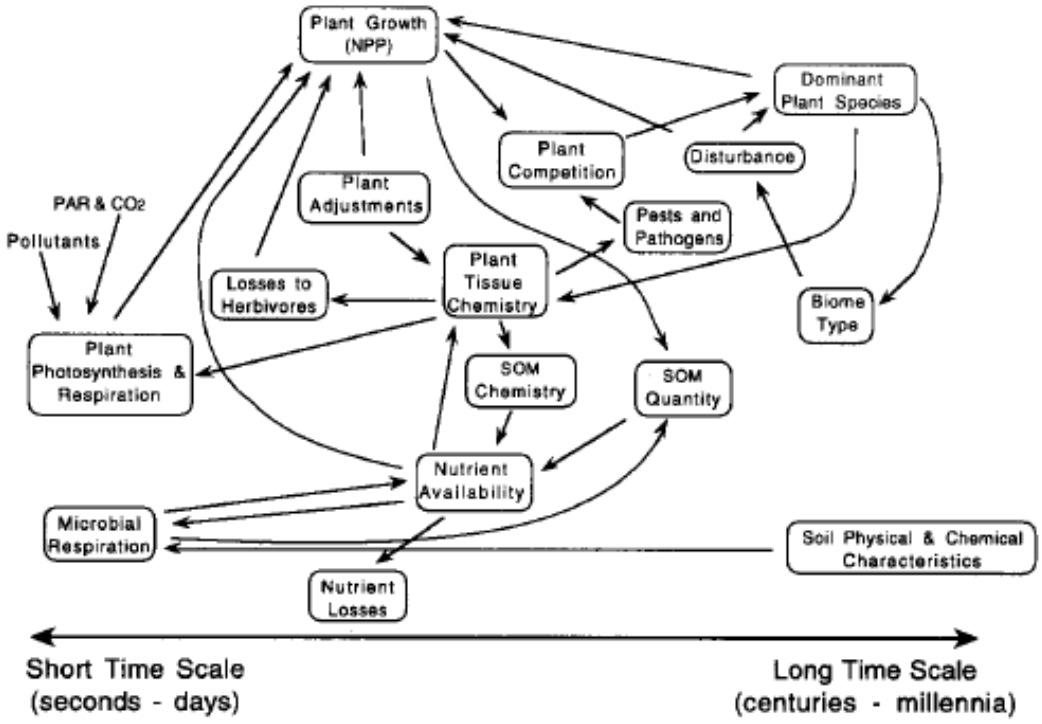

Figure 23 Major controls of NPP on the time scale (Source: Field et al, 1995)

Field et al (1995) reported that on a short time scale temperature, soil moisture, and atmospheric moisture affect the physiological processes that control plant photosynthesis and growth. It also implies that both scales are adjustable, under the presumption of looking into necessary parameters. Therefore the higher temporal scale needs not only finer measurement, but at spatial distribution, in fact more measurement. This is the limit of spatial scaling depending on temporal scaling.

This can be explained through interaction Ecosystems with the physical climate system (see Figure 24).

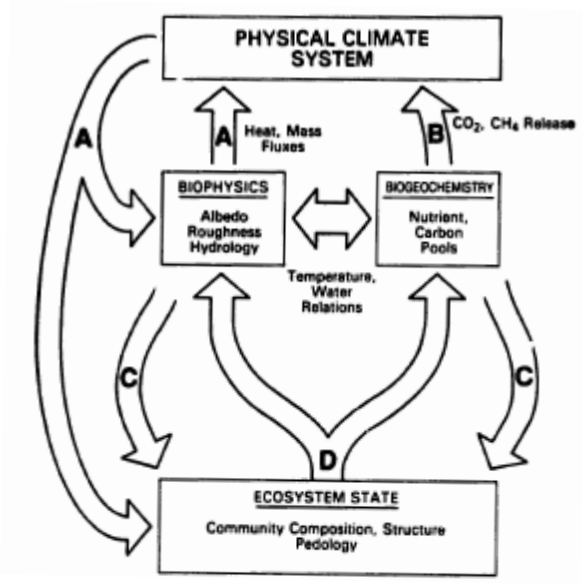

Figure 24 Interaction of vegetated Land surface (Source: Sellers et al., 1993) with different Interactions (chemical, energy etc.) between and to the ecosystem state

Vegetation in climate and biogeochemical cycles is well recognized (Sellers & Schimel, 1993;Myneni, 1997). In addition to the atmospheric carbon discussion it is proved that a quarter of atmospheric carbon is fixed by annual terrestrial vegetation (Myneni, 1997;Myneni *et al.*, ;Verstraeten *et al.*, 2006).

The changing of radiation as part of the input parameters is mainly coupled to clouds and other Atmospheric effects (see (Iqbal, 1983a). Although there is enough radiation during total cloud cover to enable Photosynthesis, but diffuse Radiation hasn't the same power density then direct irradiation (Chmielewski *et al.*, 2005), but ~75% (Schönwiese, 1997). Loveland et al (1991) described that the temporal vegetation analyses can be used to characterize major vegetation types at continental level. Potter et al (1998), DeFries and Townshend (1994) reported the dependences between the higher amplitude in NDVI temporal profiles in high latitudes forests and woodlands whereas tropical evergreen forests inhabits the highest total greenness (see Figure 25)

Vegetation Type	*Matthews Class*	*Ruimy et al.*	*CASA*	Miami NPP / GCM APAR
Equatorial, tropical moist forests	1,2,3	0.310	0.340	0.409
Tropical, subtropical dry forests	5,6,7,9,12,13, 15,17,19	0.185	0.290	0.547
Mediterranean evergreen forests				
Temperate, deciduous forests	4,11,16	0.505	0.305	0.450
Temperate, subpolar, coniferous forests	8,14,18,20,21	0.785	0.272	0.428
Temperate grasslands	26,27,28,29	0.630	0.277	0.497
Deserts	30	0.630	0.160	0.763
Tundra, bog	22	0.630	0.263	0.590
Cultivation	32	1.035		

Figure 25 Light Use Efficiencies for several models in [g C MJ^-1](Source: Seaquist, 2003)

The Light use efficiency approach (comp. (Adams *et al.*, 2004;Hilker *et al.*, 2008;Seaquist *et al.*, 2003) is only mentioned in this thesis, since the availability of light is not a deficit factor.

It assumed that the vegetation will be transformed to the most appropriate type for the environment. They are limited through the necessary to extrapolate in order to calculated the vegetation response to an environment that does not currently exist (Adams et al., 2004).

The change of soil characteristics due climate and Vegetation influences might by magnificent, but a climate-based model has no access to factors like nutrient inputs or loss of organic matter from management practices (Field et al., 1995)

In summary the assessing temporal variability in primary production is important for quantifying energetic constraints on organisms, population dynamics, and community structure (Knapp & Smith, 2001) and the understanding of the inter- and intra-annual variability of ecosystems (von Wehrden & Wesche, 2007). Together with (Potter & Brooks, 1998) they suggest that the NPP should combine with Rainfall data.

4 Data collection

4.1 Meteorological Data

Impetus operates a Meteorological network within the Drâa Catchment Area (see Figure 27). The location of the automatic registration Stations is chosen with respect to WMO guidelines (comp WMO. 1996: Guide to Meteorological Instruments and Methods of Observation (6th edition) and the multidisciplinary approach IMPETUS (Schulz, 2006). The installed Stations are automatic recording Systems of Campbell Scientific Ltd. (England). All Stations inside the Catchment share the same Equipment, with little variation. The core of every station is the Data Logger CR10X. Together with the Storage Module (SM4M), a 12 V -7Ah Battery it is stored in a weather proof Box in 1-1.5m height. Together with an external Solar Panel and a Multiplexer (AM416) it's mounted on a Tripod (Figure 26). All Meteorological Instruments are mounted outside the Logger Box and wired by protective electric cable made of copper. For a detailed listing of all used of all Sensors and a detailed description see Schulz (2006).

Figure 26 Automated Climate station ARG with of wind, temperature and radiation sensors.

The installation of the stations was done between 2000 and 2002. Besides some minor data loss it is assumed that all stations remain operational until 2014.

The raw data is stored in an ASCII, row based format. Every row contains the identification, date and time of each measurement, and the corresponding means and sums of the sensor outputs as well as internal calculation results. The post readout procedure includes a translation into computer readable, consistent data which is stored in an column format similar to Excel. The plausibility check includes a comparison of the maxima and minima. The daily averages and –sums are calculated without plausible and missing data. Extreme values are calculated retrospectively from 15 min Intervals. Precipitations during periods under 0°C are calculated by a different method. The pure Water column is comprised by the subtraction of the grand total measured rainfall from the snow equivalent. If snowfall is registered by both the snow height and rainfall sensor, the higher numerical values are taken. Delayed Snow meld is taken into account in a plausible fashion under inclusion of the air temperature and moisture, as well as the global radiation budget. It is classed either as pre or post shifted snow height.

Together with meteorological and hydrological data from our Moroccan partners (Service Eau, ABH etc.) it was possible to aggregate the available data pool with longer time series (for details comp. (Schulz, 2006)).

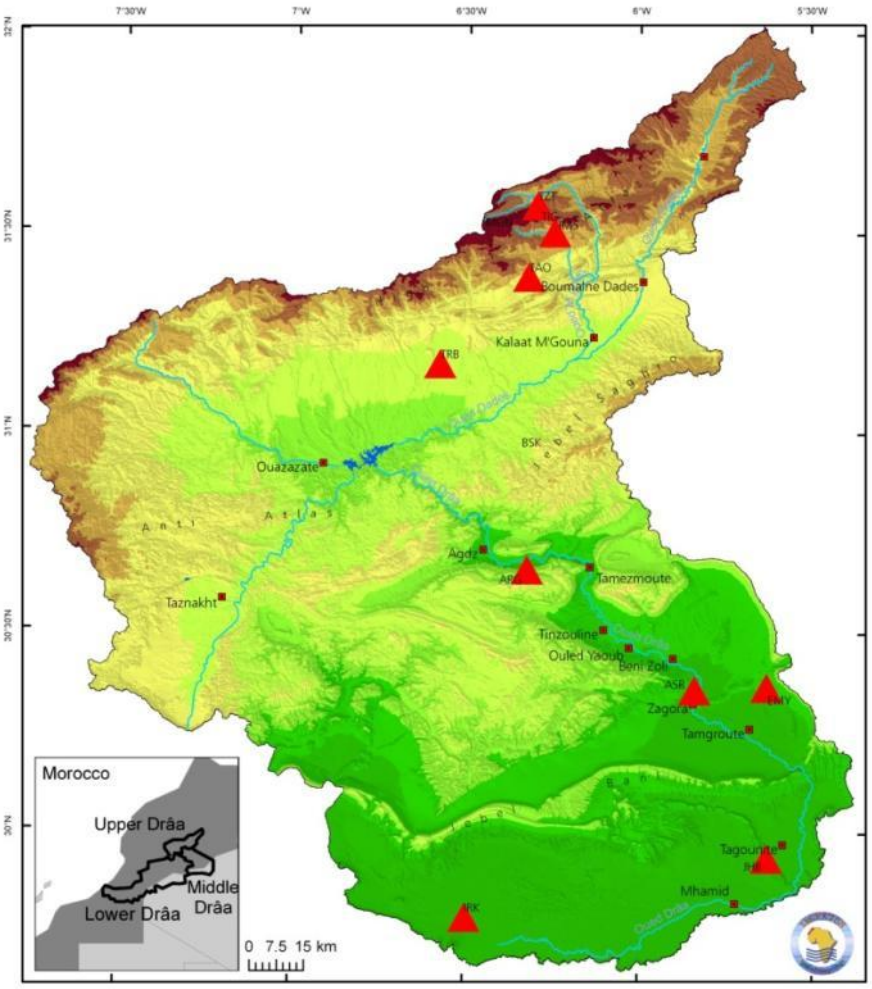

Figure 27 Climate station distribution (red triangles) inside the investigation area.

The final Data pool consists of:

- Date [dd.mm.yyyy]
- Precipitation [mm]
- Net Radiation [W/m²]
- Ground reflected shortwave radiation (outgoing shortwave) [W/m²]
- Air Temperature (1 and 2 m) [°C]
- Relative Humidity [%]
- Dew point [°C]
- Solar irradiation (incoming shortwave) [W/m²]
- Wind speed [m/s²]
- Water Vapour [mm]
- Wind direction [°]

The final Data pool is stored as tab stopped ASCII File and will be in the following format:

|Date|day|time|p|net|refl|at_1|at_2|rh_1|rh_2|dp|rad|wv_1

Where:

- Date Date [dd.mm.yyyy]
- Day Julian Day of the year
- Time Time indicator (i.e. 24 for daily)
- p Precipitation
- net Net Radiation
- ref Ground reflected shortwave radiation
- at Air Temperature
- rh Relative Humidity
- dp Dew point
- rad Solar Irradiation
- wv Water Vapour

The ASCII Format allow manipulation and updating the data file with any current text editor or spreadsheet program.

4.2 Field Measurement

4.2.1 Ground Truth Points

The intention of measuring vegetation inside the Investigation area is to acquire reliable data on the vegetation cover, its state and changes in its development as well as land cover changes. Besides long term exclosure, two approaches can be used to get information on Vegetation activity (see Figure 28):

- an investigation area - width ground truth monitoring network
- cage experimentation

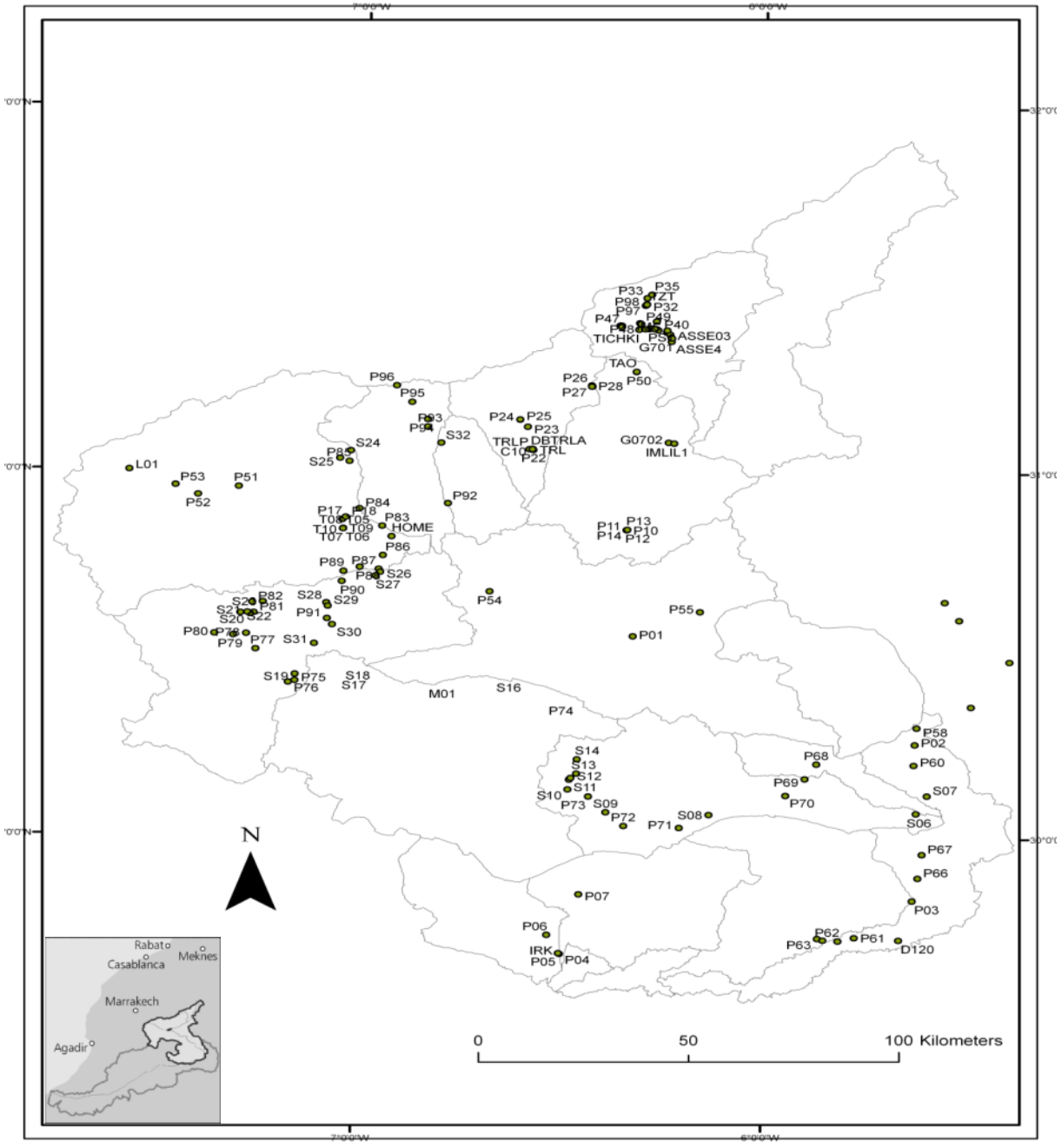

Figure 28 Schematic overview of observed GCP's points and their distribution (black dots) inside the investigation area.

The general concept of acquisition of quantitative vegetation parameters includes the measurement of the vegetation cover-density; bio volume and general conditions on 92 randomly distributed spots inside the catchment (see Figure 28). The randomizations are done on two ways:

1) The point must be reachable by car and foot in an appropriate amount of time and

2) The point must be representative for the area it lies in and be able to contain 3 or more Pixels with a size of 250*250m.

Choosing the measerument points is done by expert knowledge and estimation. No GIS System is fundamentally unable (or at least almost so) to decide how representative and reachable a point is, so no automatic distribution system was selected. This limits the ability to choose reference points, but is a fair trade off between objectivity and praxis . The selected points where treated as recommended by the research group for site field mapping (Workgroup Location Cartography (Arbeitskreis Standortkartierung in der Arbeitsgemeinschaft Forsteinrichtung., 1980). I choose a 3 by 3 m sampling design with 92 sampling points. This represents the local conditions best. This method is called Quantitative Vegetation Monitoring. It includes:

- Dominance Monitoring
- Soil texture
- Altitude/Position/Inclination etc.
- Photo Documentation

All points were monitored through field research during the spring and fall of 2007 and 2008. The results were used inside the model to estimate vegetation cover and biomass (see Chapter 5.11).

4.2.2 Long Term Exclosure

Having commenced operation with the start of IMPETUS in 2000 (eg M. Finckh) the long term exclosure (together with a km² extension) follows a north to south profile, including an Aridity and Altitude gradient, a transect of 10 Test sites with a fence line contrast observing small scale vegetation patterns on permanent plots of 1 sq km. Those plots are divided into 400 sub parcels to assess spatiotemporal vegetation patterns in order to estimate their respective carrying capacity and resilience. Parameters recorded on the plots further comprise of species composition and density as well as functional traits (Finckh & Oldeland, 2005b). These sites are monitored by Biota Morocco (http://www.biota-africa.org/).

4.2.3 Cage Experiment

Cage experimentation was undertaken in order to get more information on vegetation growth (ANPP) and standing biomass (Biomass) in the research area. This exclosure experiment was designed as 4 x 4 full factorial sample experiment. The four Test sites TRL, TAO, IMS and TZT were chosen as altitude and nomad gradients. Every experimental test site included 10 sites under grazing pressure (GXX Suffix) and 10 cages with grazing protection (CXX suffix).

Cage Experiment (overview)

- 4 Testsites with
    - 10 Cage Sites
    - 10 Grazed Sites
- Random distributed
- Outer perimeter is 40mx40m

Figure 29 gives an overview over one Cage experiment and the random distribution for the TRL- test site.

Figure 29 Sample Cage Experiment points distribution of measurement distribution (green dots) with indicator for TRL Testsite (40m x 40 m testsite)

Figure 30 Example of a typical Test Cage

Table 3 Cage Experiment Length for the used stations

TRB	02.09.2007 until 04.04.2008
TAO	22.09.2007 until 26.04.2008
AMS	13.09.2007 until 08.10.2008
TZT	17.09.2007 until 09.10.2008

This cage experiment was set up as a short time exclosure with the aim of quantifying vegetation growth during a one year period (see Table 3). During the field experiment valuable Data on the ANPP and standing biomass were gathered. For more information on said experimental results (except for some results of Chapter 5.11) and other information see (Baumann, 2009).

4.3 MODIS satellite data

4.3.1 Sensor MODIS

MODIS stands for Moderate-resolution Imaging Spectroradiometer and is a scientific sensor onboard the Terra (EOS AM). and Aqua Satellite Platform (EOS PM). It is has been launched in 1999 and is being operated since that time by the NASA Goddard Space Centre (http://modis-land.gsfc.nasa.gov/). All Data can be downloaded through this website, which also offers possibilities for an automatic download. A short technical introduction of the MODIS sensor and its characteristics is given in Table 4.

Table 4 Specifications of the MODIS sensor (Source: NASA-Homepage)

Orbit:	705 km, 10:30 a.m. descending node (Terra) or 1:30 p.m. ascending node (Aqua), sun-synchronous, near-polar, circular
Scan Rate:	20.3 rpm, cross track
Swath Dimensions:	2330 km (cross track) by 10 km (along track at nadir)
Telescope:	17.78 cm diam. off-axis, afocal (collimated), with intermediate field stop

Size:	1.0 x 1.6 x 1.0 m
Weight:	228.7 kg
Power:	162.5 W (single orbit average)
Data Rate:	10.6 Mbps (peak daytime); 6.1 Mbps (orbital average)
Quantization:	12 bits
Spatial Resolution:	250 m (bands 1-2)
	500 m (bands 3-7)
	1000 m (bands 8-36)
Design Life:	6 years[7]

The MODIS Terra sensors cover the area of the Drâa Catchment at ~10:30 UTC. MODIS Terra has been operational since early summer 2000. Version 5 of the data processing (used here) includes all available data right up to the end of the vegetation period of 2006 (which was August 31, see chapter 6.3.2) for building up MD. The years 2007 and 2008 serve for validation purposes.

4.3.2 Data format and handling

There are different methods to store data and describe geographical locations. MODIS Data is stored in a digital data format called Hierarchical Data Format, commonly abbreviated to HDF (versions HDF4 and HDF5 are used for this work). HDF and its versions are a library and multi-object file format for the transfer of graphical and numerical data between computers (HDF Group). HDF was created by the National Centre for Supercomputing Applications in the 1980s and is now bundled in the HDF group. The HDF Data Format is organized into groups and datasets. A group consists of zero or more HDF5 objects. The object itself is made up by the data array with a separate Header.

Following data types are supported by HDF:

- Integer data types: 8-bit, 16-bit, 32-bit, and 64-bit integers in both small and big-endian format
- Floating-point numbers: IEEE 32-bit and 64-bit floating-point numbers in both small and big-endian format
- References
- Strings

Besides the data format it is important to know that MODIS products are delivered in a Sinusoidal projection grid based format (see Figure 31).

[7] The designed lifetime is extended to 2012 due to the execellent performance with nearly no breakdowns since launch. (NASA 2009)

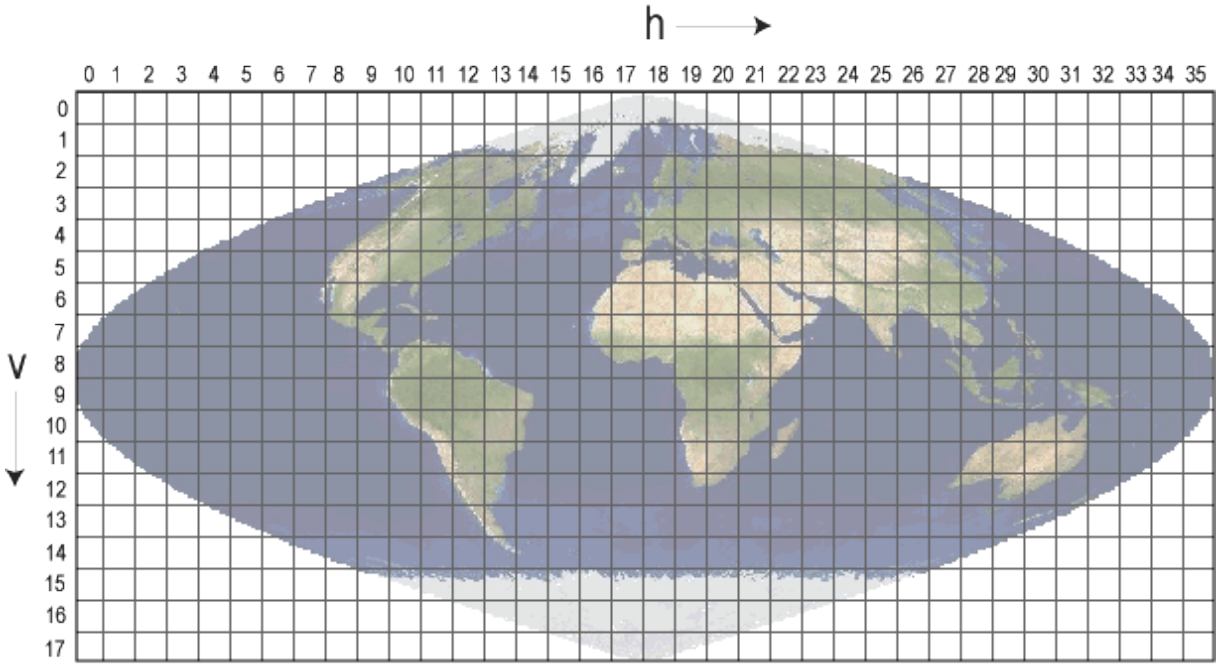

Figure 31 Sinusoidal Projection for MODIS Products (Source: NASA)

During this process a simple ftp script is used to download the data (just search for h17 v 5 and 6 on the NASA FTP Server). For data processing the following steps are carried out successively: layer stacking, mosaicing, and finally reprojecting the data into the Lambert conformal conical projection (which preserves angles,for details see USGS)). Run time quality assurance data, specific to the land cover parameter, is given separately as an 8-bit land cover assessment data field. This labels the confidence of each grid cell (Strahler *et al.*, 1999a). This group stores Quality Assurance (QA) metadata as long integer values. The QA are indicated and assessed through the generation process. The QA metadata include a document production for every pixel. For a first impression it is possible to look at the usefulness index, delivered by NASA for every pixel. This is calculated by scores which are computed to weights, determinating the usefulness (for details see MODIS User Handbook).

Table 5 Usefulness Index (MODIS User Handbook p.17 fig 6)

Parameter Name	Condition	Score
Aerosol Quantity	If aerosol climatology was used for atmospheric correction (00)	2
	If aerosol quantity was high (11)	3
Atmosphere Adjacency Correction	If no adjacency correction was performed (0)	1
Atmosphere BRDF Correction	If no atmosphere-surface BRDF coupled correction was performed (0)	2
Mixed Clouds	If there possibly existed mixed clouds (1)	3
Shadow	If there possibly existed shadow (1)	2
View zenith angle (q_V)	If $q_V > 40^o$	1
Sun zenith angle (q_S)	If $q_S > 60^o$	1

The metadata behind the usefulness index are encrypted in an integer data format which can be retrieved via a reverse binary transformation. The QA are stored in a 16 Bit (2Byte) long order. The QA Flag content is slightly alternated in V5 (see Figure 33 and Figure 32).

Bit No.	Parameter Name	Bit Comb.	Description
0-1	VI Quality (MODLAND Mandatory QA Bits)	00	VI produced with good quality
		01	VI produced but with unreliable quality and thus examination of other QA bits recommended
		10	VI produced but contaminated with clouds
		11	VI not produced due to bad quality
2-5	VI Usefulness Index	0000	Perfect quality (equal to VI quality = 00: VI produced with good quality)
		0001	High quality
		0010	Good quality
		0011	Acceptable quality
		0100	Fair quality
		0101	Intermediate quality
		0110	Below intermediate quality
		0111	Average quality
		1000	Below average quality
		1001	Questionable quality
		1010	Above marginal quality
		1011	Marginal quality
		1100	Low quality
		1101	No atmospheric correction performed
		1110	Quality too low to be useful
		1111	Not useful for other reasons (equal to VI quality = 11: VI not produced due to bad quality)
6-7	Aerosol Quantity	00	Climatology used for atmospheric correction
		01	Low
		10	Intermediate
		11	High
8	Atmosphere Adjacency Correction	0	(No) No adjacency correction performed
		1	(Yes) Adjacency correction performed
9	Atmosphere BRDF Correction	0	(No) No atmosphere-surface BRDF coupled correction performed
		1	(Yes) Atmosphere-surface BRDF coupled correction performed
10	Mixed Clouds	0	(No) No mixed clouds
		1	(Yes) Possible existence of mixed clouds
11-12	Land/Water Mask	00	Ocean/inland water ? Shallow ocean ? Moderate and continental ocean ? Deep ocean ? Deep inland water
		01	Coastal region ? Ocean coastlines and lake shorelines ? Shallow inland water
		10	Wetland ? Ephemeral water
		11	Land
13	Snow/Ice	0	(No) No snow/ice
		1	(Yes) Possible existence of snow/ice
14	Shadow	0	(No) No shadow
		1	(Yes) Possible existence of shadow
15	Compositing Method	0	BRDF composite method used for compositing

Figure 32 QA Flag MODIS for Version 4 of the MODIS Algorithmen (Source: NASA Handbook)

Bit	New QA map (C5 and later)
0	MODLAND QA
1	
2	VI usefulness
3	
4	
5	
6	Aerosol
7	
8	Adjacent cloud
9	Atm. BRDF correction
10	Mixed cloud
11	Land/water flag
12	000: Shallow ocean 001: Land (Nothing else but land) 010: Ocean coastlines and lake shorelines 011: Shallow inland water 100: Ephemeral water 101: Deep inland water 110: Moderate or continental ocean
13	111: Deep ocean
14	Snow/Ice
15	Shadow

Figure 33 QA Flags for Version 5 of the MODIS Algorithm (Source: NASA Handbook)

During the programming of MOVEG a routine was implemented and programmed to transform the integer values into binary values (for details see chapter 5.2). Bits 0-1 and 2-5 give a first glance about the quality of a pixel. Ever since Version 5 of the QA channel bits 14 and 15 have been exclusion parameters and bits 0 to 10 warning and exclusion parameters. In practice this means the excluding of all snow and ice, as well as shadowed, aerosol and too cloudy pixels. This can be seen as a first step towards data correction, ensuring data quality and integrity.

All data was preliminarily processed during the NASA pre-processing phase (see Figure 34).

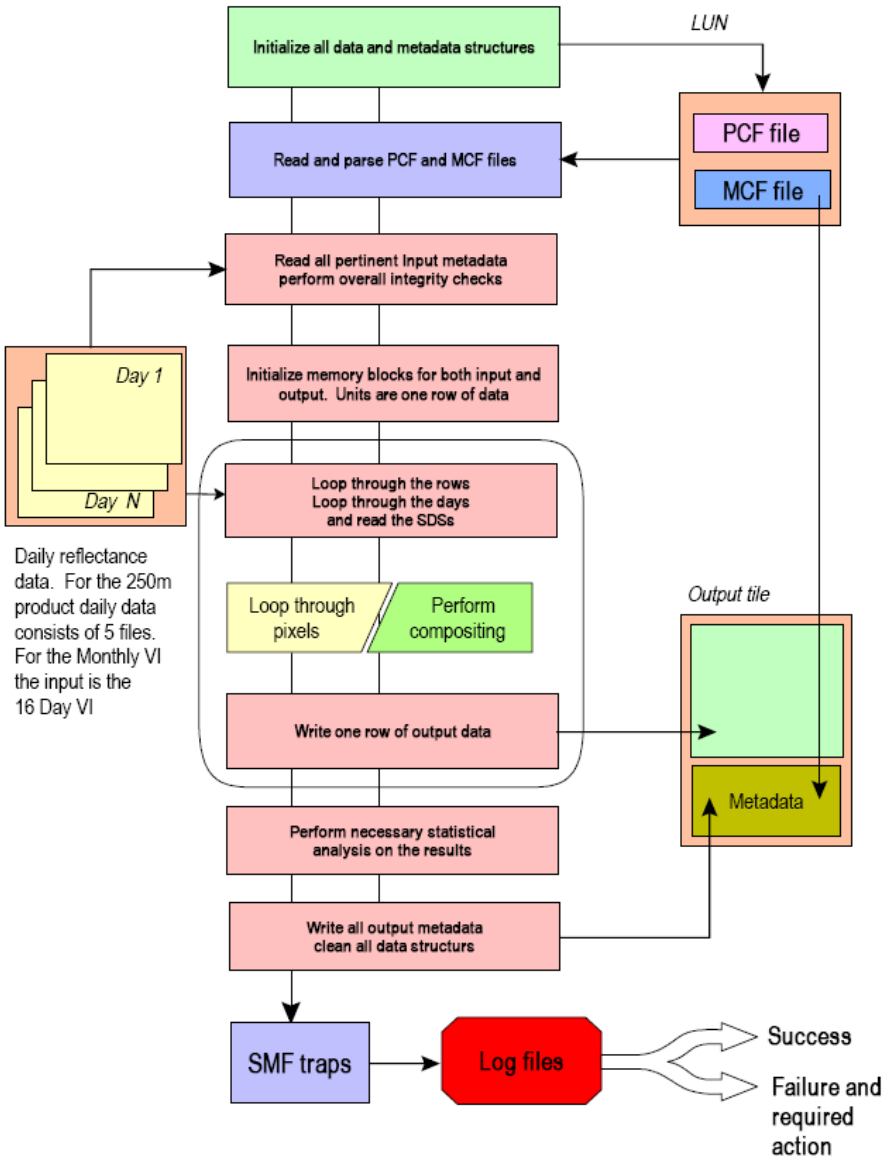

Figure 34 NASA Vegetation index algorithm major components flow chart. The chart details the different phases of the algorithmen. Process Controll File (PCF) and Status Message Files (SMF) ensure that all quality information, calculated during the process, are stored into data output metafile. (Source: Modis Handbook)

Data inspection and correction after downloading have been conducted in two ways. Primary checked whether the Data has a correct geo-location and secondly inherits inconsistencies (see: Chapter **5.10.1**).

4.3.3 MODIS NDVI

MODIS NDVI is a calculated index of the MODIS Radiometer AVHRR. The algorithm provide consistent, spatial and temporal comparisons of global vegetation conditions (2006;2007;2008). It is the virtual extended of the 20 –year NDVI global data set (1981-2000) from the NOAA-AVHRR series to provide a long term data record. MODIS Data are delivered in HDF Format and the 250m Resolution is labelled as Vegetation Indices 16-Day L3 Global 250m (short: MOD13Q1). “Version-5 MODIS/Terra Vegetation Indices products are Validated

Stage 2, meaning that accuracy has been assessed over a widely distributed set of locations and time periods via several ground-truth and validation efforts."MODIS –Handbook (2007).

As Level 3 Product it is a derivate of the Level 2 daily surface products. For Details see MODIS Land Website (2009) and MODIS VI Product (Algorithm) Description(2007). All Initial Data are screened with the above described Data quality Layers and combined to the 16 – days product depending on how many good pixels (n) available (see Figure 35).

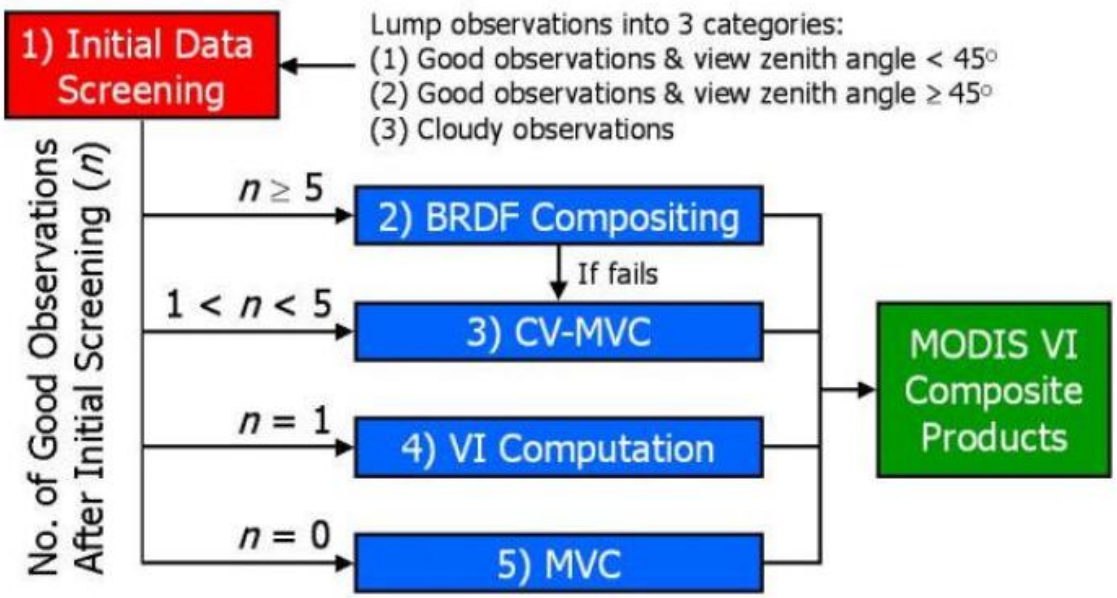

Figure 35 MODIS Composit approach flowchart design for deciding which method for Compositing is taken by number (n) of lump observations. (Source: MODIS Product algorithm base)

The product is available through MODIS Land Website and can be graphical viewed on the page as Figure 36 shown.

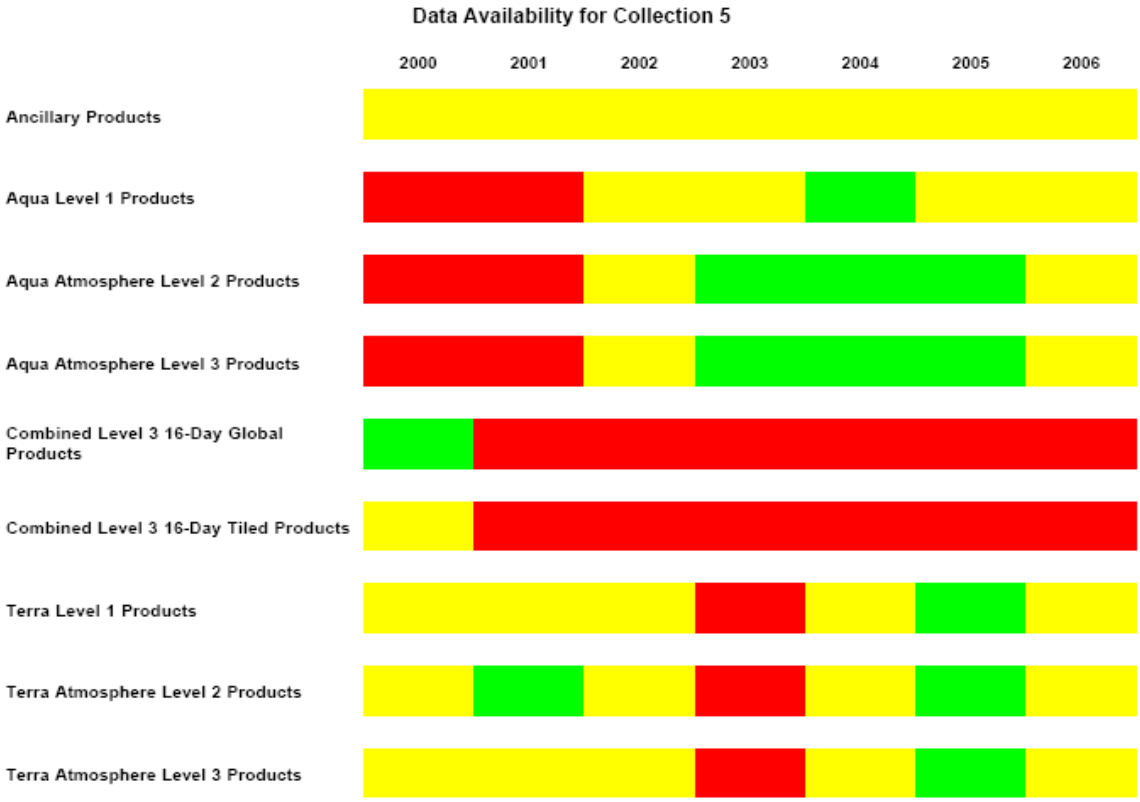

Figure 36 Data availability MODIS (Source: MODIS Land Homepage)

The data availability indicates for red missing data, yellow indicates that some data available and green all data available.

5 Development of the dynamic regional Model MOVEG Drâa

The model MOVEG Drâa („Modèle pour l´acquisition de la dynamique de la végétation dans la vallée du Drâa“) is a modular conceptual and statistical model that is extrapolating the condition inside the Catchment until 2050. As mentioned in Chapter 3 MD consists of different modules, which represent different calculation steps during compution of the model.

This chapter introduces the programming approach, the modules and routines used in MD. It gives a detailed view on every application inside MD and its boundary structure and functions. Every module introduces its core function and interfaces, as well as the combination of every module with other modules and their internal interaction.

5.1 General structure of MOVEG Drâa

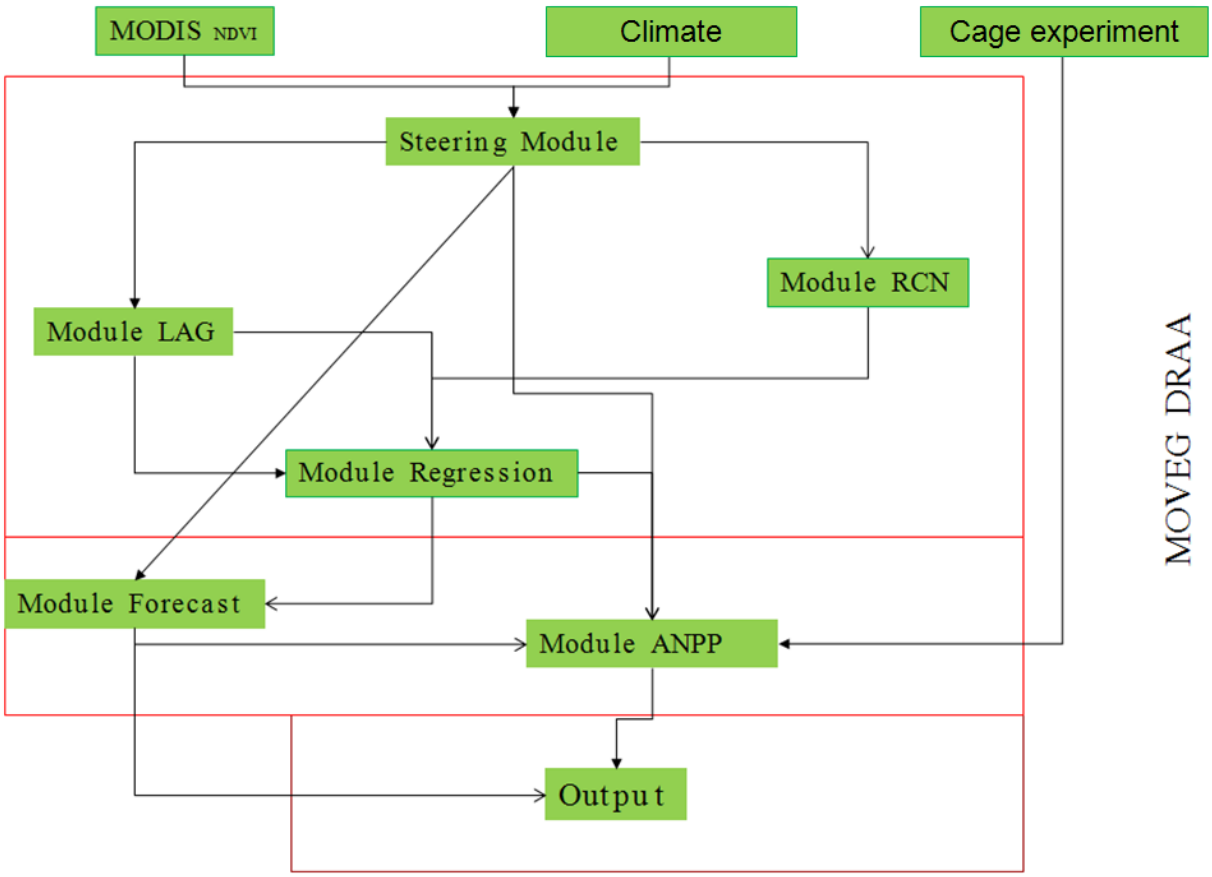

Figure 37 General flow chart for the moel MOVEG Drâa

MOVEG Drâa (MD) (Figure 37) uses and combines different scientific approaches. It is designed based on the Booch Method (Booch *et al.*, 2007) as an object-oriented analysis (Figure 38).

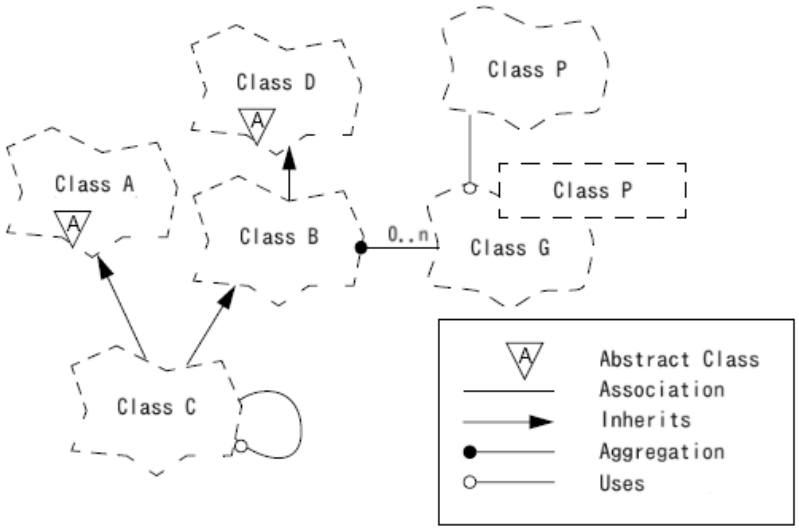

Figure 38 Booch-Methode chart (Source: Booch et al., 2007)

The intention behind a modular structure is to simulate/emulate the complex system of plant relevant processes in a structure of clusters that are able to communicate with each other. The main goal of MD is the automatic adaption and preparation of input parameters. This is done by a self adjusting semi- automatic read in mechanism of pre – formatted input data. The steering module (see Chapter 5.5) is therefore not only the core module but also provides interaction with all other modules.

- Data maintenance
- I/O routines
- Model flow control
- Output control

A restriction arises from technical issues, such as read in filters and calculation routine restrictions, and conception restrictions and limits. This is specific by every class or object and is described in the modules description or solved via a sub routine.

5.2 Enumeration of Input Parameters and Sampling Strategy

The field work (chapter 4) provided measured input data necessary for MD. As a first step MD was developed for nine climate stations (see Figure 39), along an N-S profile with every station focussing on a ~20-50 by ~20-50 pixel test area. Every test area represent the natural vegetation very near of the station, excluding the long term enclosures and agriculture areas. In a later step (see Chapter 7) the possibilities of extrapolation are discuassed.

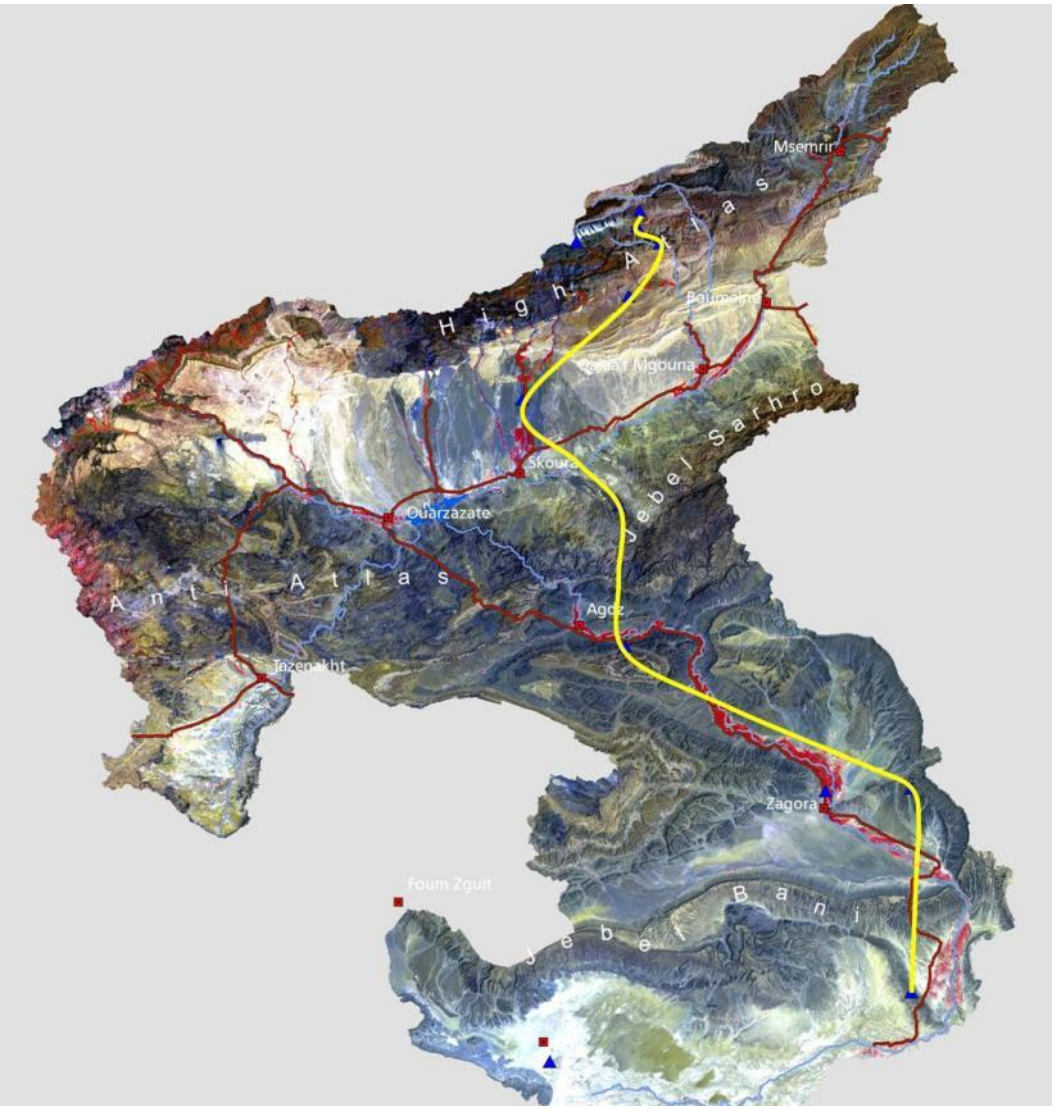

Figure 39 Transect used for development of MD

In summary the Core Input parameters are:

- Satellite Image: ENVI-Format (best: BIP Format)
- Meteorological Data (ASCII Format, tab –stop separated)
- Investigation areas (ESRI Shape file format [*.shp])
- Steering files (ASCII)
- Soil information (ENVI Format)
- Forecast Data (ASCII Format)

The output is provided in ASCII tab – stopped Format.

5.3 Conversion MOVEG Drâa to IDL

The technical requirements are an IDL and ENVI Licence with IDL Analyst running. A dual core or quad core computer (or better) with at least 1.6 GHz core frequency is recommended in order to be able to calculate the data in appropriate time. 500 MB of RAM is the minimum

required specification. The recommended specification is 2 GB of memory. ENVI IDL 4.2 is restricted to ~1.3 GB RAM.

The intention behind the modular structure is to simulate/emulate the complex System of plant relevant processes in a structure of clusters that are able to communicate with each other. MD uses the Advantages of object oriented programming and the advantages of a linear computing. Every Module is in an addressable form and adds to the integrity of the Data and the general survey of the Data processing by Flow check.

IDL inherits the advantages of being able to handle object and flow based programming. Furthermore it can handle large images and provides a large output variety. ENVI is able to handle images and data as vectors. This is a great advantage when using time series,

5.3.1 Programming with IDL

Programming in IDL can be done object oriented like C# or Java. ENVI IDL itself is a linear script language, but provides support of object oriented programming. This is possible through the utilization of functions and internal and external programs. Every module is in an addressable form and adds to the integrity of the data and the general survey of the data processing by flow check. Furthermore it can handle large images and provides a large output variety. ENVI is able to handle images and data as vectors. This is advantageous when using time series.

Memory shortage turned out to be the most complex problem in the programming process. The satellite images used, consist of roughly 1100x900 pixels with 154 channels (one for every 16 days) with a bit depth of 16bit per pixel (such images can take up as much as 1.6 GByte system memory which exceeds the maximum amount of memory used by ENVI). ENVI therefore inherits a function called “Tile”. This function tiles the image into a slice which can then be read into the main memory and to which any calculations can be subsequently applied. After that the result is stored. After the slice is deleted from memory the function continues with the next slice.

Another important factor is the right location on Earth’s surface. Therefore a sub-routine was written to use Shape files inside the model. The location information inside the shapes is read out, transformed into the projection of the image to create a ROI (region of interest). The specific image information can now be read out.

5.3.2 Parameterisation and Automation

Parameterisation is the process of defining or deciding the parameters - usually of some model - that are crucial to the question being asked of that model. MD is designed to inherit a level of automation. This process can be described by the following structure:

- Reading in data
- Checking for failures & unreliable data (is repeated on several steps)
- Handover and calculation by the MD Modules.

A key factor for consistent data is the definition of a “Backbone” or time-stamp that ensures that all data is rightfully dedicated, especially if the data is transformed during measurement and scale. The backbone of this model is called date stamp. During scaling, cutting out and transformation every data point is bidirectively dedicated.

The automation is handled by fall-back mechanisms which mostly check for a valid data range. Additionally statistical pre-tests are implemented to ensure data quality. Those tests are included and described in chapter 5.10.

5.4 Digital Elevation Model

Digital Elevation Models (DEM) are spatial representations of elevations (highest point below a nominal observer, including buildings, trees and any other objects that protrude from the earth's surface and are resolvable by the observer) in regular spaced intervals. Devoid of landscape features they are so called Digital Terrain Model (DTM), required for flood and drainage modelling. The DEM used here was set up during the Space Shuttle Mission Shuttle Radar Topography Mission (SRTM), a joint endeavour project of NASA, the German and Italian Space Agencies in February 2000. It used dual radar antennas to acquire interferometric radar data, processed to digital topographic data at one arc-sec resolution. The height of any point ht is therefore given by:

$$h_t = h_p - \rho \cos\left[\sin^{-1}\left(\frac{\lambda\phi}{2\pi B}\right) + \alpha\right]$$

where hp is the platform height (antenna altitude with respect to the WGS84 reference ellipsoid), p is the range, Φ is the measured interferometric phase, α is the baseline roll angle, λ is the observing wavelength, and B is the baseline length (Farr *et al.*,). This measurement includes all potrude on the surface.

The selected orbit of the Endevour shuttle was circular, 57° inclined, with a mean altitude of 233.1 km. This orbit repeated the same ground track in 9.8 days, after 159 revolutions. It produced ground tracks measured orthogonal to the direction of travel spaced from 218 km at 60°N and S to 252 km at the equator. Since C-RADAR had a mean swath width of 225 km, the nominal overlap was only 7 km (Farr, 2007).

There are four main error sources during the process of creating a DEM from radar:

- Geometry
- Electrical
- Interferometric
- Geolocation

Generally all sources of errors are derived within the error model for the SRTM measurements in terms of the quantities measured.

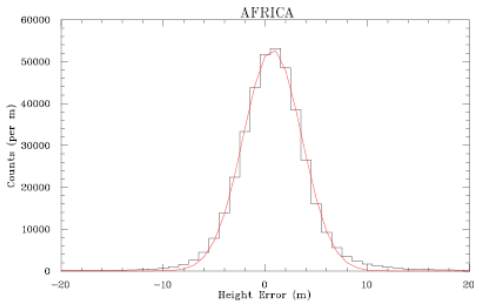

Figure 40 Histogram of the SRTM height error measured over the continent of Africa (black), with a Gaussian fit (red) (Rodriguez, 2006, p.22.).

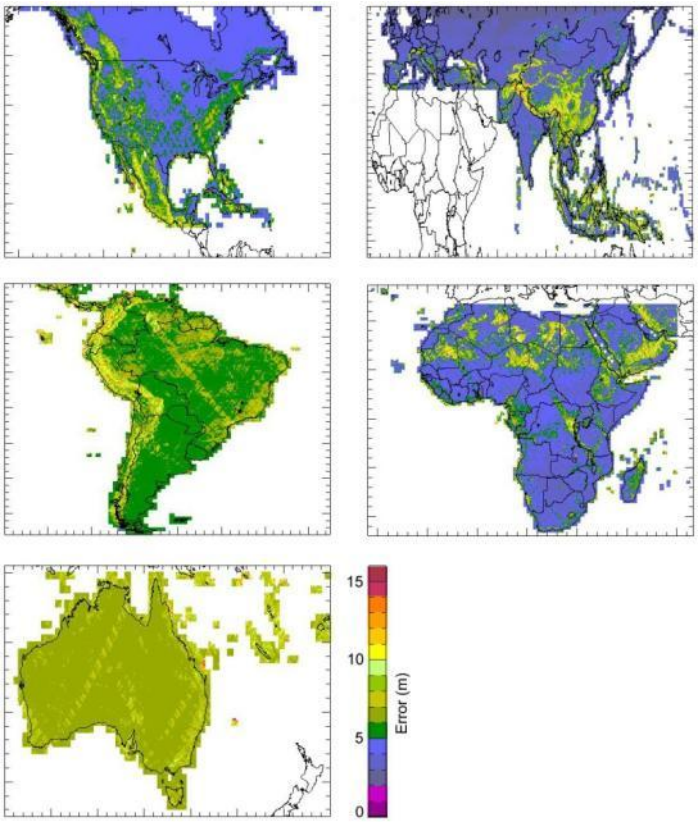

Figure 41 Histogram of the SRTM height for different continents (Rodriguez, 2006, p.22.).

The quantified by mean error is given by 1.3m on a 3.8m standard deviation and a 6m 90% absolute error (Rodriguez, 2006)(see Figure 41). For the IMPETUS project area the given root mean square error (rmse) is 18.55m (r =0.99) with a maximal variability of 97.14m, based on the measure on 194 points with a Differential GPS (Klose, 2009). The DEM, used here, has an original ground resolution of 90m which was converted to 30m.

In a first step the raw SRTM data was transformed in projected Lambert Conformal Conical. After the resampling the map was built up by rasterising and classification (see Figure 3).

5.5 Steering Module

The steering Module is the core of MD. It is the connection between the different branches of sensory input and controls how the modules work. The steering module opens and handles the steering files. A system of file based steering system allows us to define different scenarios and also the combination of test sites to be calculated without changing the model itself. Therefore there is a main script file which inherits the script file (multiple scripts files possible) and IDL specific format (*.sav) and template files

A Steering File including:

- Name of Script file to execute
- Framebox of *.sav file of Script file
- templates of Script file

The mentioned script file includes the following parameters, with X standing for:

0=RCN_file
1=NDVI_file,
2=shape file for corresponding NDVI File,
3=Key file for Date assignment
4=Climate Date
5=shape for RCN
6=Flags

The flag file inherits the ability to steer the execution of modules and is classified by the position of the flag (a,b,c……z) and their inherited command code (0,1,2,3...99). The command code is classified as 0=don't execute, 1=execute in standard 3-99=special command (for documentation: see modules specification). The position (a...z) of the flag classifies the module. The module codes are:

This design has the advantage that every user can combine the favoured settings and run the model with the desired results.

a= RCN
b= Biomass
c=lag
d=Regressions
e=LAI
f=Forecast

This design has the advantage that every user can combine the favoured settings and run the model with the desired results.

An example:

Steering File:

Path_to_file\Framebox Path_to_file \Templates Ablauf_skript

Scriptfile:

Path_to_file\SoilGroup_for_Curve_Numbers.hdf
Path_to_file\Gesamtstack_BIP_catchdraa_MODIS2000-2006_Subset_ImpetusProj_korrigiert.hdf
Path_to_file\TRL.roi
Path_to_file \Sat_Date_Key.txt
Path_to_file \METEO_TRL_tab_daily.txt
Path_to_file\TRL-Investigation_Area_RCN.roi
Path_to_file \Flag_File.txt

Beside the execution of the steering files, the steering modules also function as a parent process for all called modules. It is more or less the kernel and its process identifier (PID. That means that it also functions as a fallback routine on child process errors or exit status. This can be handled via the return command. It is furthermore important that every child process has its own variables and can't access variables of other processes or of the kernel, unless it is hand over or a global variable. This seems to be a major security feature of IDL to protect variables and demand a clear handover of variables.

5.6 Module Climate

The Module Climate calculates Potential Evapotranspiration (PET), Evapotranspiration (ET) and other meteorological data. The module calculates cumulate values (i.e. PET) or median values (temperature) for the 16 day period of each satellite image time step. A preliminary for calculating is a valid value of NDVI for each time step, otherwise no calculation is done.

Using the data of the meteorological stations enables us to calculate the estimation of the potential Evapotranspiration by using the Penman Monteith Approach ("Modified Penman-Monteith" Formula, FAO-56).

Equation 2 Penman-Monteith (FAO-56)

$$\lambda_v E = \frac{\overbrace{\Delta R_n + \rho_a c_p (\delta q) g_a}^{\text{Energy flux rate}}}{\Delta + \gamma (1 + g_a / g_s)} \iff ET_o = \frac{\overbrace{\Delta R_n + \rho_a c_p (\delta q) g_a}^{\text{Volume flux rate}}}{(\Delta + \gamma (1 + g_a / g_s)) \lambda_v} \quad (1)$$

λ_v = Latent heat of vaporization. Energy required per unit mass of water vaporized. (J/g)
L_v = Volumetric latent heat of vaporization. Energy required per water volume vaporized. (L_v = 2453 MJ m^{-3})
E = Mass water evapotranspiration rate (g s^{-1} m^{-2})
ET_o = Water volume evapotranspired (m^3 s^{-1} m^{-2})
Δ = Rate of change of saturation specific humidity with air temperature. (Pa K^{-1})
R_n = Net irradiance (W m^{-2}), the external source of energy flux
c_p = Specific heat capacity of air (J kg^{-1} K^{-1})
ρ_a = dry air density (kg m^{-3})
δe = vapor pressure deficit, or specific humidity (Pa)
g_a = Conductivity of air, atmospheric conductance (m s^{-1})
g_s = Conductivity of stoma, surface conductance (m s^{-1})
γ = Psychrometric constant ($\gamma \approx 66$ Pa K^{-1})

Using the measured Short wave radiation and calculating the long wave radiation by using a approach by (Jensen, 1990) described in (Neitsch *et al.*, 2005), pp. 35ff) it is possible to fill up gaps of net radiation measurement.

The Conductivity of stoma, surface conductance is calculated by

Equation 3 surface conductance

$$surface\ conductance\ = 1/(0.5 * 5 * LAI)$$

The aerodynamic resistance is fixed by 0.1 (Schulz, 2006). Other fixed factors are (incl. units):

- Latent heat vaporization 2.501-(2.361/1000)*temperature [MJ kg^-1]
- latent heat 2200 [kj*kg]
- specific heat= 1.0035/1000 [(MJ*C)*kg^-1] (Neitsch *et al.*, 2002),p.53)
- Heat capacity air 1.012 [J*kg^-1*K^-1 ;1.0054/10^6]
- Air density 1.2041 [kg/m³].
- emax=5.49993E-06
- Thermal conductivity 0.0261 W/(m·K)

Transpiration rate is calculated by Equation 4 from the SWAT theory (Neitsch et al., 2005).

Equation 4 Transpiration Rate

$$Transpiration = \frac{pot_{Evapotranspiration} * LAI}{3}$$

The Leaf Area Index is defined by (Huete, 1988;Myneni *et al.*, 2006) with :

Equation 5 LAI

$$LAI = ((-1/0.996) * alog(1 - FAPAR)$$

By using IGBP classification for open shrub lands, open shrub lands, unvegetated and non-vegetated land a factor of 0.996 was used as extinction factor [taken from (Myneni, 1997) Table IV p 1391 for Medium and Dark Soil on Shrubs]. Medium and dark soils were chosen to represent the dark soils in the high mountain Atlas range as well as the desert varnish (Dorn & Oberlander, 1982) on rocks inside the area.

The necessary FAPAR is calculated by the Equation after (Seaquist et al., 2003):

Equation 6 Fapar

$$\mathrm{FAPAR} = a * (NDVI) - b$$

$$a = 1.67$$

$$b = 0.07;\ for\ west\ african\ Savanna$$

The evaporation is calculated by using the Equation 7:

Equation 7 Evaporation (Source: Penman)

$$E = \frac{\Delta(R_n - G) + \rho_L c_p C_{at} \delta e}{\lambda_w (\Delta + \gamma)}$$

E = Mass water evapotranspiration rate (g s^{-1} m^{-2})
Δ = Rate of change of saturation specific humidity with air temperature. (Pa K^{-1})
R_n = Net irradiance (W m^{-2}), the external source of energy flux
c_p = Specific heat capacity of air (J kg^{-1} K^{-1})
ρ_a = dry air density (kg m^{-3})
δe = vapor pressure deficit, or specific humidity (Pa)
g_a = Conductivity of air, atmospheric conductance (m s^{-1})
g_s = Conductivity of stoma, surface conductance (m s^{-1})
γ = Psychrometric constant ($\gamma \approx 66$ Pa K^{-1})

Since Evapotranspiration is the sum of transpiration and evaporation, the actual Evapotranspiration is given by:

Equation 8 Evapotranspiration

$$Evapotranspiration\ (ET) = Evaporation\ +\ Transpiration$$

The ET and PET are stored as 16 Day sum in the designed format and is available by other Modules.

All climatic calculation are equipped with limitation checks, which holds or warn the computation if an error occurs.

5.7 Module Runoff Curvenumber

Based on the climate data, the amount of Runoff Water is calculated under the local soil type, using the empirical model Runoff Curve Number (Rallison & Miller, 1981). Different studies have shown that the infiltration depends on slope position and topographic relief parameters (Poesen *et al.*, 2003;Pachepsky *et al.*, 2001;Berndtsson *et al.*, 1989;Miller, 2002). (Cerda, 1999) has shown that infiltration depends more on temporal terms then spatial circumstances. The Runoff Curve Number Model (Curve Number or CN) is based on a concept described in (Cronshey *et al.*, 1986) and is an empirical model for predicting runoff or infiltration from rainfall excess. It is developed by the United States Department of Agriculture to provide a consistent basis for estimating the amount of runoff under varying land use and soil types (Rallison & Miller, 1981).

The runoff is described by

$$Q = \frac{(P - I_a)^2}{P - I_a + S}$$

With Q as runoff, P as precipitation, S is the potential maximum soil moisture retention after runoff begins. S and I_a are the initial abstractions before water runoff [all in inches]. The retention parameter is defined as :

$$S = \frac{1000}{CN} - 10$$

CN stands for the curve number on the calculating day. The initial abstraction, I_a, is commonly abstracted as 0.2*S.

The Curve number is a function of soil properties. This includes permeability, land use and antecedent soil water conditions. Therefore the soil was classified in four soil hydrological groups, based on infiltration characteristics. This characteristic depends on the situation of the soil, hydraulic conductivity and the minimum rate of infiltration. Klose (2009) provides those maps for the whole catchment.

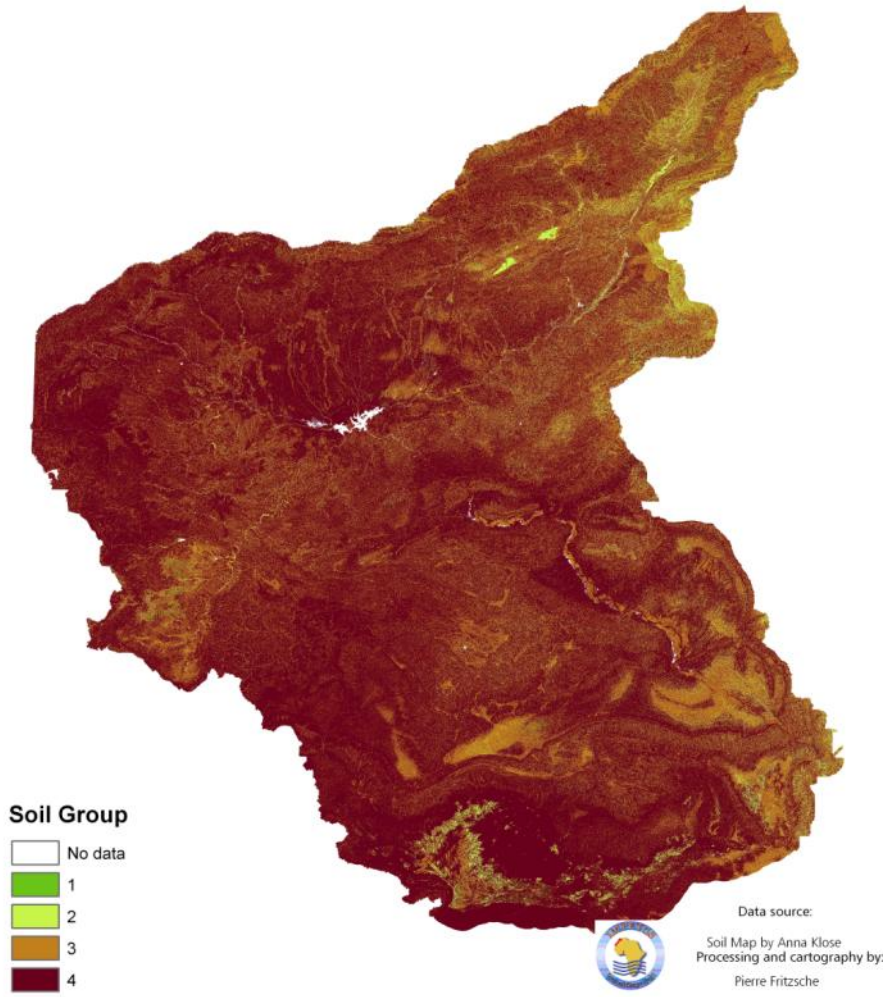

Figure 42 Soil Groups for RCN Model (Source: Anna Klose, 2009)

The four classes, shown in Figure 42, are:

1. high infiltration rate (Low Runoff potential)
2. moderate Infiltration when thoroughly wetted
3. slow infiltration rate
4. very slow infiltration (High runoff potential)

Using Retention parameters, described in (Rallison & Miller, 1981), the daily CN values where calculated as function of Rainfall. For the local parameterisation a slope adjustment from the DEM (Williams *et al.*, 1995) can be used, as well as a Soil moisture reduction after (Weber, 2004).

The previously soil moisture is calculated by:

$$CN_1 = CN_2 - \frac{20 \cdot (100 - CN_2)}{(100 - CN_2 + \exp[2.533 - 0.0636 \cdot (100 - CN_2)])}$$

$$CN_3 = CN_2 \cdot \exp[0.00673 \cdot (100 - CN_2)]$$

The slope adjustment is given by

$$CN_{2s} = \frac{(CN_3 - CN_2)}{3} \cdot [1 - 2 \cdot \exp(-13.86 \cdot slp)] + CN_2$$

The previously described formulas can be figuratively summarised as:

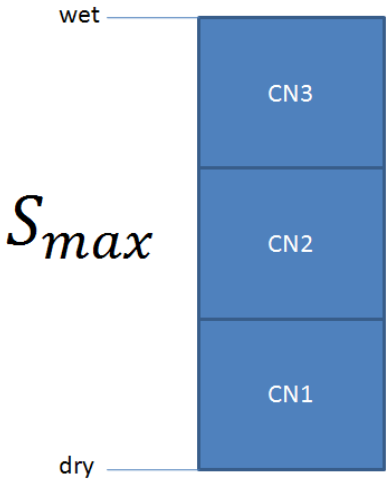

Figure 43 Graphical Illustration of CN's for different Soil conditions

The result is the infiltration runoff. Using the approach of (Richards & Wadleigh, 1952) for the available Water capacity (AWC)

$$AWC \equiv \theta fc - \theta pwp$$

With θ_{fc} as water content at field capacity and θ_{pwp} as permanent wilting point the saturation runoff can be calculated

Equation 9 Runoff calculation

$$Qsurf(i) = Precipitation(i) - AWC + Is(i-1)$$

After calculating all run off components it is possible to calculate the soil water content by

Equation 10 Soil Water content for non saturated situations

$$Soil\ moisture\ (i) = Soil\ moisture\ (i-1) + Precipitation - Qsurf\ (i)$$

Based on the investigation of (Weber, 2004) the soil moisture reduction is given by

Equation 11 Soil Water reduction

$$y_i = I_a * exp(x_s * Dry\_days)$$

Where y_i is the soil moisture on day i, I_a the antecedent soil moisture and x_s the specific component for every station. Dry days are the number of days without rainfall [8].

5.8 Development of Time Series using ENVI IDL

IDL stands for Interactive Data Language. IDL and ENVI are special developed for processing satellite and airborne images. The generation of time series is a pre-processing requirement and is a critical step of processing of remote sensing data. "*Studies on error analysis of observations in a time series are scarce"(Colditz, 2007)*. The generation of Time series, including a data analysis and the detection of noise and sources of errors. The level of accuracy is increased by using ancillary Data quality flags (see next chapter).

The temporal Information is extracted by going through every layer, extracting a pixel value (see Figure 44) for each layer. The result is a collum of numbers that can be describe like:

NDVI= [0.1, 0.13, 0.1, 0.2] ; marked with the Date vector
Date= [01.01.2001, 16.01.2001, 02.02.2001]

Those numbers can be described as Vectors, with date as unique marker. After that creation processes a first reliable check by scanning for negative NDVI or unreliable NDVI (i.e. values above 1 or belowe 0) is done. The second step is the quality filter which operates by a double standard deviation range (95% criteria). This eliminates outliners, but dumpend the variances.

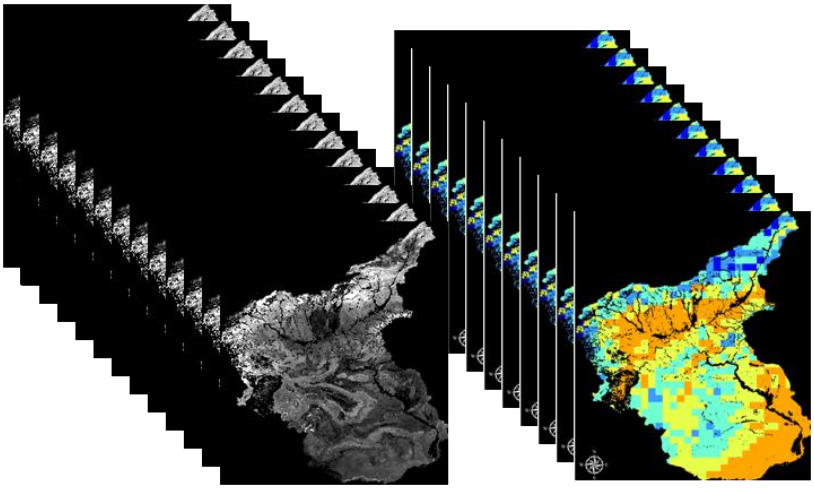

Figure 44 NDVI and Meteorological Time Series illustrated

These vectors are provide into RAM and are available during processing.

[8] all in mm

5.9 Module LAG

LAG is the act of delaying; inactivity resulting in something being put off until a later time. The presumption is that precipitation in the early rapid-growth stage has an impact on vegetation activity in the rapid growth stage. And precipitation 1–2 months before the mature stage did impact the vegetation activity in the mature stage (Schultz, 1995a;Miyazaki, 2004), precipitation in the rapid growth stage is important for vegetation activity in both stages. (Schultz, 1995b;Lambin & Geist, 2001) have investigated the relationship between temperature, precipitation and NDVI. In their time series they did not find a high correlation between monthly climate data, but their investigation implied that time lags of about one month between rainfall and NDVI are common and the onset can be derived by proxies. (Prince & Goward, 1995) reported a minor relationship between NDVI and climatology on local scale, except for marginally dry environments. Given that the vegetation cycle in arid areas is mostly linked to precipitation (Diodato, 2006;Lupo *et al.*, 2001), lag here is described as the cross covariance Rxy (L) of two sample populations NDVI(X) and Rainfall(Y) as a function of the lag L.

$$R_{xy}(L) = \begin{cases} \frac{1}{N} \sum_{k=0}^{N-|L|-1} (x_{k+|L|} - \bar{x})(y_k - \bar{y}) & \text{For } L < 0 \\ \frac{1}{N} \sum_{k=0}^{N-L-1} (x_k - \bar{x})(y_{k+L} - \bar{y}) & \text{For } L \geq 0 \end{cases}$$

Figure 45 Lag Formula (Imagesource: ENVI IDL digital Help) with R as cross covariance of xy(L), x and y as factors, N as sampling size, L as Lag and k as iteration step)

Choosing the maximum cross covariance approach assumes that precipitation peaks are followed by an increase in the NDVI. Therefore, the adapted $NDVI_{lag}$ is used from this point onwards. In this approach a lag Vector of 0 to 5 was used. By using a 16 day interval the maximum lag of 80 Days may occur.

5.10 Module Regression

In general Beven (2001) concluded that different Parameters approaches can be lead to equal results (concept of equifinality). That means that a 'optimal' Parameter combination is not always assignable. A Calibration must be done for Parameters that are not covered by measurement or be derivated from literature sources. (Refsgaard, 1997) point out three methods for model calibration:

- Manual adaptation
- Automatic calibration
- Combination of manual and automatic

This model uses an automatic calibration method. This is done by a least square approach, which is done independently for every station. The Regression Module is split up in two Sub-Modules. The first part is a statistical input and flow control module. The second part calculates the regression formula for the forecast.

5.10.1 Input and flow Indicator

This module has been created in order to calculate a statistical check on the main input parameters. At first it checks if the data are statistically significant. For NDVI data this is done by checking if 95% of the data are in a range of two standard deviations (2σ). Temperature and precipitation are checked in the same way. The second level checks if the input parameters have different variances. This is done by an ANOVA (analysis of variance) test. The input data has been checked again if they have different means by a T-Students test. Thirdly the data are checked on normal distribution using a Kolmogorov–Smirnov test (K–S test) (Kendall & O'Hagan, 1994). And fourthly the data are checked for multi-collinearity (Van den Poel & Larivière, 2004). This is done by calculating the variance inflation factor (VIF) and the tolerance factor. If the tolerance factor is lower than 0.2 and the VIF is greater than 5 (Draper & Smith, 1981;Bahrenberg, 1992;O'Brien, 2007) the model stops execution and prompts a warning.

5.10.2 Projection Sub Module

The projection sub module uses a combined linear and non- linear regression model approach. A linear regression model is a widely used tool (Bahrenberg, 2003;Verstraeten *et al.*, 2006) in remote sensing in the form of:

$$yi = \beta 0 + \beta 1xi1 + \beta 2xi2 + \ldots + \beta kxik + \varepsilon i \; i = 0, 2, \ldots, n$$

$\beta 0 \ldots \beta k$	*Regressors*
x	*Independent Variables*
y	*Dependend variables*
$\varepsilon i \; i$	*independently distributed normal errors, each with mean zero and variance σ2.*

Figure 46 Linaer Regression Formula

To take in account that vegetation growth can be divided in three phases (see Figure 47) a growing stage weighting factor is introduced.

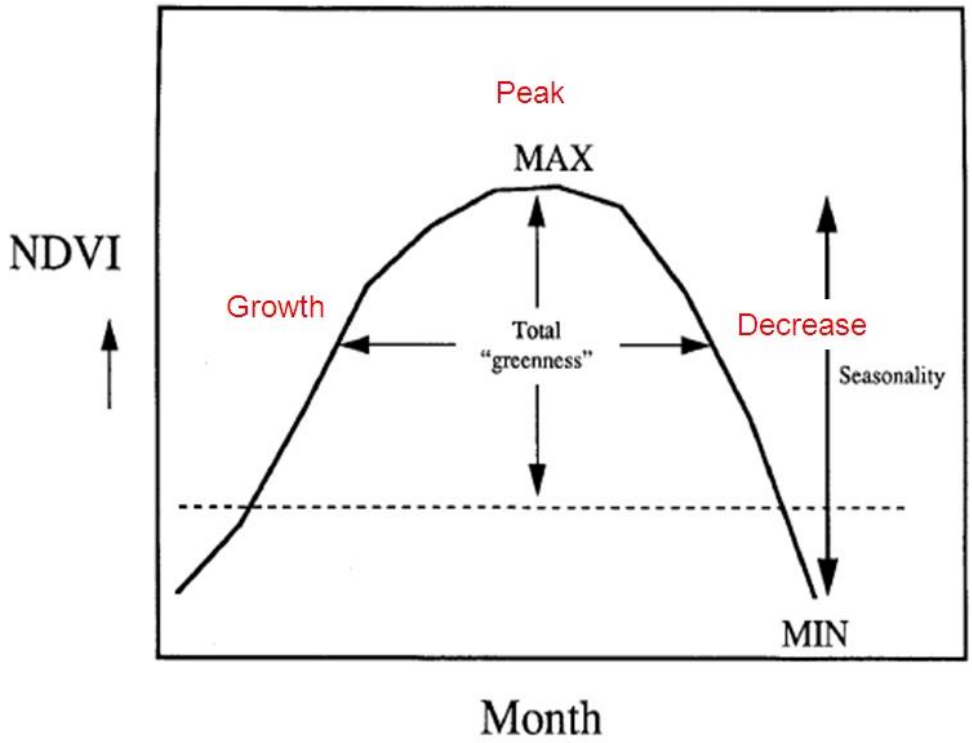

Figure 47 NDVI - Season (after Potter and Brooks, 1997)

This weighting factor w_i is designed with 0 as no weighting and 1 as absolute weighting, and a lower boarder of zero.

- Growth phase (1)
- Peak (0.6)
- Decrease phase (0.5)

Optimization here means the minimization of the weighted sum of squares (SSE) (Equation 12)of the deviations of the observed response yi from the fitted response (Draper & Smith, 1981) which is given out as variance statistic (ANOVA):.

Equation 12 ANOVA output of error sums

$$SSE = \sum_{i=1}^{n} w_i(y_i - \hat{y}_i)^2$$

SSE = sum of squares
n = number of observations
w = weighting factor
$\hat{y}_i$=fitted response
y = observed response

The Least Square solution is performed by IDL Analyst function which is based on the work of (Golub and Van Loan 1983, pp. 156–162; Gentleman1974). Inside this function an orthogonal reduction of the matrix of regressors to upper-triangular form under avoidant of the loss of accuracy that results from forming the cross product matrix used in the normal equations. The final computing of this function checks if the regressors have linear dependency. This leads to Independent Regressors and iteratively reweighted least squares regressors until the sum mean residuals are zero. The linear dependency is declared if

- A regressor equals zero.
- Two or more regressors are constant.
- The expression:

$\sqrt{1 - R^2_{i \cdot 1, 2, \ldots, i-1}}$ is less or equal to 100 x ε, where ε is the machine precision.

If a lineary dependency is declared the function will prompt an error. If the Results are declared not linear dependent the residuals, which are in sum 0, can inherit a bias for large variances. This can be seen by:

$$S^2 = \frac{1}{n}\sum_{i=1}^{n}(X_i - \overline{X})^2$$

With S as quadrate mean variance of the Residium X_i to the mean Residium (X). That is iterated until the Variation of S^2 is different of the Standard Variation.

$$\mathrm{E}(S^2) = \frac{n-1}{n}\sigma^2 \neq \sigma^2.$$

After getting an approximation of the linear trend, a second non linear optimization to minimize the existing bias is used. Choosing a non-linear approach try to explain the dependency between depended factors and residuals due to the least square mechanism as

described by (Rousseeuw, 1984) and (Gentleman, 1974) (see Figure 48 and Results from this Regression in Figure 49).

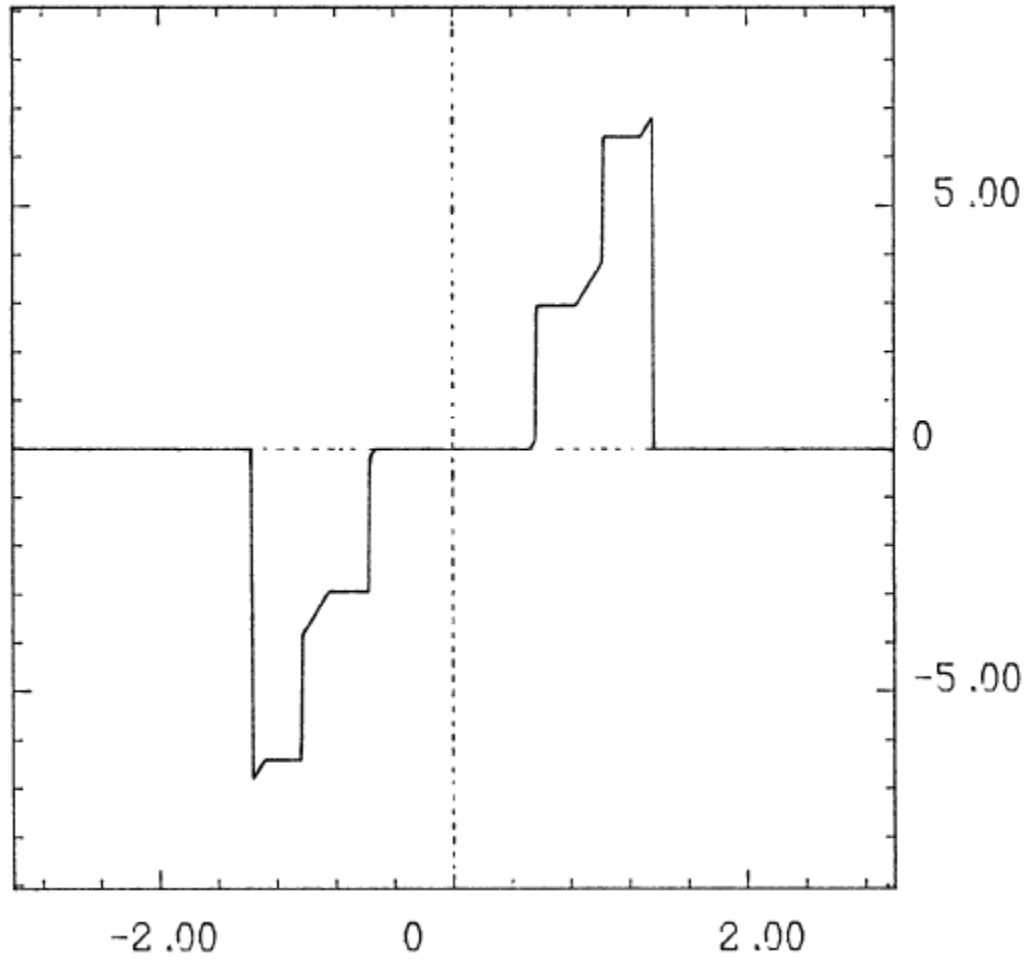

Figure 48 Least square sensitivity (Source:Rousseeuw,1984)

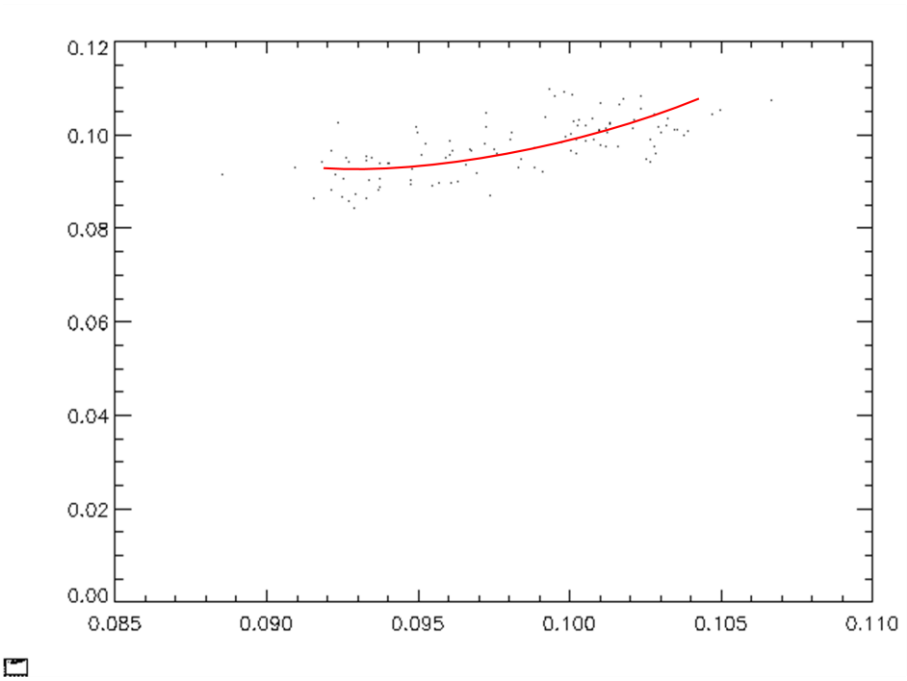

Figure 49 Residuals after Linear Regression. Inside the cloud of residuals a red demonstrational function is shown as example for the possible solution of the non-linear regression. (dimensionless)

There's an increase of residual with an increase of variance, so this distance is to close by using a formula that best fits the data. To solve that problem the Equation:$yi = f(xi;\theta) + \varepsilon$ with $i\ i = 1, 2, \ldots, n$ is used.

With Result y_i as function of the input parameter x_i (which here are the Residuals) by using the functionθ. This uncertainty is illustrated by the machine precision ε. The function x_i of θ is definied by:

$f(xi) = \theta_1(0) * e^{x(0)*\theta_2}$

With $\theta_1$and θ_1 as parameters to iterated by using the Residuals: $e_i(\theta) = yi - f(xi\ ;\ \theta)\ i = 1, 2, \ldots, n$ with y_i as observed Parameter. The iteration minimizing the equation

$$\Sigma_{i=1}^{n}[e_i(\theta)]^2$$

The result is a approximation which is, like the linear equation, the best solution. This is also done separately by growing and decreasing days.

This combined linear and non-linear approach is the attempt to approximate the variations in temporal progress by finding the best general linear dependency of the input parameters completed by the approximation of peaks and outliners.

5.11 Module ANPP

As discussed in chapter 3.3 the observation of natural vegetation and land cover, as well as their change, is an essential part of this work. For Grassland the annual change in carbon stock can be approximated by (IPCC, 2003):

$$\Delta C_{GG} = \Delta C_{GG_{LB}} + \Delta C_{GG_{Soils}}$$

ΔC_{GG} = annual change in carbon stocks in grassland remaining grassland, tons C yr-1
$\Delta C_{GG_{LB}}$ = annual change in carbon stocks in living biomass in grassland remaining grassland, tons C yr-1
$\Delta C_{GG_{Soils}}$ = annual change in carbon stocks soils in grassland remaining grassland, tons C yr-1

Calculating the change in the living, photosynthetic active, biomass (Monteith, 1965;Monteith, 1972;Potter & Klooster, 1999;Fensholt *et al.*, 2004;Fensholt *et al.*, 2006) is the main intention of this module. The ANPP Module is broadly based on the Dissertation of (Richters, 2005b). His Model *Regionales Biomasse-Modell* (RBM) Kaokoland provides a basis for this model. Kaokoland is a part of Namibia and describes the geographical origin of RBM development. Namibia can be classified as semiarid/ arid with arid desert hot to cold arid (Köppen, 1923;Köppen, 1901) Climate (Sander & Becker, 2002). The Fact that the Drâa Valley has a comparable climate (see chapter 2.2) and that the source code of RBM is written in ENVI IDL are strong arguments to use RBM. But more important is the fact that RBM uses similar Input parameters (Climate, DEM) as well as it optimized for MODIS Terra NDVI.

RBM is an approach to calculate daily ANPP (see chapter 3.5) on the basis of radiation transfer in different solar spectra measured on images of satellite based sensor. Besides the satellite images, a DEM and soil information are used (Richters, 2005b). The model uses the remote sensing-based LUE (Light Use Efficiency) approach of (Monteith, 1972;Monteith, 1981;Prince, 1991a;Running *et al.*, 1999). This can be summarised into the following formula:

Equation 13 NPP calculation (from Richters, 2005)

$$NPP = \varepsilon \cdot FPAR \cdot PAR \quad \textbf{(Monteith, 1977)}$$
$$\approx \varepsilon \cdot NDVI \cdot PAR \quad \textbf{(Running et. al., 2000)}$$

Equation 13 implements the NDVI as Vegetation activity measurement, PAR as Input Radiation and ε as biophysical Conversion Factor or LUE factor as core variables for calculating ANPP. RBM includes a mathematical approach on calculating the photosynthetic active radiation on the base of latitude, relief and time of calculation (Swift, 1973;Swift, 1976).

The factor ε is defined by

Equation 14 Epsilon Definitation

$$\varepsilon = f(Biom, Relief, Boden) \cdot f(Klima)$$

The factor ε can be divided into two parts (Figure 50).

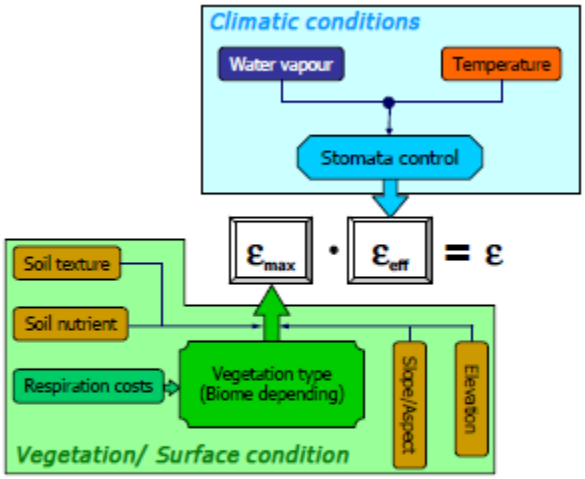

Figure 50 Flow chart of RBM (Source: Richters,2002)

The factor $\varepsilon eff\ (x,t) = T''(x,t) \cdot W''(x,t) \cdot \varepsilon max(x,t)$ includes the temperature and water stress and the potential growth component εmax. The equation $\varepsilon max = \varepsilon p * xRelief * xBoden$ inherits the factor εp, which represents the LUE efficiency factor. The derivation of εp will be discussed in Chapter 6.3.5. After calculation all necessary factors of the ANPP Modul it is able to calculate the ANPP.

There are three main modifications to the original RBM approach:

- transformation to a 16 day module
- including climatologically data instead of remote sensing data
- calibration with measured biomass and ANPP data

Since RBM was designed to calculate daily ANPP it has to transform into a 16 day cycle. This could mainly be carried out without major changes in the source code, but small adjustments in conversions. Those conversions were due to the different inputs. RBM original uses MODIS products as input. The measured climate data is for example in W/m² and RBM calculates in MJ, with every value now standing for mean or total value (depend on factor[9]) during the 16 days measured by one climate station. For example the temperature and water stress equations remained unaffected, but the calculation has been taken from Chapter 5.6. The e_p or LUE efficiency factor is modified by using field data. Chapter 6.3.5

[9] Precipitation and Radiation parameters are used as 16 day sum, while temperature i.e. reflects the minimum temperature during the period.

presents the results for the Drâa Catchment. As Cloudiness Data are rarely, only a few Data from end of 2006 until end of 2008 are used.

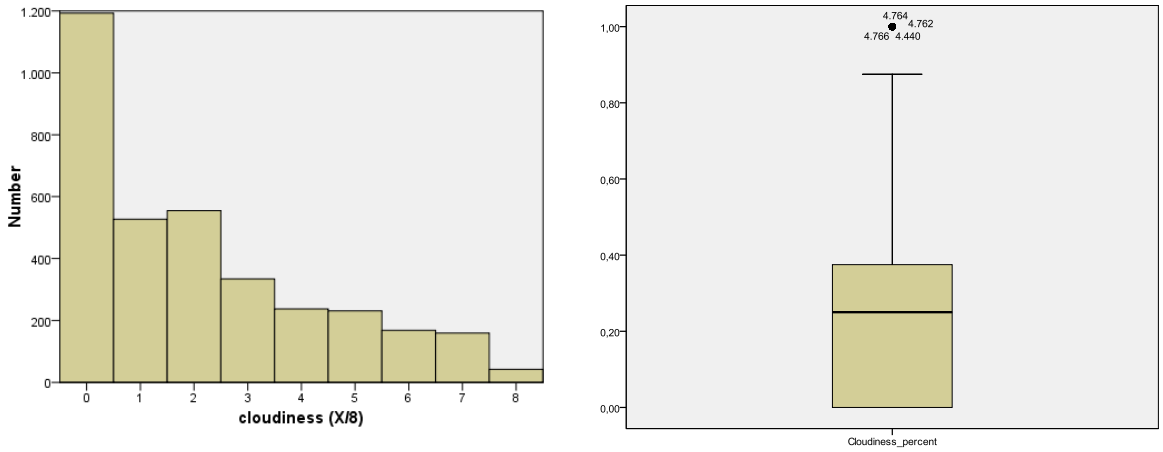

Figure 51 Histogram of Cloudiness for the period 2006-2008 for station Ouarzazate Airport

The Cloudiness is not normal distributed; so it is decided to set the Median value of 25% as fixed cloudiness (Figure 51).

5.12 Subroutines

During the conception two major Sub-Routines are implemented, which are vital for the calculation. The plant cover calculation and the Leaf Area Index are regressions from the results of the Fieldwork. For both calculations the NDVI and measured data are taken and an approximation algorithm was developed to simulate LAI and total plant cover using a regression approach in order to give an exact result for every NDVI value. For details and results consult Chapter 6.3.3 and 6.3.4.

5.13 Quality Criteria

The Process of assessing the performance of a model requires to estimate the “closeness” of the simulated behaviour of the model to the observation (Krause *et al.*, 2005). After the sensitivity analysis it is necessary to quantify a mathematical efficiency criteria contain a summation of the error term and reported value ranges and performance ratings (Krause *et al.*, 2005;Moriasi *et al.*, 2007). During this work three main quality Criterions used:

- Pearsons r² (Quadrate of the Correlation)
- Nash Sutclifffe efficiency (after Nash and Sutcliffe, 1970)
- Index of Agreement (after Willmot, 1981)

R² can be expressed as squared ratio between the covariance and the multiple standard deviations of observed and predicted values .

Equation 15 R² (after Krause et al, 2005)

$$r^2 = \left(\frac{\sum_{i=1}^{n} (O_i - \bar{O})(P_i - \bar{P})}{\sqrt{\sum_{i=1}^{n} (O_i - \bar{O})^2} \sqrt{\sum_{i=1}^{n} (P_i - \bar{P})^2}} \right)^2$$

Therefore it estimates the combined dispersion against the single dispersion of the observed and predicted series. The range lies between 0 and 1 which described how much the observed dispersion is explained by the predicted. A value of 0 means no correlation at all and a value of 1 a perfect fit. The problem with r² that only the dispersion is quantified is a mayor disadvantage of r². A model that systematically under or over predict all the time will also result in a good r² even if all predicted values are wrong. R² only analyse the linear relationship between observed and simulated data and is oversensitive to high extreme values (outliers) and insensitive to additive and proportional differences between model predictions and measured data (Legates & McCabe, Jr., 1999).

The efficiency proposed by Nash and Sutcliff ((Nash & Sutcliffe, 1970)) is a dimensionless indicator which is defined by:

Equation 16 Nash-Suthcliff index

$$E = 1 - \frac{\sum_{i=1}^{n} (O_i - P_i)^2}{\sum_{i=1}^{n} (O_i - \bar{O})^2}$$

The Nash-Suthcliff efficiency indicator normalized the variance which results in a relative higher value of E, especially in Observations with higher dynamics and lower values of E in Observations with lower dynamics (Krause et al., 2005). This is important because of

observed higher dynamics in mountainous areas and lower dynamics in arid (desert) areas. The Nash-Suthcliffe coefficient range between 1.0 (perfect fit) to -∞. An efficiency of lower than zero indicates that the mean value of the observed time series would have been a better predictor than the model. The Nash-Suthcliffe coefficient is calculated as difference between the observed and predicted as squared values. The Result is that larger values in a time series are strongly overestimated whereas lower values are neglected (Legates and McCabe, 1999). This leads to an overestimation of model performance during peak flows and an underestimation during low flow conditions. E is oversensitive for extreme values because of it squares the values of paired differences (Legates & McCabe, Jr., 1999;Daren Harmel & Smith, 2007). Similar to r^2 the Nash-Sutcliff is not very sensitive to systematic model over- or under prediction especially during low flow periods.

Using the Index of Agreement as developed by Willmott (1981) as a standardized measure of degree of model prediction error (varies from 0 to 1). 0 indicates no agreement at all (Willmott, 1981). It represent the ration between the mean square error and the “potential” error (Gaile & Willmott, 1984). The potential error is defined as the sum of squared absolute values to the mean observed value and distances from the observed values to the mean observed value.

Equation 17 Index of Agreement

$$d = 1 - \frac{\sum_{i=1}^{n} (O_i - P_i)^2}{\sum_{i=1}^{n} \left(|P_i - \bar{O}| + |O_i - \bar{O}|\right)^2}$$

The index is sensitive to extreme values due to squared differences. (Legates & McCabe, Jr., 1999) suggested the alternative IA, which is less sensitive to extreme values. The Reason is that errors and differences are given appropriate weighting by using the absolute Value of the difference instead of using squared differences. Although IA alternative has been proposed as an improved statistic, its limited use has not provided extensive information on value ranges (Moriasi et al., 2007).

5.14 Module Forecast

*Forecasting is "An ordered sequence of values of a variable at equally spaced time intervals" (Engineering Statistic Handbook).*Forecasting, as technique, is used for:

- Obtain an understanding of the underlying forces and structure that produced the observed data
- Fit a model and proceed to forecasting, monitoring or even feedback and feed forward control[10].

By using a Deterministic forecasting model, it became possible to predict the futures if assumed that physic Phenomena's are nearly constant. In order to assess the future climate special computational models of the climate system have been developed. Based on physical principles and laws their simulating the Earth's atmosphere as well as other climate subsystems and the regression equation of chapter 5.10 an Forecast of the vegetation situation until 2050 can be done.

The Meteorological modelling has been undertaken with the Atmospheric Model REMO. REMO is a RCM (Regional climate modelling) developed by the Max-Planck-Institute for Meteorology (MPifM) Hamburg. It is based on the hydrostatic approximated set of hydrodynamic equations (Born et al., 2009). REMO is nested in Echam5 and the package of physical parameterization is near similar (Born et al., 2009). Details of the model physics are described in (Jacob *et al.*, 2001), the application of REMO for RCM in the Mediterranean and Africa has been presented by (Paeth *et al.*, 2006;Paeth *et al.*, 2005a). These studies focus on the evolution of RCM Data as well as the assessment of extreme events in the Mediterranean. (Paeth & Hense, 2005) also shown that shape of the two dimensional distribution is shifted torwards higher values, which implies that REMO produces stronger spatial maxima in the MTR seasonal precipitation than the CRU data. (Paeth & Hense, 2005) related that to the better representation of orographic effects in the non-linear dynamical downscaling approach than the CRU data.

The used Data are distributed in 12 zones over the catchment (Figure 52). These 12 zones inherit the statistical distribution of the REMO results for the Drâa Catchment based on the period of 1960 to 2000.

[10] Engineering Statistic Handbook

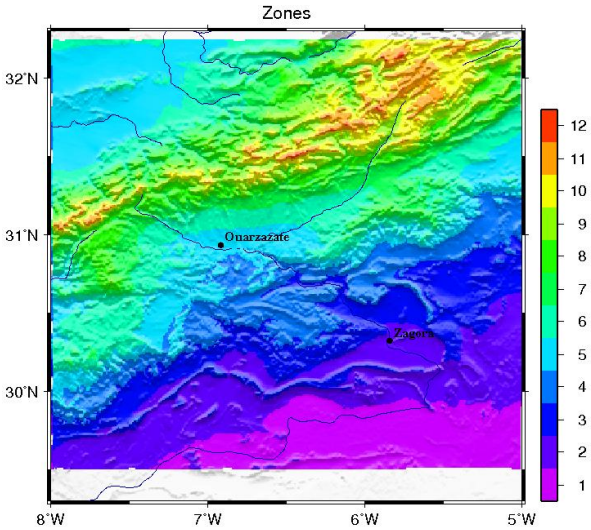

Figure 52 Forecast Zones (Source: Kai Born)

Forecast Precipitation (Figure 56) is distributed with an N-S gradient und inherits a large Variance.

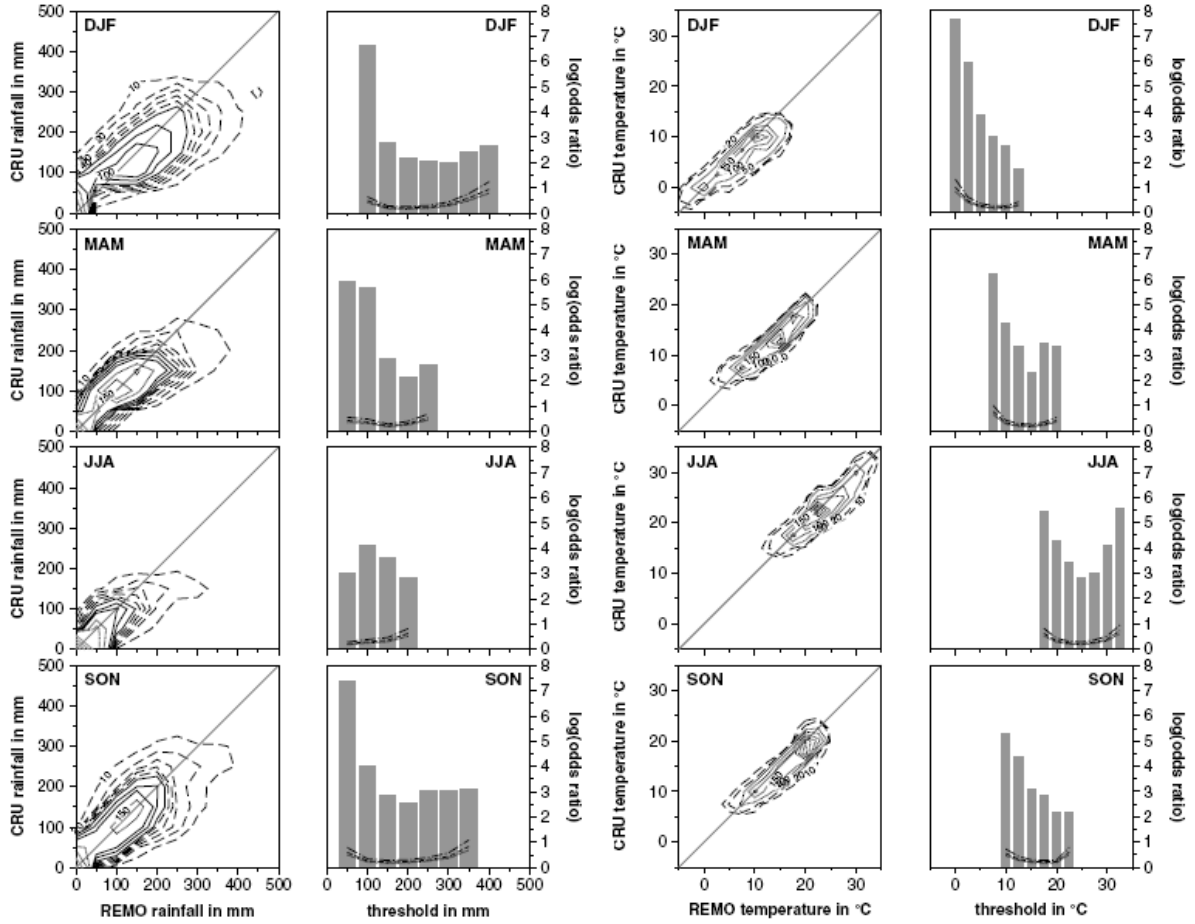

Figure 53 Validation of REMO Szenarios (from Paeth, 2005) for quarterly parts of the year.

The higher the log odds ratio in the Precipitation, the more grid boxes are consistent with respect to the simulated and observed threshold exceedance(Paeth,2005).

It is possible to show the signal –noise Ratio can be calculated from each k-year Return Value(KV) of daily sums of (precipitation) or means (temperature) devited by the Standard Error (STE) over 1000 bootstrap samples (Kharin and Zwiers, 2000, Park et. al, 2000). If small than the RV is uncertain und not appropriate. In our investigation Area the signal-to-noise ratio is quite high.

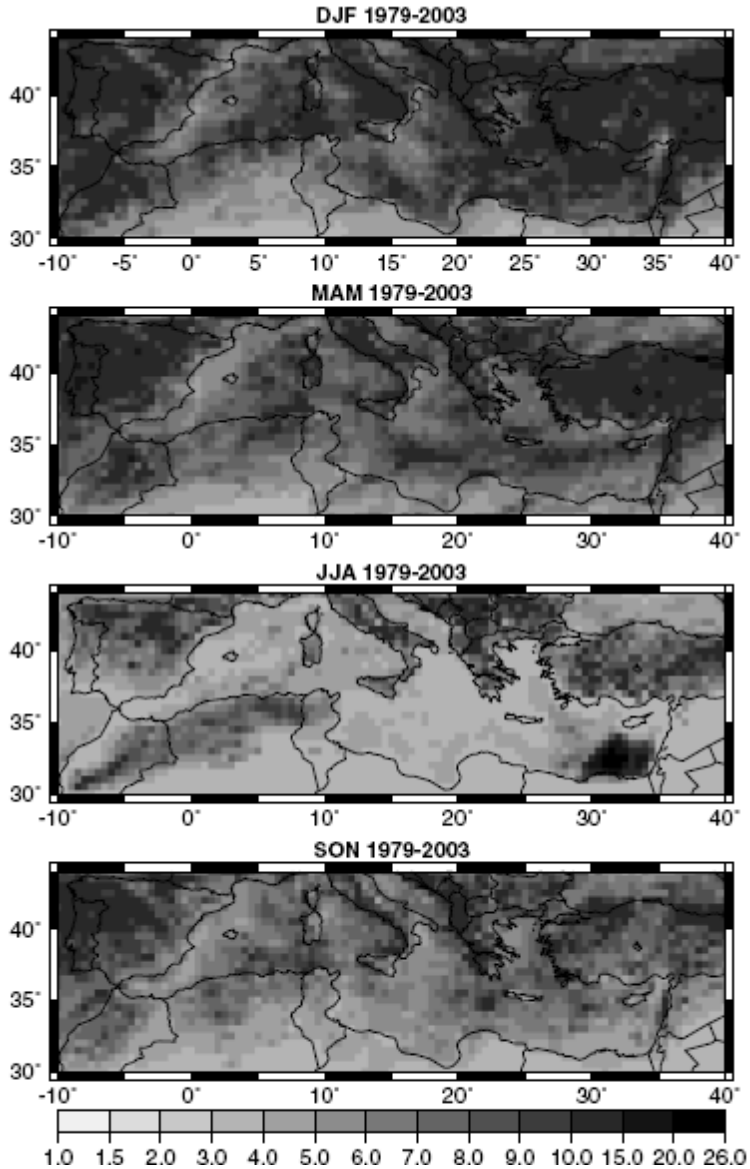

Figure 54 Signal to Noise ratio of the estimate of 1-year return values of daily rainfall based on 1000 bootstrap samples (source: Path (2005))

For this Study the IPCC SRES scenarios (Nakicenovic and Swaart, 2001) was used. Each scenario and the 20th century simulations are represented by three ensemble members in order to obtain a measure of uncertainty (Born et al., 2008). All scenarios are realized with transient forcing, extending from 1960 to 2050. Our RCS uses a stochastically land-use change model which is based on assumptions for population growth and urbanization in Africa (comp. Paeth et al. 2005, Born,2008).

Born (2008) had show that Trend of this results shown that the error probability for this focus is low, with an greater error in summer (Figure 55)

Table 3: Trend matrix for temperature in K/91 years from REMO A1b and B1 scenarios, for the period 1960-2050. For all values, the error probability for the rejection of the no-trend-hypothesis is less than 1%. Again, the range of uncertainty is given as the averaged deviation from the ensemble mean trend.

Temperature trend	ATL	MED	SOA
Winter	**1.37 ± 0.28**	**1.33 ± 0.22**	**1.27 ± 0.18**
Summer	**1.75 ± 0.49**	**2.04 ± 0.55**	**2.02 ± 0.52**
Year	**1.56 ± 0.29**	**1.69 ± 0.31**	**1.64 ± 0.29**

Table 2: Trend matrix for rainfall indices in standard deviation units / 91 years for the period 1960-2050. The bold values are trends, for which the error probability for rejection of the no-trend-hypothesis is smaller than 10%. Additionally, trend uncertainties as mean deviations from the ensemble mean trend are given.

Rainfall Index Trend	ATL	MED	SOA
Winter	-0.73±0.30	**-0.86±0.36**	-0.71±0.37
Summer	-0.73±0.42	-0.46±0.38	-0.63±0.41
Year	**-0.91±0.29**	**- 0.91±0.25**	**-0.83±0.26**

Figure 55 Trend matrix (Source: Born, 2008)

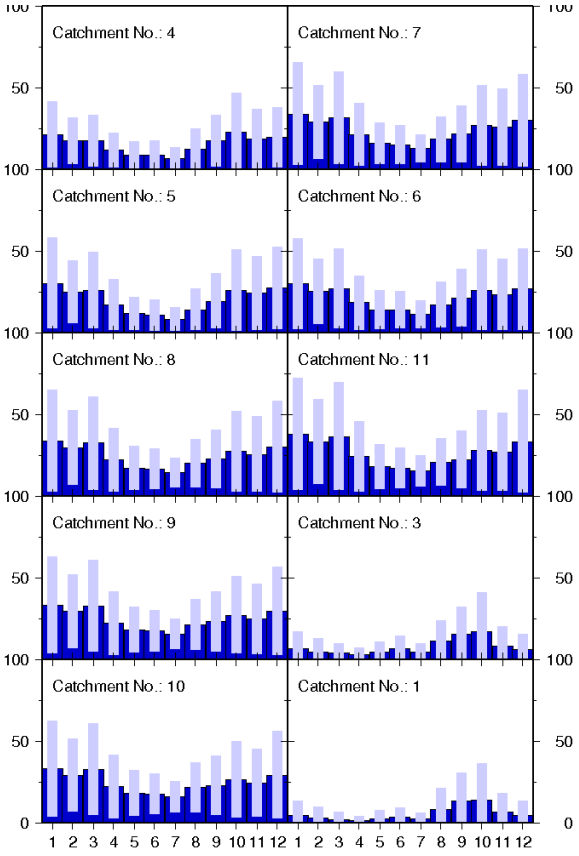

Figure 56 Forecast Zones Precipitation Seasonal cycle (Source: Kai Born)

Using the zones from Figure 52 Born shows the shifting of rainfall events from south (cathcment1) to north (catchment 10) is not only in the amount of rain but rather the

distribution. Catchment 1 shows a clear fall precipitation peak during Catchment 4 to 10 shown a dual peak precipitation distribution.

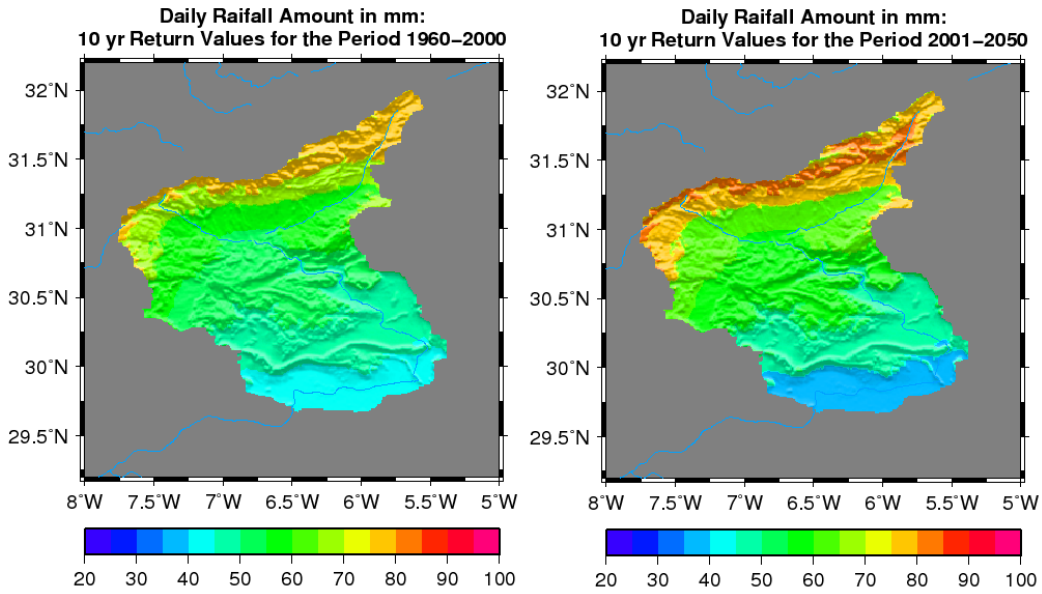

Figure 57 Forecast Daily Rainfall Amount [mm/d] (Source: Kai Born)

By using the Harmony Analysis approach of chapter 7 a classified Station Data map is can be created, based on Vegetation response Units. This Classification is Cluster mean approach with a manual assignment of Climate stations. Inside the Atlas Mountain not all station can be assigned. In this approach all agriculture areas are mask out.

5.15 Output format

MD supports multiple image output or text-based output formats. The most used here is ASCII text files or ENVI files. The output files are stored at the determined destination and are ready for analyzing or further use. This interface allows an easy coupling with other programs or models.

6 Results of Moveg Draa

This chapter presents the results of all approaches and routines stated in the previous chapters. Guided by the module structure, it concluded all results in two parts. The first part concluded all results based on the measurements of station based results. This part also included an overview of the results of these methods. The second part gave an overview of multi-station results, like gradient and other spatial outcomes.

6.1 Results Climate Data

This sub-chapter summarizes all calculated measured and calculated meteorological data along the transect given in Figure 58.

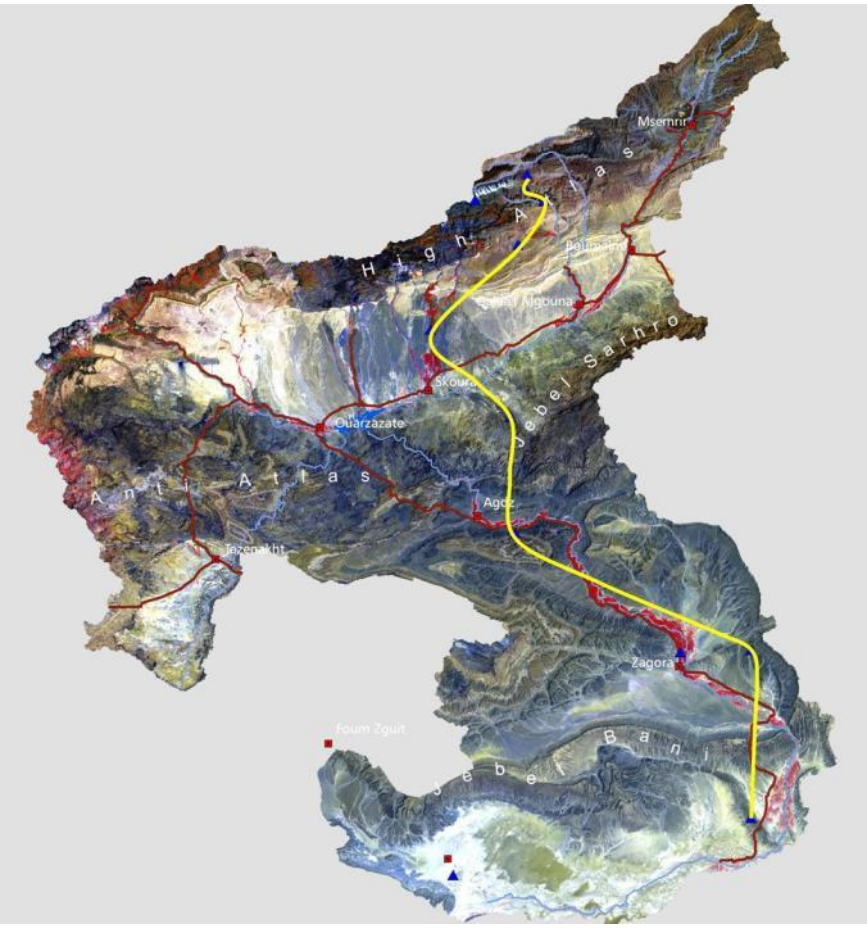

Figure 58 Measurement gradient

Using the transect given in Figure 58 this chapter presents an overview about the situation inside the catchment, picking example data to demonstrate certain facts.

6.1.1 Wind

Wind is the driving factor for all particle incidents in the athmosphere (Oke, 2003). The wind speed inside the catchment is investigated on two selected stations, TZT and TAO. Both are inside the High Atlas mountain range. The exact orientation of the mountainous plateau of TAO is SW to NE and TZT is located on a platform that is framed S to W by mountains. Both stations have a wind direction that follows the orography of the location.

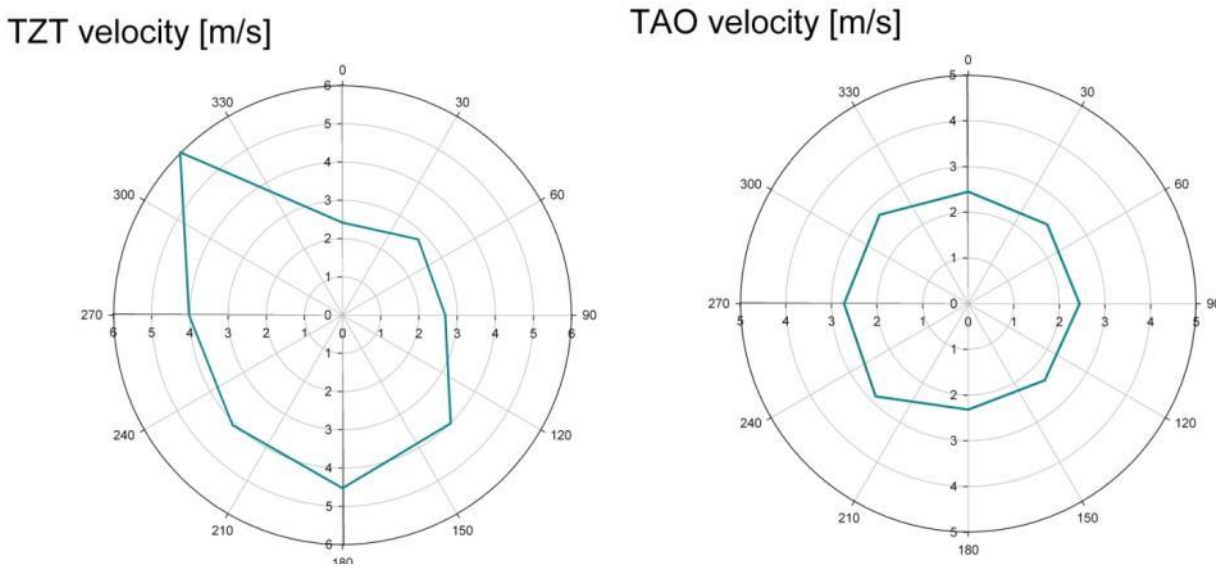

Figure 59 Wind velocity station TZT and TAO

The velocity of stations TZT and TAO (Figure 59) shown that wind direction has no significant influence on the mean win velocity. This is important because it is now possible to negate wind direction in calculating transpiration rates and evaporation, but keeping in mind that the wind direction is rather important for Luv/Lee effects, as well as the dew point.

6.1.2 Temperature

The temperature inside the investigation area follows the classical seasonal climate (Figure 60) that can be expected in arid areas (Le Houérou, 1996;Born *et al.*, 2009).

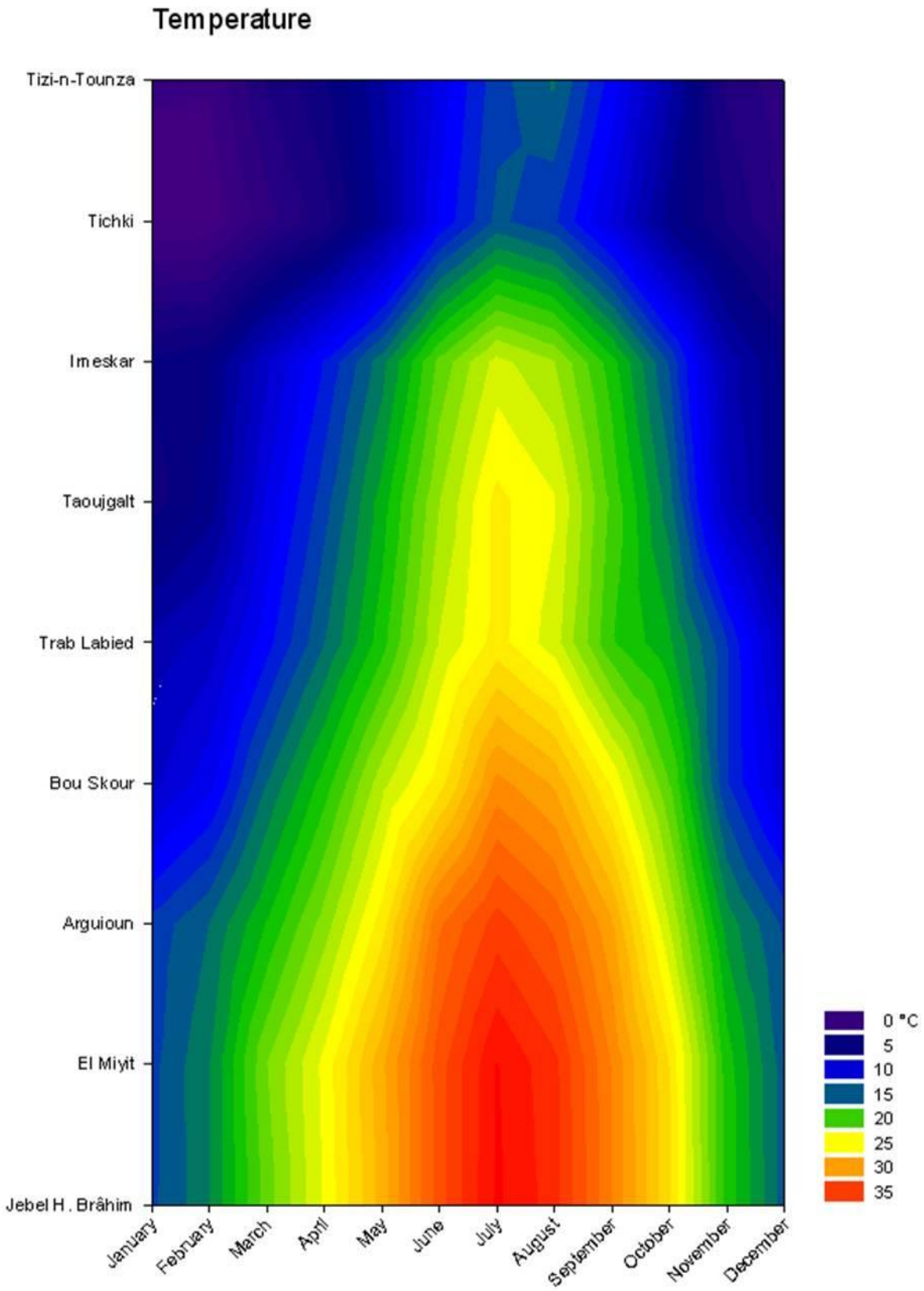

Figure 60 mean monthly Temperature inside Drâa catchment from measured station data (own graphic)

Figure 60 includes all data measured starting in 2000/2001, till the end of 2008. The temperature ranges from cold winters to hot summers. The yearly temperature gradient varies from 15° up to 30° in the southern areas. According to (Potter & Klooster, 1999)

savannas and wooded grassland stretch at least 16 to 11315 GDDs. By taking Toujgalt as example a total of 4032 GDDs on the base of 280 days over 5° C (see Chapter 5.6 for details) and a mean air temperature of 14.4°C was calculated.

6.1.3 Precipitation

Following the vegetation classification of (Potter & Klooster, 1999), semiarid shrub land inherit a rainfall ranging from 276 to 0 cm per year. Looking at the examples in Figure 61 and

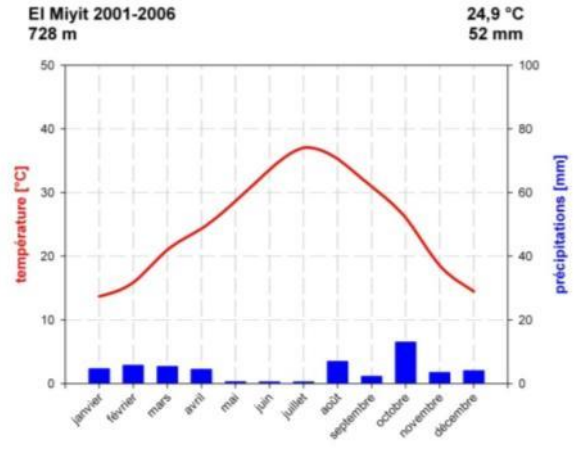

Figure 62 the mean annual precipitation varies from 52 to 300mm.

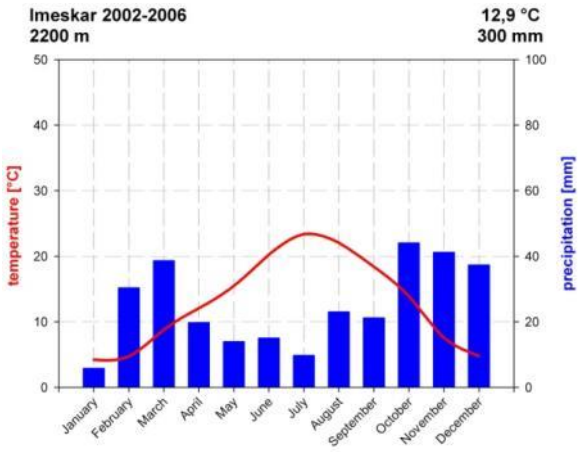

Figure 61 Climate Station EMY

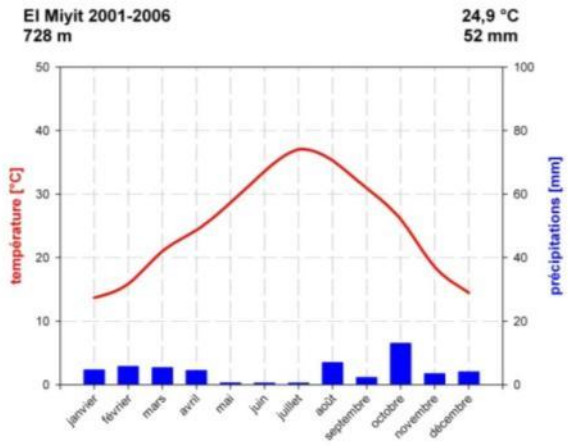

Figure 62 Climate Station IMS

The high atlas mountain range is then to be classified as savanna and wooded grassland (comp. (Finckh & Oldeland, 2006)). By looking at the spatial distribution in Figure 63, it becomes clear that the mean distribution of rainfall events (daily based) inside the area, indicates no significant yearly varying distribution of rainfall south of the Anti Atlas (Bou Skour).

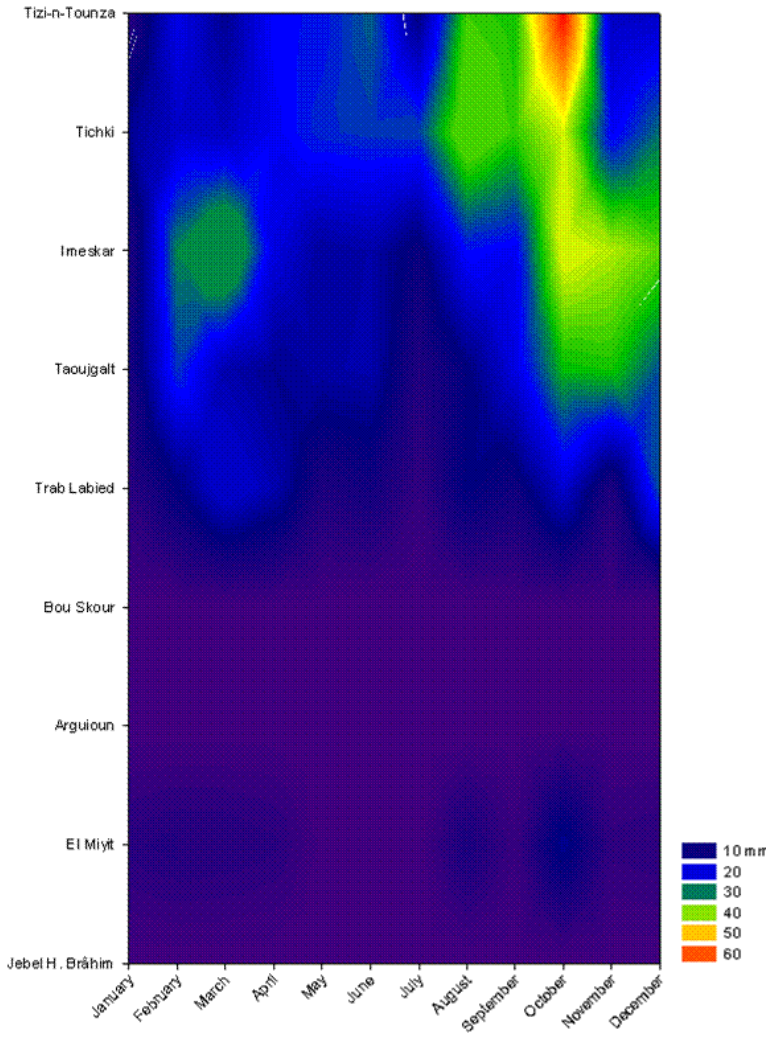

Figure 63 monthly mean precipitation (2000-2008)

For the stations south of Bous Skour the most notable rainfall occurs during September to November. For stations north of Bou Skour precipitation takes place mainly in March/April and October though it has a high variance (comp.chapter 5.6).

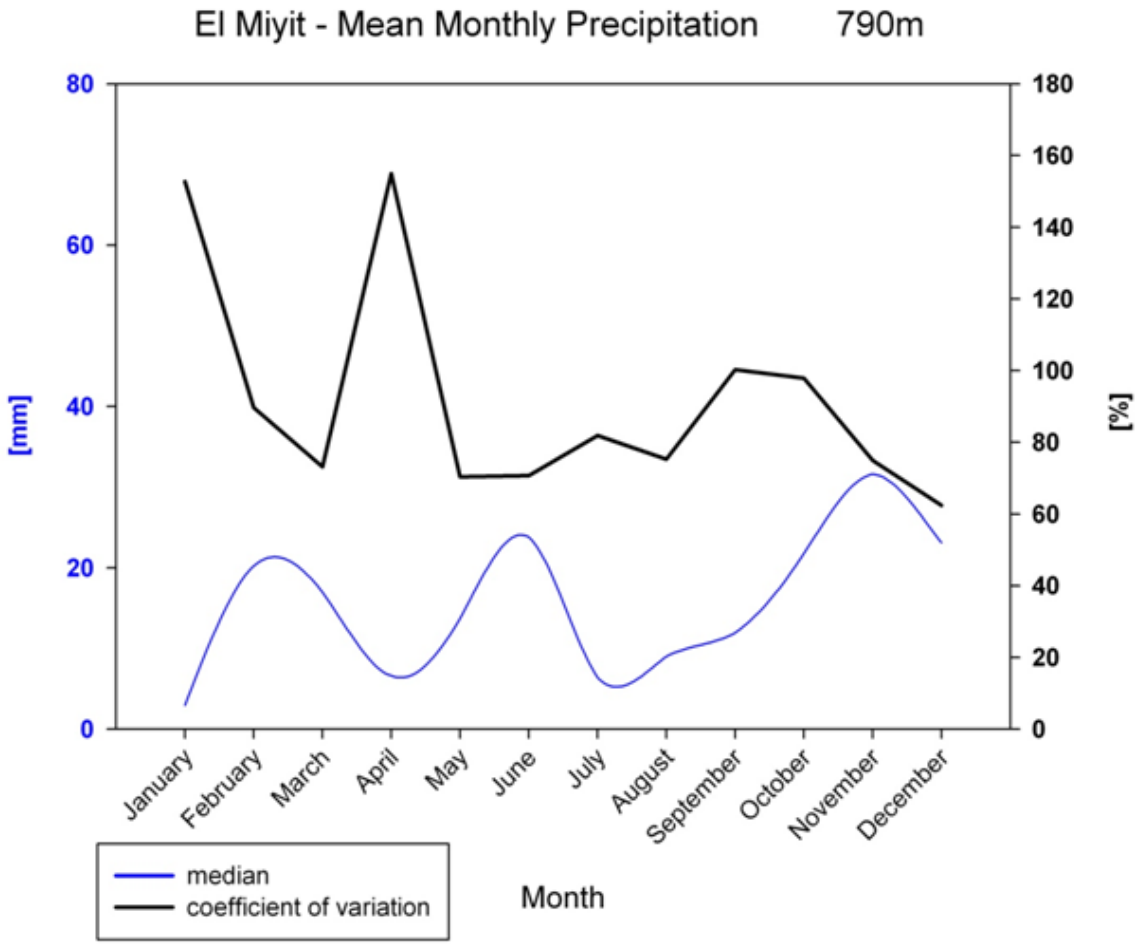

Figure 64 climat station EMY coefficient of variation(black) and median precipitation (blue)

Figure 64 shows the precipitation in the southern areas (represented through EMY here, more stations and figures can be found in the appendix) are on a very low level with a high variation coefficient throughout the year. This means that the small amount of rainfall strongly varies and is only predictable through the general weather situation rather than by climatology.

For the northern stations (Anti Atlas and northward) the variation coefficient remains at a high level for all stations with high variation (as seen in Figure 65) in winter and spring. But one can see in Figure 65 that the fall/winter rainfall is much more reliable than that in the southern part of the investigation area.

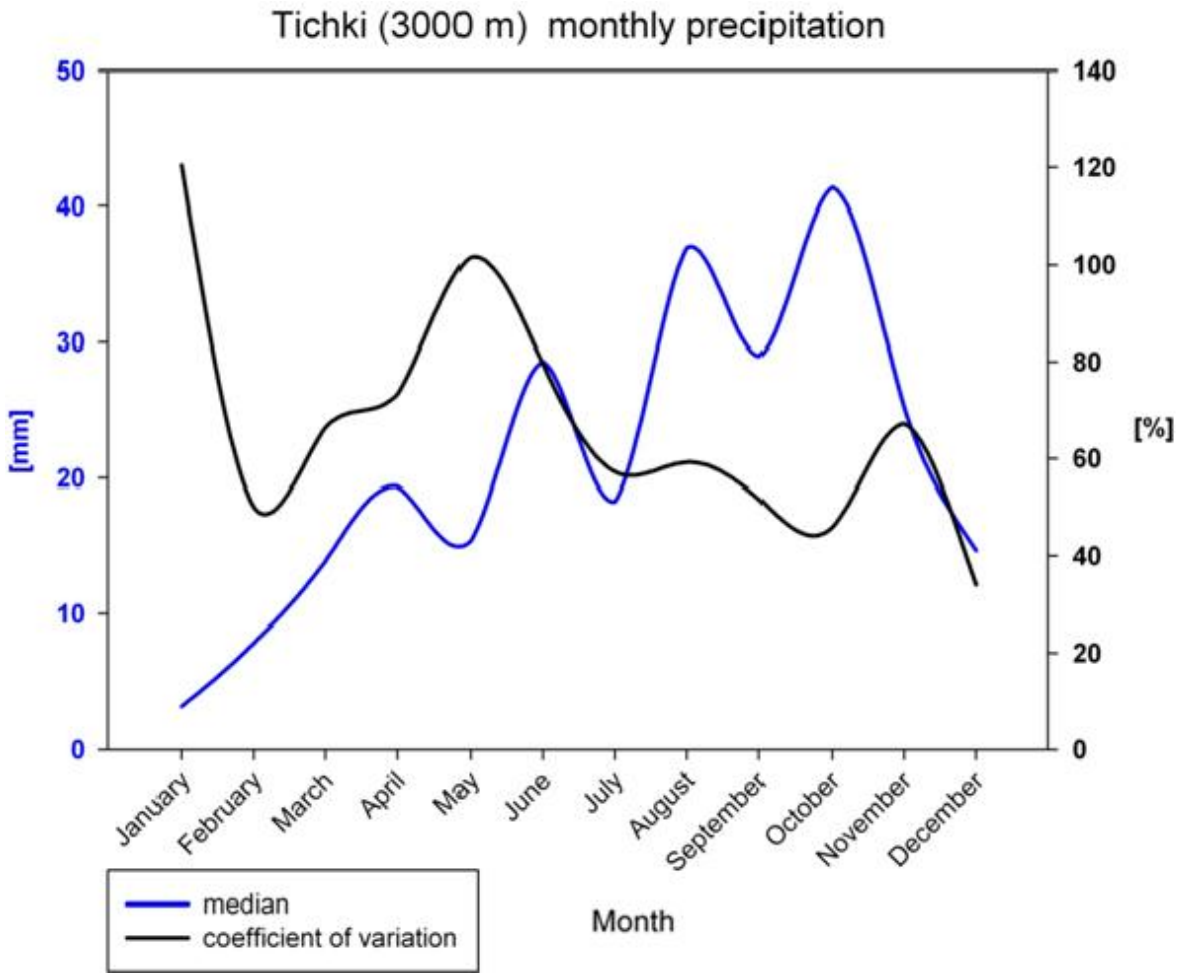

Figure 65 Percipitations coefficient of variation (black) and median precipitation (blue) for the period 2001 until 2009 for the high mountain station TZT

All stations north of the Anti Atlas show a significant fall/winter/spring rain regime. This is confirmed by looking at historical long term development. This confirms the fall/winter/spring rain regime (see Figure 66.)

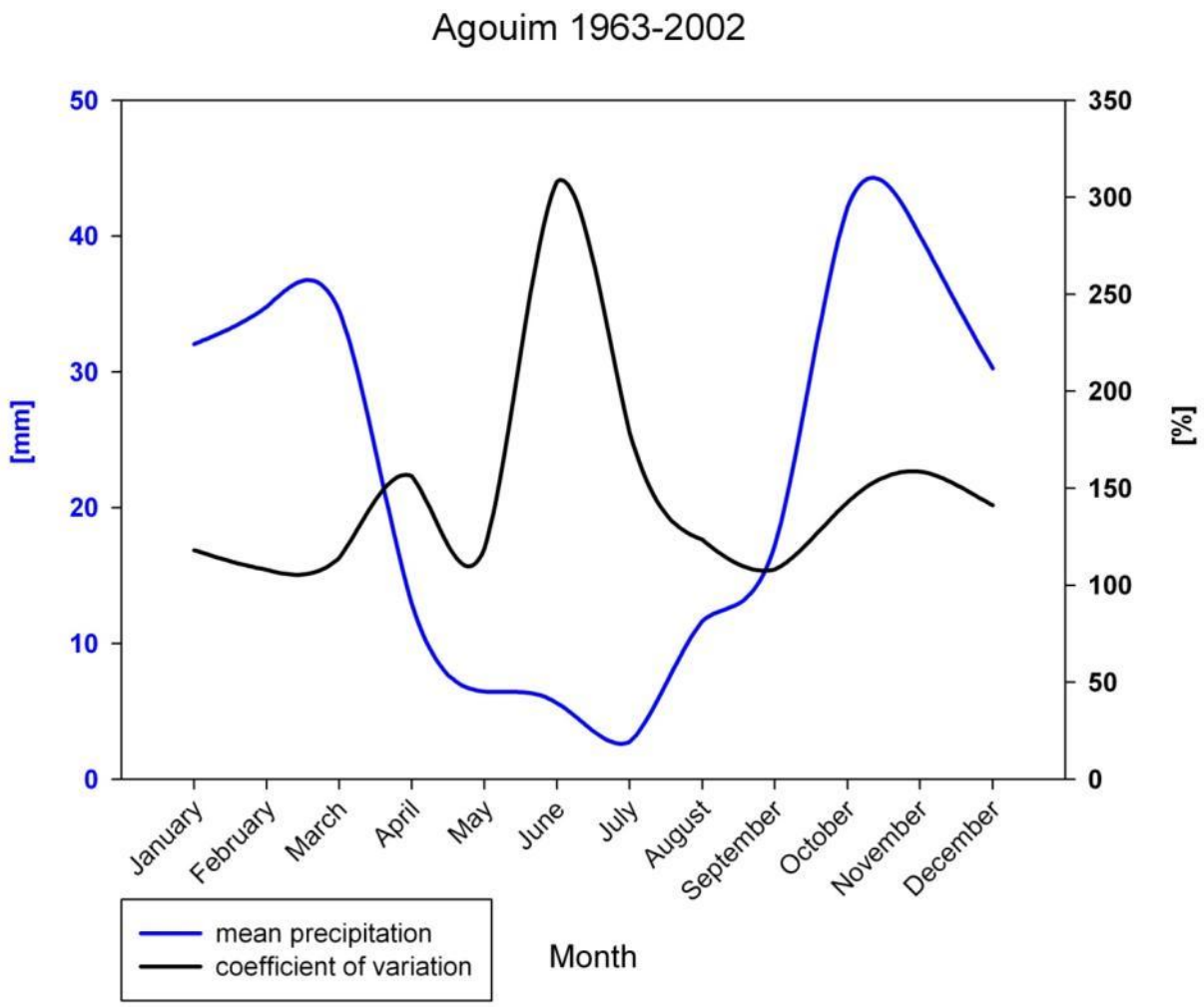

Figure 66 long term Agouim coefficient of variation (black) and the mean precipitation (blue)

High values in coefficient of variation in summer are due to the difference between wet and dry years. On the long term track the regime is very constant in October/November but variable with regards to rainfall amount (Figure 67).

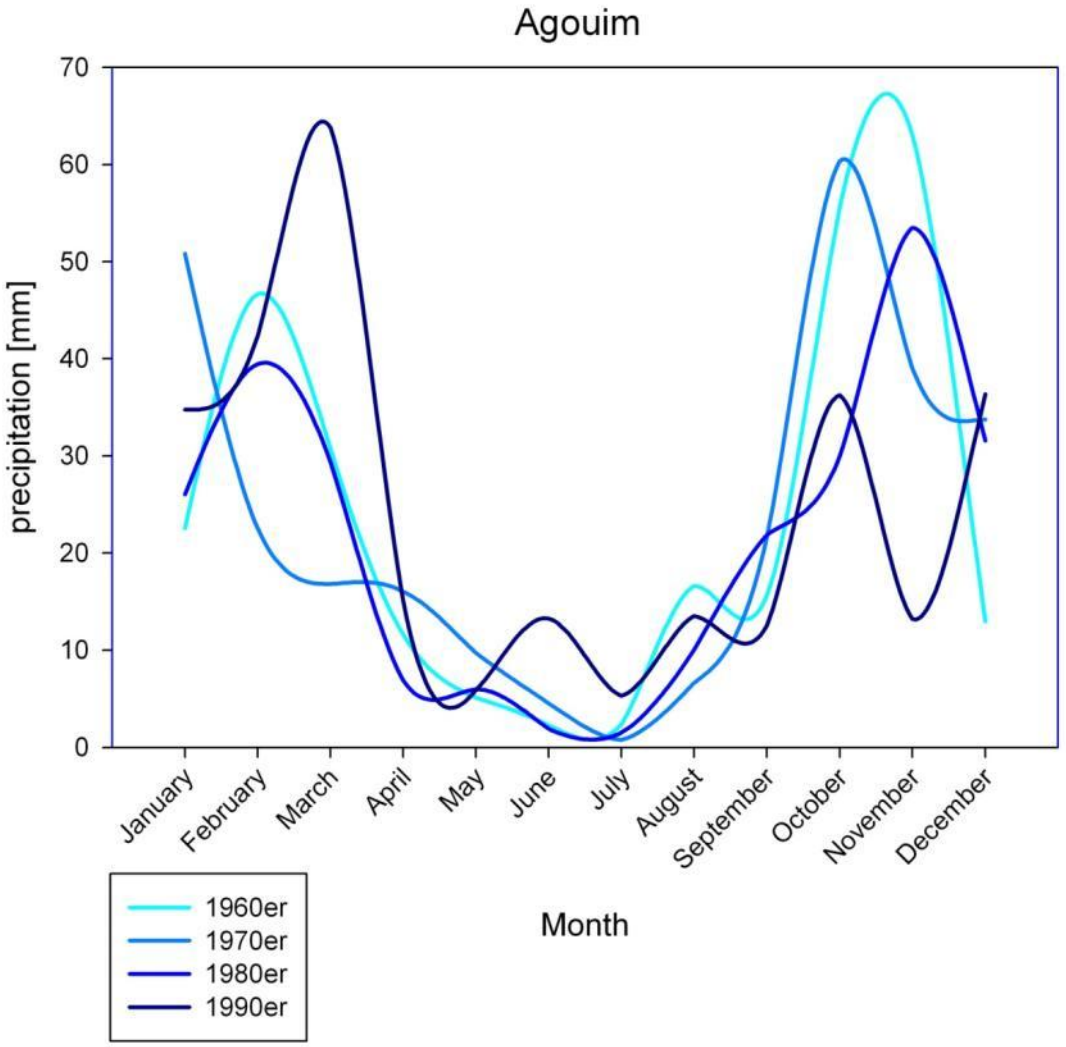

Figure 67 mean rainfall during various Decades for the station Agouim

These tendencies are further strengthen when taking a look at the relative anomalies of a drought year (Born et al., 2008).

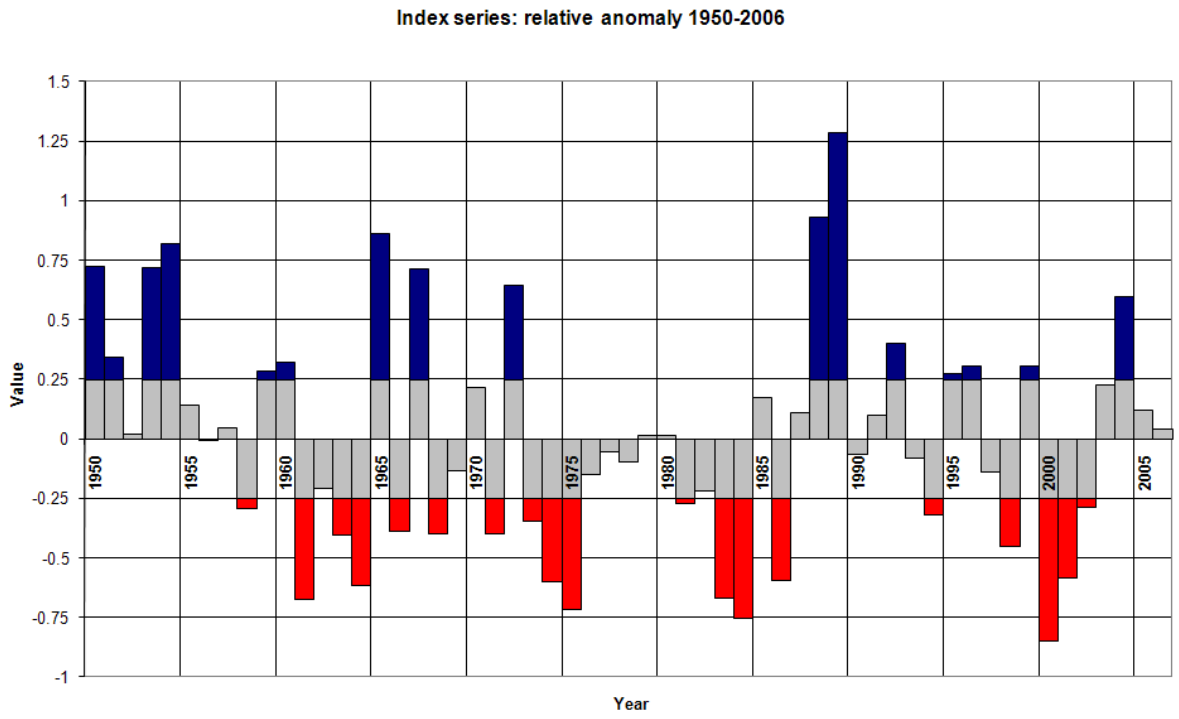

Figure 68 Relative Anomalies for station OZZ (Source: Kai Born)

The larger dry (marked red) and wet periods (marked blue) indicate large inter-annual variations, which have a great impact on food production systems (i.e for the sub-Saharan system: Nicholson et al, 2006; Benson and Clay, 1998).

In conclusion it can be stated that the precipitation variation is stable over the last 30 years. The precipitation fluctuations over the last 50 years are an alteration of dry and wet years, but always with reliable precipitation

6.1.4 Transpiration and Evapotranspiration

Using the formulas described in Chapter 5.6, transpiration rates, like PET and ET, was calculated. These rates are an important factor for the percentage loss of water for plants (comp. (Kolb & Sperry, 1999) and used in the ANPP module.

Looking at the N-S profile, an increase in the total sum of PET from North to south can be seen (Figure 71). The TZT station has great standard deviations because of failures (due to vandalism).

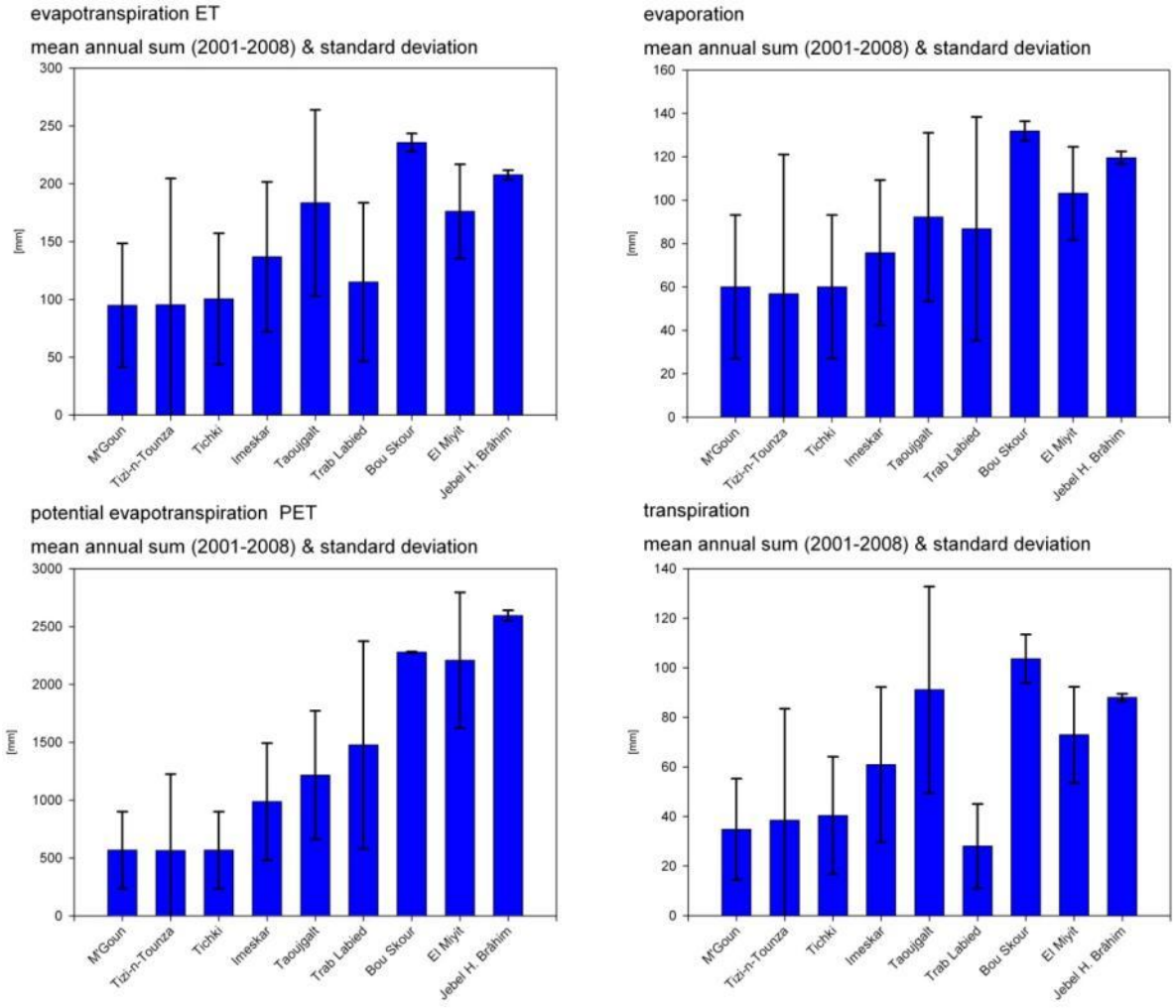

Figure 69 mean annual sums ET, PET, evaporation and transpiration rates with their standard deviation forselected stations. Note: Tizi-n-Tounza Station inherits noncredible data

One interesting fact is the increase of transpiration rate when going southward. The only exception is Trab Labied, which has a very low vegetation cover. Notice that the really substantial standard deviations occur due to cloudiness, wind and exposition. For example in JHB, you see a very small standard deviation. One reason my be that JHB station is a south oriented, small vegetation cover and high net radiation area. This caused a very small variarion throughout the year, which is reflected in the measured data.

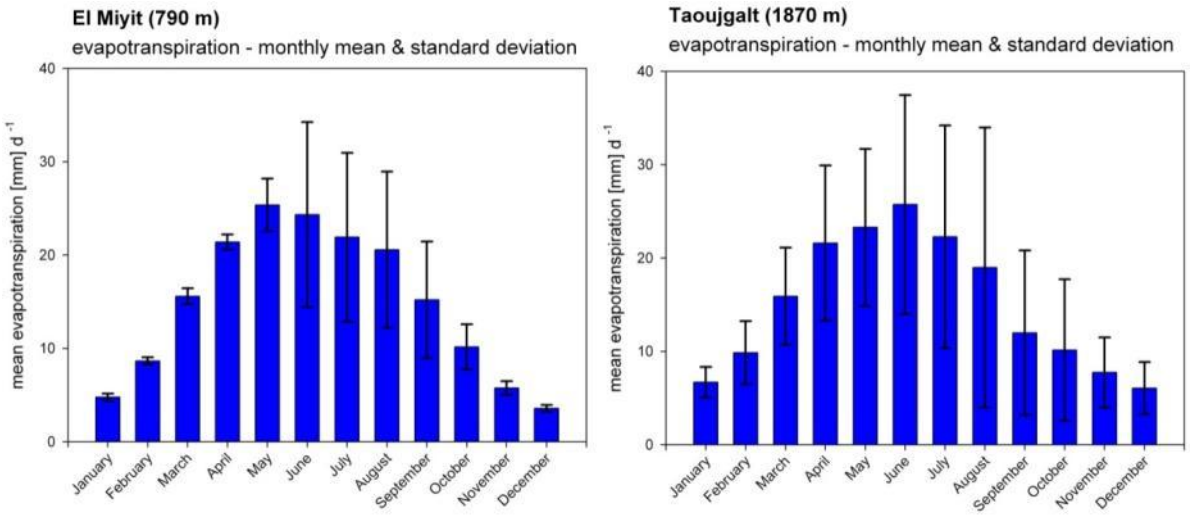

Figure 70 Evapotranspiration stations TAO and EMY

When looking at the TAO station one can be notice that the greatest ET occurs during May. This shifts to June for the southern area of EMY (Figure 70).

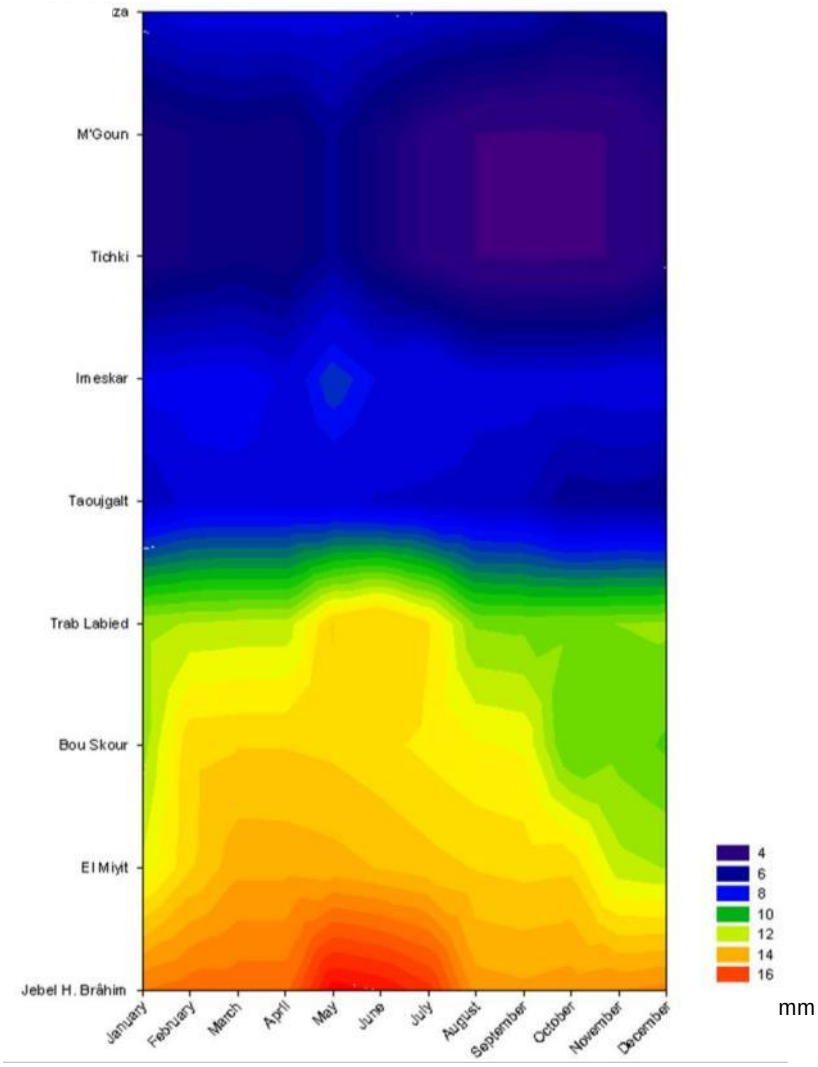

Figure 71 mean daily sum Potential Evapotranspiration [mm]

The calculated pattern of ET (Figure 71)reflects the N-S profile and the seasonal peak (June-August). Although the calculated values for the Atlas mountain range are less seasonal than rates calculated for the basin of Ouarzazate (TRL) and southward, there is, as expected, an notable increasing inside the catchment.

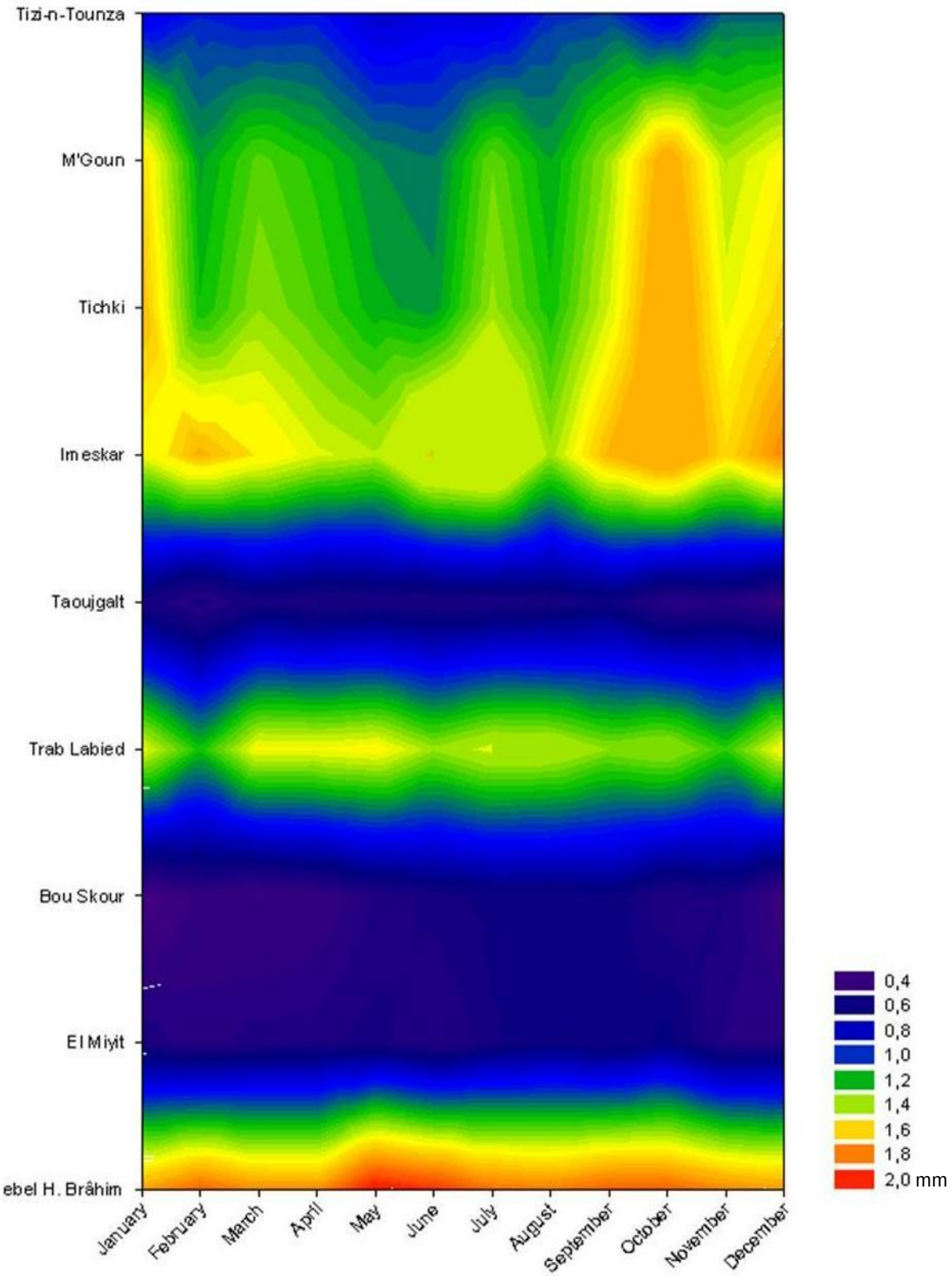

Figure 72 daily Evapotranspiration [mm]

This trend is turned for the evaporation rate (Figure 72) with a more seasonal signal for the atlas mountain range. Although the N-S profile is more dominant then in PET, the clear breaking is shifted from TRL to TAO station. The calculated ET reflects the presented vertical altitude profile of the vegetation signal (comp. MODIS NDVI4.2.1).

6.1.5 Radiation

The mean short wave net radiation, a standard measured parameter, is an important parameter to estimate the radiation balance.

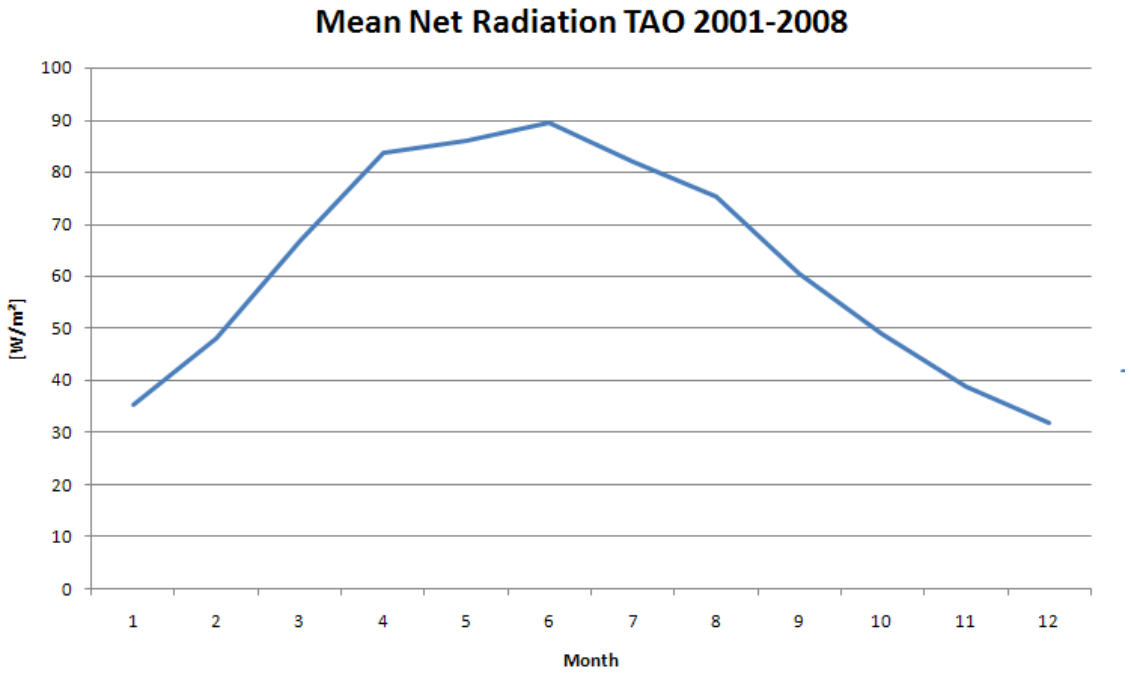

Figure 73 monthly mean Net Radiation TAO station

The measured seasonal trend of the measured radiation (Figure 73) peaks during June and is lowest in Dec/Jan. The yearly cycle of the inclination angle, which reaches its peak during June/July is, as expected, repeatable by the measured values. The net radiation, or radiation in general, is the driving factor for plant productivity. Due to failures during operational time this factor is not used for productivity calculation. Instead an atmospheric radiation model is used to simulate the energy input on the system (see chapter 6.6.).

6.2 RCN Results

The RCN module is designed to calculating the actual soil moisture depending on precipitation and preliminary moisture. Although it was designed to calculate runoff, the Run-Off Curve number is the most important module to calculate the plant available water.

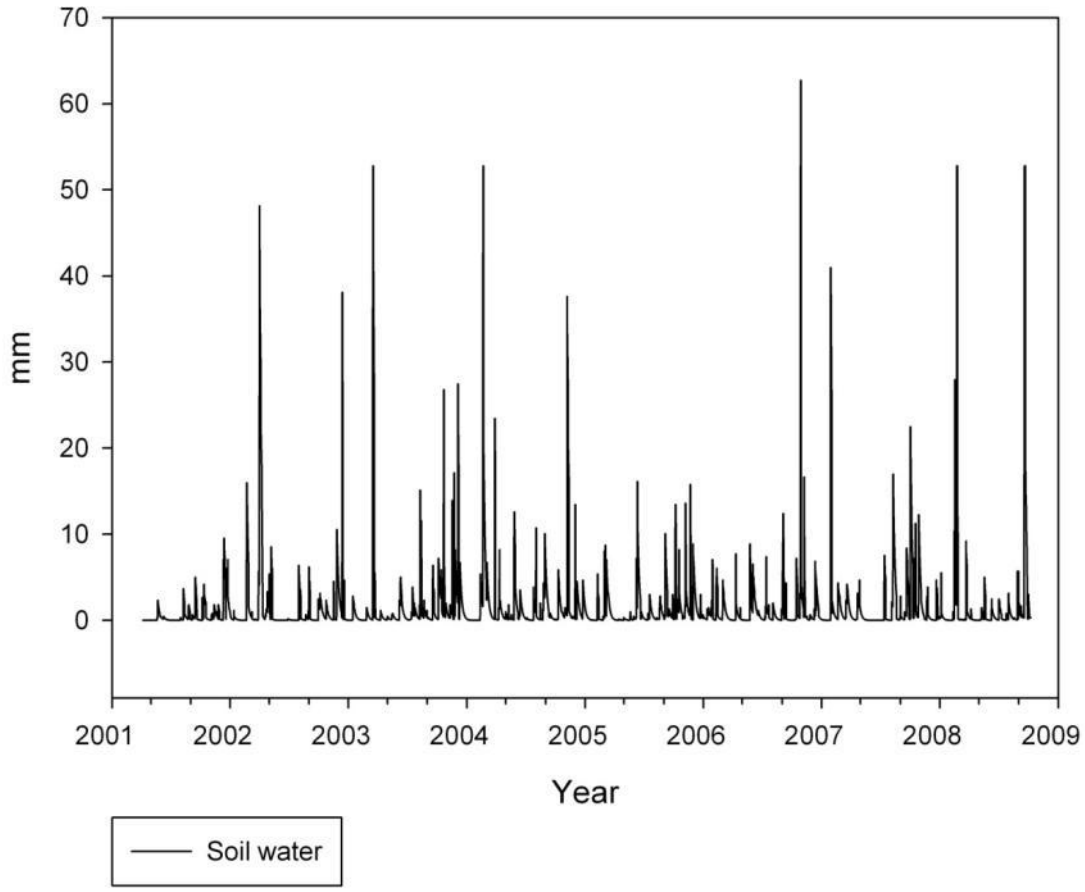

Figure 74 RCN IMS Station (16 day)

The module calculates soil moisture from 2001 (start of the climate measuring) until the end of 2008 as a 16 day sum. This sum is the available water to plants. The predicted values (Figure 74) are fluctuation and representing the great amount of storable water.

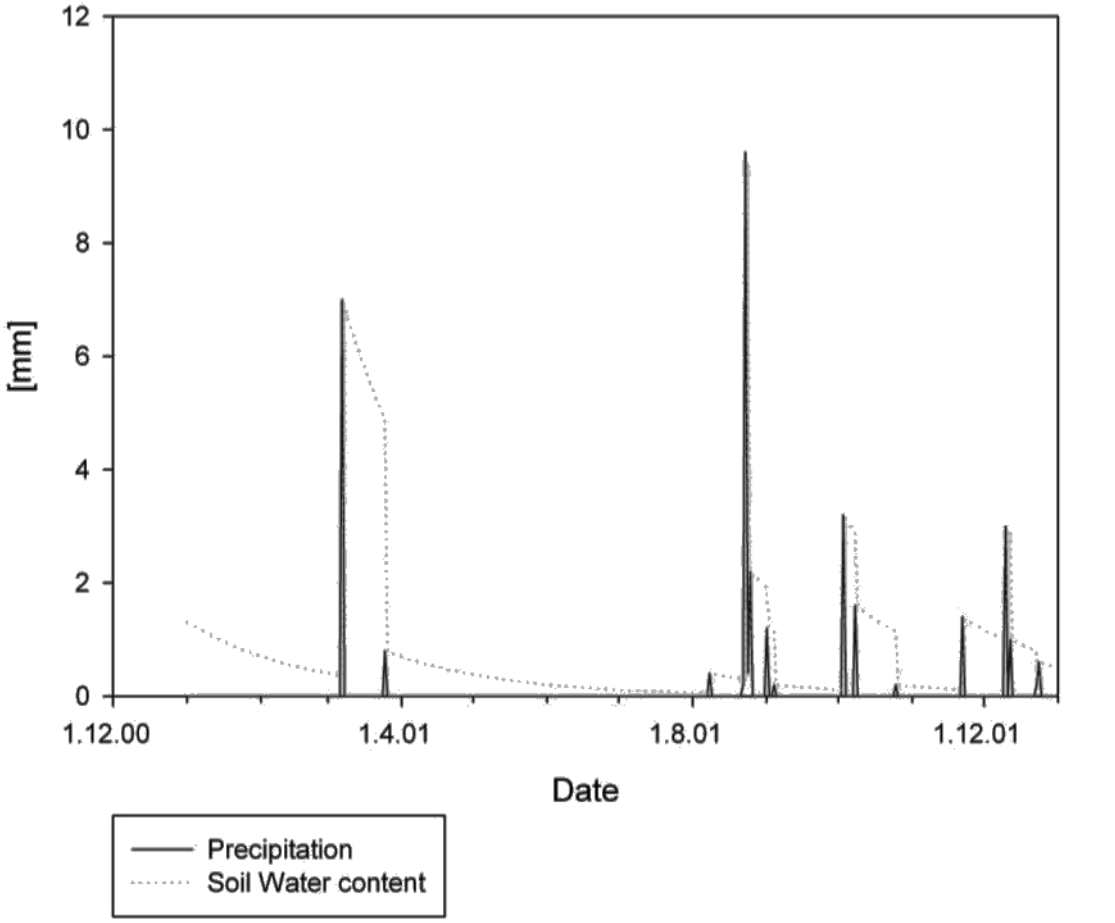

Figure 75 Function of RCN for station EMY 2001

Soil water as function precipitation indicates the amount of water inherited by an soil profile, defined by the amount of water capacity (AWC). The damping effect is to the evaporation, based on the calculation (Weber, 2004).

Since there is no other soil moisture available, since (Weber, 2004), a comparable validation method has to establish. RCN originally calculates run-off, it is possible to validate the model with other hydrological models. The SWAT calibration for the upper catchment of the valley Drâa (Busche, 2009), integrated in the IMPETUS ISDSS HYDRAA, are served as validation data

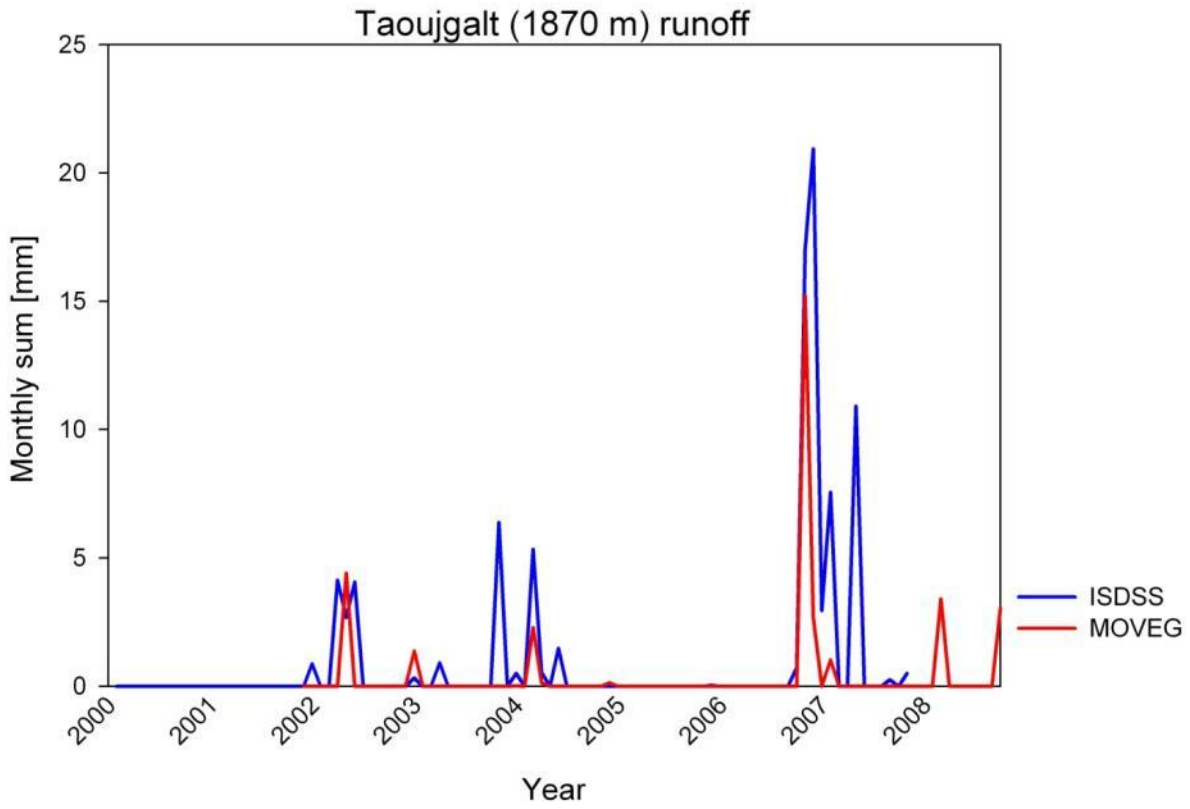

Figure 76 Compare ISDSS and MOVEG Drâa for TAO Station

The runoff, calculated by both models, differs significantly. MD always underestimates the runoff by SWAT (Figure 76). This overall underperformance reflects in the different driving factor of precipitation (comp. Figure 77).

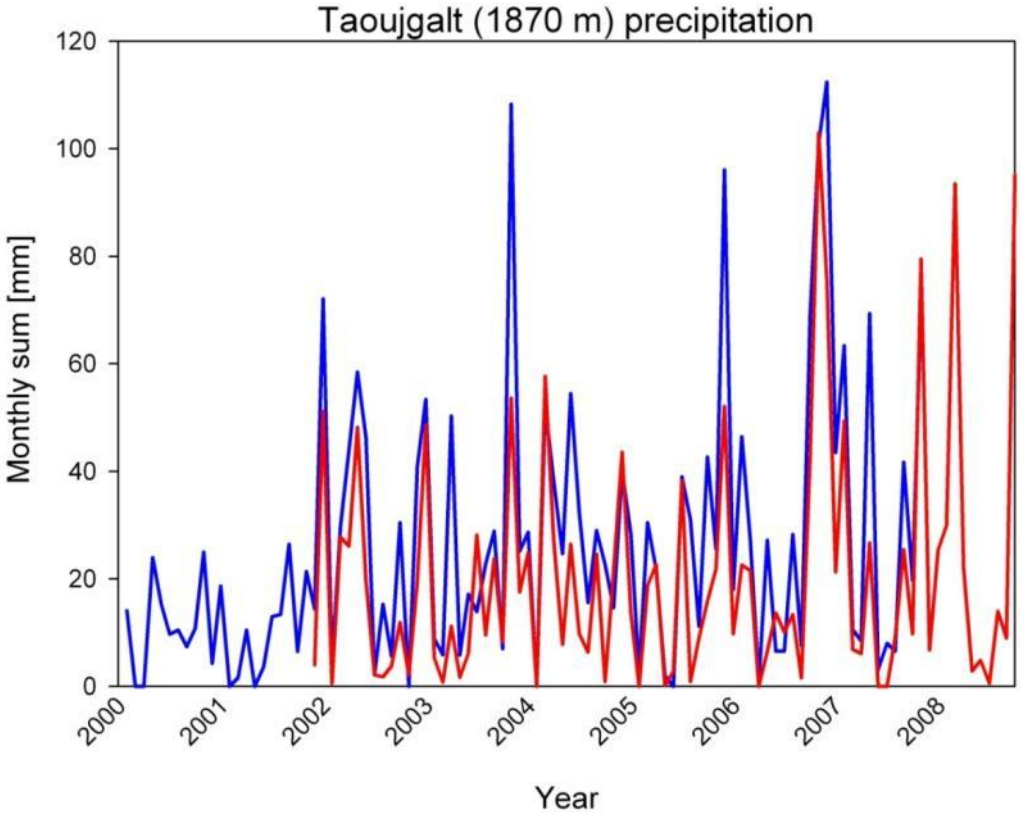

Figure 77 Compare Precipitation of MOVEG Drâa and SWAT (note that MD only calculates until end of 2008)

SWAT calculates an altitude based virtual climate station, which is slightly different to the measured data. The principal higher rainfall (Figure 77) indicates SWAT approach to recalculate the measured precipitation to an slightly higher altitude sub catchment.

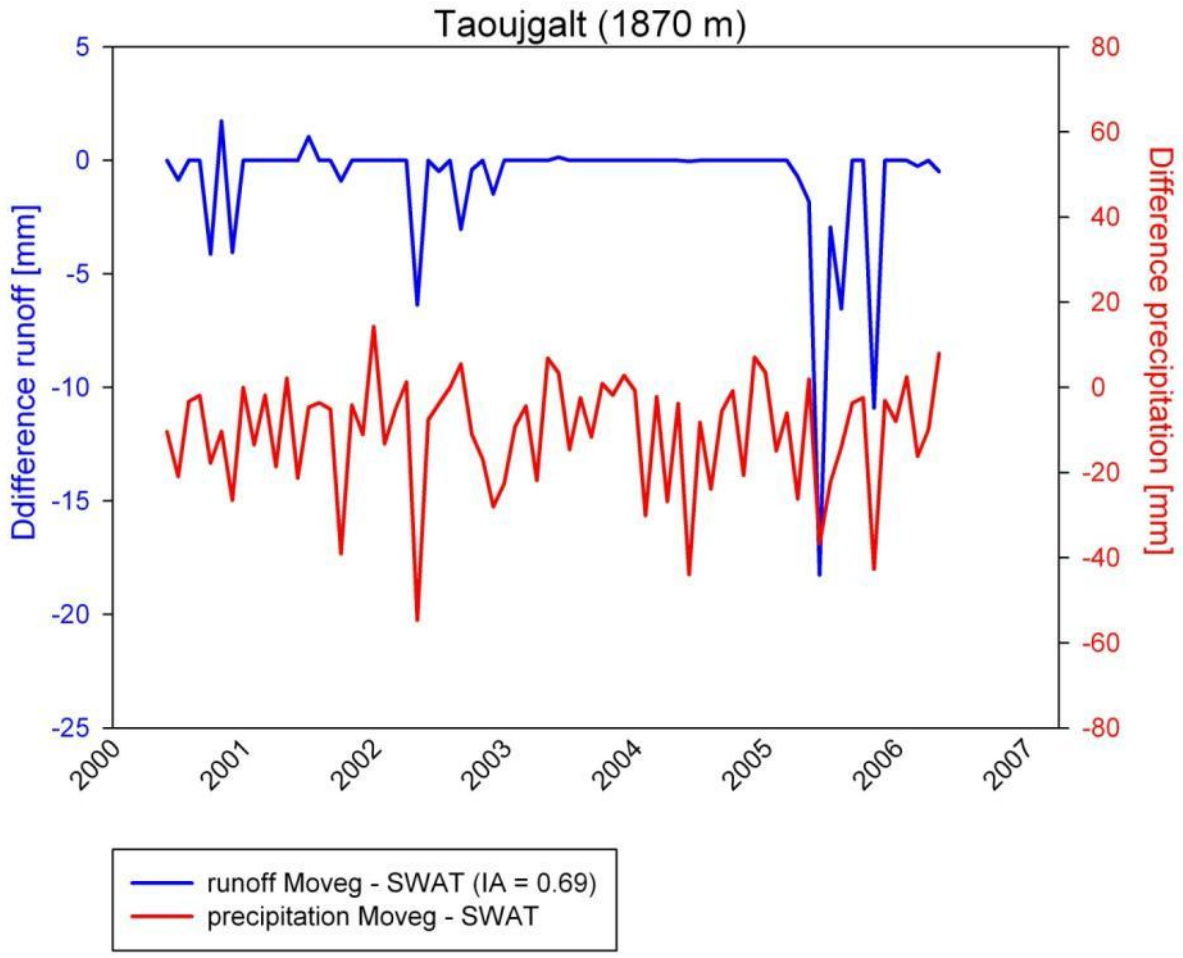

Figure 78 Difference MD to SWAT for station TAO

The compared result for the station TAO (Figure 78) and IMS (Figure 79), as proxy, indicates a significant coherency between both models.

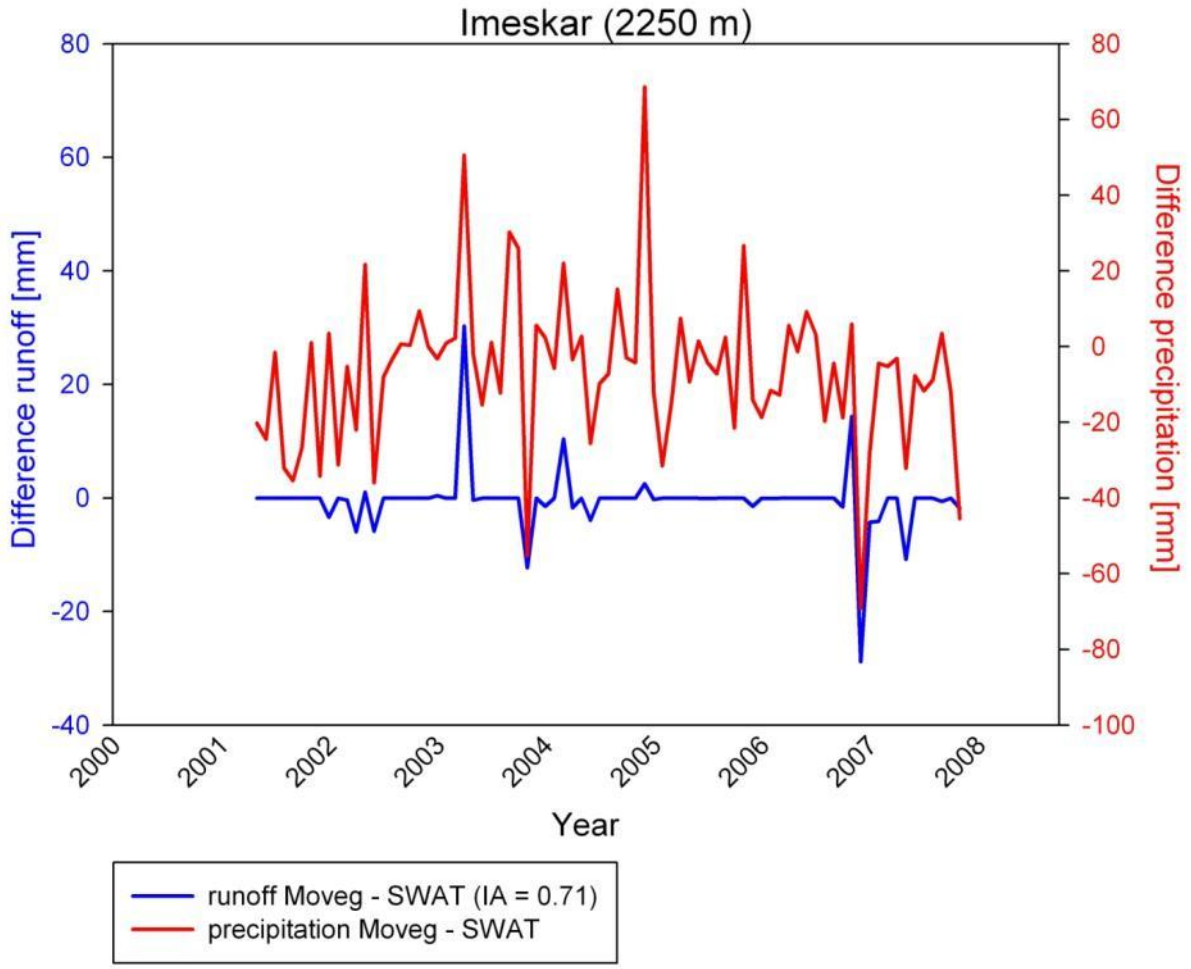

Figure 79 IMS Precipitation Runoff difference between ISDSS-MOVEG

The RCN module results described in this chapter is intended to calculate the amount of available water in the soil profil. The temporal agreement for all stations ranges from an IA of 0.71 to 0.5., providing exact information about the amount of water for all investigated stations. Our RCN algorithm are calibrated for the stations inside the investigation area by the measured values and cross-validated with SWAT model results. The results seems to be highly robust, as it not depend on a particular soil typ or set of field measurements,as used on the stations.

6.3 Temporal and spatial calculation on the Vegetation cycle and Land Cover dynamic

6.3.1 Lag Results

Precipitation in the rapid growth stage is important for vegetation activity in both stages (under the assumption that precipitation impacts the vegetation activity in the rapid growth stage, and there is not a large time lag and precipitation 1–2 months before the mature stage impacts the vegetation activity in the mature stage (Schultz and Halpert 1993; Miyazaki et al. 2004)).

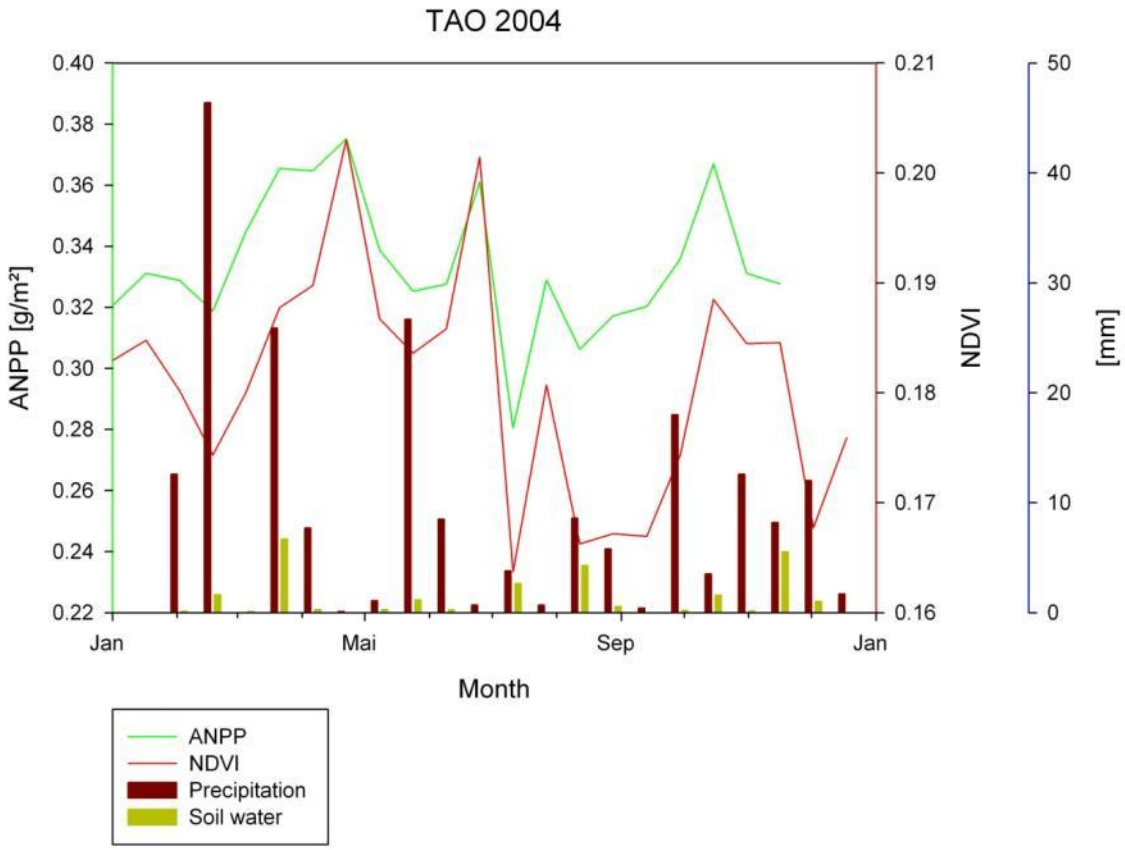

Figure 80 TAO Station monthly distribution of plant relevant parameters

Lag as described in Chapter 5.9 is here displayed as a number of scenes (16 days) during which the delayed reaction occurred. The Lag factor is calculated as a yearly factor for every vegetation period, which are defined from September to August.

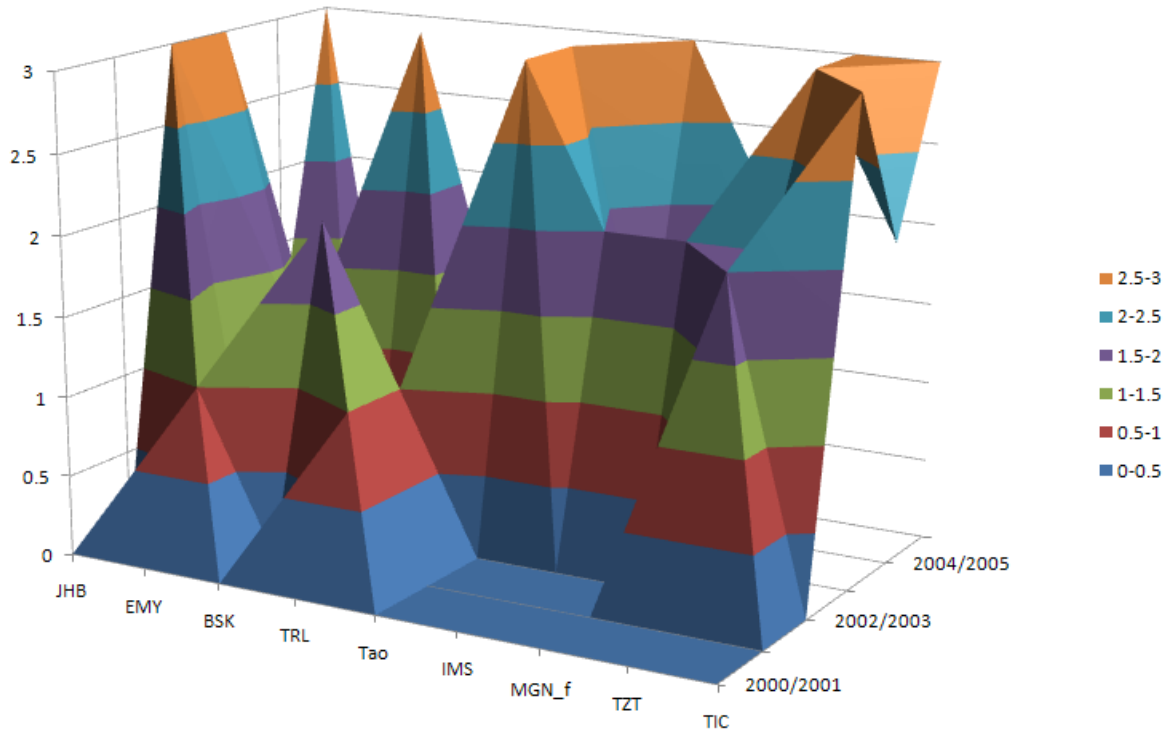

Figure 81 LAG factor for phenological years 2000to 2005 (dimensionless)

Lag is seen as a temporal and spatial calculation of the vegetation cycle, under the presumption that rain is one of the driving factors for land cover dynamic, for a given rainfall input. Using the maximum co-variance method it can be shown that most of the moisture given by rainfall is correlated to a vegetation growth offset of 16 to 32 days. This means that rainfall is converted to vegetation activity with a delay of roughly half to one month. This must be seen in the context of plant nutrification documented in chapter 5.9. Figure 81 shows that the lag is increasing for the phenological years 2002/2003 and 2004/2005. This might be explained through a dry year 2001/2002 and more wet years afterwards.

Therefore the phenological reaction and the phenological cycle can be described as an reaction of temperature and precipitation.

6.3.2 Phenological Cycle

The phenological cycle can be displayed as a deviated product of climatologic data or as product of the earth observation systems. This chapter introduce the climatologic phenology.

The length of the vegetation cycle is a good indicator for describing the possibility of vegetation growth and therefore the activity period of a vegetation formation or location. This can be expressed as pluviothermic ratio (Emberger, 1939). Figure 82 shows the vegetation length inside the high mountain Atlas range. The Figure reveals two important things: Firstly, the decrease of total days of the vegetation length with increasing altitude. Secondly, temperature stress having relevance, since temperatures below 5°C are a significant limiting factor.

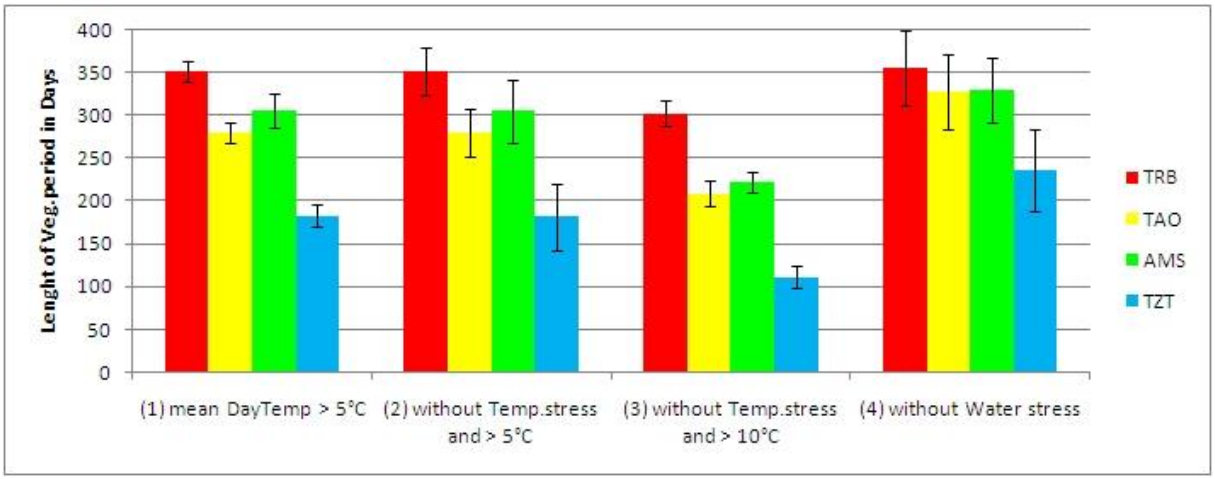

Figure 82 Length of the Vegetation period

Figure 83 shows us that the same data without water stress enables a significantly greater number of vegetation growth days. And it gives a short view on the TRB station. Water stress seems to be no significant problem there (Figure 83).

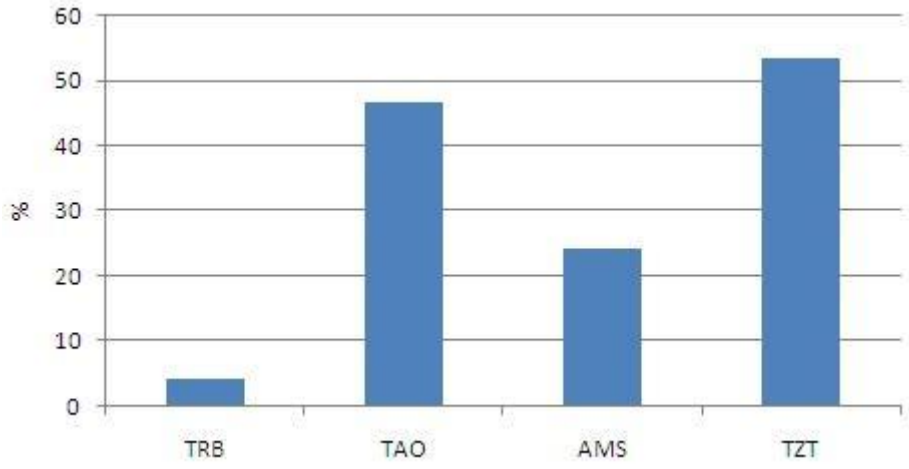

Figure 83 Difference % of Vegetation growth days without Water stress to normal Vegetation growth days (>5°C)

It can be concluded that number of growth day's whitout water stress is even higher inside the Atlas mountain range and very low inside the basin of Ourazazate. That means that the climatology derived water stress significantly dropped within stepping into the mountains.

Figure 84 shows an increasing Emberger index corresponding to altitude. .

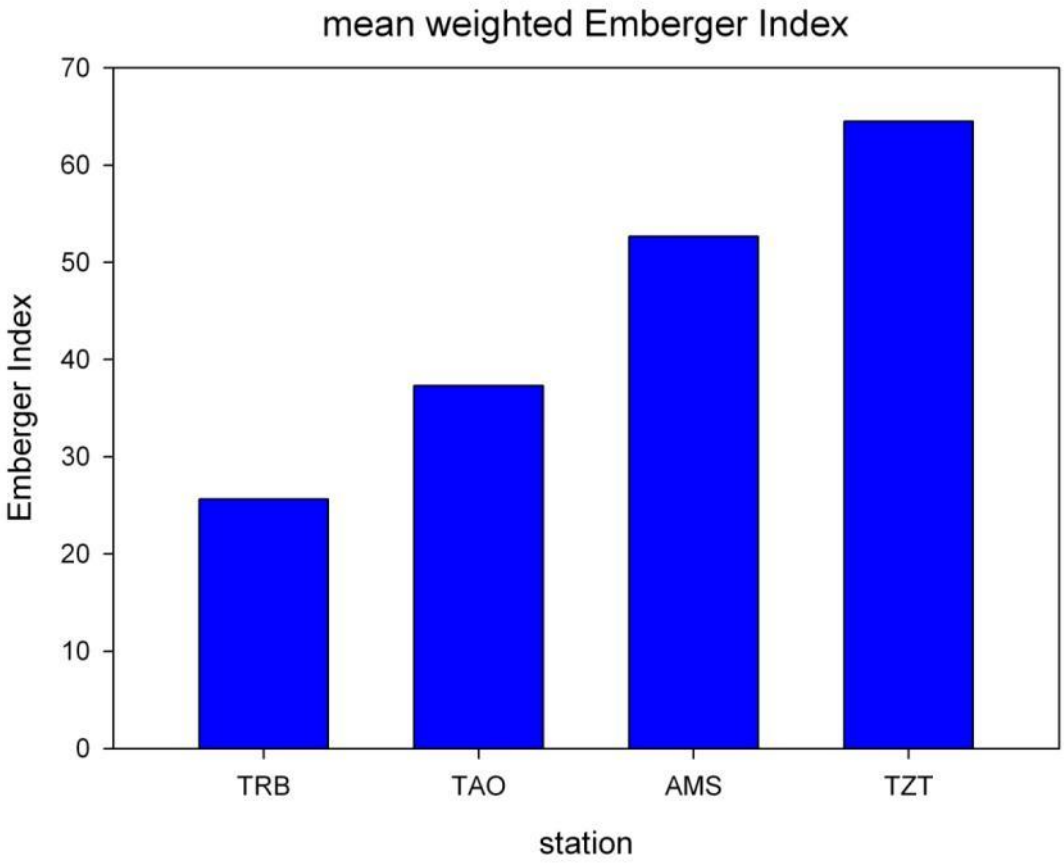

Figure 84 weighted mean Emberger Index

With increasing altitude an raising Emberger Index can be stated (Figure 84). This is confirmded by the Aridity index.

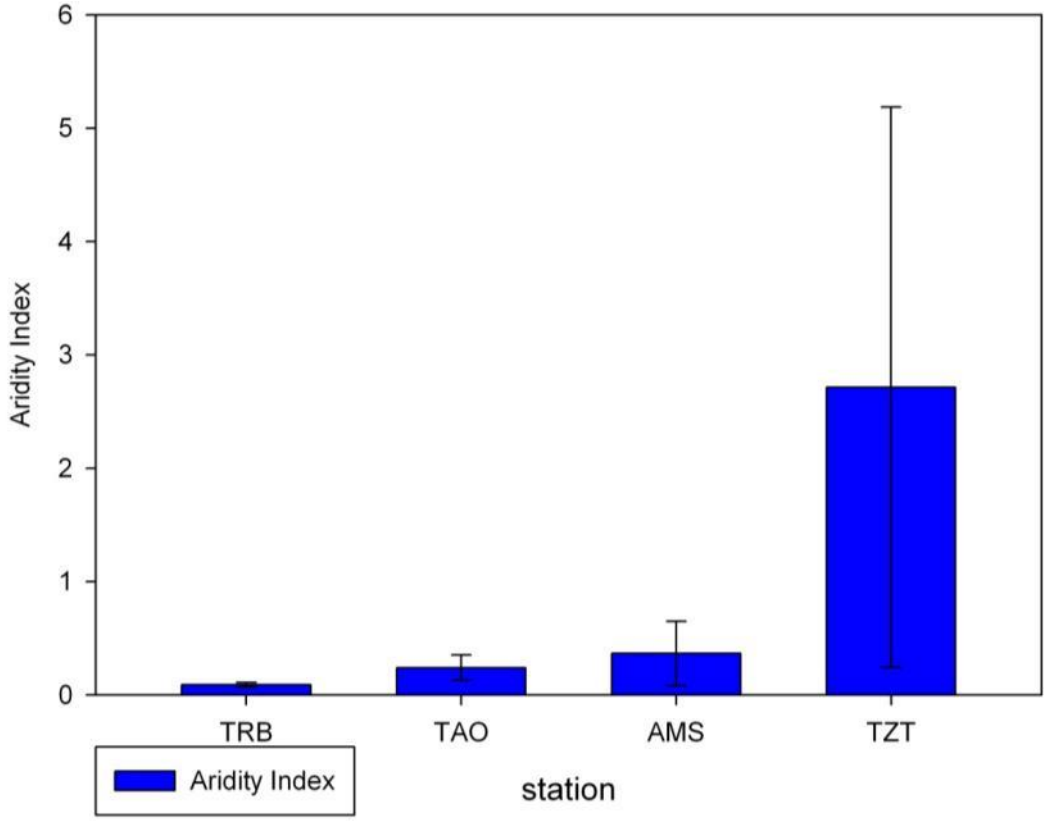

Figure 85 Aridity index (2001-2008)

The Aridity index at Figure 82 and Figure 85, calculated after Middleton and Thomas (1997) stated that the vegetation length actually decreases with altitude and aridity also rises with altitude. This can be explained not only by rising water stress (Figure 84) but also by higher water variability with higher relief energy and therefore faster drying of top soil because of lower soil profiles (see also Klose, 2009).

This is of relevance for land use, because a higher stress factor (comp (Baumann, 2009) for vegetation suggest a differentiated land use.

6.3.3 Vegetation Cover Calculation

The vegetation cover calculation is based on the monitored ground truth points (comp. Chapter 4.2.1). As stated in Chapter 5 the regression approach should reflect the relationship between different NDVI and their corresponding total ground cover. This is done automatically inside the module. Table 6 shows an example of the Geodata base excerpt for the station EMY.

Table 6 EMY Ground Cover data

EMY			
	Date	**Vegetation Cover [%]**	**NDVI**
P2	08.03.2007	7.5	0.1027
	06.09.2007	5	0.0977
	05.06.2008	5	0.0890
	01.10.2008	2	0.0865

Table 6 shows the acquired data for the ground truth point P2, which is very near to the climate station EMY.

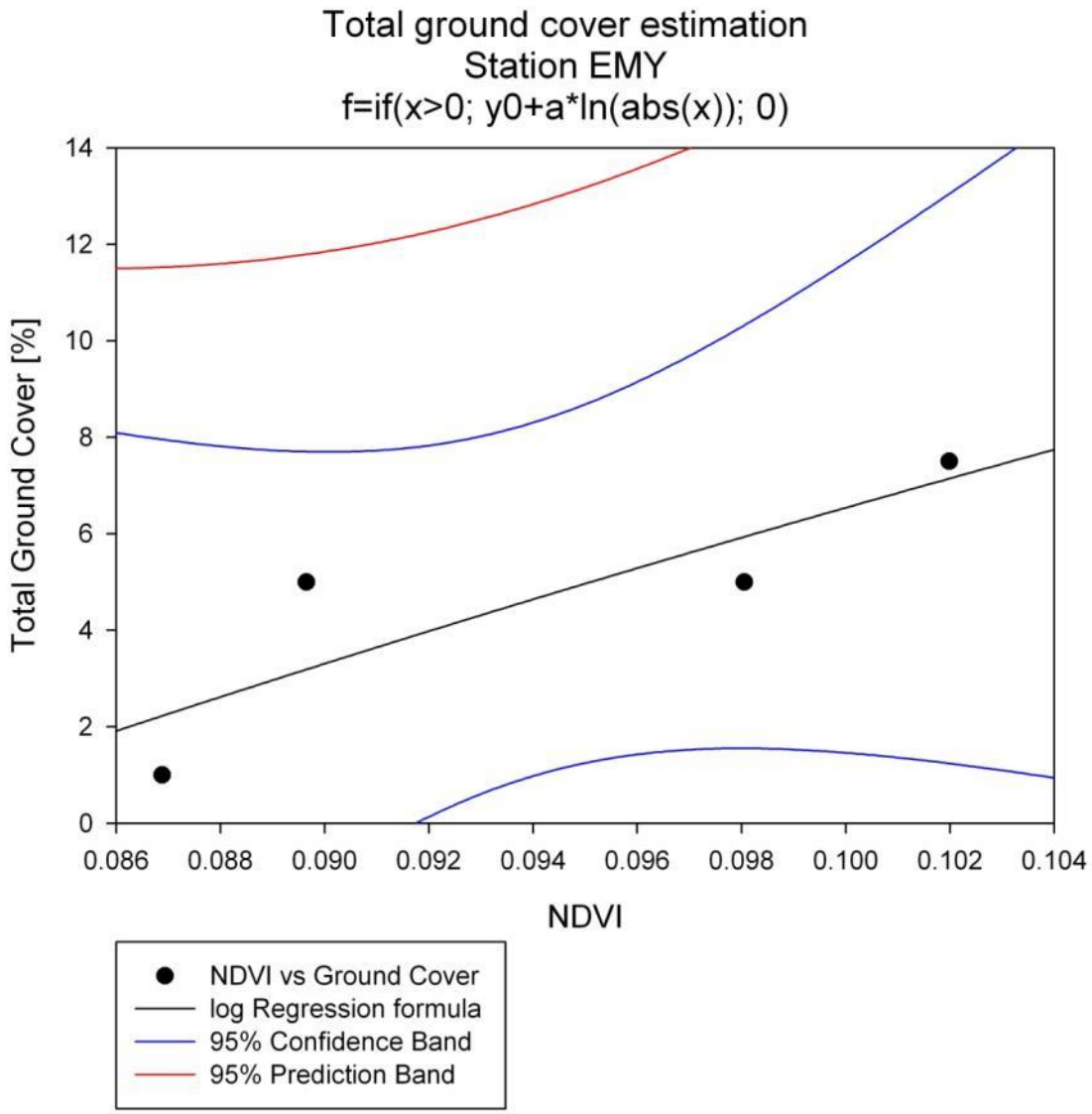

Figure 86 Total ground cover estimation for station EMY

It is now possible to use those four points per GCP to calculate a logarithmic regression formula. Why use a logarithmic approach? As seen in Figure 87 the logarithmic function approximates the asymptote to the maximum.

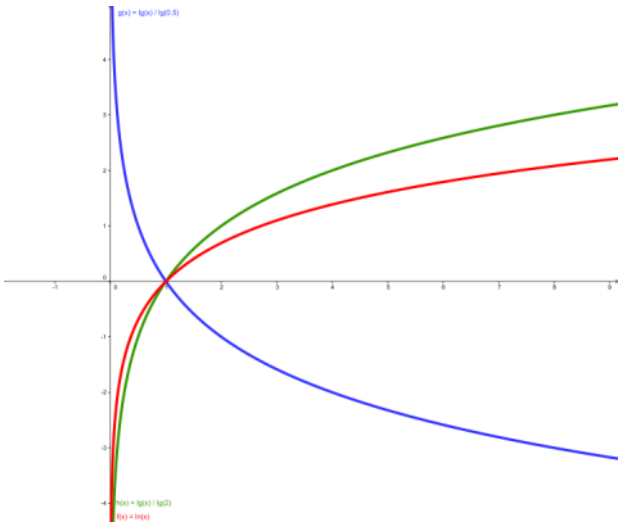

Figure 87 different Logarithm function(Source: (c) Marcel Marnitz) Colors are different functions

This is crucial, because buffering the vegetation cover against high NDVI is difficult (comp. (Bannari *et al.*, 2002;du Plessis, 1999;Geerken & Ilaiwi, 2004). It is neither plausible nor logical that the vegetation cover extends maximally. In this case the maximum vegetation cover is 62.819 % if the NDVI is 1. The quality criterion for all stations is listed below. The complete list of all points is available at the appendix.

Table 7 Quality Criteria Cover function

Station	GCP	R
EMY	P2	0.73
ARG	P1	NaN
TAO	P26	0.74
BSK	P10	0.39
MGN_f	P43	0.2
TZT	P32	0.97
TIC	P37	0.98
IMS	P39	0.99
TRL	P19	0.86
IRK	P4	NaN
JHB	P3	0.44

The calculation itself is a non linear iteration approach getting the data from the database and a corresponding image by using the formula Y=theta*ln(x)+theta. The results are acceptable for most stations. Unsatisfactory stations, like MGN_f and JHB are explained by their terrain and vegetation configuration. The JHB Station for example is a very thinly vegetated station in a rocky environment. The MGN and BSK Areas seem problematic because of steep hills and assumed high land use pressure.

6.3.4 Leaf Area Calculation

The Leaf Area (LAI) calculation was not available through the standard NASA Land product series since NASA declared most of the natural vegetation area as bare surface/desert and therefore with a vegetation cover of 0, which is wrong.

The Lai is described as leaf area (m²) per ground area (m²). In today's remote sensing literature numerous approaches exist (Burrows *et al.*, 2002;Carlson Toby N. & Ripley David A., 1997;Carlson & Ripley, 1997;Chen Jing M. & Cihlar Josef, 1996;Foetzki, 2002;Law Beverly E., 1995;Myneni *et al.*, 2006;Patenaude *et al.*, 2008;Qi J. *et al.*, 2000;Tian *et al.*, 2004;Turner *et al.*, 1999;White Michael A. *et al.*, 2000;Wisskirchen, 2003). There are other, non remote sensing, scientific approaches like (Diekkrüger, 1996), which are determined by

Equation 18 LAI Diekkrüger (1996)

$$LAI = \frac{ln(1 coverdegree)}{-0.4}$$

This Diekkrüger approach is based on the ground cover and seems predestined. Nevertheless an approach after (Myneni *et al.*, 1995b) was also tested. It determined a specific leaf area index (leaf area (m²)/leaf mass (kg) from field measurement.

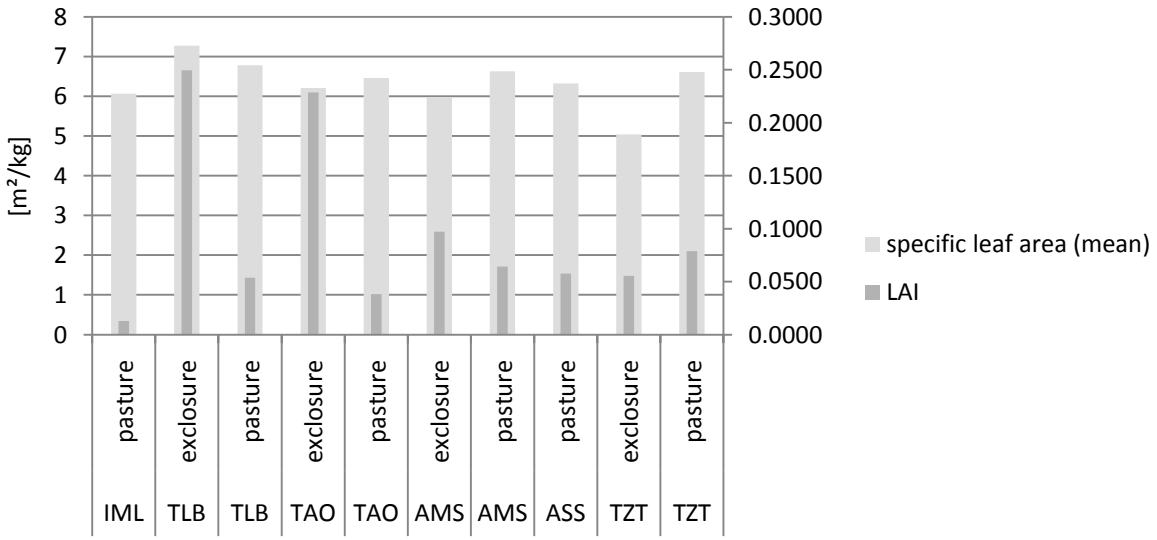

Figure 88 SLAI and LAI comparison (Source: Baumann (2009))

By using the approach of (Myneni *et al.*, 1995c) it was possible to develop a specific approach, which is separated into separate altitude steps of 400 - 1200m,1200-2300m as well as above 2300m (Figure 89).

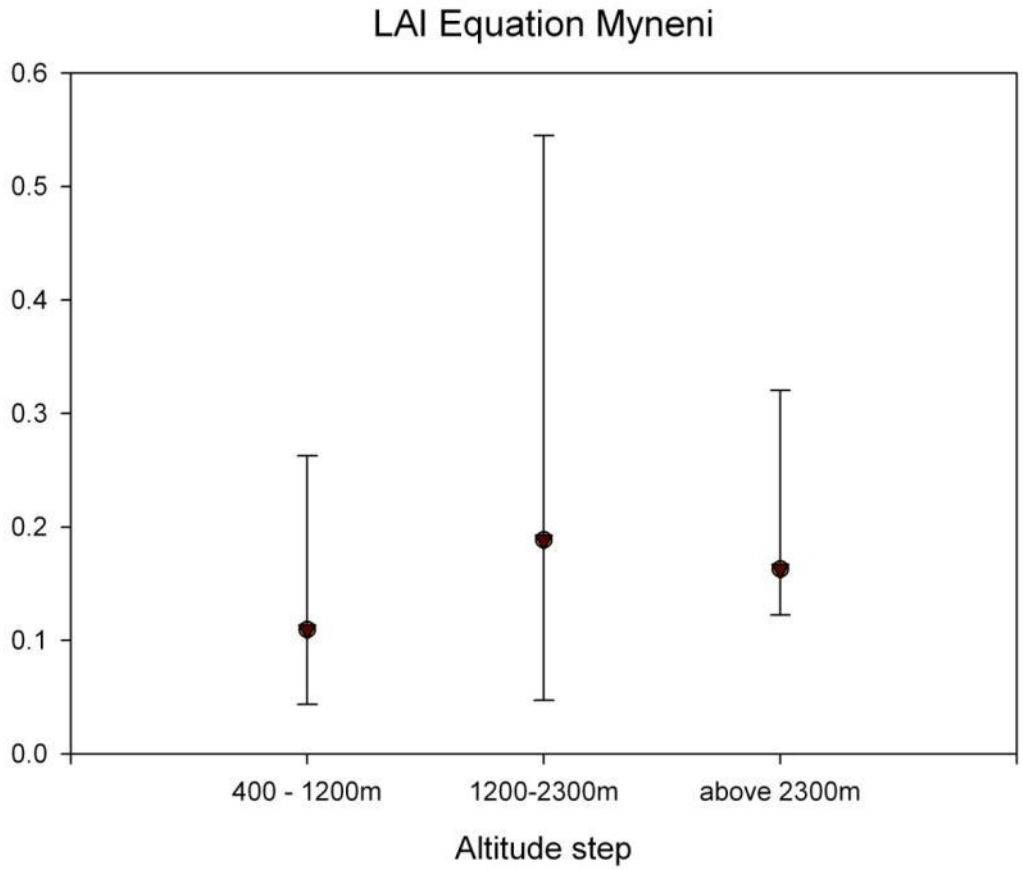

Figure 89 LAI approach after Myneni (see text)

Since LAI is coupled with the standing biomass (Figure 90), a great variance in biomass between 1200 to 2300 m and in the quantiles of the biomass which might explain the higher median in Myneni approach for this area.

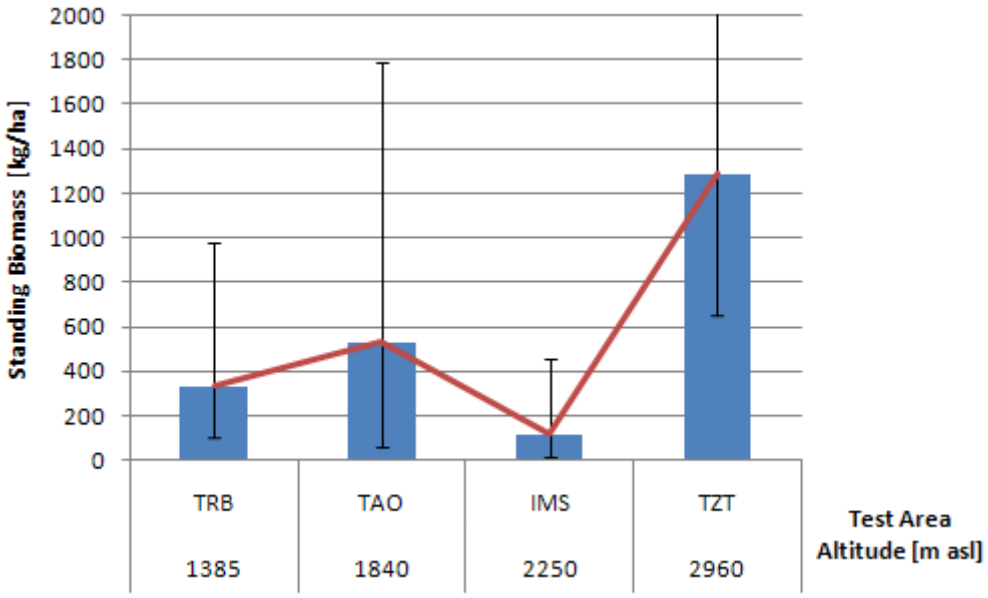

Figure 90 Standing Biomass for grazed Areas (Bauman Testplots) (Source:Baumann (2009))

The overall performance by the Diekkrüger remains unsatisfactory, because of there high variation.

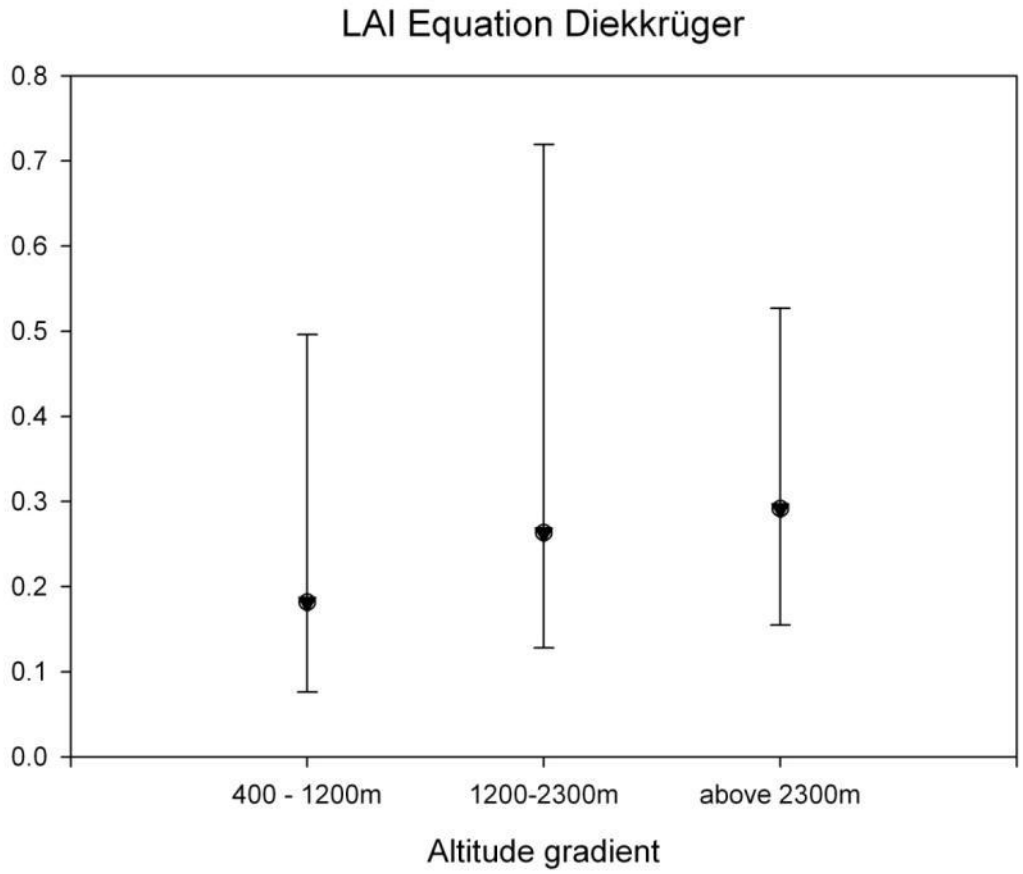

Figure 91 LAI Equation boxplots, calculated with the Diekkrüger approach for three elevations

Especially the great standard deviation makes this approach less useful. This can understood in greater detail through a comparison of both approaches and the LAI measured by Baumann (2009).

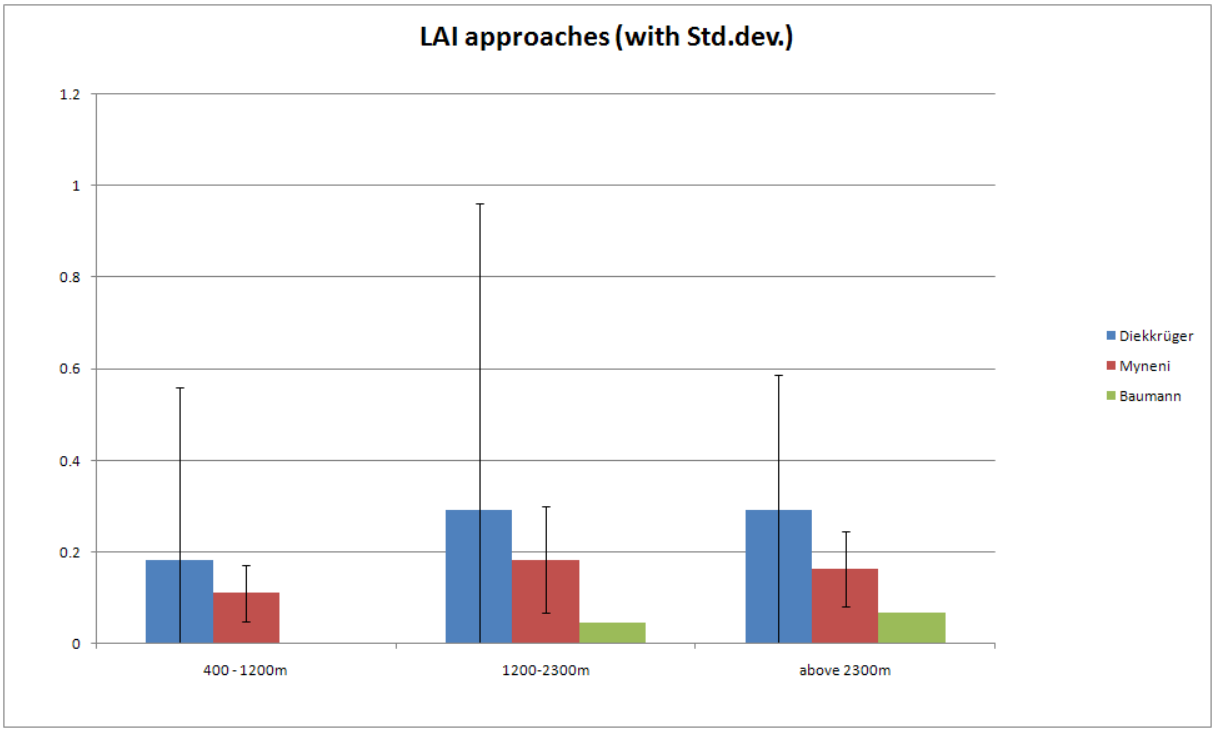

Figure 92 Comparisons of the 2 LAI calculation approaches (Diekkrüger and Myeni) and measured by Baumann (2009) in 3 different Altitude steps

The different methods for calculating LAI display that the measured LAI is significantly different from the calculated LAI's. This can be explained by two reasons. The measured LAI is calculated on the basis of about 60 of 300 species inside the area (oral, Baumann) and is only representative for all species that have leafs. That excludes mainly *Hamada spec* and *Juniperus spec* . Hama sccoparia is the name giving dwarf shrub in inside the area between 1200 and 2300m a.s.l. The Juniper tree and Chushion bushes inside the high atlas mountain range add a significant amount of LAI to the measured (comp. (de Jong *et al.*, 2008;Finckh & Oldeland, 2006). Baumann's LAI is a measure of the feedable (i.e. green) biomass and the Specific Leaf Area Index. The feedable biomass is calculated by a factor that represents the fraction of feedable biomass to total biomass per plot. This means that the factor is a mean average of all plants per altitude and use. The biomass per plot is calculated by another factor from the total cover of all species to biomass per plot. This factor is calculated by a regression of the investigation area, namely the high Atlas mountain cover and biomass. The specific leaf area index for every species is calculated by taking 10 individuals and 10 of their leafs. Knowing the mean SLA/per species and knowing the coverage of every species Baumann calculated the weighted SLA/per plot. The result is a mean value of SLA per altitude and usage (pastures or exclosure).

This is also calculated from two different sources. Calculating LAI from a remote sensing perspective means in this case to extrapolate LAI from the FAPAR and therefore from the NDVI. The NDVI represents the vegetation activity (Myneni et al., 2006). Therefore it represents the sum of chlorophyll that uses PAR radiation and is described by the fraction of the incoming solar radiation in the photosynthetically active radiation spectral region that is absorbed by a photosynthetic organism (Details are discussed in Chapter two and three, as well in chapter four).

By comparing degraded areas (25% percentile of all LAI in 3 different altitudes) of the Diekkrüger and Myneni approach (including Standard deviation) with the pastured median of the cage experiment, the difference is inside the standard deviations of the methods. This leads to the conclusion that the method of Diekkrüger is insufficient because of its relatively great standard deviation. The method of Myneni seems to be appropriate because it reflects a common method in remote sensing, has an acceptable standard deviation and represents the measured LAI under the circumstance that the measured LAI does not include all green active vegetation.

By using this approach it is possible to calculate the LAI for the whole catchment (Figure 93).

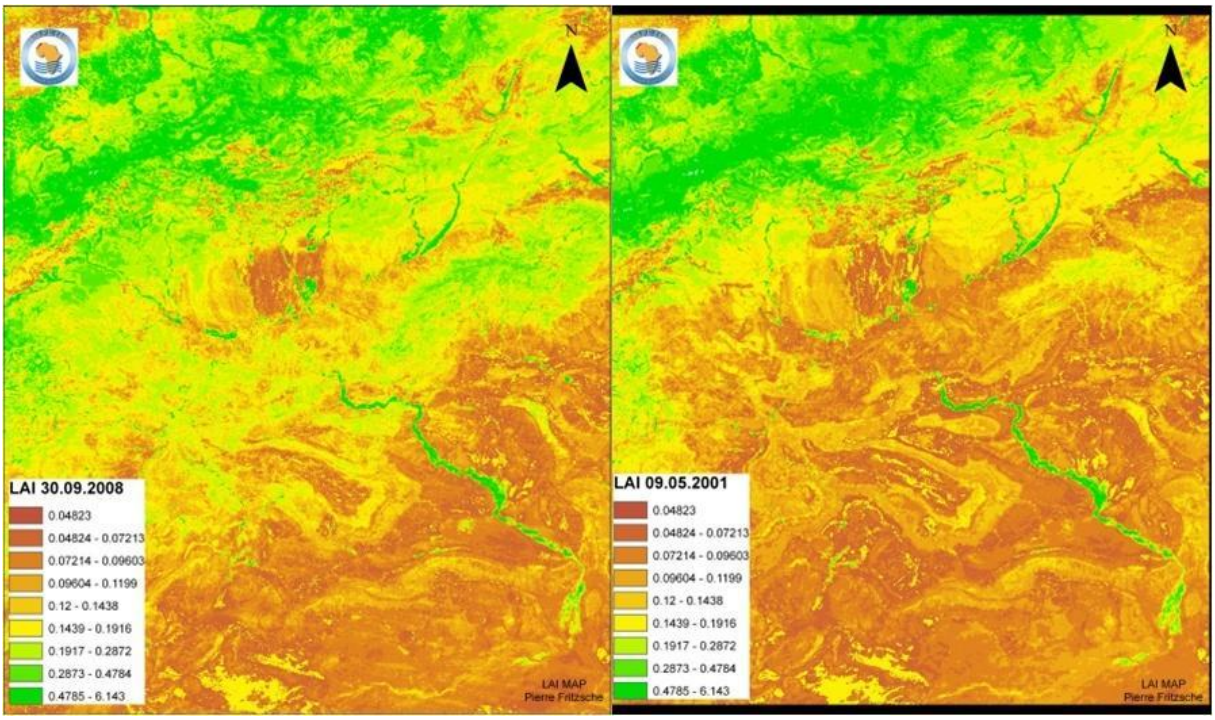

Figure 93 Result of spatial calculated LAI for a autum and a spring date after the Myeni method using the local adopted regression

The spatial analyse can be summarized for all stations by Figure 94.

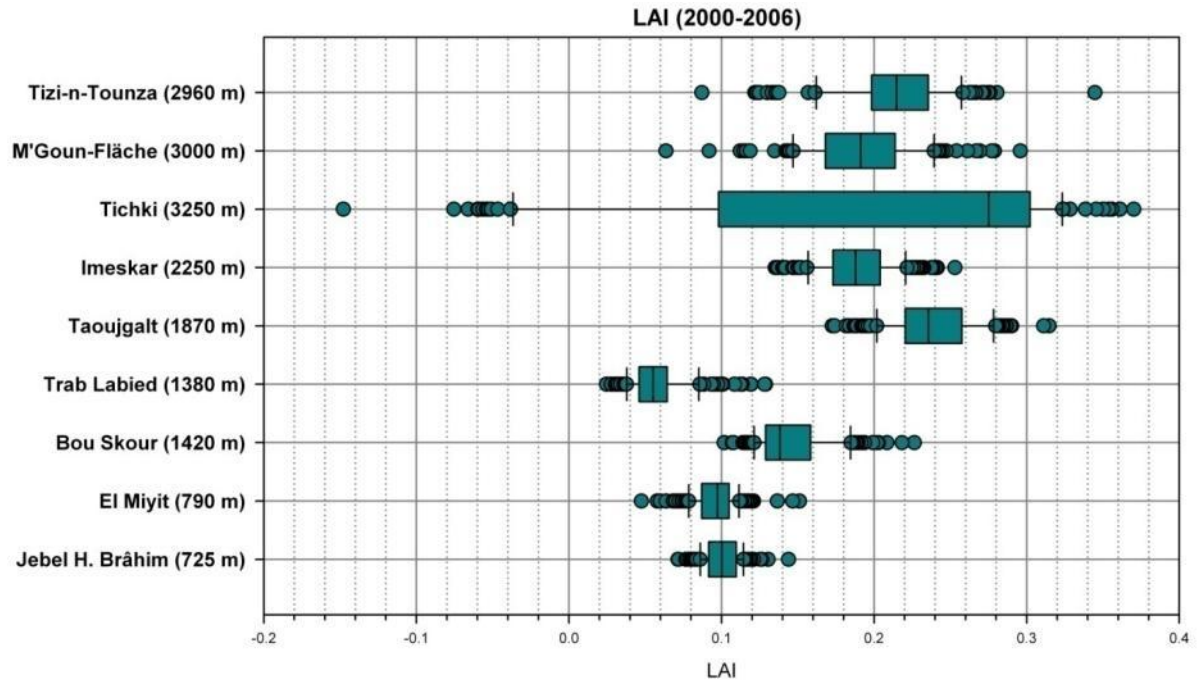

Figure 94 calculated LAI Box plots for all Stations for the period 2000-2006 after Myeni approach ,including all shadowed pixel which are clearly visible.

In Figure 94 it is visible that the high Atlas mountain ‘stations inherit a much larger variation than the more southern stations.

6.3.5 Carbon Fixing estimation

Carbon fixing is the process of accumulating carbon in stable organic matter. The carbon fixing approach was developed from field experimentation. Therefore the measured difference in standing biomass is taken and calculated in regression with the amount of PAR during the experiment time.

Table 8 Calculated C-Fix Factor

	NPP Experiment	DoM[11]	NPP/day	NPP in g/m²	Radiation	C-Fixing Factor
TRLG10	103.8	215	0.482983282	0.00482983	210.873095	0.005863418
TAOG10	48.2	217	0.221904847	0.00221905	233.298358	0.002434978
AMSG10	63.7	391	0.162857653	0.00162858	242.732462	0.001717593
TZTG10	195.2	388	0.50299855	0.00502999	147.947653	0.008703594

The result is the dependency of carbon fixing on incoming radiation. A first approach uses linear dependency as indicated in Figure 95.

A linear regression comes to its limit when encountering varying radiation amounts. To compensate this effect a decreasing, polynomial approximation was used. This function imitates the biophysical process of an optimal radiation process, based on the measured data. The results are shown in Figure 95.

[11] Days of Measurement

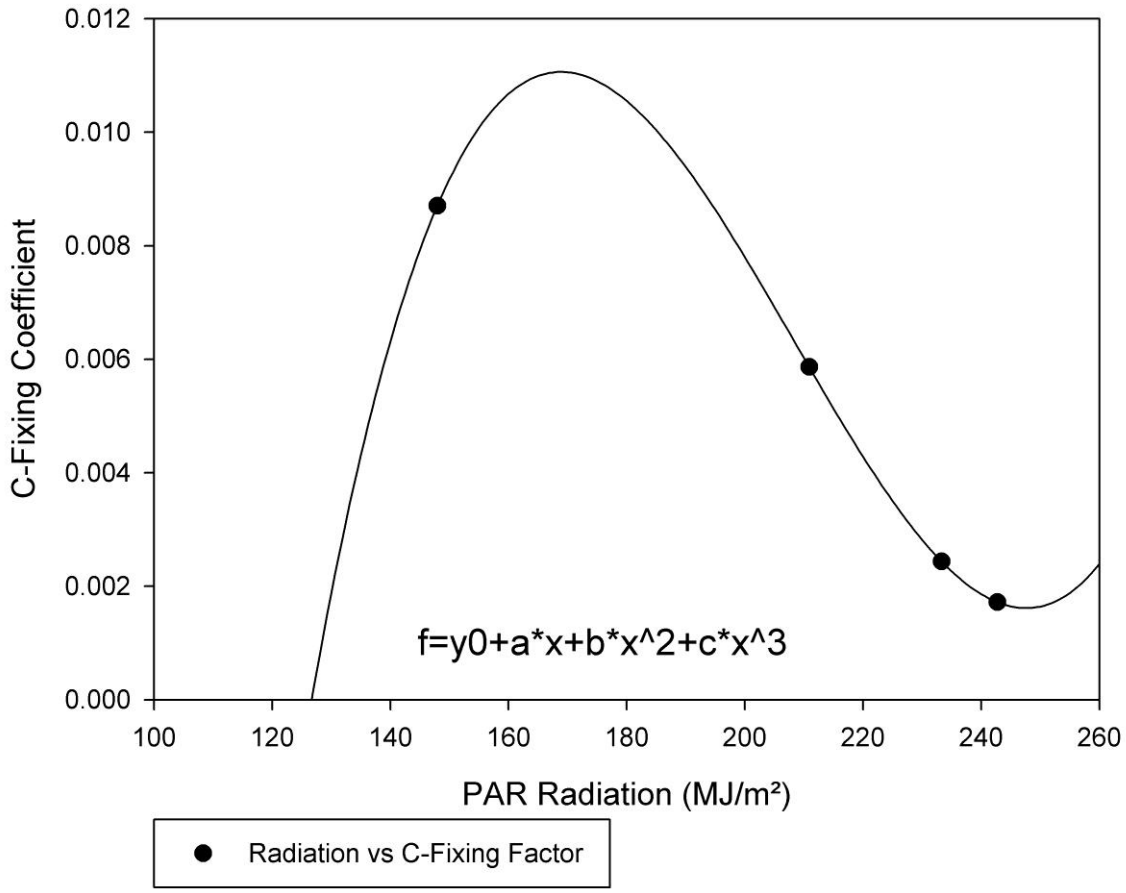

Figure 95 C-Fixing approximation whitout all erroneous data calculated after the field experiment

This approach has two restrictions:

It is limited to 125 and ~250 MJ/m² and the calculation of the maximum point is an approximation and is not regarded as universally valid or may not be effective outside the catchment.

First test indicated the calculated carbon fixing (or LUE) factor to be valid. This factor is strictly speaking only valid for the northern area of the catchment, but is used on all stations under the presumption that carbon fixing is stable over the whole region.

6.4 Pre Regression Results

First generalized linear model (GLM) tests reveals that the combination of rainfall, temperature and ground water seems to be a good approach to fit the data and is therefore used inside the regression formula. The ANPP is not used for forecast purposes because of its usage of meteorological data (like Evapotranspiration) and a possible collinearity. Furthermore the ANPP needs NDVI as an key input parameter.

Before starting the regression, the data needs to be checked for significance and other statistical data that could be preliminarily necessary for a regression. All tests that are presented here are encoded into the model and combined with statistical limits. This produces an error message if one test fails. In this way the user is able to analyze the error and fix the data or even drop the data set. An alpha level of 0.05 is used for all statistical tests. All input parameters are checked whether they are usable inside the regression.

As already stated the time period of 2000 to 2006 is used for calibration purposes, and 2007-2008 for validation purposes. The original NDVI signal (as exampled here for the TRL-station) can be described as Figure 96.

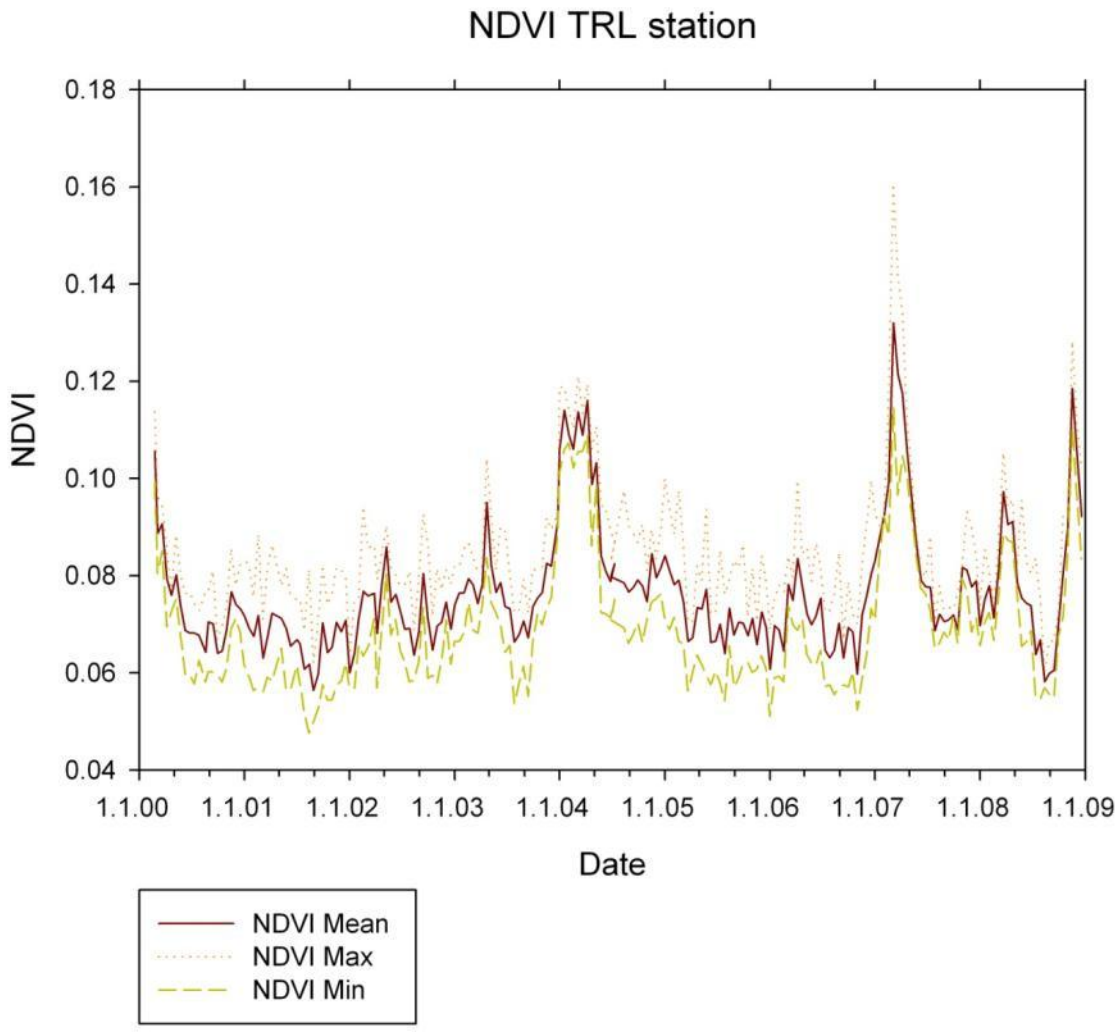

Figure 96 Raw - NDVI signal for the station TRL over the period 2000 until 2009 showing the inter-annual vegetation signal fluctuations

Since data harvesting for every station is taken from an bounding box near the stations, fluctuation is averaged but indirectly inherits the spatial fluctuation around the station. By taking the mean for every time step the temporal fluctuation can be shown in a box plot.

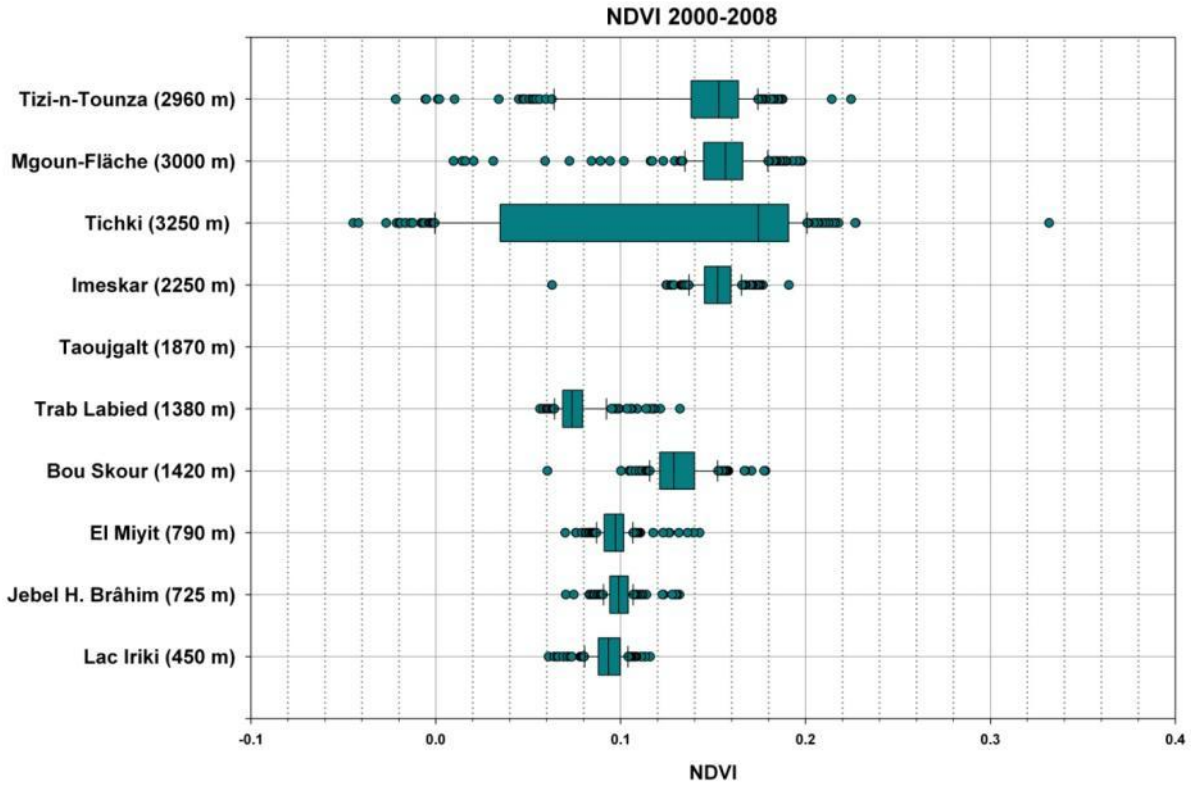

Figure 97 Raw (including erroneous pixels) NDVI Data for 10 stations along the N-S gradient

As Figure 97 shows the raw data entails some failures (below 0) and some stations, like Tichki, indicate a high amount of outliners and a high variance. This was used as base of the definition for the data filter, which is fixed to a double standard deviation. This eliminates outliners and improved the signal quality. With this applied filter, the data is checked for multicollinearity.

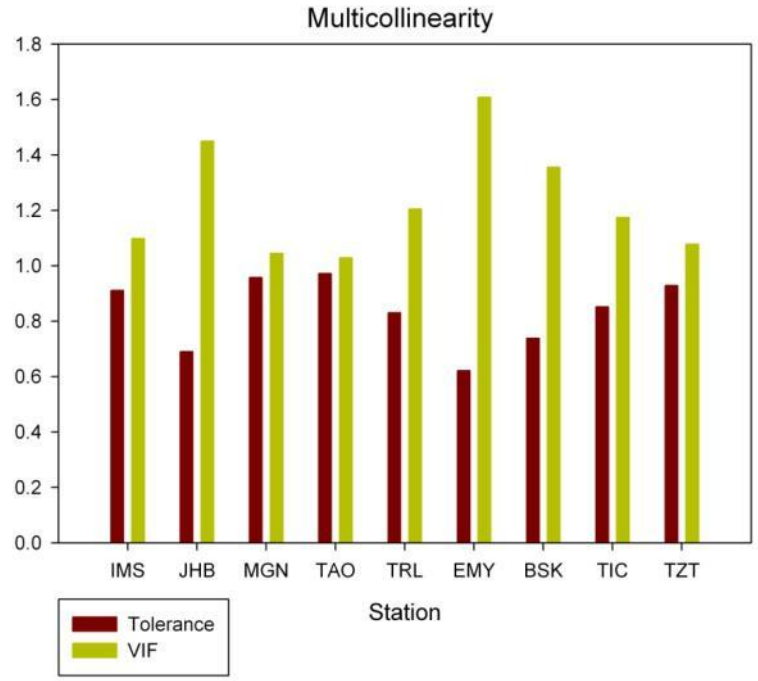

Figure 98 VIF and tolerance (method see chapter 5.10)

As seen in Figure 98 all data used is below a VIF of 5 and greater than 0.2. This enables the predictors realiabel.

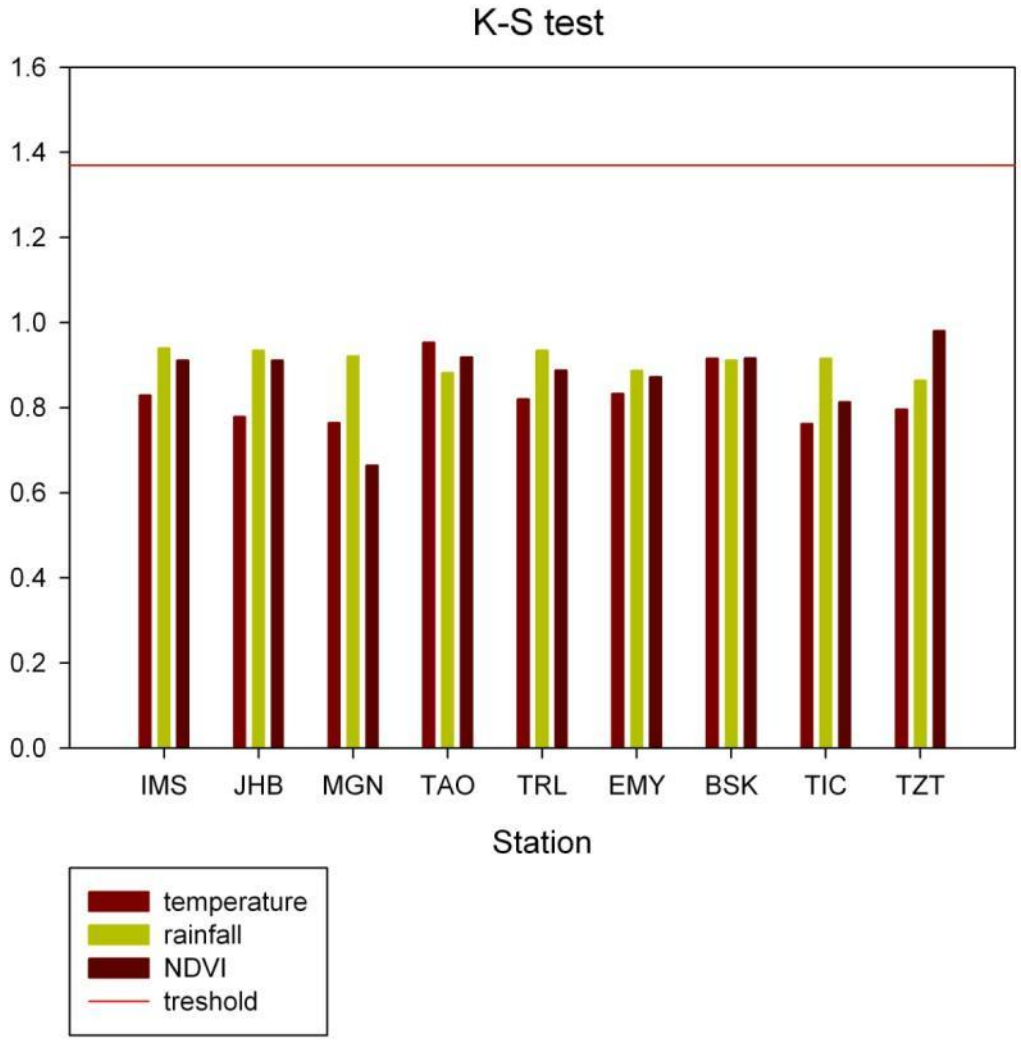

Figure 99 K-S Normal distribution with threshold limit

The normal distribution test in Figure 99 shows that the data is below the threshold. The treshold is calculated by number of case and level of significance . This means that the data is normally distributed and usable in a regression. On the base of this knowledge the significance of the NDVI signal is tested by the probability of valid data within a two standard deviation area.

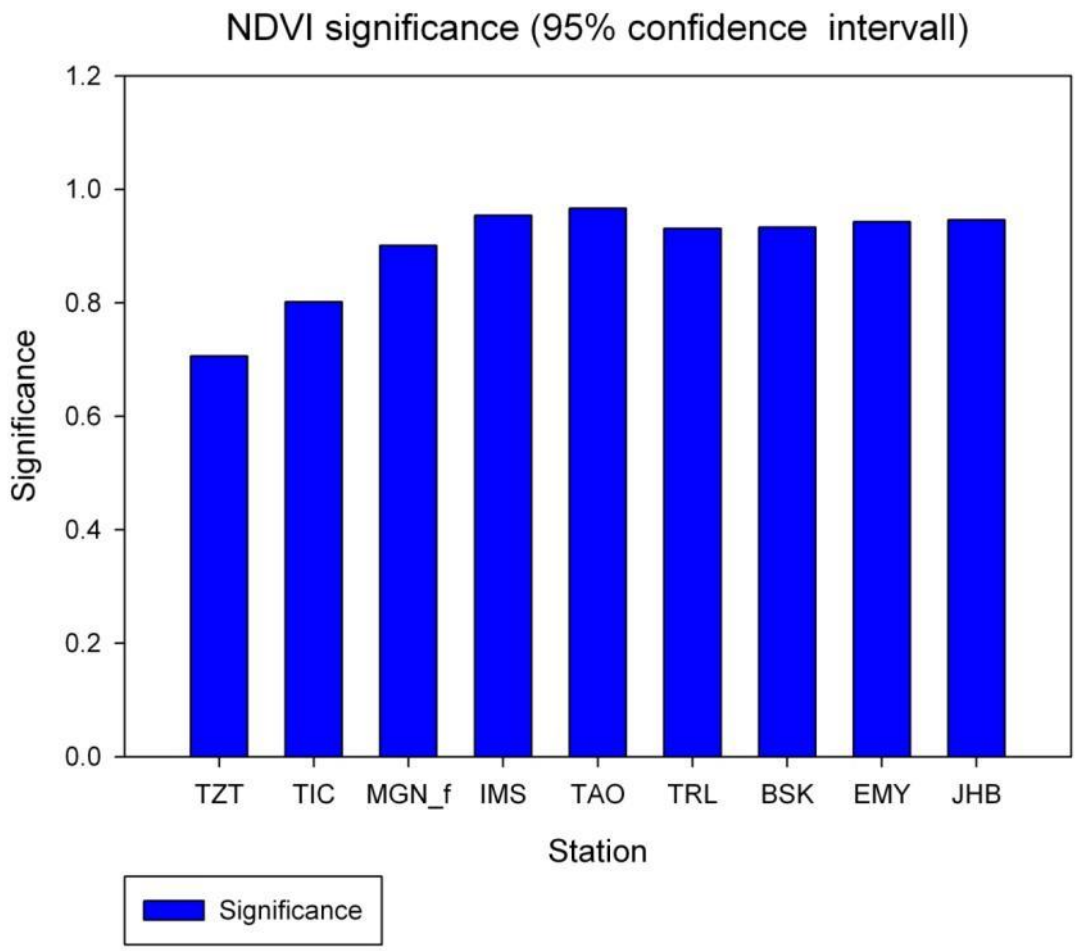

Figure 100 NDVI significance with confidence level p=0.05

Figure 100 shows that most of the NDVI signal is significant. There are some problems inside the high mountain Atlas range due to shadow and dust effects (see 'known problems' on the NASA website).

6.5 Regression

This chapter introduces the results of the calibration and validation phase of the NDVI regression. It uses the approach introduced in chapter 5.15. This chapter concludes the theories from Chapter 5.1 and presents in which way the chosen input parameters influence the NDVI. This chapter is divided into two main subjects. Calibration and quality assessment, as explained in chapter 5.10, are done in a calibration and validation phase. By minimizing the differences between observation and model output the model is altered until an optimum (Daren Harmel & Smith, 2007). Goodness-of-fit indicators (defined in chapter 5.14) for the training phase 2000 until 2006 and the validation phase 2007-2008 indicates the calibration. This chapter presents should give an excess overview on how the calibration was done, and under which quality. As explained in chapter 5.10 the data is separated into increasing and decreasing data. Figure 101 shows an example distribution chart. The red line indicates the separator for increasing and decreasing data.

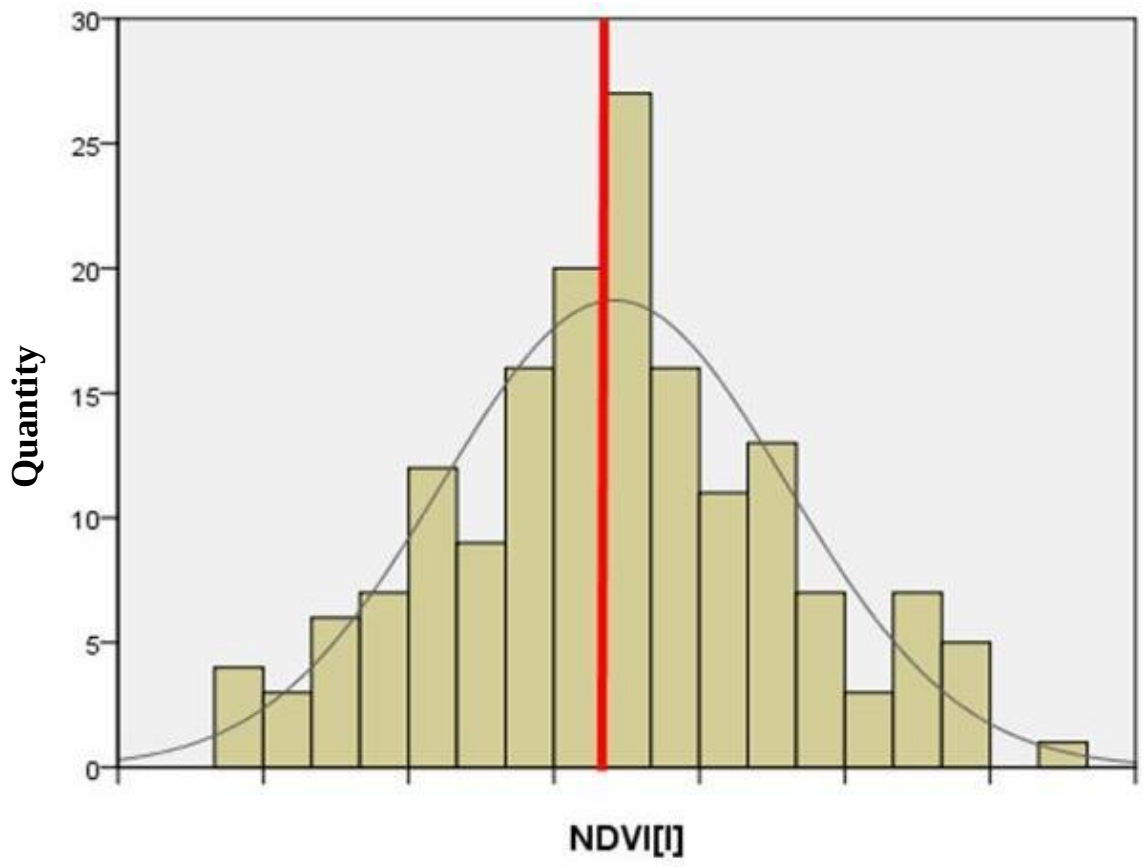

Figure 101 NDVI data separation (demonstration data)

By using the regression approach described in Chapter 5.14 a multiple linear regression formula is calculated for every station. The quality of the linear regression is at first evaluated by a t-test. The null hypothesis here is that the predicted output of multiple linear regressions is the same as the observed NDVI signal.

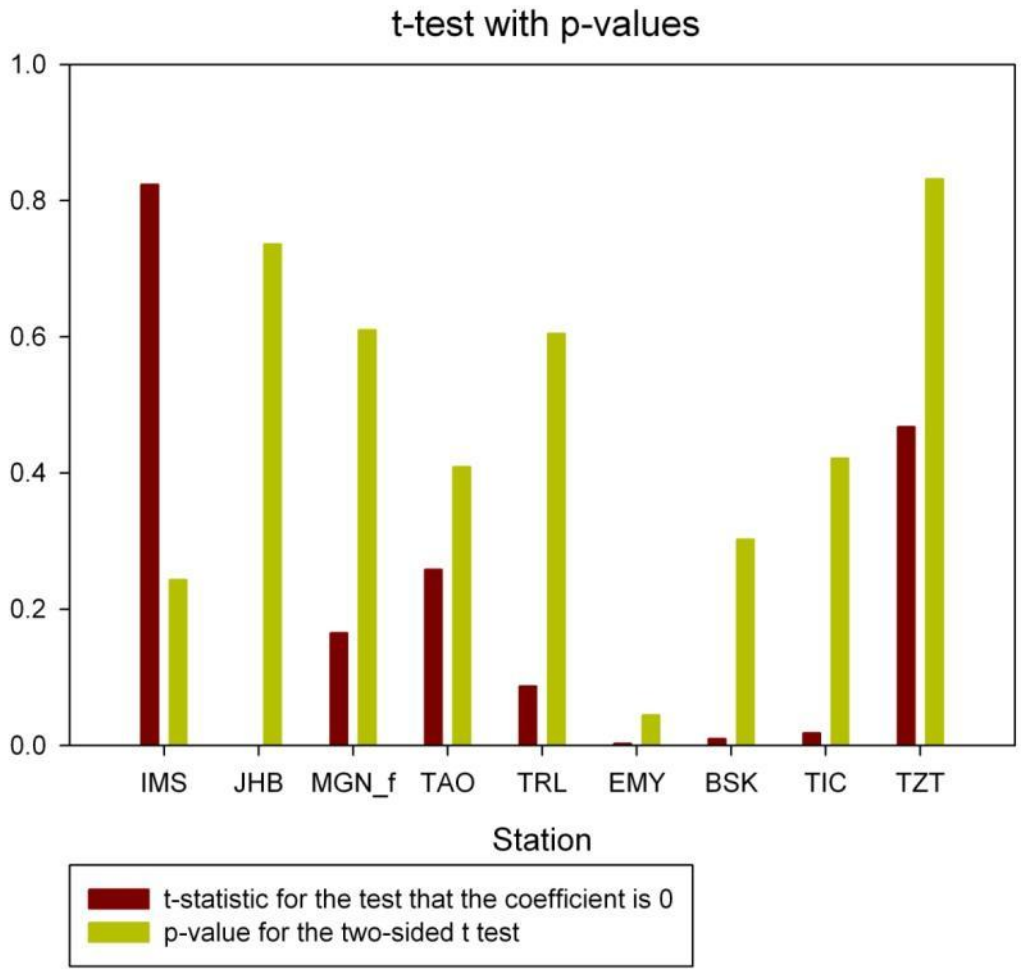

Figure 102 t-test statistics with p-vlaues for all selected stations

The t-values indicate that the Null hypothesis declines the 0,95% confidence interval for some stations. This means that the linear regression didn't fit the original NDVI signal. The R^2 (as explained in Figure 103) will not be used any further, because of the unsteady NDVI signal and the very low variance (see (Colditz, 2007) and chapter 4.3).

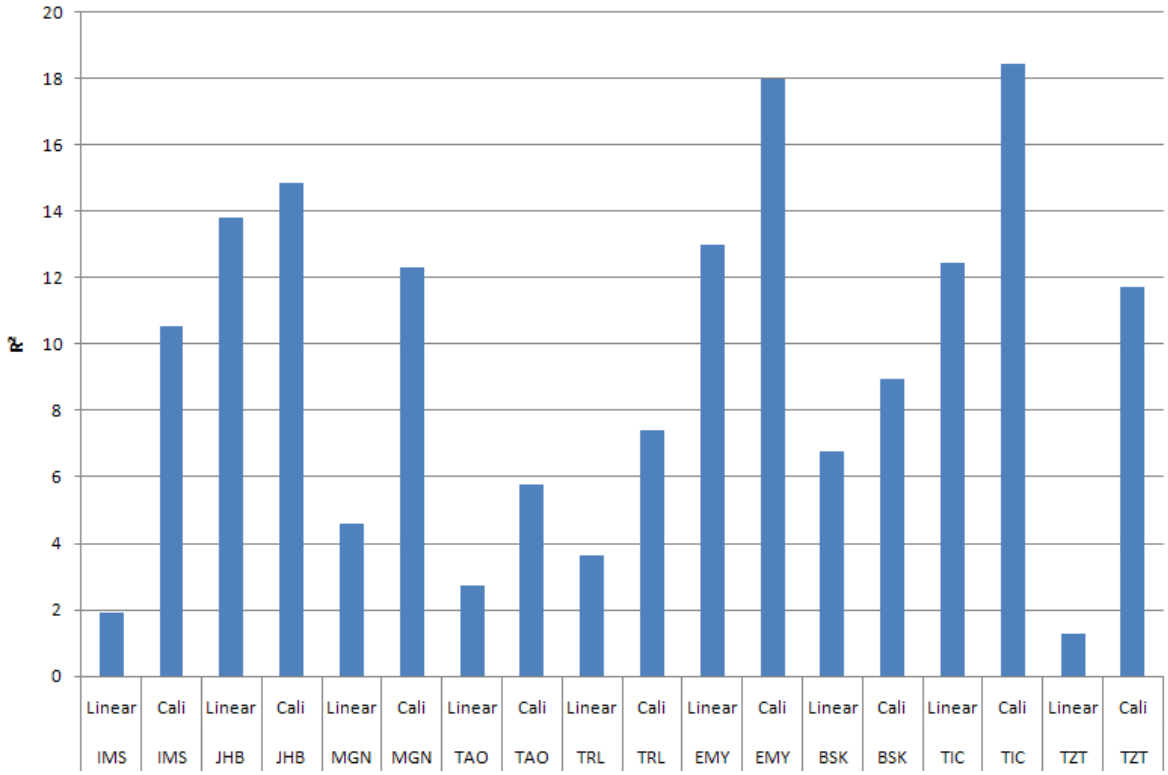

Figure 103 overall R^2 comparison between linear Regression (Linear) and after non linear Regression (Calibrated regression) for 2000 until 2006

The next step to improve the results is using non linear regression. By using this technique I compared the predicted NDVI signal with the observed original using a linear regression.

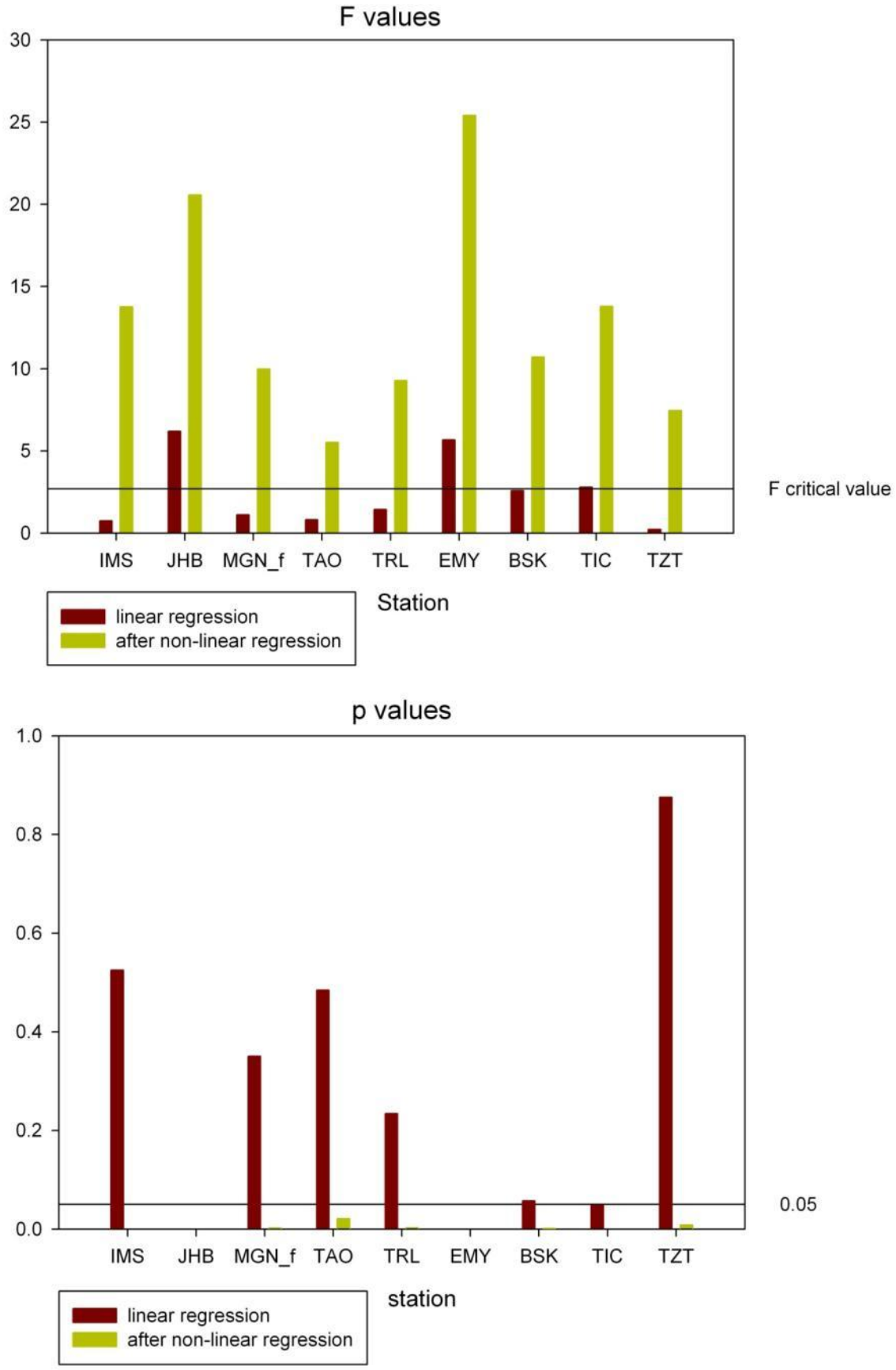

Figure 104 F- and p-Value after the linear regression step and after the non-linear regression step

In Figure 104 the F-Values can be significantly reduced during the nonlinear regression. The F-Test in regression models should test if the coefficient of determination is zero. This can be denied, because the F-Value is significantly greater than the critical F- Value (3,120)~2,70. The corresponding p values in Figure 104 show that it can be assumed that the result is significant, because the Null hypothesis that the p-value is smaller or equal to the significance level (in this case the usually 95%) can be rejected. This can be underlined by the reduced sums of square error (Figure 105).

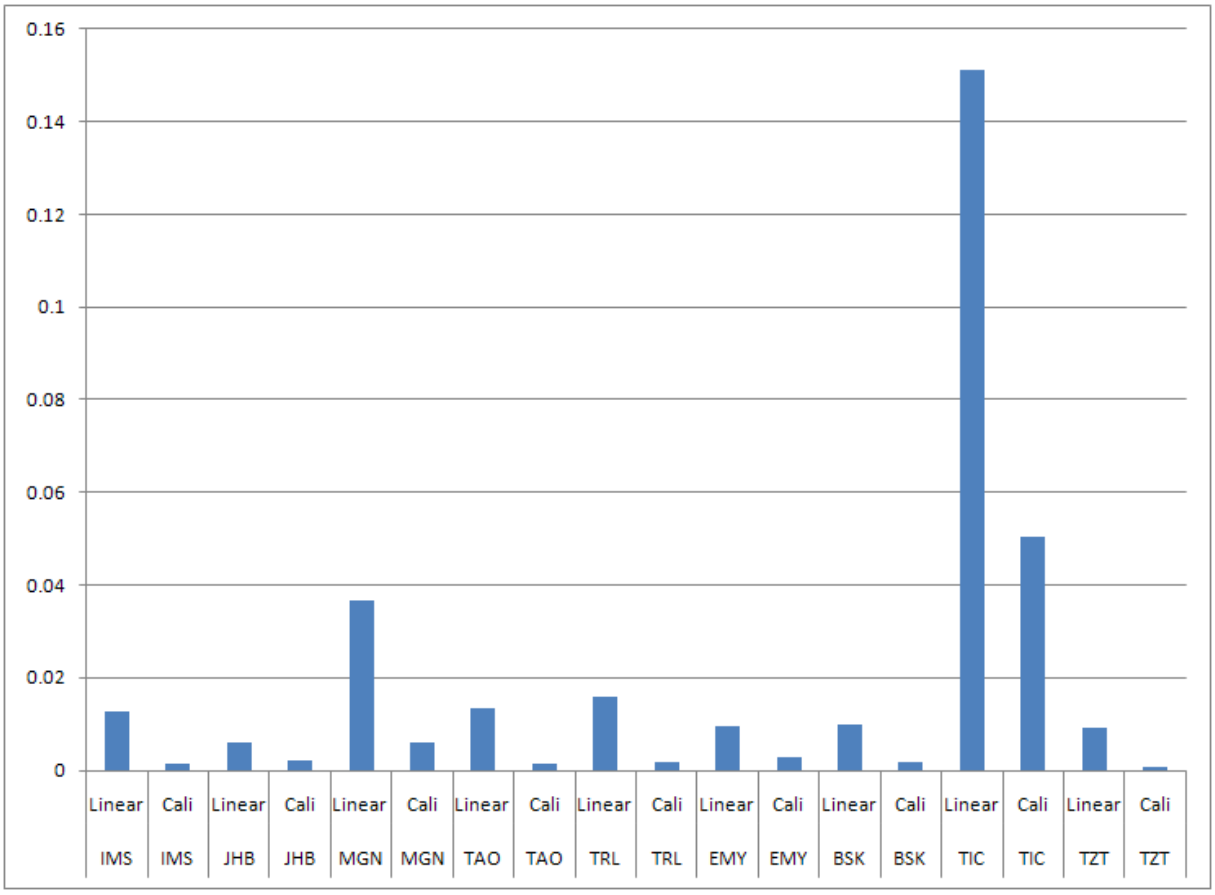

Figure 105 total (corrected) sum of squares after the linear regression step (Linear) and after the non-linear regression (Cali)step

The regression quality shows that the regression result can be significantly improved by using the described regression combination. The estimation of the regression coefficients (or predictors) is stable which is shown by the total (corrected) sum of squares. The predictors are not affected by multi collinearity (Figure 106). In sum the regression can be declared significant.

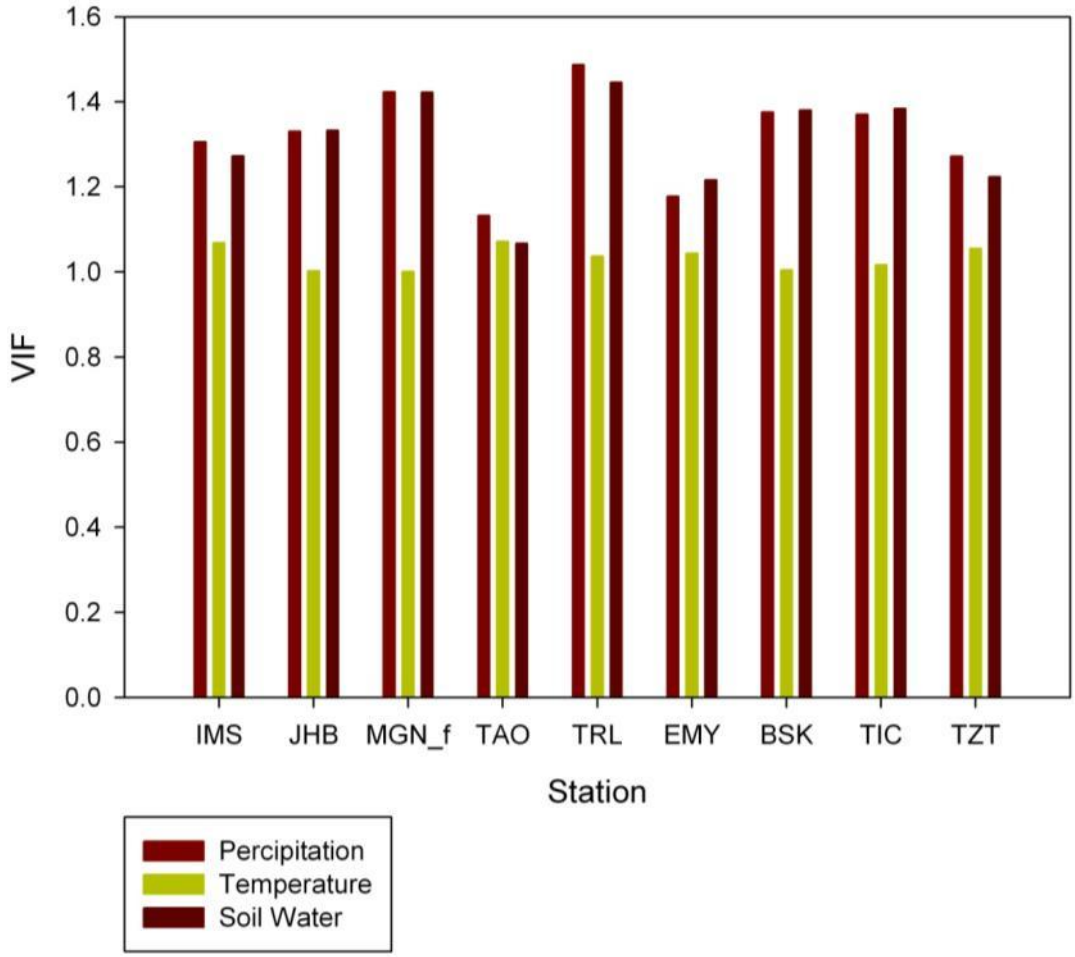

Figure 106 VIF acore for linear regression

But more important is the question: Does the data fulfil the temporal aspect of vegetations trends? By using the quality criteria introduced in chapter 5.13 this hypothesis can be confirmed during the calibration phase (Figure 107).

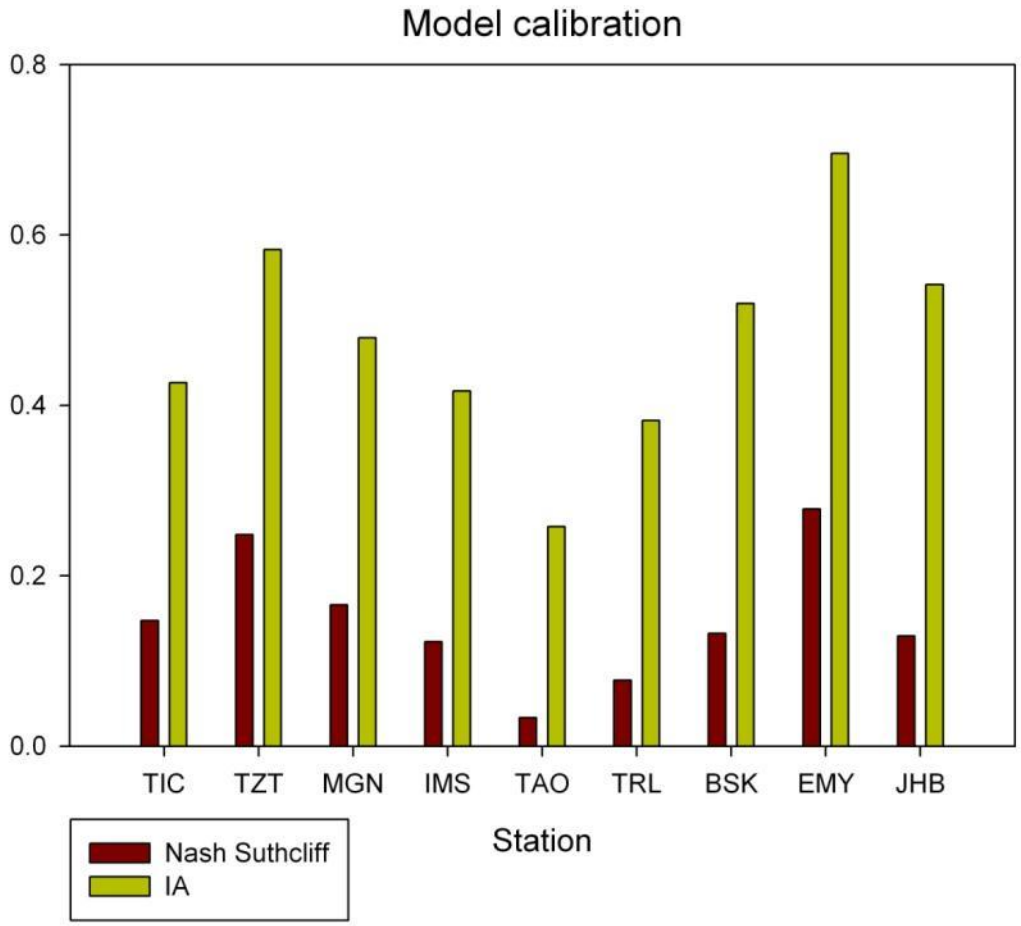

Figure 107 Quality criteria Calibration

The results show that a good agreement in the temporal course can be archived. The overall performance (Nash Suthcliff) indicates that the regression did not catch all peaks and lows.

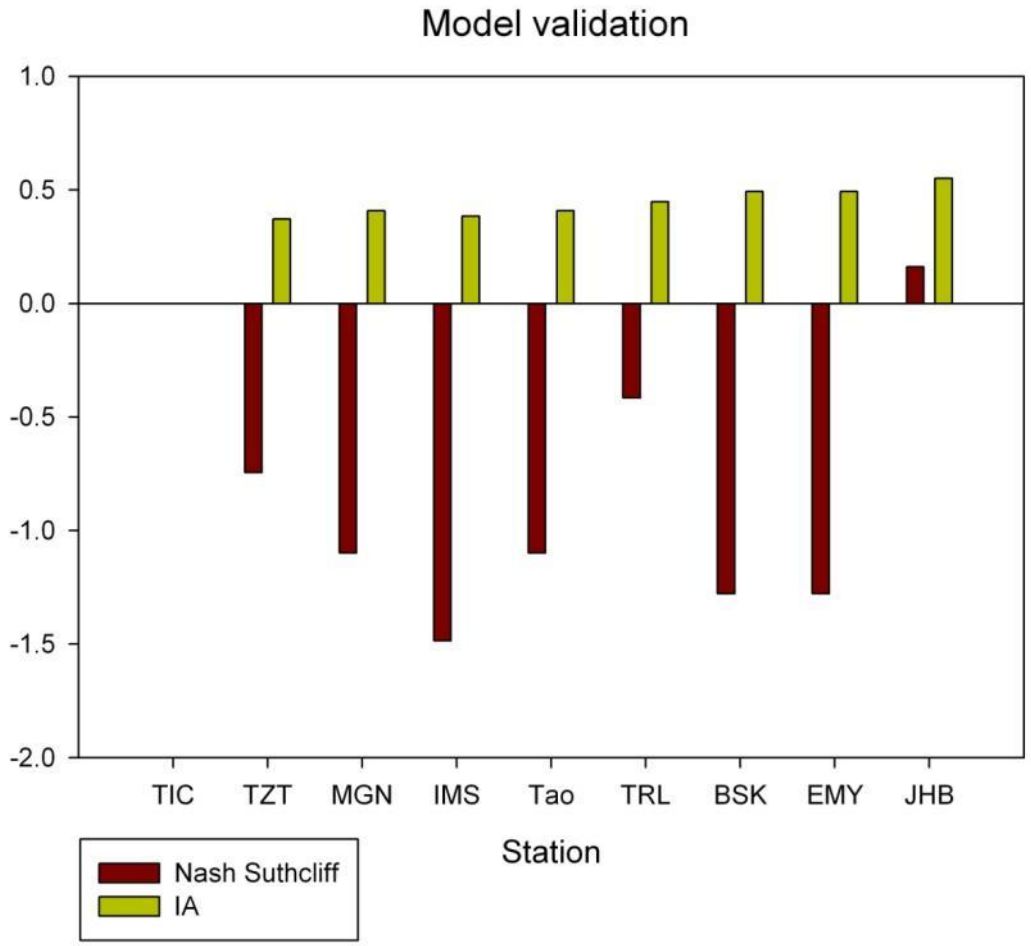

Figure 108 Quality criteria validation

The model validation (Figure 108) reveals that the regression reflects the temporal trend, but fails at the overall performance. One reason is the calibration of MD is focusing on the temporal gradient of the NDVI, not the overall gradient. Under that perspective the IA reflects that the temporal integrity is at a fair level.

6.5.1 Peaks and missing data inside the vegetation signal

The temporal course, e.g. EMY station (Figure 109), indicates a good statistical fitting.

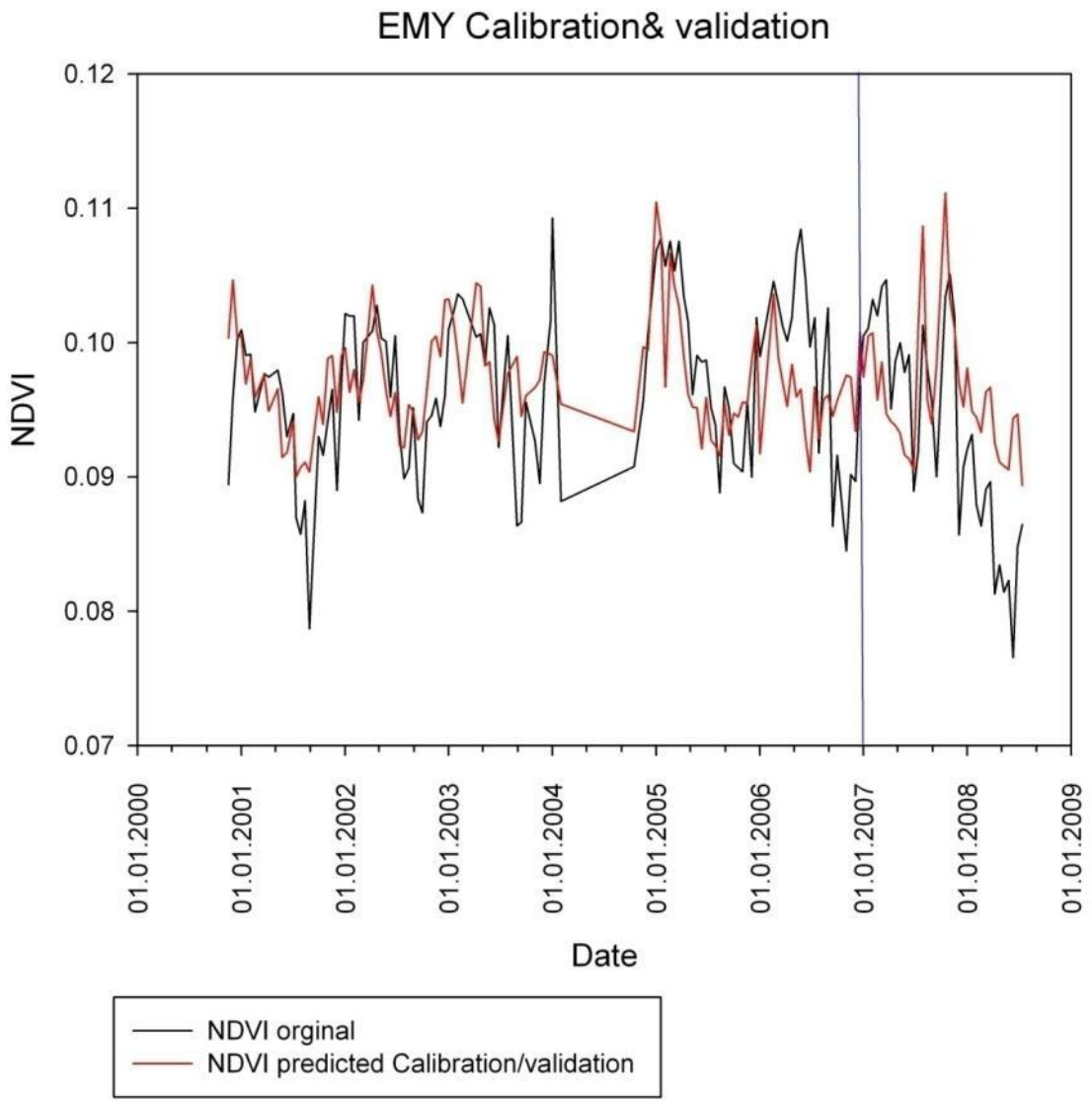

Figure 109 Validation of the Calibration result with a temporal extrapolation for 2007/2008 (Validation phase) for Station EMY (blue: boarder between Calibration and Validation phase)

There are some non explainable peaks and lows left inside the signal. Since they are not classified as wrong, because they are passed all statistical filters and tests, it can be assumed that this remaining outliners are taken in account but gained a low weighting during the statistical fitting. That means that the model can't resolve a statistical dependency between those peaks and the independent parameters.

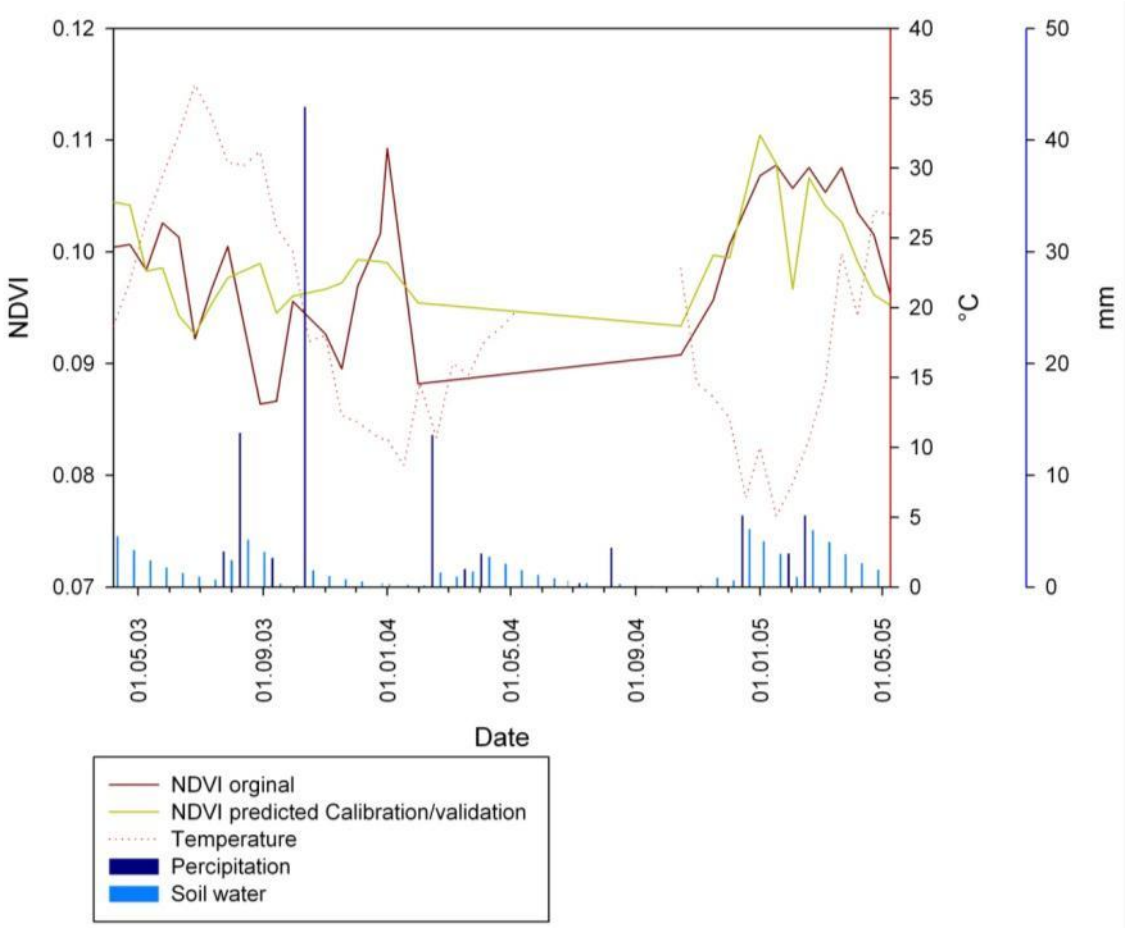

Figure 110 In depth graphical NDVI regression result comparison to the independent parameters for Station EMY (2004)

It is important to say that the elimination of outliners is done for every data pair and is therefore consistent. However, it is possible that soil water artefacts from rainfall events (which are dropped out due to missing dates from other sources (e.g. NDVI)) are included in the data because of the diminishing character of soils. A graphical interpretation of the signal shows that the predicted signal is very close to the observed signal. The difference, which can be expressed for example in the variance, is only 0.04 for the displayed figure. By keeping in mind that the signal can vary between 0 and 1 this is a very low change. But the statistical tests are sensitive to the whole spectrum (which is low here) and interpret even very low differences as significant. From this point of view a difference of 0.01 is different on a variance of 0.04 a 25%. This can also be shown in the very low standard deviation of 0.007130163 for the observed NDVI and 0.004505853 for the predicted. The general problem is that the approach lowers the signal amplitude (see Theory/Chapter5, least square effect) and therefore reactions, especially fast reactions, cannot be captured. By trying to understand the nature of these little changes it seems that there is no visible reason inside the used independent data for a reaction in the depended data (compare Figure 110). Therefore the regression can only unsatisfactorily address the reaction of the vegetation,

especially sudden peaks and lows. Also the temporal character of the signal must be kept in mind. Since most of the images are MVC it is possible that between 2 pictures there may be up to 32 days. This can have a significant statistical effect.

The second reason may be the most common land use. It cannot be excluded that some changes are due to grazing and other forms of land use. By keeping in mind that up to 90% of the vegetation productivity is grazed, it is very likely that these changes have significant influences.

Thirdly these peaks can also be due to radiometric and other failures. Therefore see MODLAND QA - Known Product Issues – Terra homepage. Especially SD_MOD13_03113 is very valuable in this context.

6.5.2 Sensitivity of individual Parameters

One of the core elements of this study is to investigate the statistical influence of meteorological data on vegetation activity. Using the explained variance of the regression provides a first result.

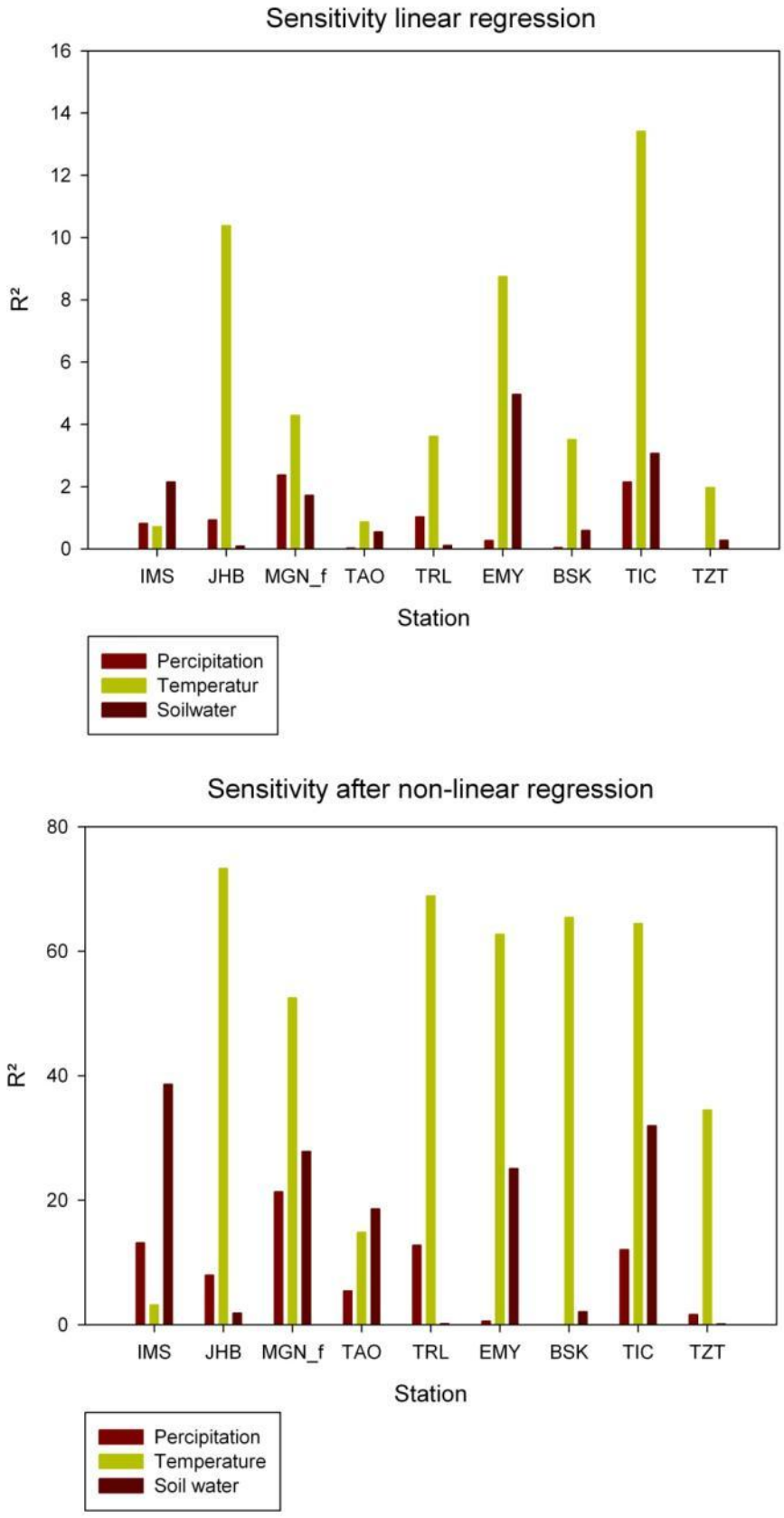

Figure 111 Explained Variance Independent Parameters Linear (top) and Non-Linear (bottom) Regression

Figure 111 shows that the explained variance is raised significantly during the regression approach. It is also shown that for most of the stations temperature is the dominant factor. At

the IMS station the temperature seems to have a much lower influence than ground water. This can be explained by the steepness of the area and the resulting rapid drying of the upper soil. At the TAO station the influence of all parameters seems significantly low. This is an indicator that this station is influenced by other steering parameters than the given ones.

6.6 NPP Results

This chapter introduces all results from Chapter 5.11 (ANPP Module). It will give an overview of the results of MD and validate it with other data sources.

RBM uses its own incoming radiation calculation, depending on latitude and longitude as well as on terrain parameters like slope, aspect, inclination and albedo.

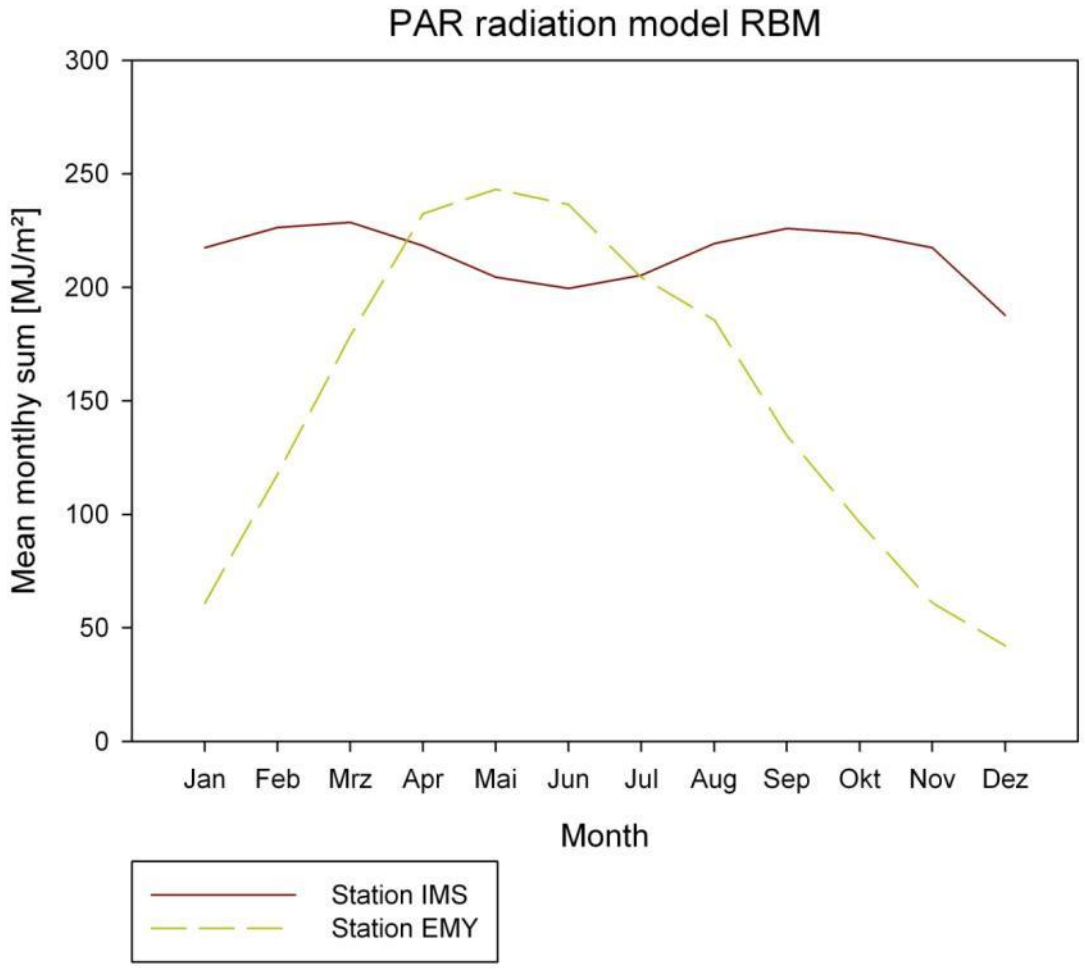

Figure 112 PAR Radiation calculated by the ANPP module

Calculating the radiation for all stations, Figure 112 shows the yearly distribution of PAR radiation for IMS and EMY stations as examples. The IMS station has the interesting characteristic that the direction of its IMS exposition (which is south) provides a nearly constant influx of radiation referring to a near azimuthally inclination angle. Only in midsummer the inclination angle is too steep so a little more radiation gets reflected by

albedo. The EMY station shows a typical yearly distribution on a flat area on the tropic of cancer. It is also visible that the max radiation is negligibly higher than in the IMS station.

6.6.1 Spatio temporal Results

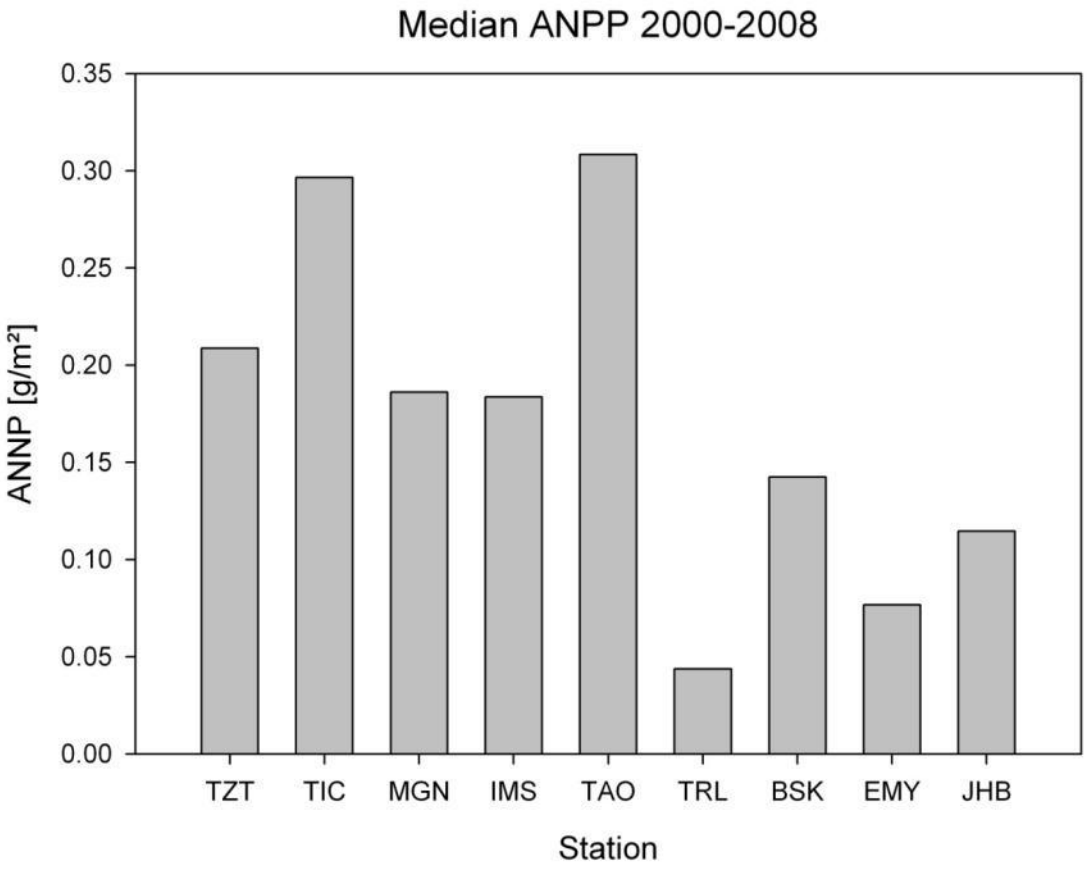

Figure 113 Median ANPP output all stations

The ANPP is highest for the mountainous areas, dropping down to a lower level at the basin of Ouarzazate (TRL station) and going down to a very low level in the southern part of the area. TRL is a special station with has almost dry conditions (Aridity index 0.07 (Baumann, 2009)) and a high percentage of yearly grass (e.g. *Stipa carpensis*). This result is coincident with the activity map of the Investigation area, which is calculated by the sum of activity on every pixel (Figure 114).

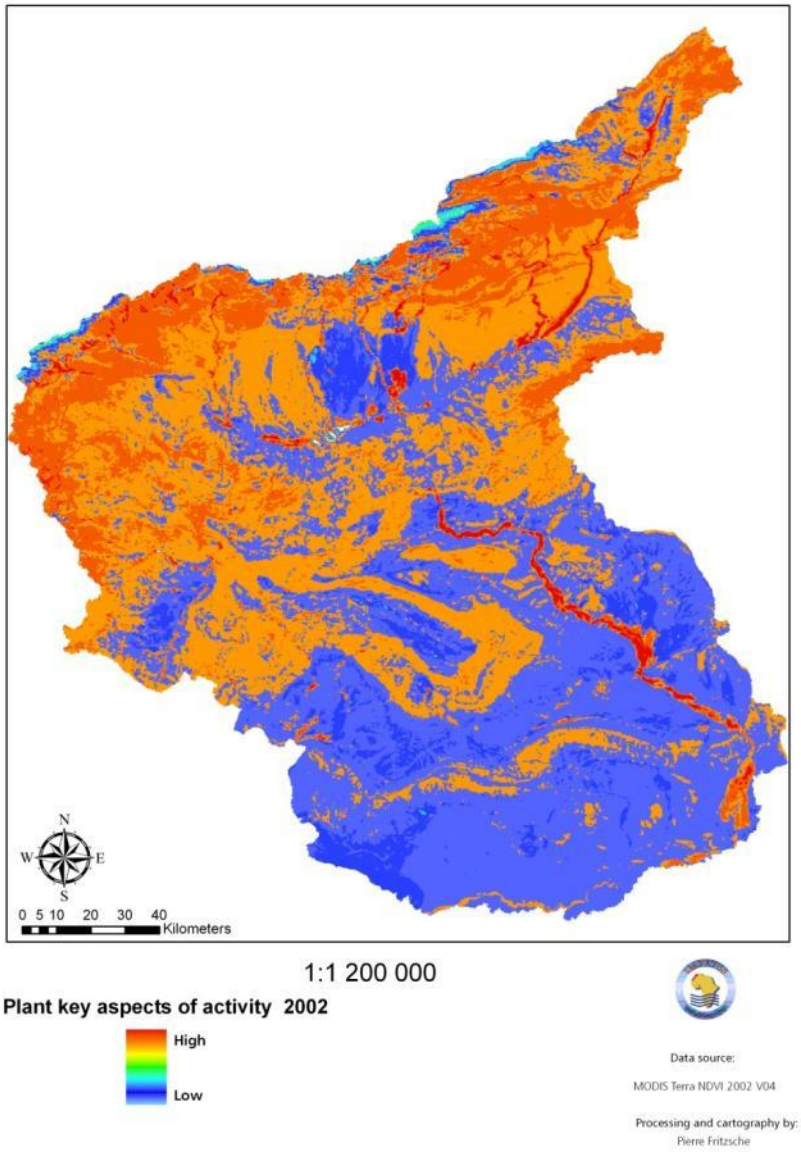

Figure 114 Plant Activity map (sum of NDVI/number of observations per pixel)

The output of the ANPP module shows a clear N-S profile (Figure 113) and altitude gradient (Figure 115)

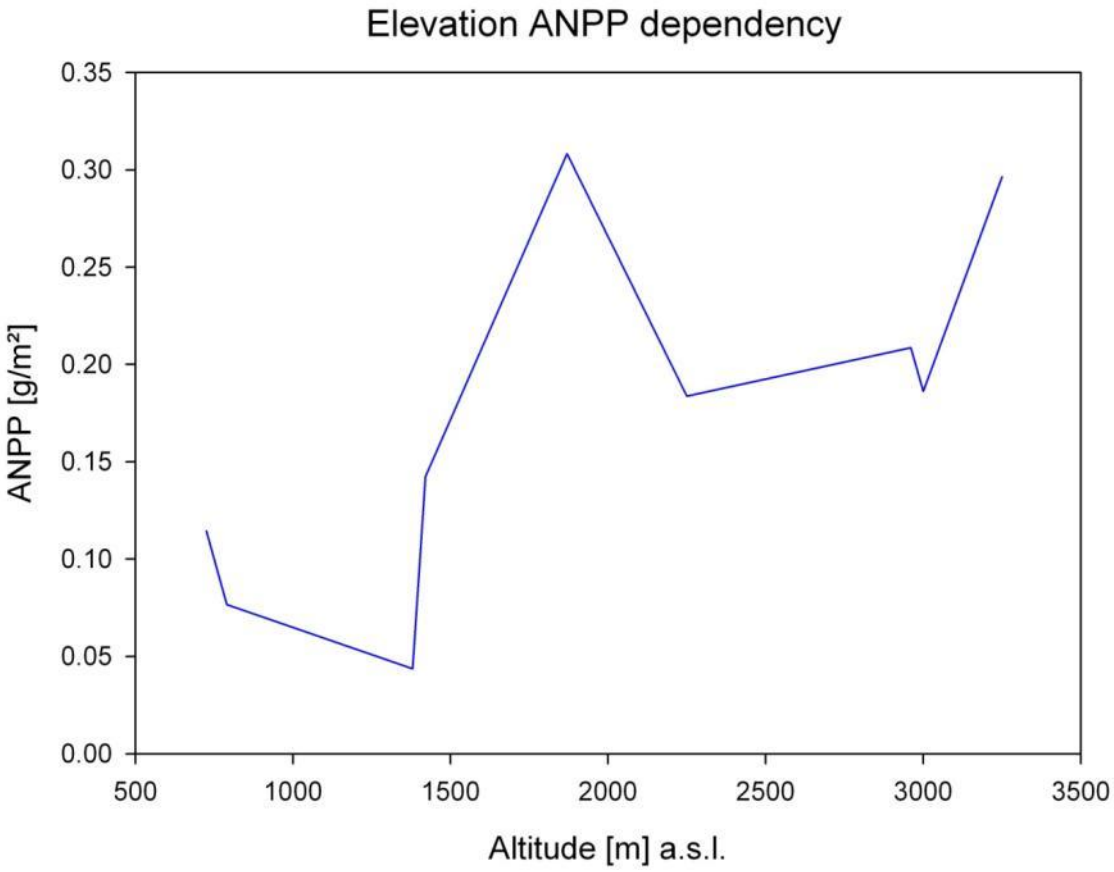

Figure 115 Elevation ANPP gradient

This altitude gradient shows that the productivity is highest in the area around 2000 m a.s.l. . By looking at the overall variance for all stations it can be shown that there is a very heterogeneous picture (Figure 115).

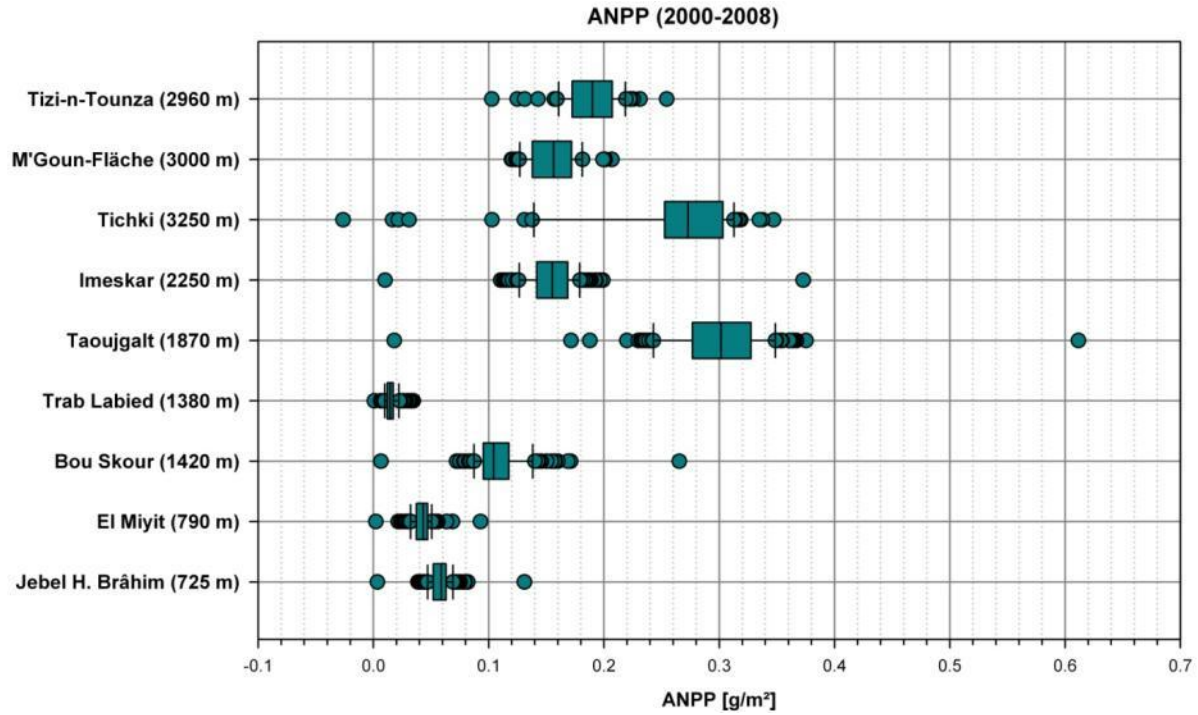

Figure 116 mean ANPP [g/m²] Boxplots

The stations with the highest mean productivities also inherit the highest variances. This must be put into perspective by looking at the temporal characteristics.

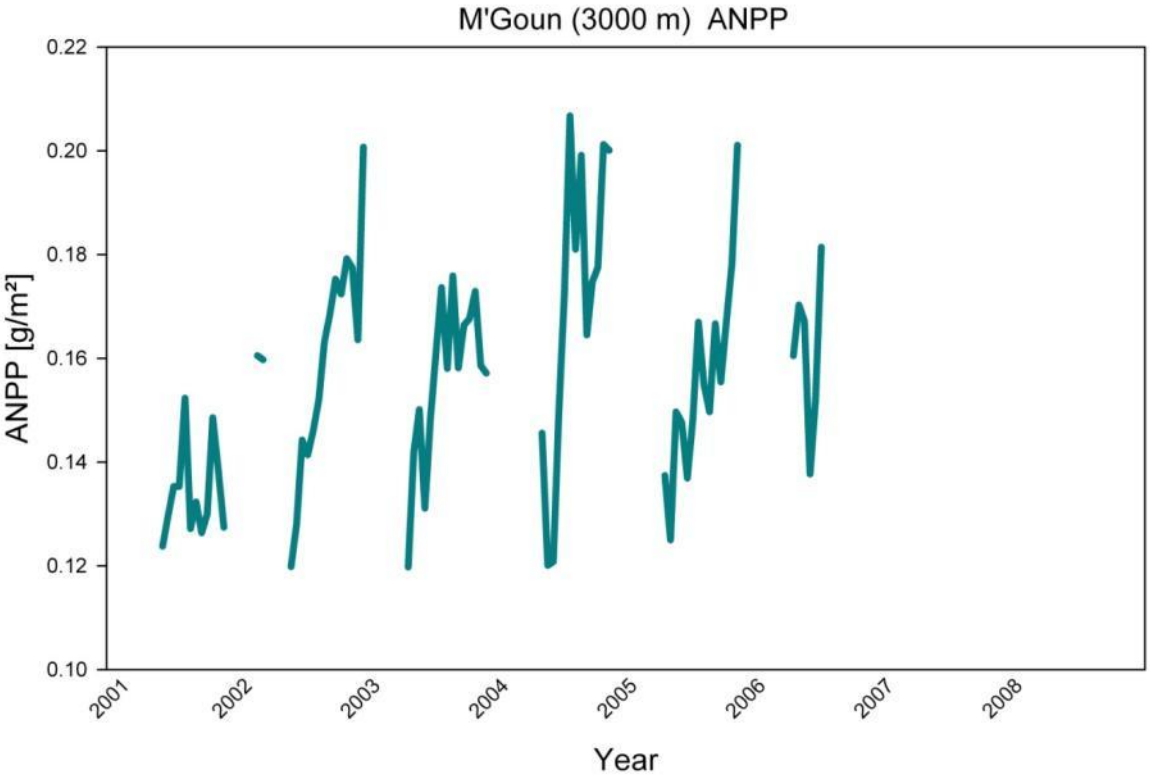

Figure 117 M'Goun area temporal characteristics of ANPP, including data gaps through erroneous data

Figure 117 reveals the problem of calculating ANPP in a high mountain area. By dropping out all snowy days and data which are corrupt due to shadow effects or particular

atmospheric corrections problems, only the spring to fall data remains. In the case of the M'goun area data the problem of missing meteorological data in 2007/2008 can be demonstrated. If any of these data are missing the model cannot calculate a result for the time steps. For the M'goun area this means that the model has no output on productivity. By looking at the TRL station (Figure 117) it can be shown that the model also reflects a decreasing productivity. Since TRL is at much lower elevation there are less snowy days and less missing data.

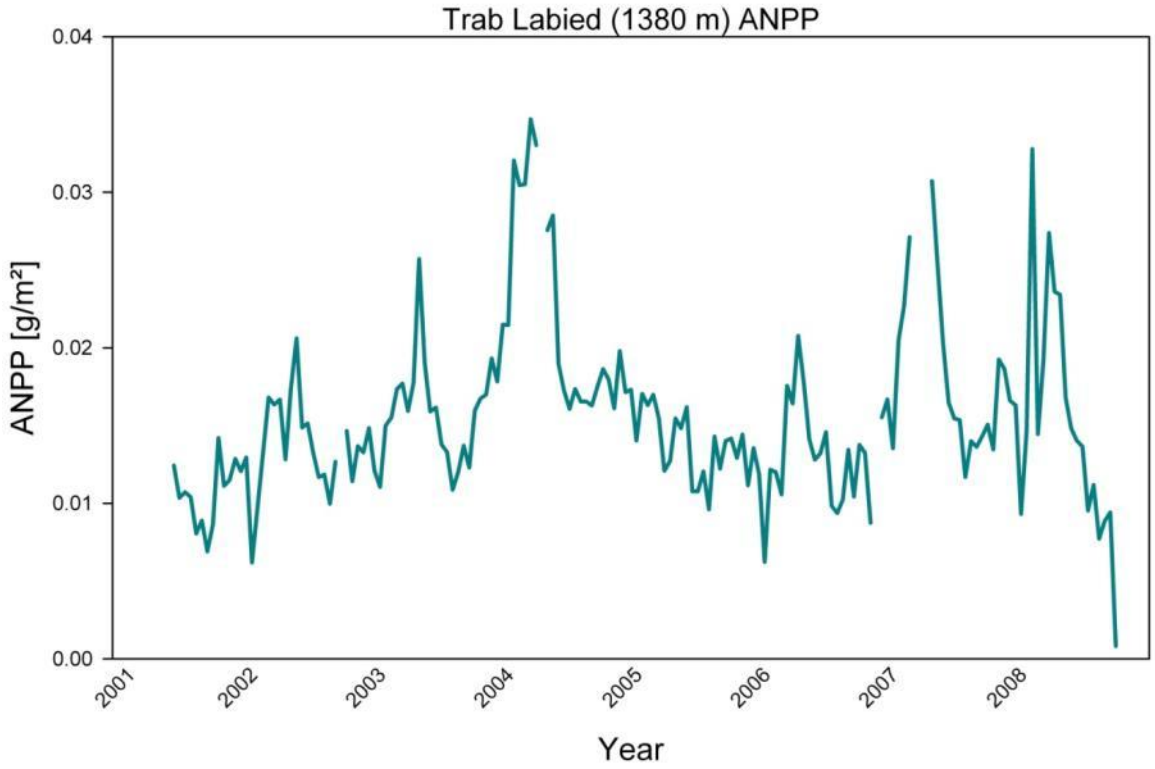

Figure 118 ANPP Results for the period 2001 to 2008 for the Station TRL

The question of Figure 118 is: Is this temporal gradient an typical annual ANPP trend? By calculating a summarized (2 events per month due to 16 days) monthly mean it can be shown that there is a clear yearly gradient (Figure 119).

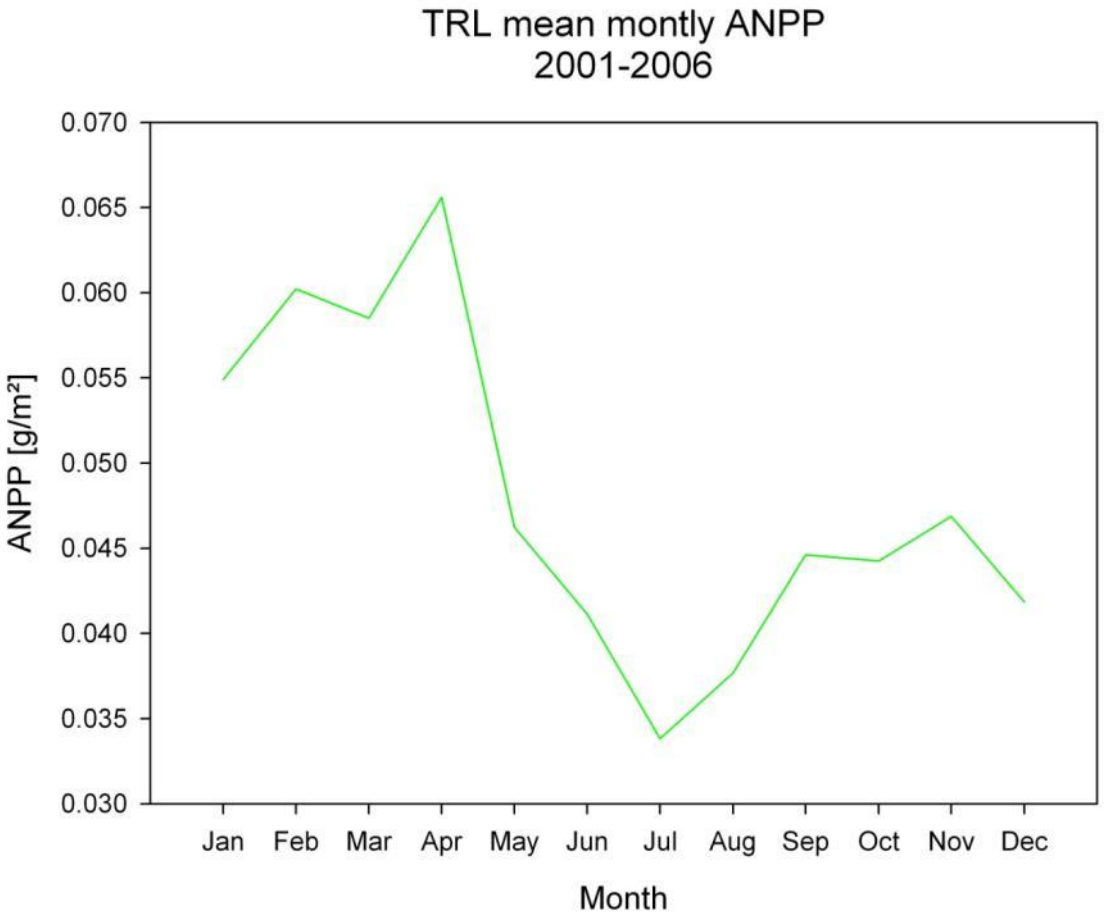

Figure 119 Mean NPP TRL for all months

TRL (as example) has a clear early spring maximum of vegetation growth and a second in late fall. The model calculates a result for every station, as long as there are data available.

One example for temperature and precipitation influences of the yearly (here 2007) gradient for temperature, precipitation and ANPP are shown for TRL station Figure 120.As expected the main peak in ANPP is in Feb/Mar. With increasing temperature the ANPP rate drops to a minimum during summer and a small peak is observed in late fall.

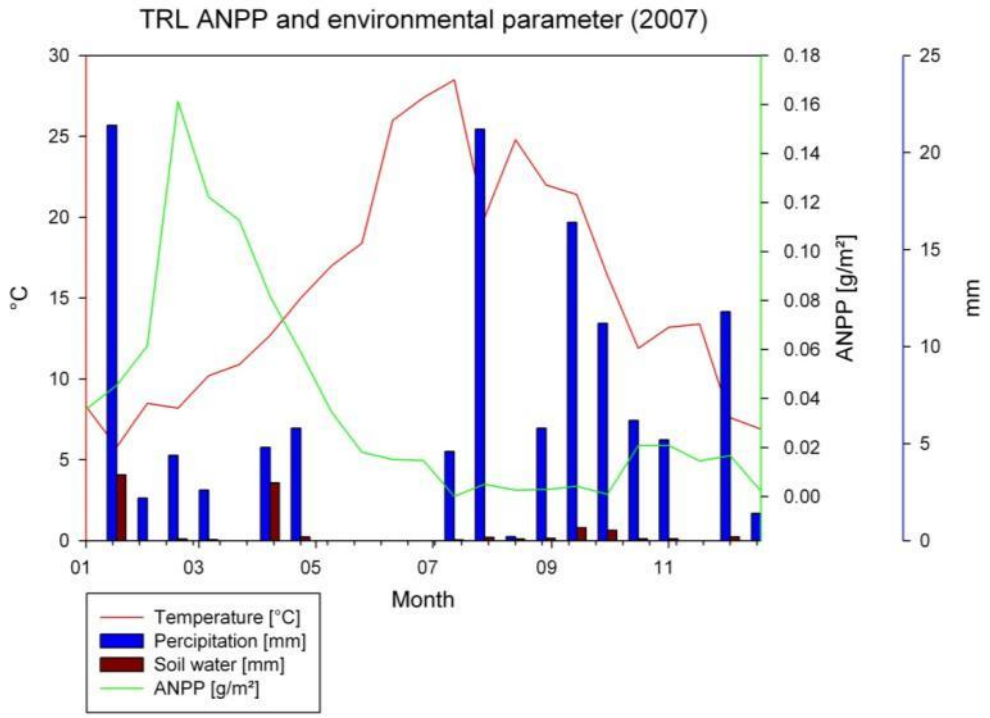

Figure 120 ANPP for station TRL during the year 2007

This underscores a trend that was already mentioned during the regression discussion. Rising temperature combined with missing rainfall tends to lower productivity.

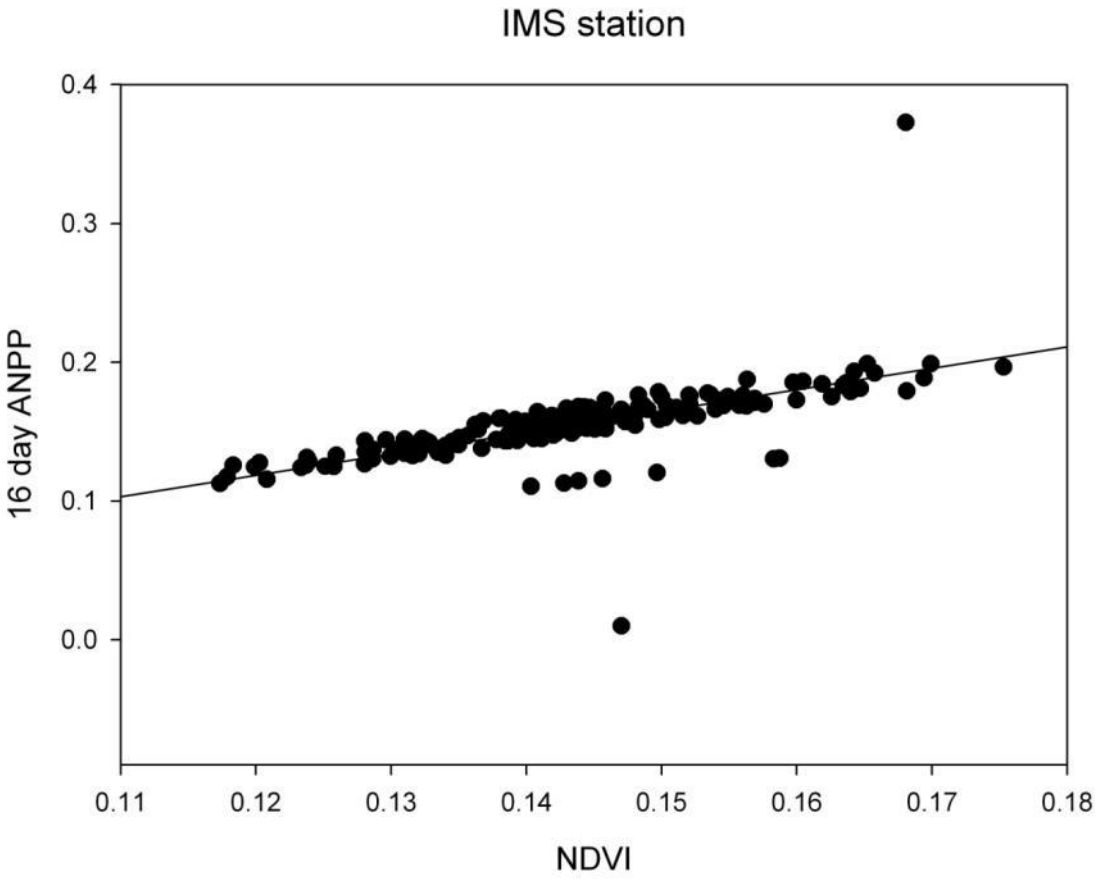

Figure 121 NDVI ANPP Scatterplot for the period 2001 until 2006 (n=158)

The NDVI Biomass relationship is quit satisfactory (Figure 121). In comparison to the investigation of (Fensholt *et al.*, 2006) it can be stated that the NDVI/ANPP relationship is difficult to handle in interannual variations, but the weighted approach minimized the problem (Figure 122).

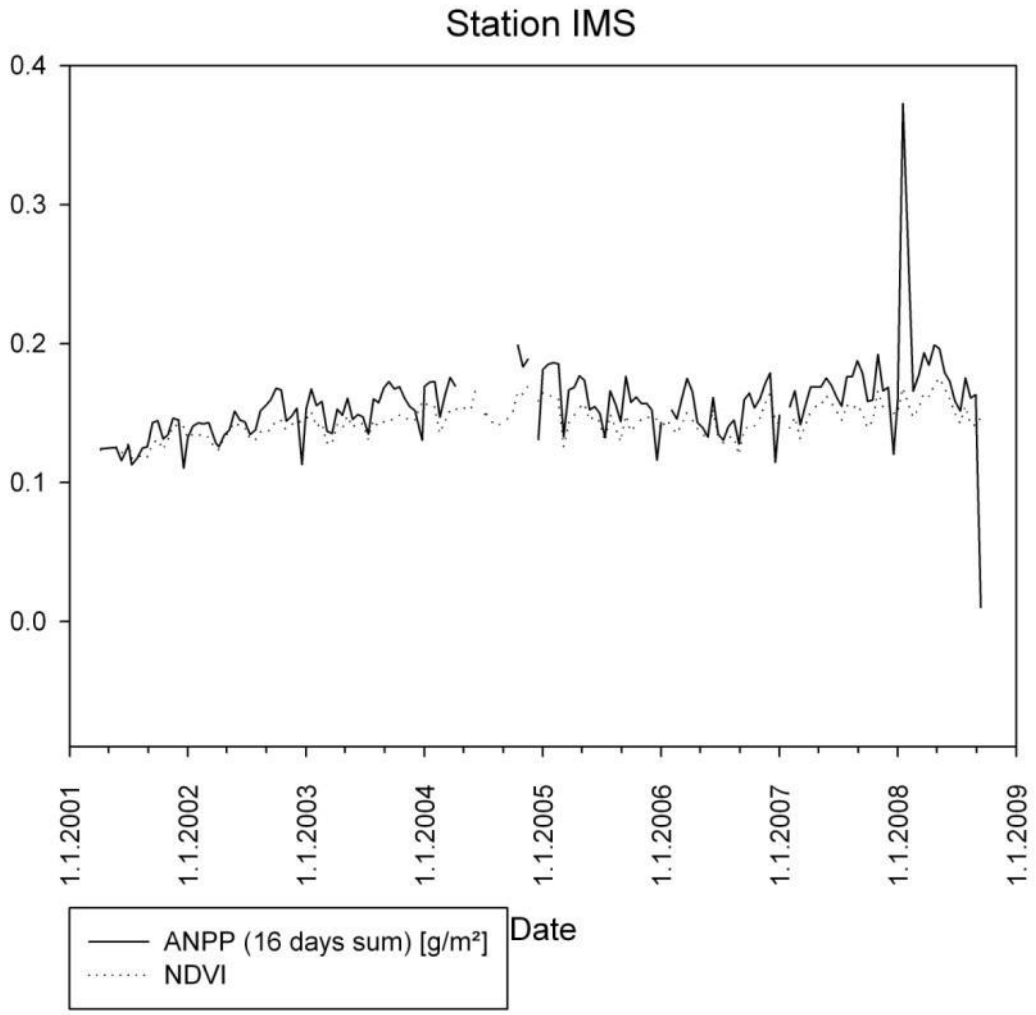

Figure 122 NDVI/ANPP interannual comparison

The inter annual comparison shows that the courses of both parameters is graphically very similar. The statistical key data on the other hand is relatively low (IA=0.59). By looking at the overall picture (Figure 123) this picture is much clearer.

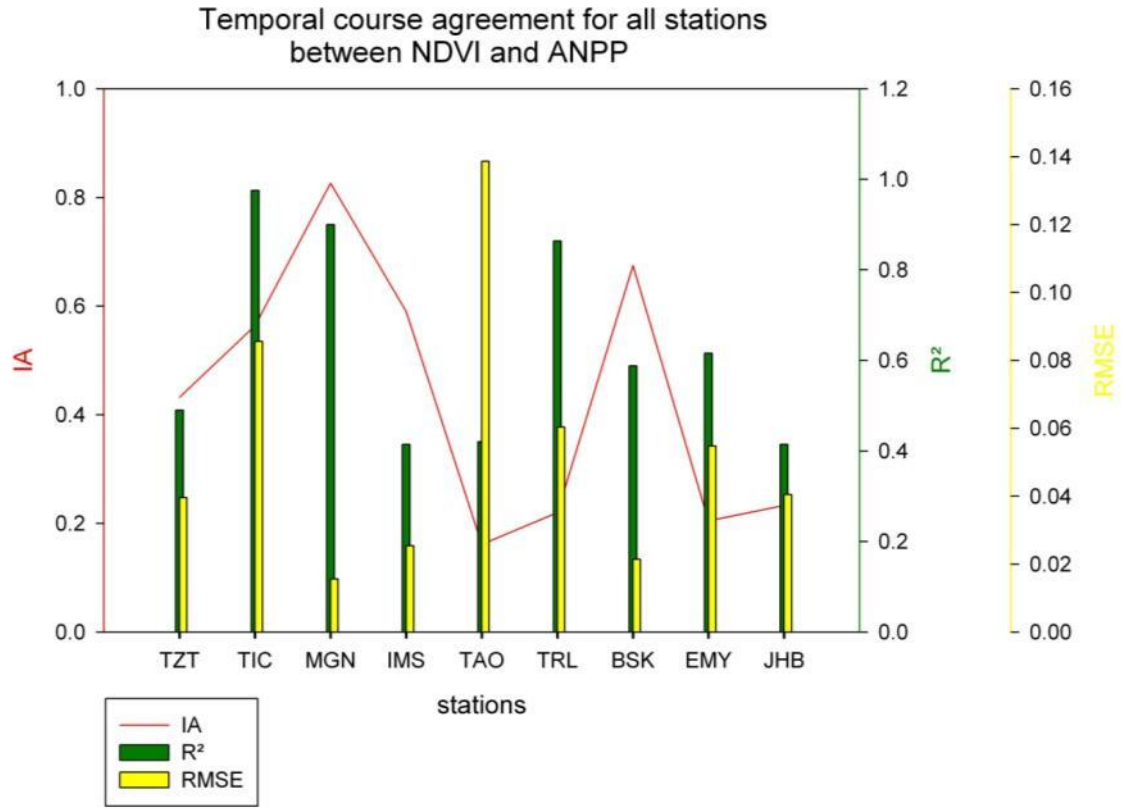

Figure 123 Statistical key data for NDVI-ANPP relationship (without missing values) for 2000 until 2008

The overall NDVI-ANPP Relationship is relatively good by looking at the coefficient of determination. The RMSE indicates indirect that the more outliners the lower the temporal agreement. This indicates that a few outliners (like seen in Figure 121) can significantly decreasing the quality of the key data. Since graphically interpretation is not objective and and some key data are sensitive to the (very low) variance (eg. IMS NDVI/ANPP relationship: 0.00081949!) it is suggested to always take normalised Indicators. For the temporal agreement of the NDVI Biomass relationship it can be concluded that the biomass model didnt react directly to greater NDVI hops, but follow the general trend of the vegetation activity course. Therefore the Biomass model must be declared stable in terms reflect vegetations lag of reaction.

6.6.2 Validation against Field Data

In order to validate the results of MD a field experiment take place (comp chapter 4.2). Using the data und the number of days the experiment lasted, it is possible to calculate a daily ANPP for MD and then compare it to the field experiment.

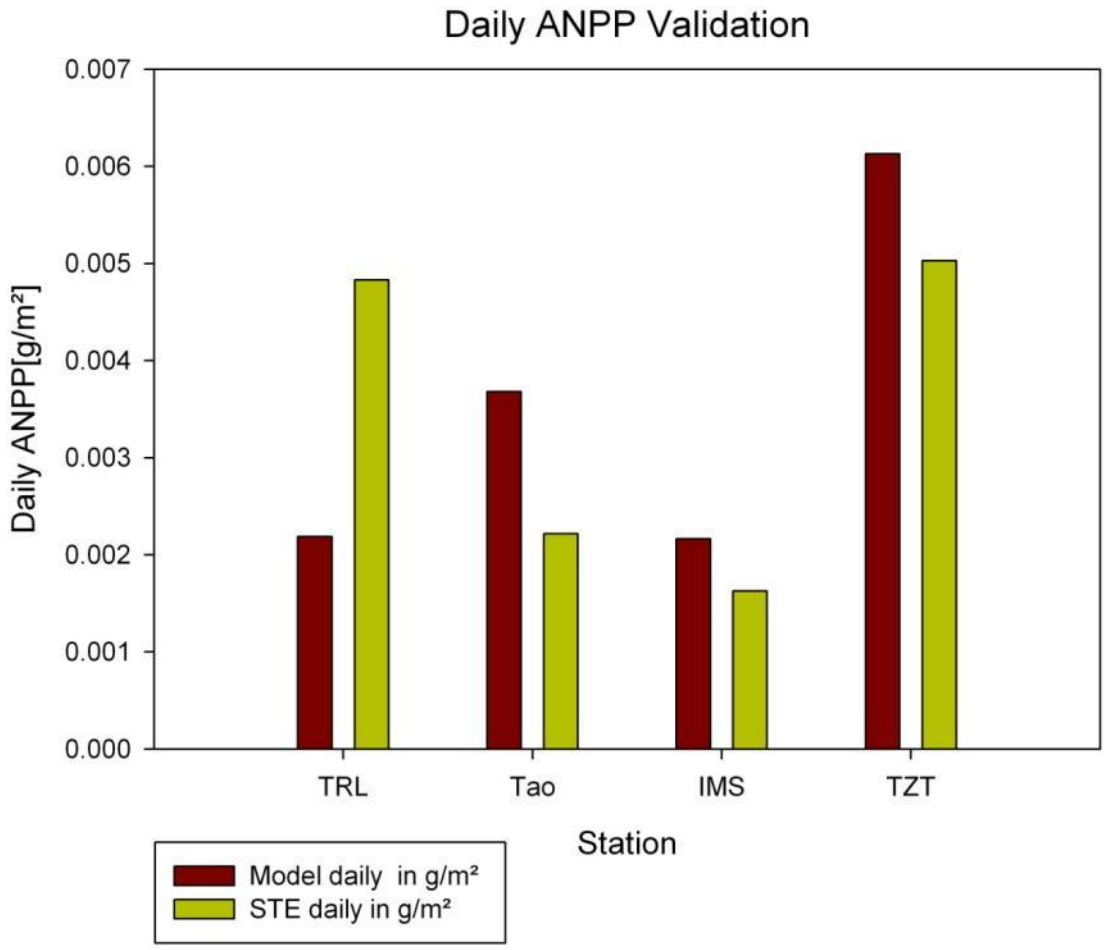

Figure 124 Daily ANPP for STE and MD

Figure 124 shows that the daily output of MD is close to the measured productivity. Only the TRL station underestimates the real productivity.

6.6.3 Influence of Cloud cover and Radiation

Several reasons lead to the decision to use a generic radiation scheme instead of a real measured one. The main reason is that the climate stations do not measure PAR. Also the net radiation instruments inherit a lot more downtimes than other instruments. Secondly the RBM model inherits a radiation routine. Thirdly, the climate scenario does not inherit PAR radiation.

Another problem is that the model works with 16 day cloudless MVC Level 3 data. The first intention to use daily data was dropped because of the required increase of computing time (16 times more) and because one intention was to use readily usable data. And, on the other hand, only cloudiness data from Ouarzazate was available. The core of the question must be this: would measured PAR radiation and/or used cloudiness data improve/impair the result? This study answers this question by investigating the uncertainty analysis by finding out if cloudiness significantly influences the outcome of ANPP model results. Since this model operates with cloud free pictures we can only say something about cloud free vegetation

activity. It should be mentioned that the direct radiation in this region is maybe stronger coupled to Mie scattering on dust particles (see (Iqbal, 1983a) p. 116f). Since no data on dust particles is available, this can only be an initial, unfounded guess.

6.6.4 Comparison to other models and temporal comparison

By comparing the results of MD to other models the problem of getting a comparable dataset occurs. As far as I know no regional biomass or productivity dataset for southern morocco exists. There are only global datasets available. Most of this dataset, regardless of the method used, inherits a global land cover for parameterization. These soil or land cover tools mainly classify most the Drâa investigation area as desert or non classified areas. This leads to the presumption that there is no vegetation at all inside these areas. (Field et al., 1995) gave a short overview on the topic of light use in different productivity models.

To demonstrate the problem results from the model C-fix (Veroustraete *et al.*, 2002;Verstraeten *et al.*, 2006;Verstraeten *et al.*, 2008) have been acquired and recalculated on a monthly base.

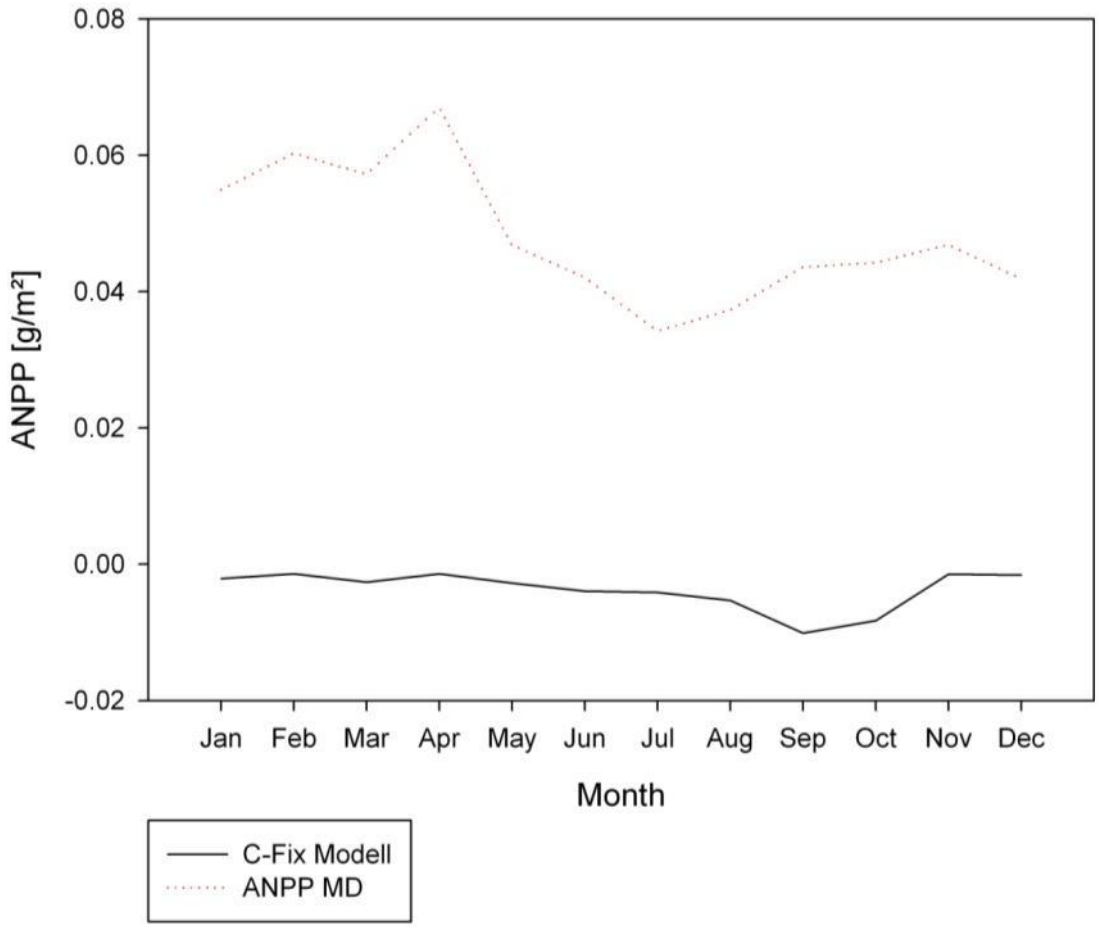

Figure 125 Comparison between monthly mean MD and C- fix for station TRL (2000-2008)

TRL is chosen as representative of the first comparison station (Figure 125). The C-fix model result here inherits a zero production. The same results occur for all stations southwards. By looking at the results inside the Atlas the difference between both models become visible.

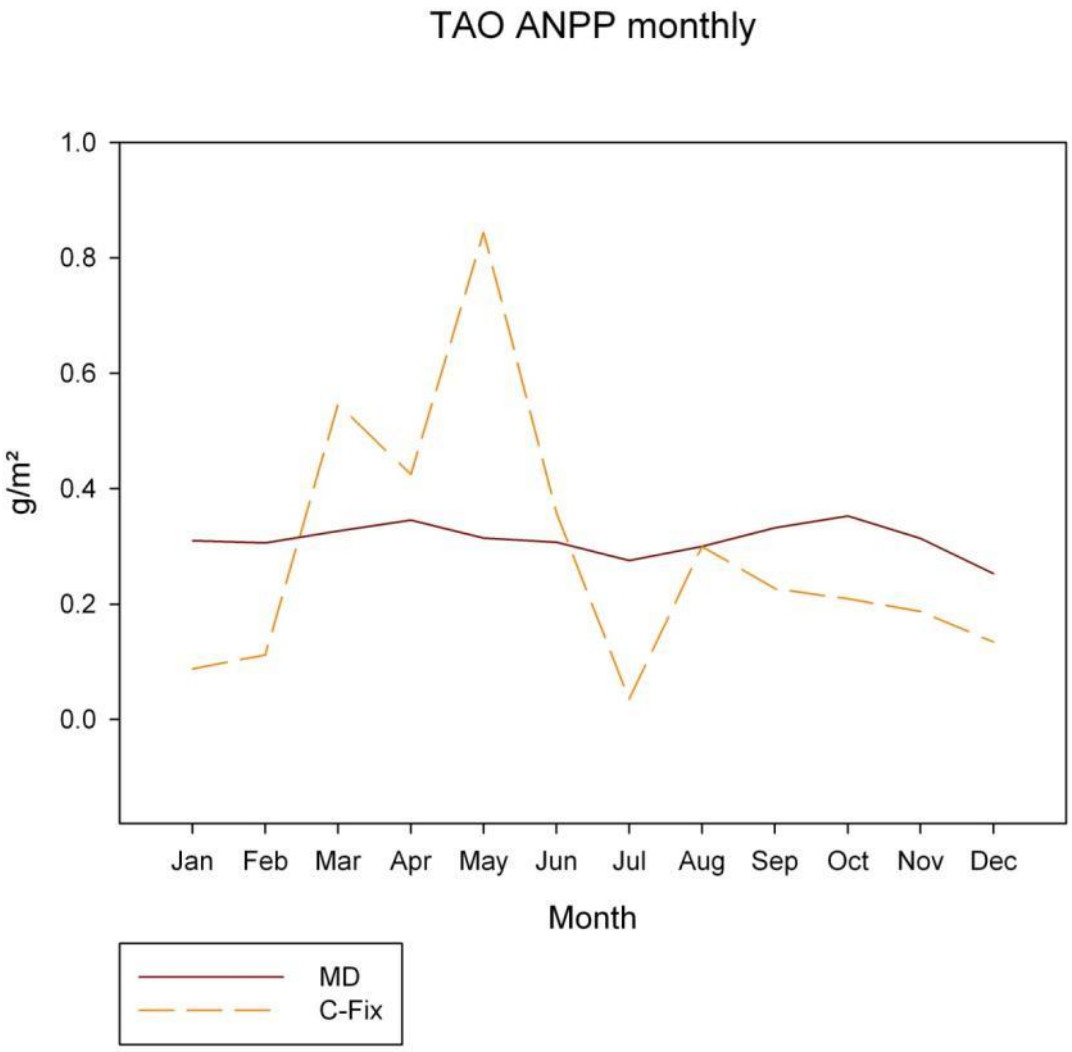

Figure 126 Comparison of MD and C- fix for station TAO (2000-2008)

Figure 126 shows the main differences between both models. MD is developed and parameterized on the actual land use (since NDVI reflects that) and soil conditions. The C-Fix model is only parameterized by climate and respiration rates. C-fix therefore entails higher yearly amplitude and a clear maximum at April/May. MD has smoother yearly amplitude with two peaks in one year.

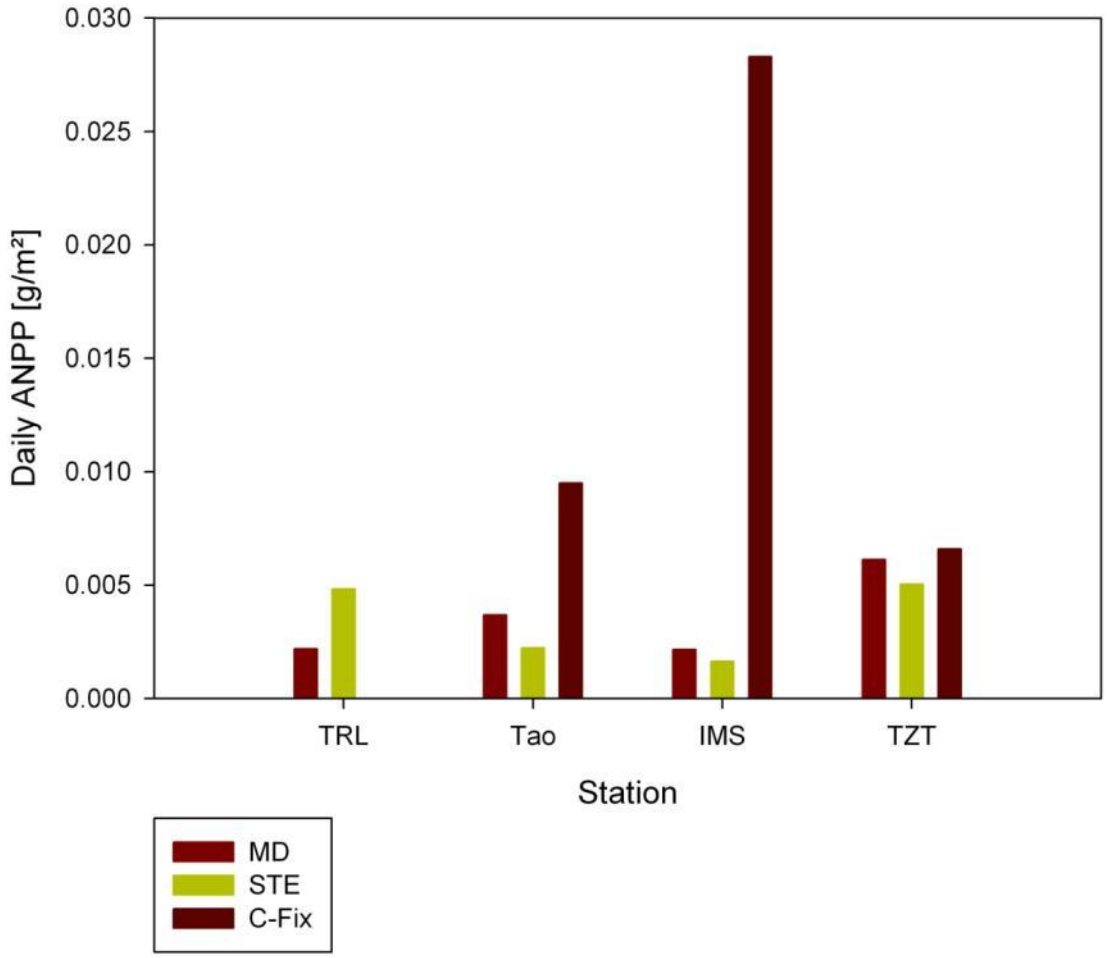

Figure 127 Comparison of C-Fix, MD and Measured Data (STE) on a Mean Daily Base (2000-2008)

Figure 127 indicates that the C-Fix model overestimates the productivity in comparison to the measured field data. It can be argued which model reflects the better temporal trend, but MD definitely is an improvement for the investigation area since it is locally parameterized to a better degree and also functions in the arid areas of the southern parts of the investigation area.

6.7 Spatial Extrapolation

Investigating the phenological cycle is a presumption to understand vegetation dynamic. Since regional or global Field experiments are very expensive or not possible, remote sensing analysis can fulfil that gap. It is possible to extract phenological parameter like length, begin, end or intra- and interannual amplitude on low cost for greater areas (White et al, 1999) by monitor vegetation activity with remote sensing sensors. Satellite born Phenology is subjective, because an objective Start and End is not ascertainable due to errors, uncertainties and other effects. The vegetation signal is a measurement on rising and falling NDVI, alternated by noise (See pre-processing and method).

Using the definition of White et al (1999), the NDVI can be described as phenological phase with Onset, green up or sequence. The extraction /derivate can be done in different ways:

- Defining limits (Adams et al., 2004) of the phenological phase, which can be over- or under run.
- gradient model (Jönsson et al 2002)
- Eastman, et al. (1993) und Hirosawa (1996) introduced a principal component method on spatio-temporal derivation African Vegetation and the western USA.
- The Harmonic Analyse or Fourier Transformation analyses the amplitudes and phases of the vegetation period in a temporal manner (Bradley *et al.*, 2007)

MOVEG Drâa investigates the following methods:

- White, Running und Thomton (White *et al.*, 1997b)as enhanced NDVI threshold Method
- The Fourier Analyse (Olsson & Eklundh, 1994)

Both Methods examine different Aspects of the Phenology. The threshold analyses of Phenology can produce start, end and length of the vegetation period. A Standardized Principal Components Analysis can identify potential cyclic and acyclic changes. The method of (White *et al.*, 1997a) was investigated in the thesis of (Elbertzhagen, 2008). The method of Olsson & Eklundh (1994) will be used to introduce as method to classify the investigation area based on the intra and inter annual cycle.

"[...]every pixel in a temporal data set is a time series, showing the value of, for example, reflected light or a vegetation index, at a particular time" (Olsson , Eklundh,1994). The amplitude and characteristics of the annual and inter-, as well as intra, annual cycle are examined by the Fourier transformation proposed by Olsson and Eklundh (1993) (c.p. also Davis 1973, Christensen 1991)

$$f(x) = f(x)_{mean} + \sum_{r=1}^{r=N/2} [a_r \sin(2\pi r x/P) + b_r \cos(2\pi r x/P)] \qquad (1)$$

where:

P = the fundamental period of the data; $P = 12$ for one year of monthly data
N = the number of observation in the series
r = the harmonic; between 1 and $N/2$
$f(x)_{mean}$ = the mean of the whole time series

Figure 128: Fourier Formula (Source: L. Olsson and L. Eklundh, 1993: 3736)

The Fourier transformation is originally designed to extract noise from an image (Richards, 2006). It is a description of a periodic function in terms of a sinusoidal function. By use the

method to extract phase and amplitude functions from NDVI data, so called Harmony's. The result of the function is the characteristics (min, max for one series) as rating for the time change inside the data set. By using the program Hants from L. Olsson and L. Eklundh (1994) a Fourier transformation is don, calculating Harmonys. Every Harmony stands for a derivation of the Fourier Transformation.

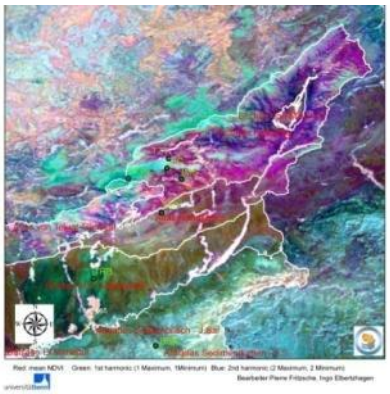

Figure 129 composite picture of the Fourier classification. The image contains 2 Levels of Information: Colormixture and Intensity. The brighter an area the higher the activity. Redish means annual constant vegetation. Green means uni-modal and blue bi-modale distribution of the vegetation signal.

The composite picture in Figure 129 shows a graphical illustration of the function with Red for mean NDVI, Green for 1st Harmony (6th on 6 year cycle) and Blue for 2nd (12th on 6 year cycle) Harmony.

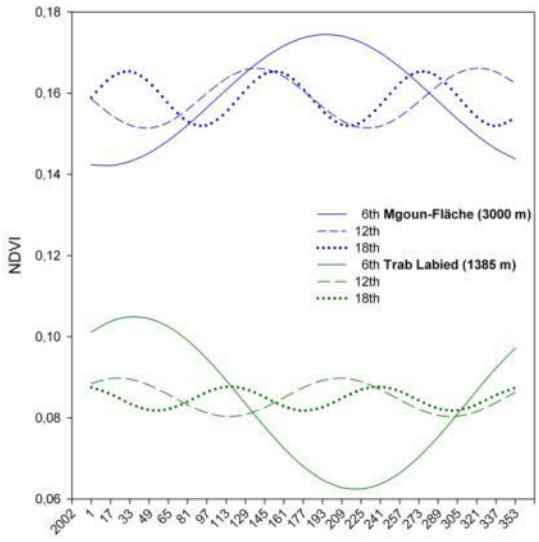

Figure 130 sample Fourier functions for 2002 (source: Elbertzhagen (2008)

As seen in Figure 130, the 6th harmony can be interpreted as unimodal distribution of the vegetation period, represented by the NDVI, inside the area. Figure 130 shows also that the Fourier function phase a little in time and differs in the amplitude of the function. As shown in the priviosly chapters the vegetation inside the Atlas Mountain is on a thermal gradient.

The results of the Fourier analyses show that the higher a Harmony the better the altitude explains the vegetation activity (R^2 = 51.83 for 3th Harmony). This means that short time vegetation activity changes are as expected. Finally, I compared the classification result with the existing vegetation map (Finckh, in prep.) and the derived natural units by using a confusion matrix. Therefore, the derivate classes arranged in proper order to vegetation classes and natural units map that occurs in the area.

vegetation classification (percent)					
Class	unclassified	pediment	bare surfaces	mediterranean high Stepps	oases
unclassified	99,04	0,12	0,43	0,59	0,01
9	0,52	91,10	28,50	0,89	0,93
5	0,13	4,20	41,00	38,23	5,84
10	0,27	0,01	26,17	24,72	0,94
2	0,05	4,57	3,90	35,57	92,28
total	100,00	100,00	100,00	100,00	100,00

natural units classification (percent)					
Class	unclassified	Atlas of Teluat-Ghassat	Basin of Ouarzazate	Central lime Atlas	Atlas marginal Catenarian
unclassified	0,00	0,04	0,15	0,09	0,07
3	0,00	0,00	27,54	0,41	4,91
8	100,00	95,94	0,00	0,00	52,36
10	0,00	0,01	65,74	27,22	19,08
5	0,00	4,01	6,58	72,28	23,58
total	100,00	100,00	100,00	100,00	100,00

Figure 131 Confusion matrix for classes inside the atlas region

Figure 131 illustrates the shifts and differences inside the area. The vegetation response units get an overall accuracy of 73.96% (Kappa Coefficient = 0.6245) compared to the vegetation classification. By comparing the results with the derived natural units we get an overall accuracy of 84.01% (Kappa Coefficient = 0.74). The overall accuracy results show that our unsupervised classification characterises the area very well.

Additionally to the quantitative accuracy assessment, the result was compared graphically. The differences between the automatic classification and the manual expert classification are in the arbitrary delineation in the case of the natural units inside the area. The natural meso-units are drawn according to fundamental geologic criteria and relief parameters. Widely both appendages share the same criteria, but vegetation formation has an environmental performance indicator that is not strictly bound to river boundaries or geological boundary. As investigation inside the Drâa Catchment shown is that, the Biomass increase is significant under non-grazing conditions inside the Atlas (IMPETUS, 2003). This method allows an exact classification of spectral information given on one to three steps in time. Nevertheless, the bottom line is the (mono) temporal character of the supervised classification. The Fourier transformation gives the opportunity to classify multi-temporal vegetation response units. Those areas are useable as input classes for modelling, as we classified them as identical on climatic influences. We are dealing with two uncertainties at this point. Firstly, we do not know everything about the processes that are going on, but try to reduce them mathematically. Secondly, we try to quantify process parameters, boundary conditions and starting points through the variability of the process, but analyzing them are more than statistic (Diekkrüger, 2000).

Vegetation Response Units Classification (Figure 132) are units, which can associate with non spatial meteorological data During the Forecast process the module access Figure 52 to determinate the Zone and Figure 132 to determinate the Regression Formula.

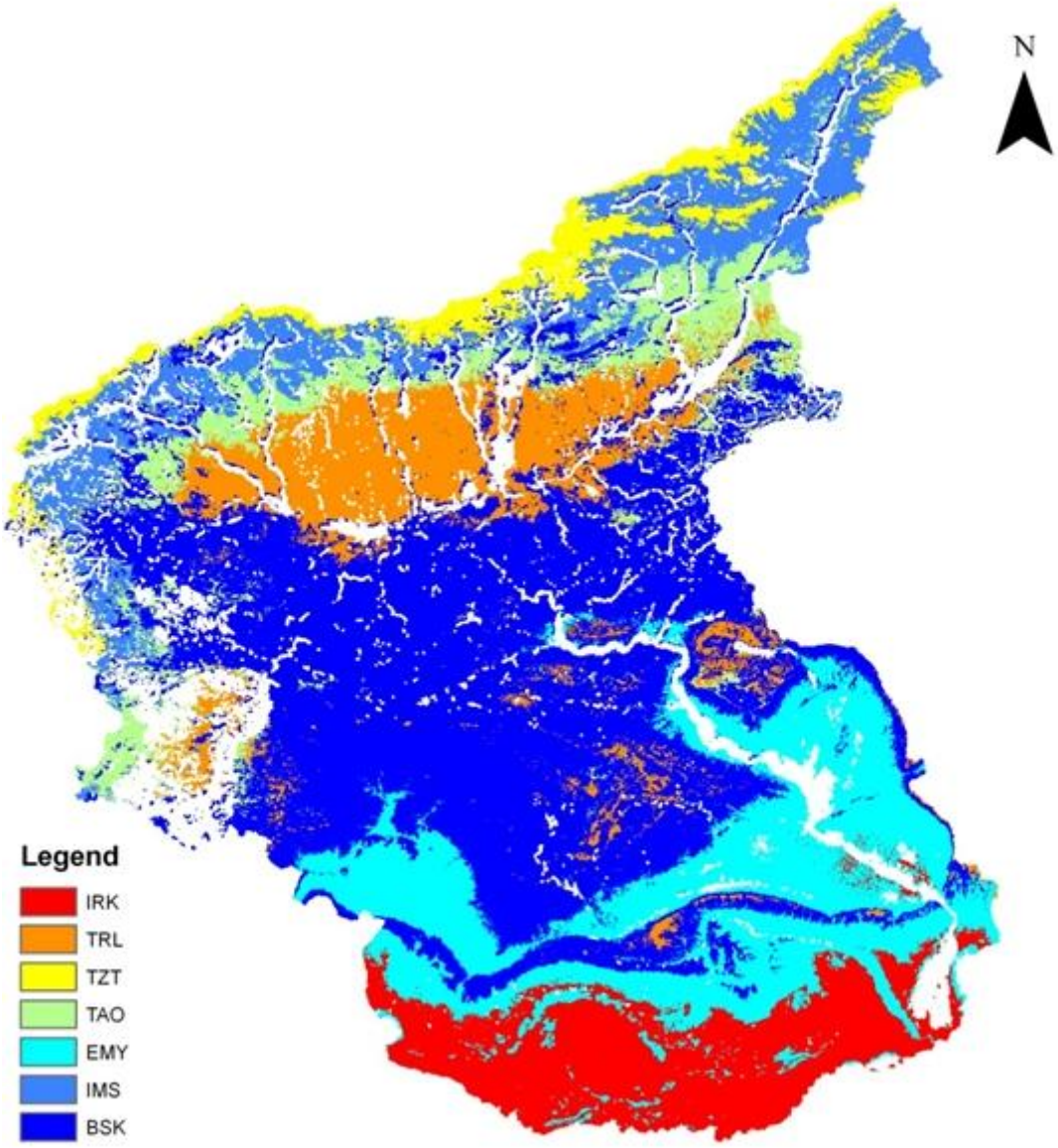

Figure 132 Fourier method classified Image

The result contribute to a future spatial extrapolation, by using a activity dynamic based classification. Every class can be sorted to one station and is therefore extendable to station and measurement density. Secondly the result gave an information of the usability of the area, sparse modeling computing speed and results are machine ready for further calculations. Also the lower computing steps are useable in case if you want to fast predict

an area for disaster management. This advantage, especially in developing countries, is crucial because of the lower computing power.

6.8 Forecast Results

This chapter presents the results of the forecast module. It first uses the regression formula generated in Chapter 5.10 and applies it to the climate data described in chapter 5.14 by using the two different scenarios A1B and B1 of IPCC. In a second step the results are used together with the ANPP module described in chapter 5.11.

6.8.1 NDVI Prediction

The future climate dates, described in Chapter 5.14, are now used together with the regression built up in Chapter 5.11 of the NDVI to calculate the NDVI from 2001 to 2050.

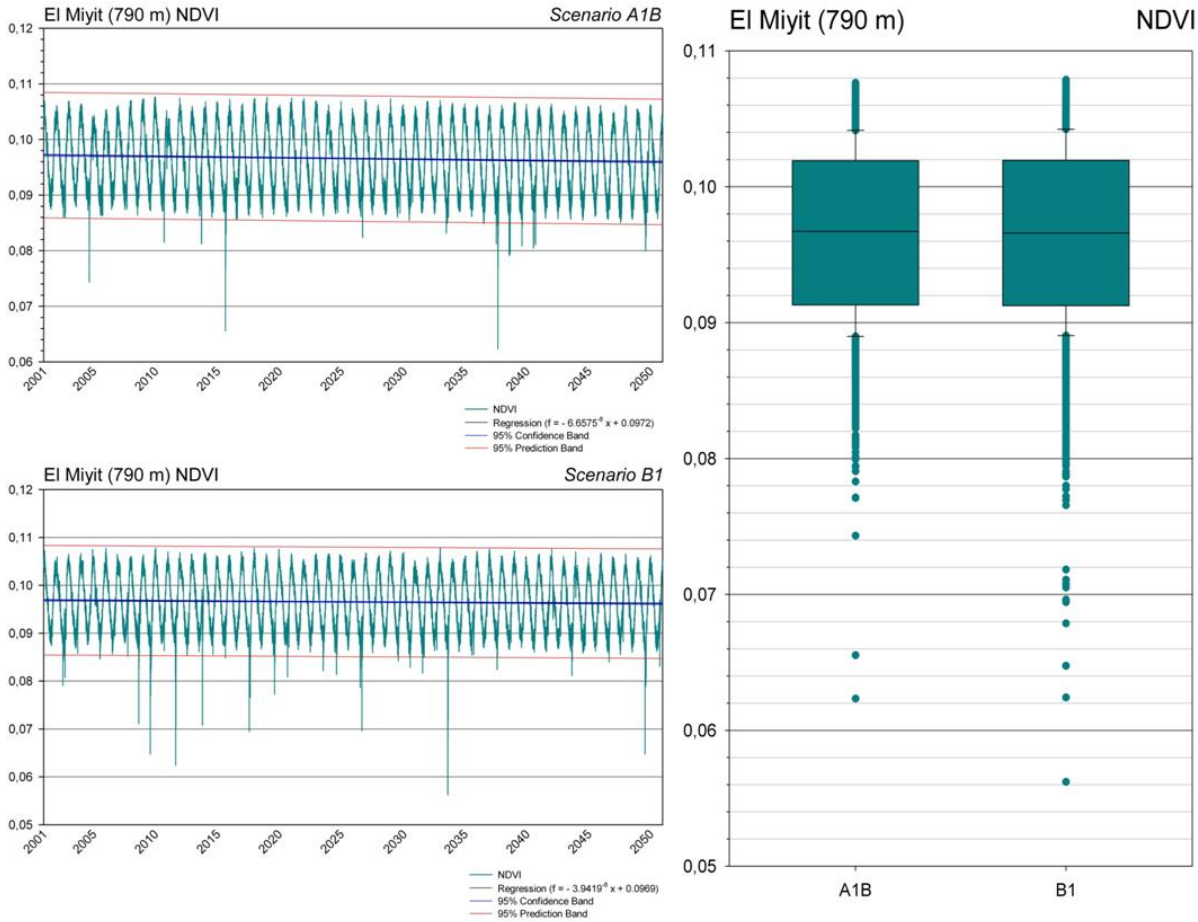

Figure 133 Prediction of NDVI (y-axis) for Station EMY with Scenario A1B and B1 as daily forecast and Box-Whiskar statistical overview

As seen in Figure 133, the results for both scenarios indicate that the plant activity decreases slightly, including some outliners. These are dry years (model data) or real outliners due to an overfitting of the regression model. On the right side the box plots for the displayed time are shown. The variances are very low. And the visual numbers of outliners are very few, due to the amount of data. This is done for every station used and for both scenarios.

6.8.2 Dominance results of the long forecasting module

One of the first things to be calculated with the NDVI data is the dominance or total vegetation cover. The variation coefficient shows that the ground cover varies up to 30 % (not displayed).

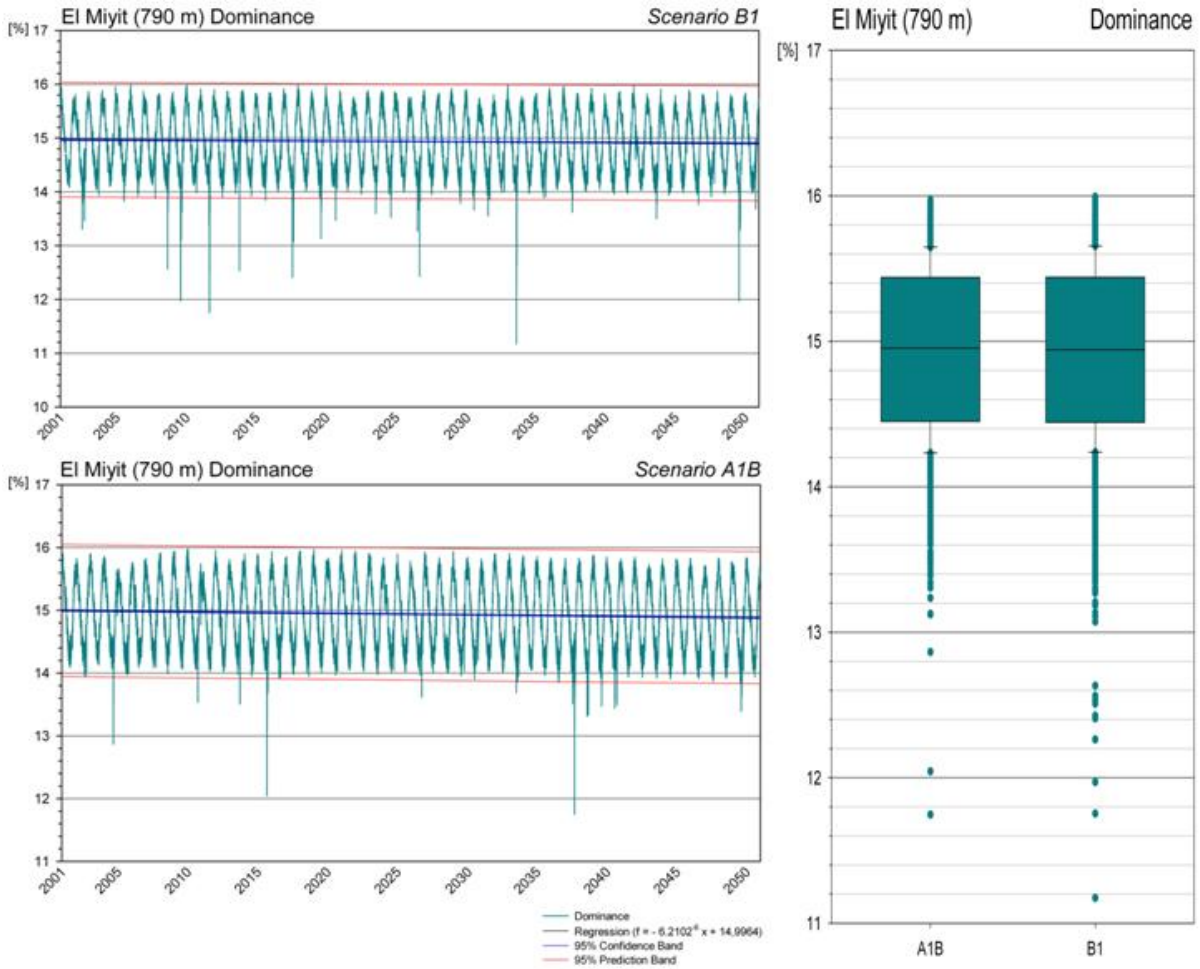

Figure 134 Forecast of dominance for Station EMY (y-axis) with Scenario A1B and B1 as daily forecast and Box-Whiskar statistical overview

The displayed dominance in Figure 134, e.g. for station EMY, is integrated into the ANPP calculation. For EMY station it can be shown that the mean ground cover decreased over the time of the projection. This occurs on a very low level.

6.8.3 ANPP Results

Using the RBM module, as in the ANPP calculation for 2000 to 2008, the calculated NDVI values are used to calculate the productivity based on the climate data from the IPCC scenarios A1B and B1.

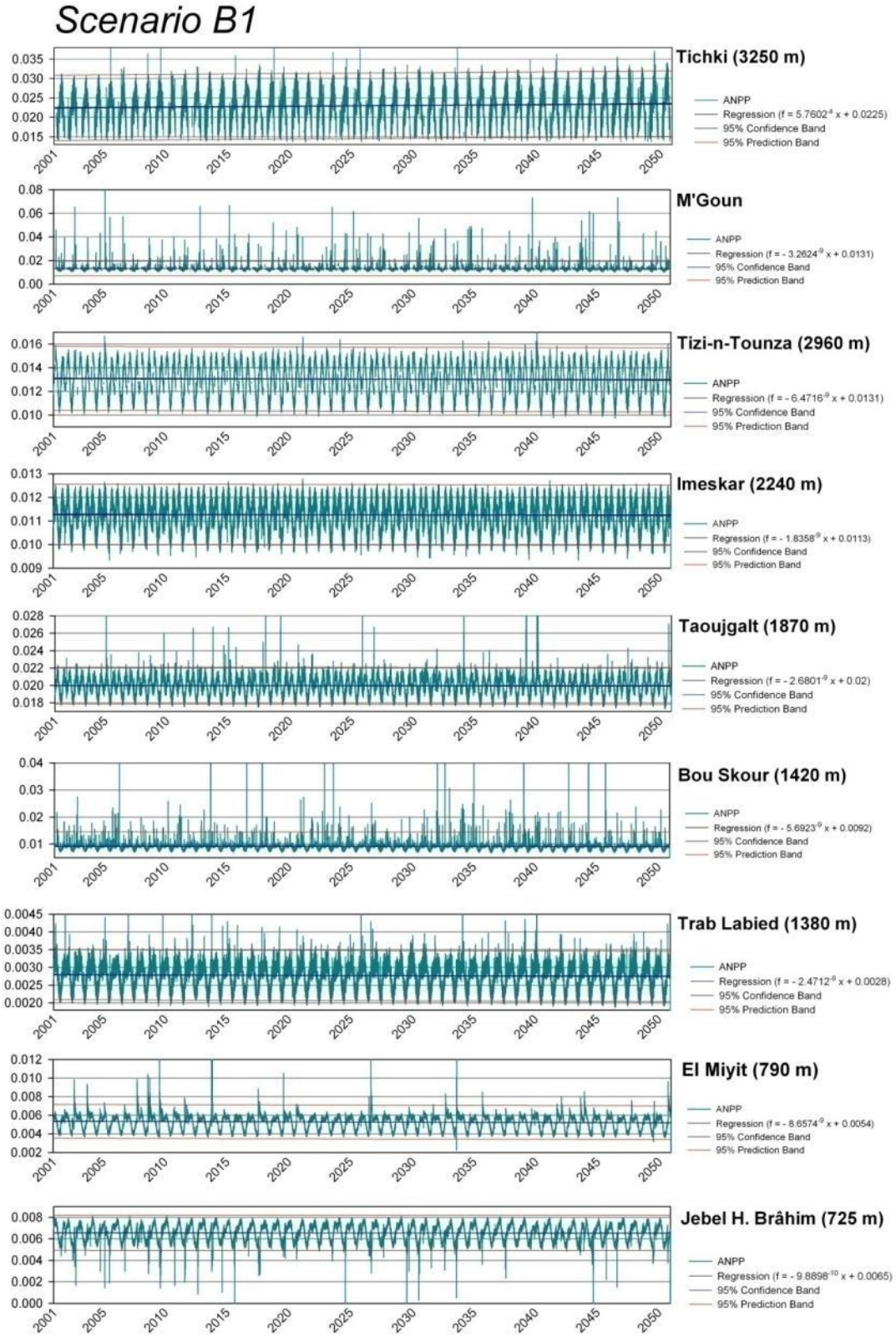

Figure 135 ANPP Forecast for IPCC scenario B1 for all stations (Units in g/m²/day)

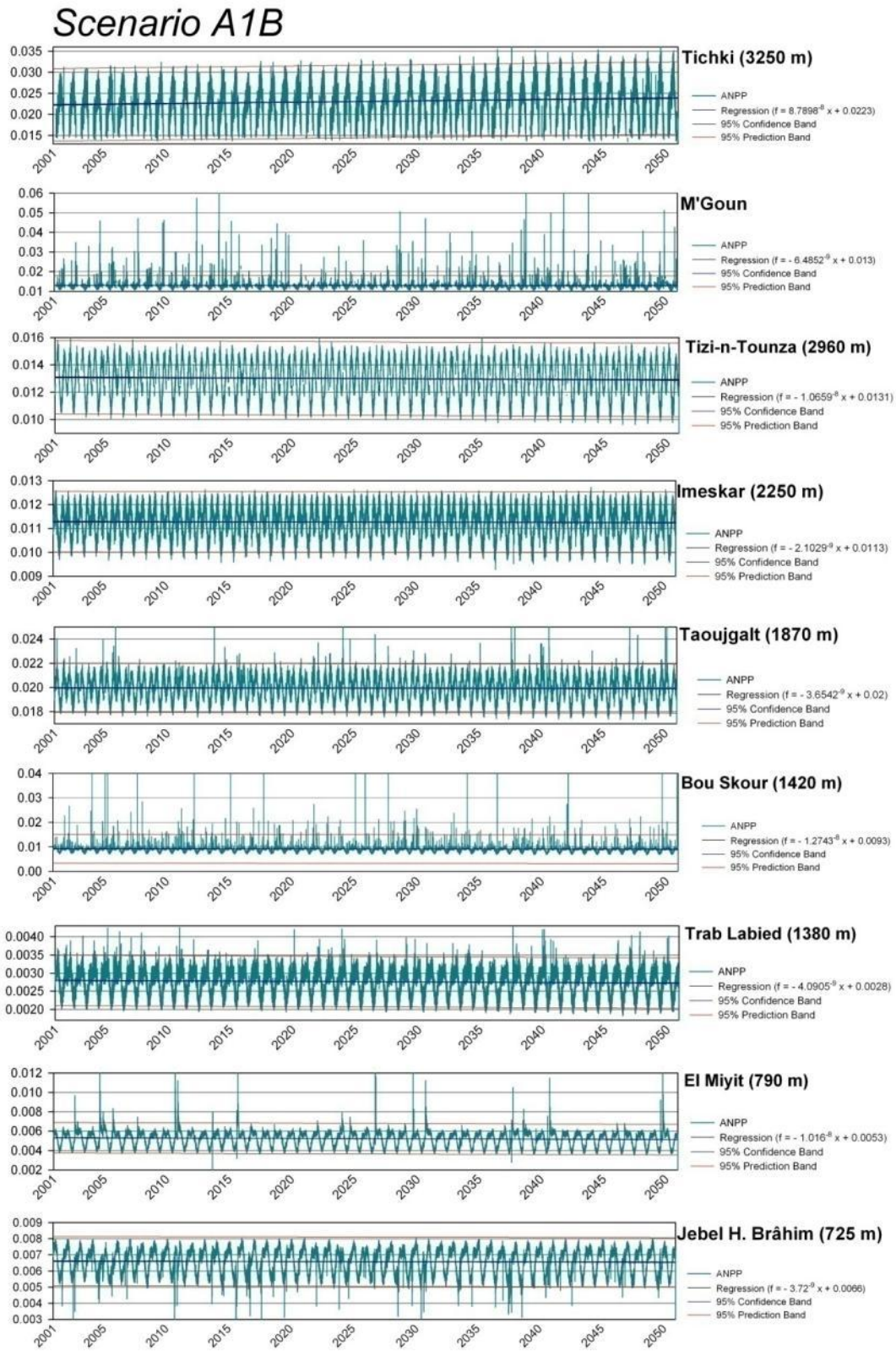

Figure 136 ANPP Forecast for IPCC scenario A1B for all stations(Units in g/m²/day)

The Figure 135 and Figure 136 shows the daily calculated ANPP for all 9 Stations used in this study. In general it can be stated that the vegetation productivity is changing on a very

low level. This slow change is consistent with the results from Finckh (oral). Secondly the yearly (anual) and interanual cycle can be shown and used for further studies.

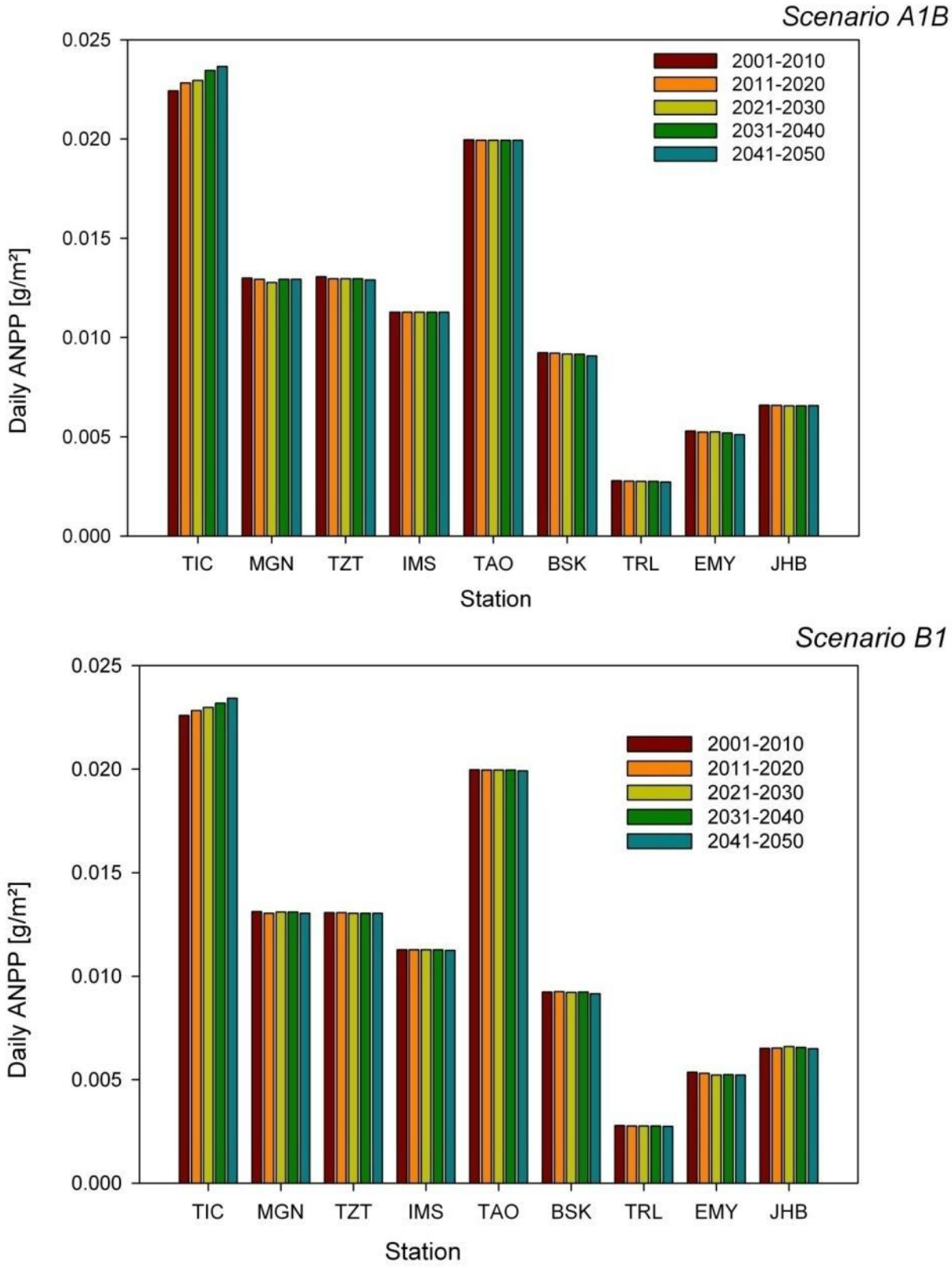

Figure 137 decade mean long term trend of ANPP for all stations (daily ANPP)

The long term trend can illustrated by the long term change mean (Figure 137). the changes occur only on very low levels for both scenarios. It is visible that the mountain stations (TZT to TAO) are on a stable, sometimes slightly increasing level. The stations BSK to JHB are also stable, albeit slowly decreasing.

6.9 Uncertainty Analysis

This chapter investigates in which way errors influence the results and on which magnitude said results are influenced. Uncertainty analysis in complex models is a necessary step to evaluate if the model is stable, and under which conditions. This can also be seen as a sensitivity analysis, but with the exception of summing up the input parameters.

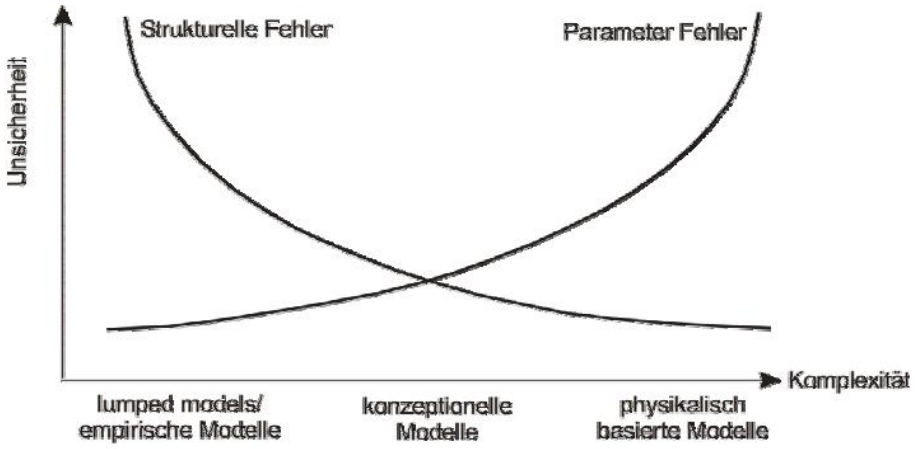

Figure 138 Failure analyses and sources depending on model type (after Grunwald, 1997)

The starting point of uncertainty analysis is the presumption that the full parameterized model rightfully describes the analyzed processes, as long as data is available (Diekkrüger *et al.*, 2006). Input uncertainty is a result of errors in input data such as rainfall, and more importantly an extension of point data to large areas in distributed models. As errors can have a structural model or parameter source, the uncertainty in physically based process models is normally smaller than in conceptional models (Giertz, 2004). For all models the following applies: The more input parameters, the more uncertainty (Giertz, 2004;Refsgaard, 1997). This chapter describes in which way and under which conditions the uncertainty analysis takes place.

6.9.1 ANPP Uncertainty

The uncertainty analysis for the ANPP module is done in three steps. Firstly those parameters are identified that are equable for an uncertainty analysis. Secondly the parameters are tested for consistency and model stability (parameter sensitivity). Thirdly, uncertainty limits for every parameter are set.

The result is an output for all investigated cases. By taking limits on the 0.025 and 0.975 percentile on the results a p-value of 97.5% of all values is acquired. This excludes extreme parameters and the percentiles give a better impression of the occurrence frequencies than other methods e.g. mean.

This following data is subject of a possible uncertainty analysis:

- CN2 (Runoff Curve Number Parameter)
- Total Ground cover
- C/N coefficient
- Field capacity
- Cloudmask

The Curve Number (cn2) is taken as the parameter which determines the amount of water that can be held inside a soil profile. As parameter of the runoff, it is a quite an important parameter to plant water availability (Cronshey et al., 1986). For this study the soil characteristics are altered on the mean in a variation of 4 points. That essentially means that we influence the infiltration and runoff by ~8%.

As described in chapter 5.10 a regression approach for calculating ground cover, on base of the NDVI, is used. For testing uncertainty on this parameter it is assumed that the approximated ground cover, determined during fieldwork, is slightly of scale. Therefore it is altered by a normal distributed value with a mean of 0 and a 4 standard deviation width based on the measured ground cover. This generates a measure error of up to +- 15%.

The C/N coefficient is a valuable parameter for describing plant nitrification. Under the presumption that this parameter is not estimated correctly and may change (Cronshey et al., 1986), an altered value on a normal distribution with a mean on the specific station is generated.

The field capacity is a factor on how much water, and therefore how long, is stored inside the soil profile. The field capacity is provided by Löose (2009). The field capacity is not constant and is in fact changed by many factors. By approximating that changes are continuous and occur in both directions, and that measurement errors can go in both directions, a mean for every station is taken and altered on a normal distribution with a deviation of 4 standard deviations.

Cloudiness is important in terms of the input energy into the system (Iqbal, 1983a;Richters, 2005a). Since RBM uses a linear function using the extinction coefficient to calculate the PAR irradiation the parameter is very sensitive. Since cloudiness is randomly distributed (see chapter 5.11) a uniform distribution is chosen (and therefore near random) to simulate the cloudiness between 0 to 100%.

The factor of carbon fixing was not included because this factor is bounded too close to radiation, and a high collinearity is taken. Secondly the low quantity of data does not allow a founded choice of an alternating level. The factor radiation is covered by cloud mask.

The firstly analyzed parameters are the RCN and CN2 parameters. Both parameters don´t affect the final result due to the effect that arid soils rarely reaches their potential water capacities (Simmar, 2003) and therefore the effect tends to be zero. The same goes for saturation runoff. Only very low profile soils and very humid months in higher areas are capable of saturation runoff (eg. Mountain ridges). Because of the rare occurrence this factor is dropped on further analyses, but kept in the model for two reasons. Firstly it is a good quality parameter for the soil module. Secondly it enables the model to work in higher mountain areas und prepares for other working areas.

The selected Parameters (Table 9) can be declared independent.

Table 9 Correlation matrix of Input parameters Uncertainty IMS Station

	Ground_Cover	cncoef	CLOUDMASK
Ground_Cover	1	-0.00364806	0.0245299
cncoef	-0.00364806	1	0.0143404
CLOUDMASK	0.0245299	0.0143404	1

The Uncertainty Parameters can be graphically displayed (Figure 139).

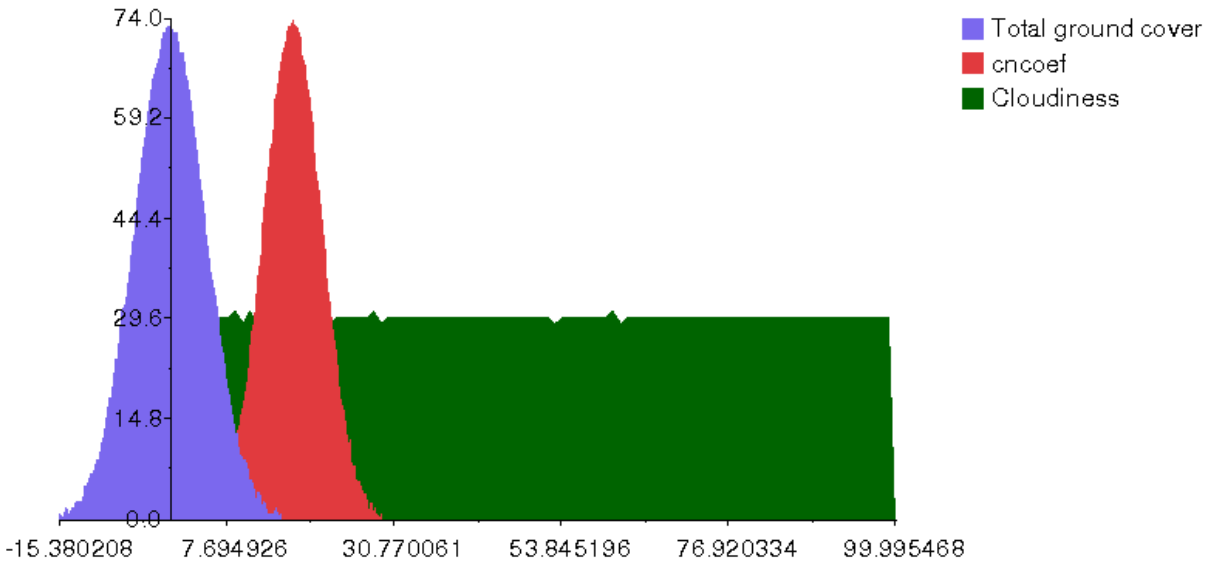

Figure 139 Distribution of altered Input parameters Station IMS

These are the uncertainty assumptions.

6.9.2 Sensitivity of the selected Input parameters

By using these three parameters the uncertainty analysis takes place by combining the Monte Carlo Analysis with the Latin Hypercube Method of (Diekkrüger *et al.*, 2003). An

uncertainty dataset for each parameter is created including 3000 combined iterations. The result is calculated and analyzed by calculating the three percentiles (0.025, 0.5 and 0.975) and graphically plot them. In a further analysis the 0.5 quantile is compared to the values of the original calculated ANPP.

6.9.2.1 Cloudiness

Using the 3000 iterations it is possible to reveal the influence of cloudiness on the productivity of the model.

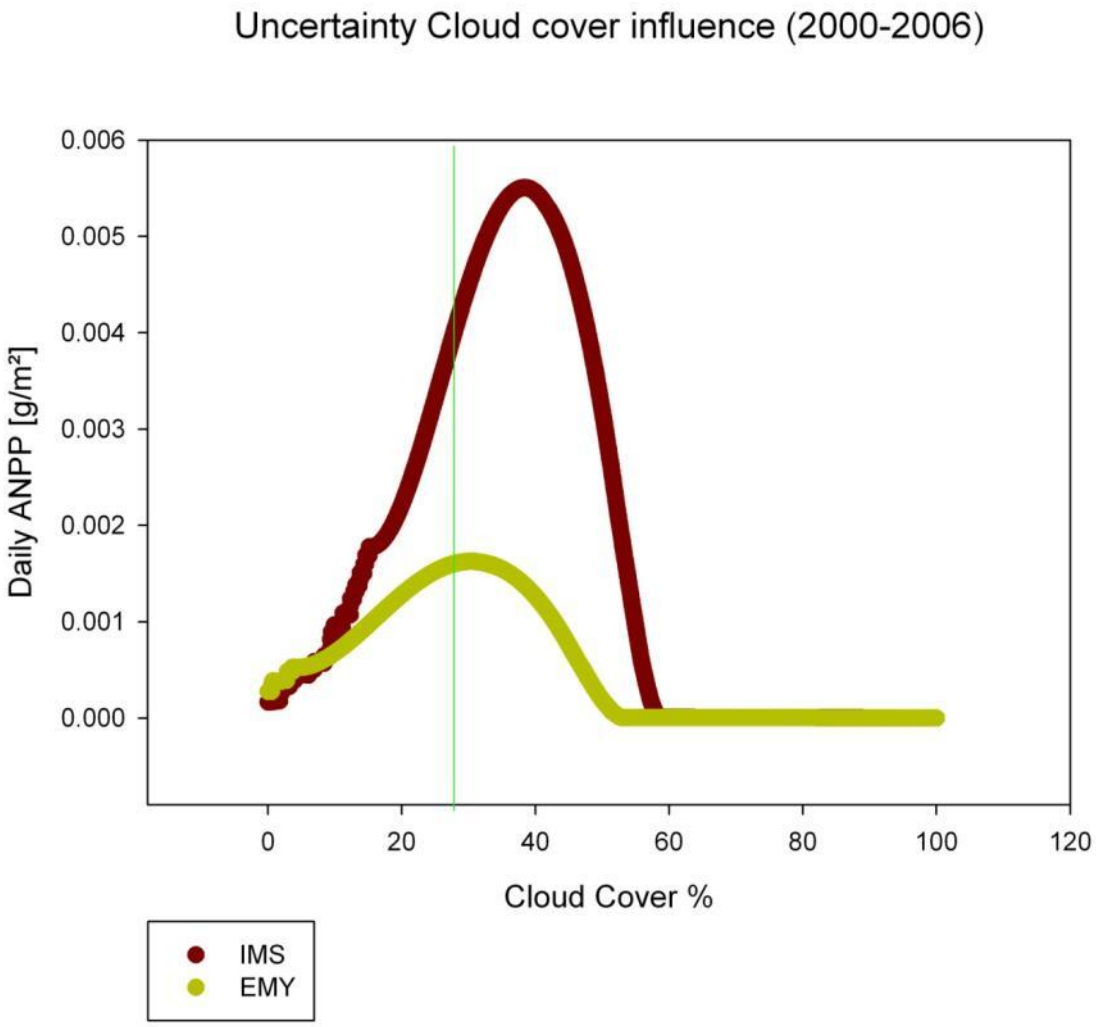

Figure 140 Uncertainty Cloud cover influence IMS (2000-2006). The green line marks the mean cloudiness at Ouarzazate Airport, the only WMO-Station inside the area.

Investigation of the cloud cover influence reveals that for every station a maximum productivity can be calculated which shifts to slightly higher cloud coverage in the north. Secondly it can be shown that the model slows down the productivity at a cloud cover of around 55% to a minimum. This can be explained by the fact that a cloud cover over 50% is never used during the parameterisation of the model and the productivity below that points is not exactly 0. It is more that the model asymptotic goes to a minimum.

6.9.2.2 Ground Cover

The ground cover is an important quantitative parameter for estimating the density of vegetation that is on an area and influences the productivity of the area (comp. Chapter.6.6)

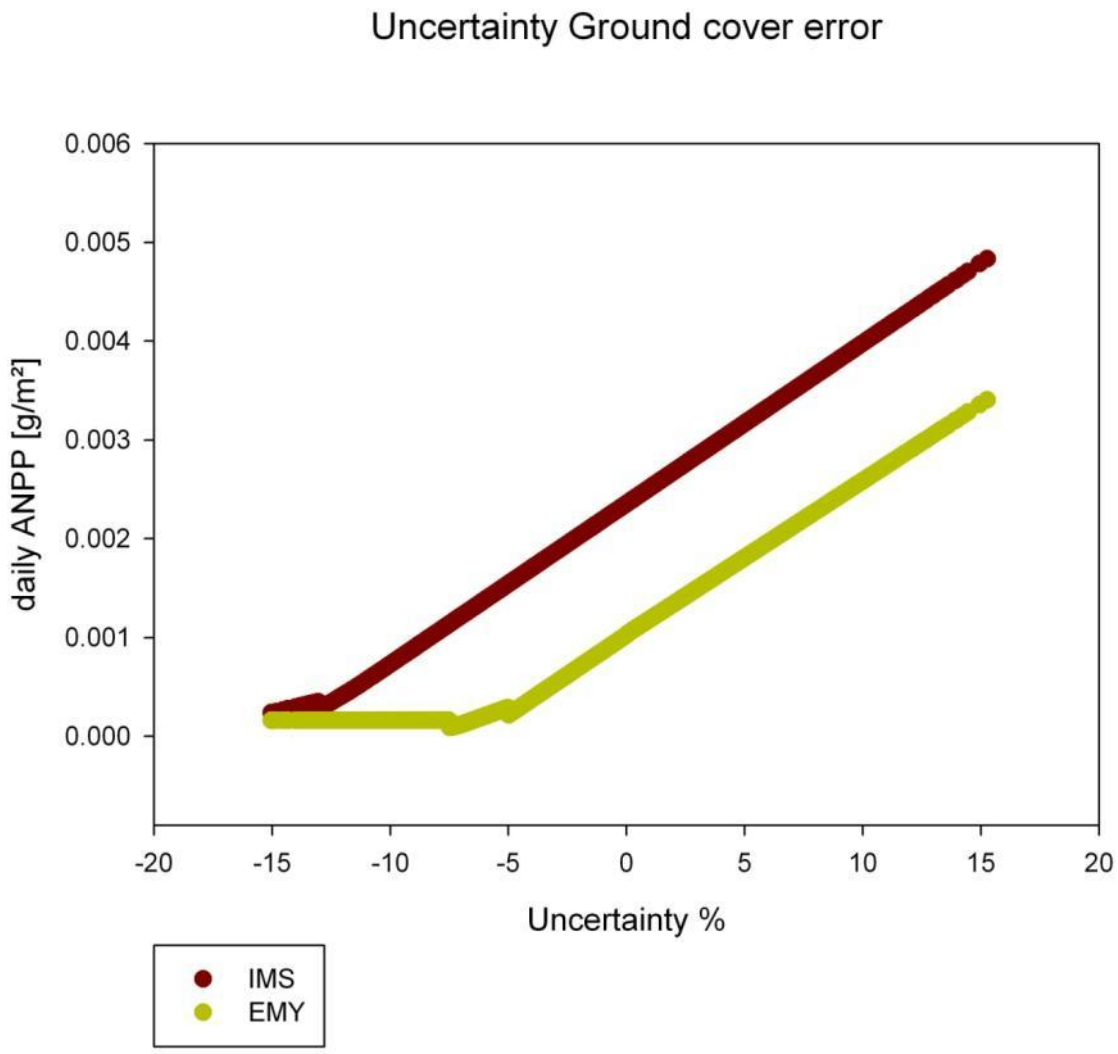

Figure 141 Uncertainty Ground Cover error

The uncertainty in ground cover shows that there is a linear relationship for ground cover influence on ANPP. The ANPP values of 0 are due to the fact that the calculated ground cover was capped at 0 to prohibit a negative total ground cover.

6.9.2.3 Carbon to Nitrogen coefficient

The C/N coefficient is one of the most important factors to measure plant nutrient supply.

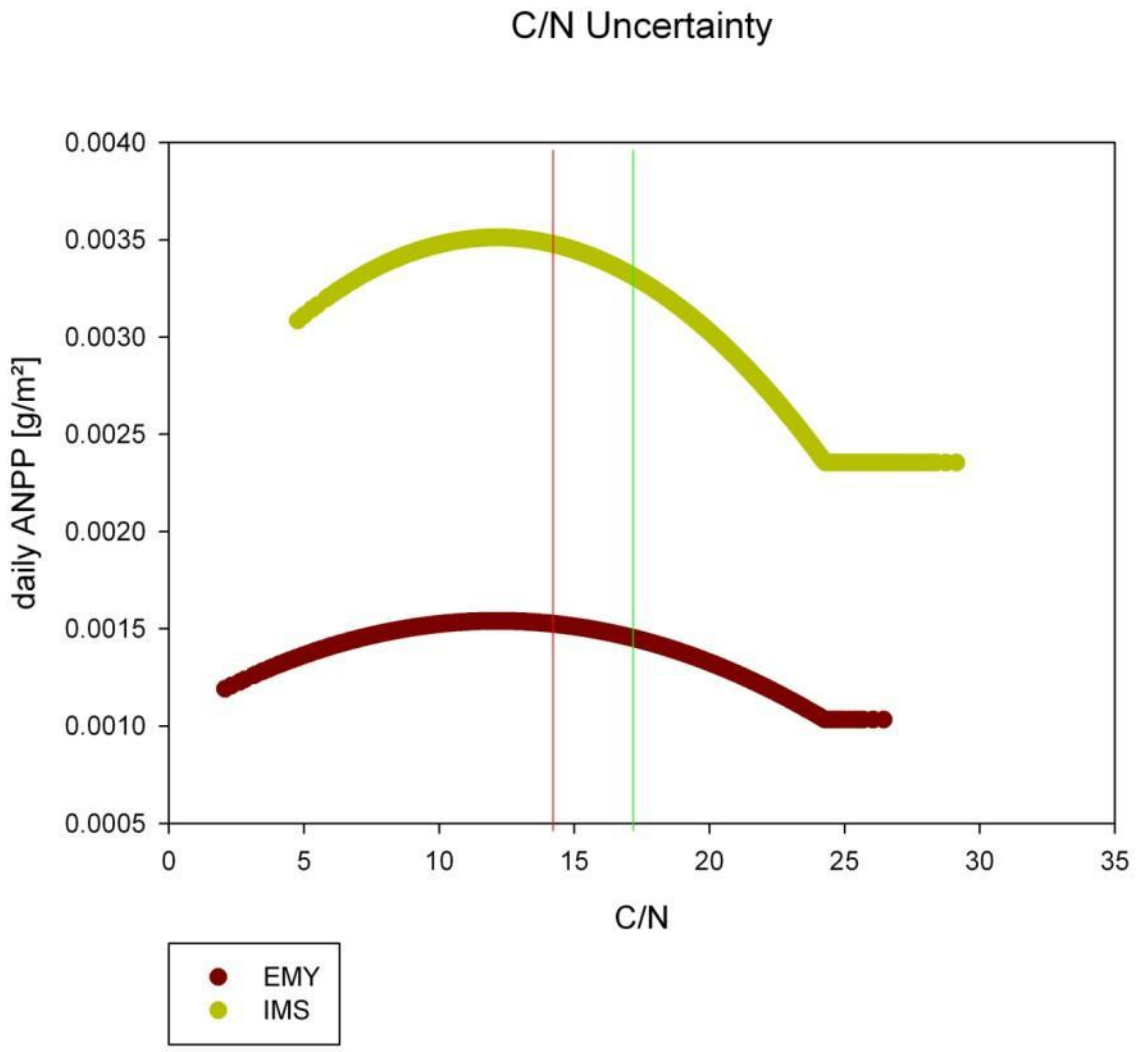

Figure 142Uncertainty C/N

The C / N uncertainty relationship shows that productivity is in a hyperbolic relationship. All values above a c/n of 25 are negated by the model. This uncertainty reveals also that the highest productivities are on a lower level than the actual value. A lower level means that the nitrate availability increases. This in turn means that for the two displayed soils N is not optimal. It can therefore be stated that nitrate is at a minimum of plant productivity in the system.

6.9.3 General uncertainty

Using all uncertainty parameters together, a general uncertainty can be calculated for every station from 2000 to 2006 (Figure 143).

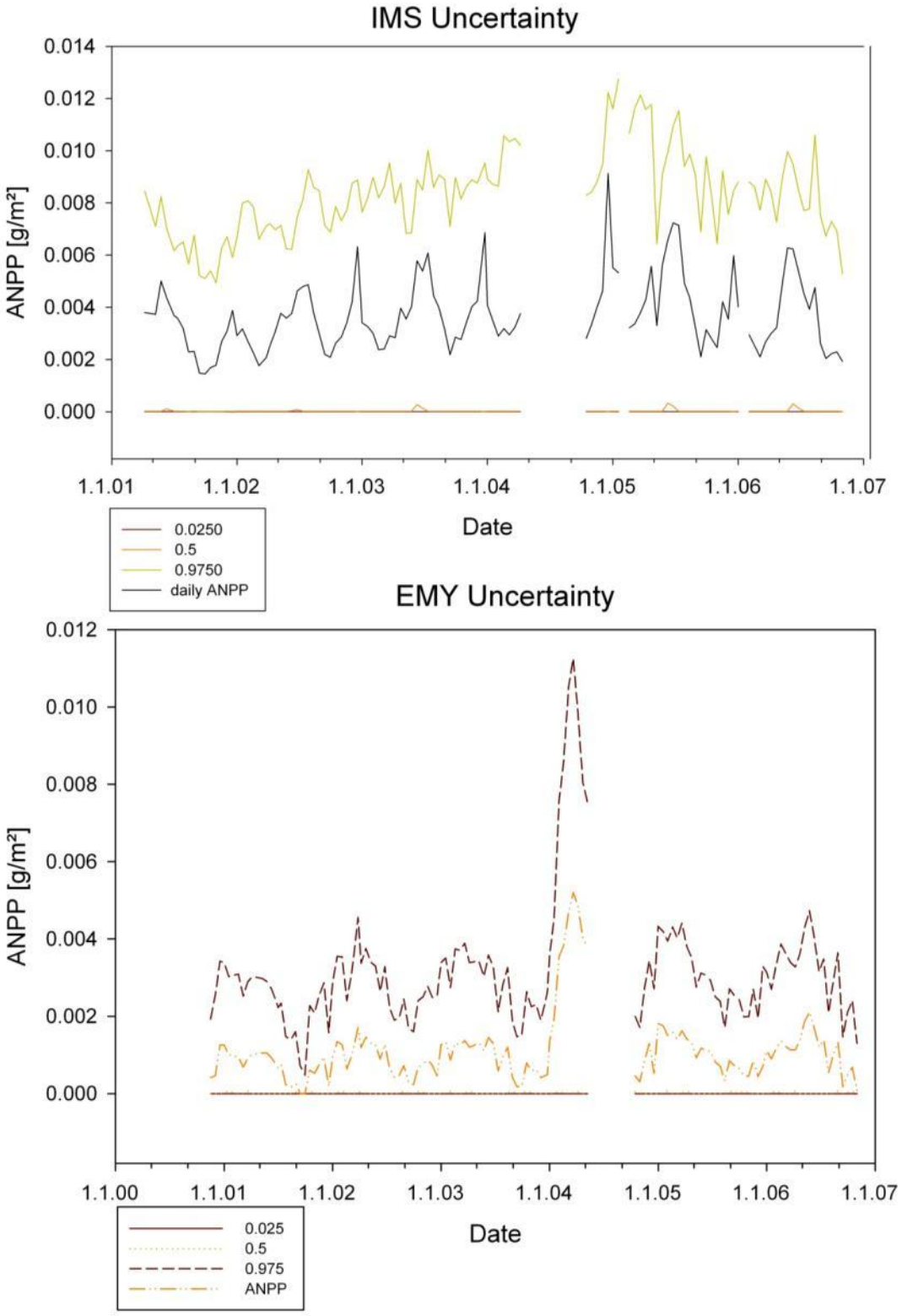

Figure 143 IMS and EMY uncertainty Quantiles and the orignal calculated ANPP

Figure 143 shows that uncertainty can be at a relatively wide value between 40 to 100 % around the original value. The lower level is always 0 because zero productivity is always possible. The upper limit is a given upper limit of the model for all possible influence combinations.

This high variation of up to 100 % is not quite satisfactory, but the 0.5 quantile is quite lower than the normally calculated ANPP (Figure 144).

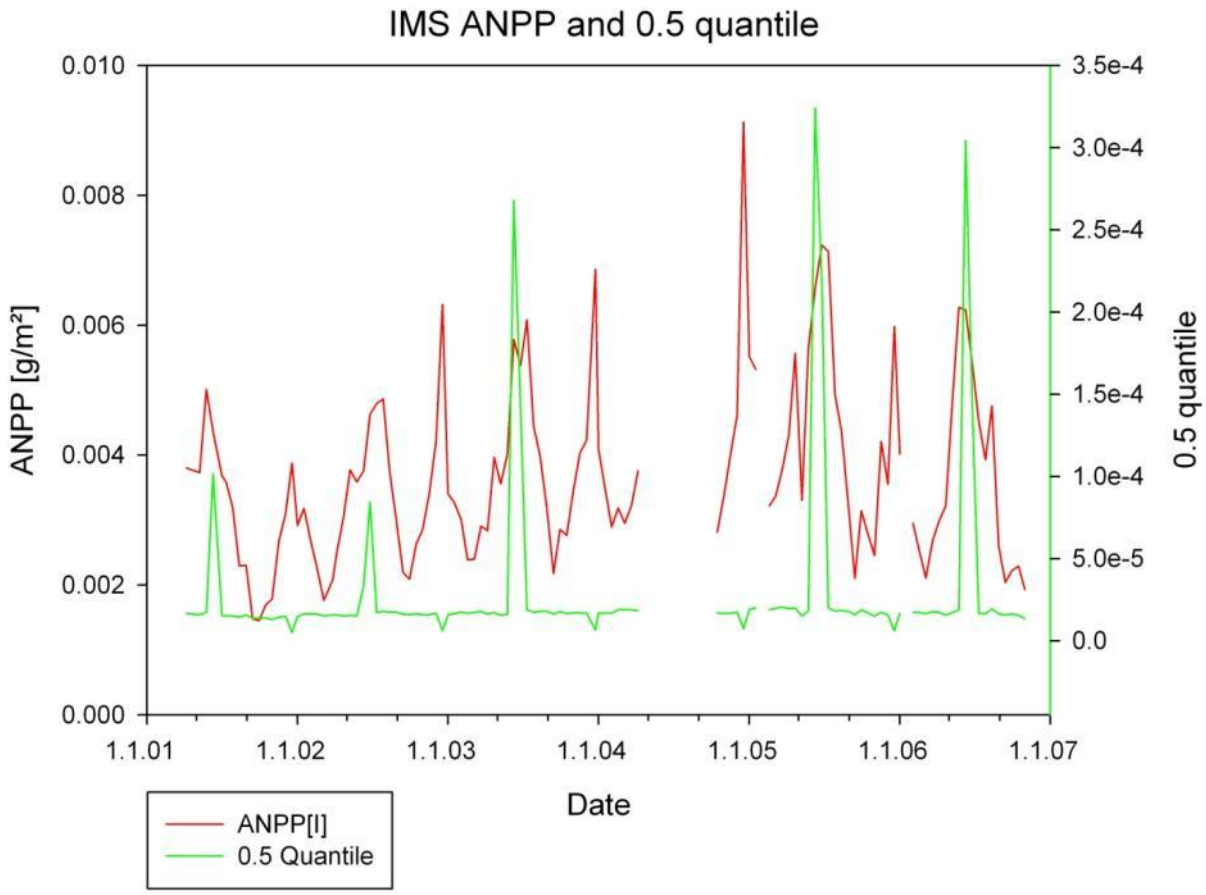

Figure 144 ANPP and 0.5 quantile comparison

This is an indicator that most of the calculated values are below the calculated ANPP or quite small. This is also an indicator that the productivity can be much lower in certain circumstances. In summery the ANPP can be displayed by its calculated value and the error bar provided by the uncertainty analysis.

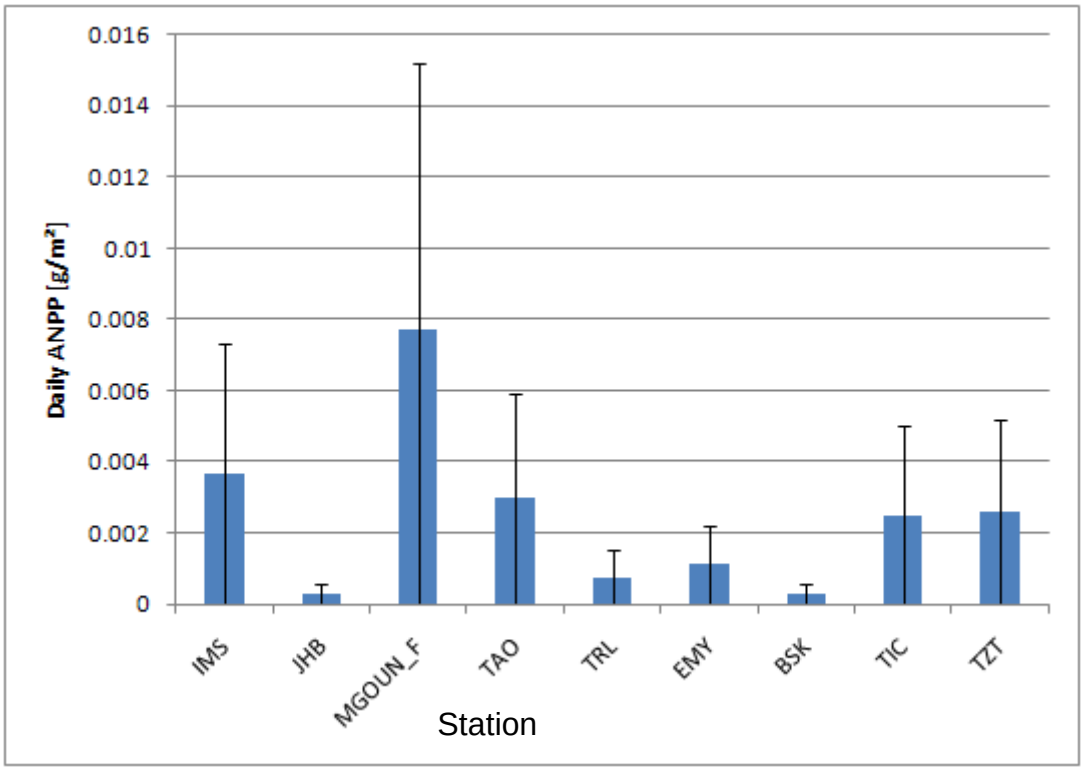

Figure 145 ANPP uncertainty 0.5 Quantile

By taking the mean difference between the 0.5 quantile (which is the median value in this case) of all calculated values and the calculated ANPP from the model driven by the measured values, a near symmetric distribution of errors in negative and positive direction can be stated. This means that the model entails a nearly 100% variety in both directions. Figure 143 demonstrated that this can go up to 500% for extreme combinations. This extreme variety is due to the relatively low numbers.

7 Conclusion and Discussion

Modelling is a game, but it is a serious game (Beven, at the 2001 EGS conference in Nice).

Core objective of this study was the interdisciplinary approach of analysing vegetation activity on the base of satellite and meteorological data. Therefore the vegetation course for the years 2000 until 2008 inside the Drâa valley was investigated by using NDVI Data in order to understand the principals of vegetation dynamic. Nine corresponding climate station data was analysed to investigate the climatic situation. The main challenge of this research has been to unite diverse scientific disciplinary approaches to develop a model that can provide a robust semi-automatic analysis of vegetation dynamics including most vegetation relevant environment parameters for the semi arid region of the Drâa Valley in southern Morocco. By using sophisticated mathematical approaches the results show it is possible to analyse and simulate natural processes on the basis of their dependencies. This final chapter will conclude all results from chapter 6 and 7.

7.1 Regression approach

These studies show that the vegetation activity mostly depends on temperature. It can also be shown that the temperature goes from a positive correlation inside the Atlas mountain area to a rising negative relation in the south. This shows that with rising temperatures (positive correlation) the vegetation starts to react and with temperature above a certain level the NDVI declines. This also seems to highlight the models problem in higher mountain areas of capturing vegetation activity, especially in winter. Since we already sort out temperature below 5°C, the vegetation growth seems too unsteady. This model was tested on its quality behaviour and in a split sample test for calibration and validation.

The low level soil water content (in comparison to the total water capacity) corresponds to long lasting water stress. Combined with often high water vapour pressure deficits, arid plant life has adapted by creating mechanisms against water loss (Lajtha & Whitford, 1989;Snyman, 2005). The original thesis that only rain is the steering factor for plant growth must be rejected and replaced by a rain steered water pressure deficit minimisation in a plant physiological sense. This means that rain minimizes temperature and decreases the water vapour deficit, due to which said reason temperature inherits greater explained coherency. This doesn´t change the fact that rain, or general water availability, is a prerequisite for plant activity. More water doesn´t effectively mean more nutrification (comp. (Lajtha & Whitford, 1989;Snyman, 2005). In this context it is not surprising because plant physiology is in the balance of energy gains and energy losses (see Baumann, 2009). More rain doesn't mean more nutrificants, and this in turn means that the physiological reaction is slowed down. And

the other factor, that of extensive evaporation, is also involved. A possible improvement can be achieved by introducing a more detailed investigation between usable nutrificants and soil water content. This is not included here because there is no detailed study on this topic for this area.

7.2 Biomass

The ANPP module calculates the highest production rates inside the high mountain Atlas range. This is comparable to the results of (Baumann, 2009) and other data sources.

As for pastoral use the grazing value is not only determined by high production of forage, but the predictable availability of forage(Baumann, 2009), its most important to forecast the seasonal production.. As shown in chapter 6.6 the that forecast can be done on a reliable basis. The model is stabile (comp. Chapter 6.6. and 6.8) and reflects the annual and interannual course without following hops of the input data. This is remarkable since the ANPP model has now kind of memory. MD is therefore optimized on the mid to long term prediction.

Since nomads and their herd's use surplus of vegetation, the vegetation signal is dampened by higher use and amplified by lower usage. This may explain some outliners that are inside the activity data. If one area is not used during one time the signal may be outlining because of that effect.

It is always a problem to transfer NDVI and NPP results to other areas or to use other sensors. This will always come with high failure rates and under or overestimation (Menz, 1996). Typical problems that can be lead to over or underestimation are

- Non consistent measurement (shifting of stations, change of Sensors)
- Non-sufficient pre-processing (pixel location, radiometric shifting, cloud influences)
- Possible under- , overestimation of standing crop and NPP in field measurement
- Mathematical problems due to applying regression results on an area with a high wood content

This study avoids these problems by using a defined product and a semi automatic approach which is self adjusting with new data. Based on the work of (Diouf & Lambin, 2001) this investigation firstly discusses the issues of climate variability and prepares it for a automatic modelling.

The comparison with other models (comp. Chapter6.6.4) reveals that MD has a lower yearly amplitude, but on overall a better parameterisation of the mean daily productivity. The great advantage of MD is the individual parameterisation for the whole Investigation area and the possibility to integrate more data. This open standard is an advantage for transferring the

model to a greater area or other areas. (Richters, 2005a) also mentions that a scaling on higher resolutions will in general improve the possibility to describe and identify more structures on a small scale. This is done by MOVEG DRAA by improves the spatial resolution by factor 16. The discussion of primary production is interwoven with the carbon fixing discussion. Carbon fixing is coupled with significant sinking of carbon dioxide (Schimel, 1995;IPCC Working Group3, 2001) and the role of vegetation inside the global cycle. Primary productivity is more concerned with the roll of vegetation depending on energy provided and used by plants (Le Houérou, 1984;Oke, 2003). (Monteith, 1972;Monteith, 1965) goes one step further by bringing aspects such as the efficiency factor into the discussion.

The greatest advantage of MD is that it can improve the spatial understanding by integrating data of a long time series, which is hard to survey by other means. This is something which can typically only be provided by remote sensing data. By using a modular structure all options for extensions are wide open. MD is a self calibration, semiautomatic model which

- Test the input parameter with an automatically Error handling
- Self assimilation, depending on the combined length of all input factors
- Self calibration, depending on condition given by input parameter.

7.3 NDVI forecast

The long term forecast of the model is a bit static in terms of the long term trend (comp. chapter 6.7.). This is an indicator that the long term relationship of NDVI / atmosphere is not fully explained by the model. This is partly due to the modelling strategy (see least square problematic in Chapter 5.10) and partly to the MVC composite. The MVC composite problematic can be viewed as a problem of brightest glowing. Ultimately, MVC means that pixels of brightest value (eg. greatest value) are taken. Under the assumption, and this is not always true, that the brightest signal is also the date of its neighbour, it can be assumed that there are pixels in neighbouring different states. This can cause unexpected spatial shifting. One of the main problems in this work is that the real day of the MVC NDVI measurement is unknown. This can raise the problem of temporal unsteadiness, because two time steps can have a range between 1 to 31 days. Therefore only one value of meteorological measurement for that period can be associated with one time step.

7.4 Summery

This study raises the frequency of vegetation monitoring inside the Drâa catchment from a few observations by hand to a every 16 days observation by increasing the timespan to 8 years by using MODIS NDVI time series. Supplemented by a vegetation monitoring network and 10 years of measuring meteorological network a entire usable phenological database

was created. Furthermore this study also takes the impact of soil water as a main water source during draught into account. It also considers the time delayed reaction of plant activity after rainfall events. MOVEG Drâa provides a robust analysis of the phenological cycle with a robust productivity output and allows out long-term predictions based on the basis of the IPCC scenarios.

8 Outlook

This work closes the link between the lower atmospheric situation and the depending vegetation activity. One of the mayor problems will be the extrapolation of point data for an area. Especially small meteorological events (like thunderstorm events) can cause great differences in spatiotemporal measurement. Therefore remote sensing imaging sensors can spatial fill the gap between climate stations, although they cannot completely substitute them (Remsberg, 1994;O'Donnell *et al.*, 2000). Future sensors will increasly close this gap.Sensor combinations, like NASA A-Train, future meteorological platforms like MTG (Meteosat third generation) mission and environmental missions like the LDCM (Landsat Data Continuity Mission misson (Figure 146) will substantial contribute to this goal.

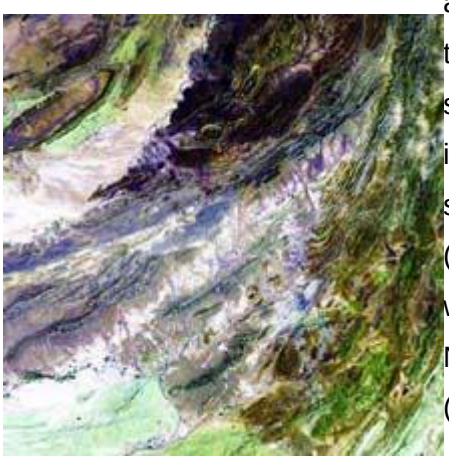

Figure 146 Image that represents the LDCM mission (source: NASA)

The IMPETUS projects aims to provide the availability of water. Answer questions such as in which way a better management of resources can improve the quality of life for land users. Since one of the main extensive land use in southern Morocco is extensive pastoralism (comp. (Baumann, 2009;Kemmerling, 2008), a major improvement would be the combination with land use models. (Richters, 2005a) already mentioned that one of the primary extensions of the RBM approach should be to include the sustainable survey grazing. This should close the gap between production and consumption. Since the survey inside the Drâa catchment is not available, it is not possible to close that gap. One of the most important things is that the production calculated by this model is the real production minus the biomass used up by grazing. As (Baumann, 2009) mentioned grazed biomass can make up to 90% of all consumption (Figure 147).

The model itself is fixed on this grazing rate, because it includes the carbon fixing rate of the grazed area (which includes the grazing loss). It is therefore possible to give a productivity potential, but since the grazing rate is still unknown this will for now remain a hypothetical number. Modelling reaches its limits at this point.

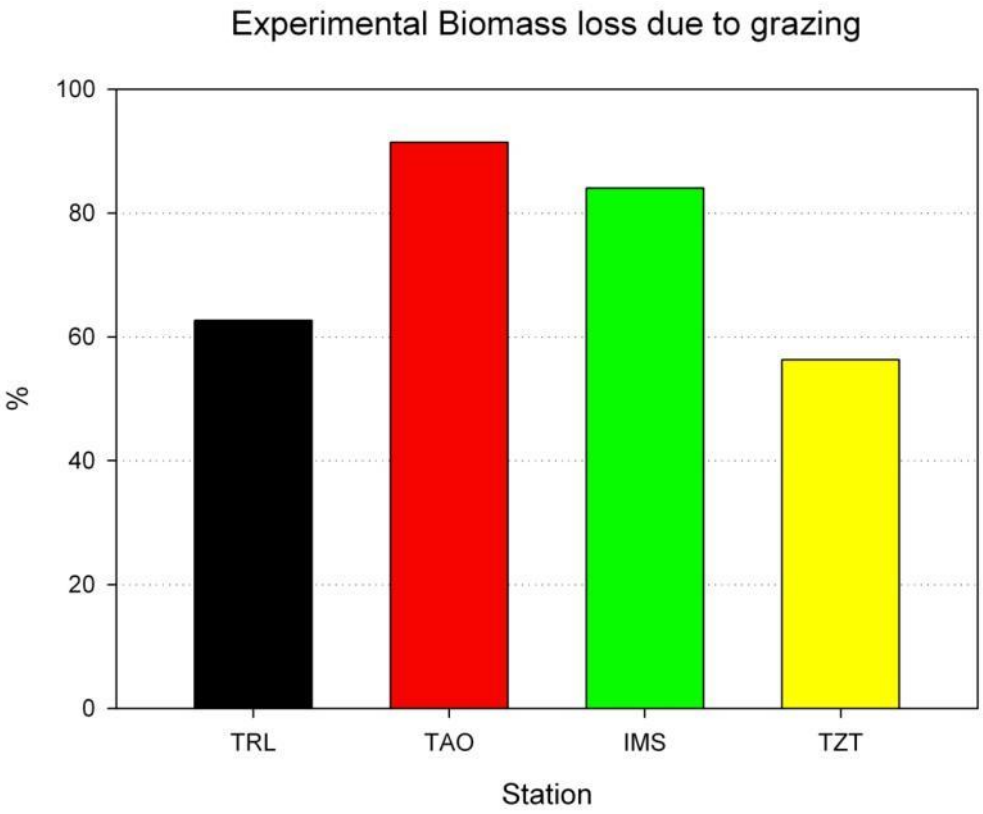

Figure 147 Experimental measured Biomass loss due to grazing influences on 4 stations along a S-N gradiant, which is also a altitude gradient. (Source: Baumann, 2009)

Figure 148 explained that the total number of sheep and goats has been rising in the last 20 years, including all the problems that come along with that fact.

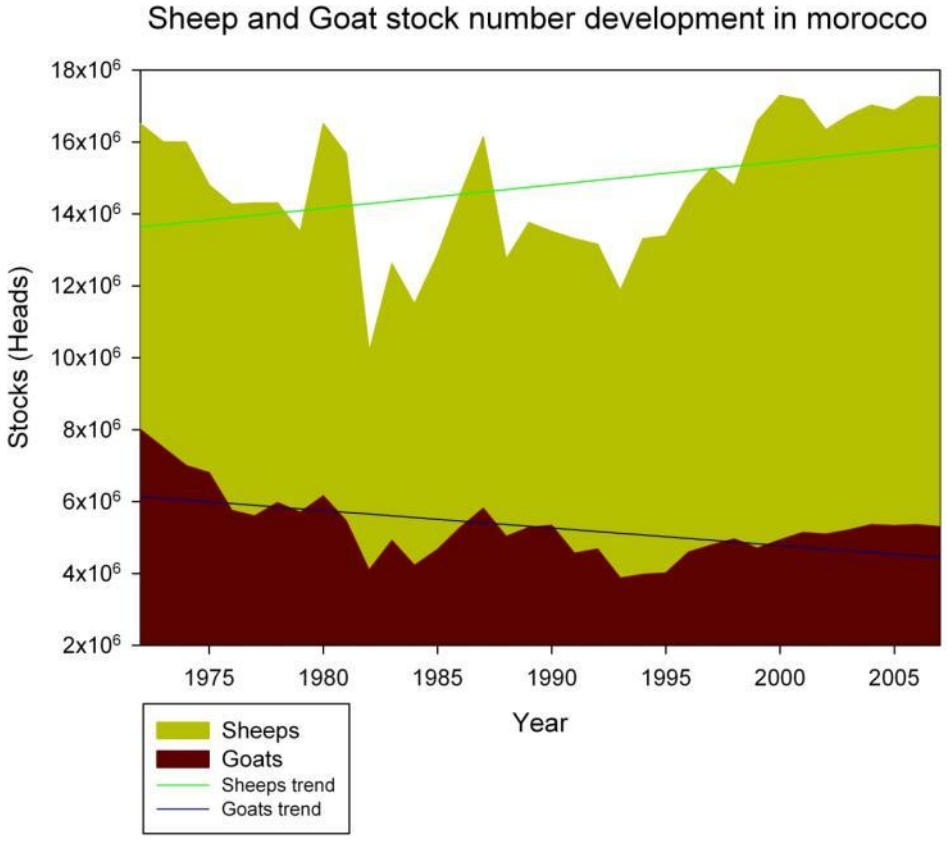

Figure 148 Sheep and Goat development in morocco (Source: Service d´elevage)

As an example, the increasing trend of sheep population increases pressure on useable biomass very likely. Since the ecosystems are in transition between a degraded state to equilibrium state of transition (Finckh & Oldeland, 2006;Finckh & Staudinger, 2002;Finckh & Oldeland, 2005b) more, and finer, vegetation information are needed. Newest studies indicate that the eg ANNP is a poor indicator for degradation in this highly variable landscape (Baumann 2009). Therefore it is important to improve the carbonisation parameterisation with land use (models) and further investigations on plant growth (increasing part) and pastoralist science (decreasing part). (Finckh *et al.*, 2009) states that the long term shift in vegetation composition gains in importance and desertification is more likely caused by firewood cutting and overgrazing. Using this regression result it can be stated that under the land use during the parameterisation phase (2000-2008) and under the climatic changes of the climate model, only minor changes in vegetation activity will occur in both scenarios. This is only a generalized output in terms of vegetation composition, but it inherits the conclusion that for ANPP calculation the general productivity change is only minor.

MD introduced a new toolset to handle low and unsteady Vegetation activity investigation on a regional scale. Its contribution of tools is set, but certain parameters undergoing a further development by improving space technologie. It is most certain that remote sensing in all scales will be constantly increasing it’s contribute to earths observations and the benefit it provides to the understanding of the interactions inside all processes on earth.

Reference List

Reference List

MODIS Level 1B Algorithm . http://www.mcst.ssai.biz/mcstweb/L1B/L1B_OVERVIEW.html . 2006.
Ref Type: Electronic Citation

MODIS VI Product (Algorithm) Description. http://tbrs.arizona.edu/cdrom/VI_Intro/VI_MOD_VI_Prod.html . 2007.
Ref Type: Electronic Citation

MODIS Level 1B Calibrated, Geolocated Radiances (MOD 02). http://modis.gsfc.nasa.gov/data/dataprod/pdf/MOD_02.pdf , -1. 2008.
Ref Type: Electronic Citation

MODIS Land Website. 2009.
Ref Type: Internet Communication

Adams, B., White, A., & Lenton, T. M. (2004). Am analysis of some diverse appraoches to modelling terrestrial net primary productivity. *Ecological Modelling* **177**, 353-391.

Agarwal, C., Green, G. M., Grove, J. M., Evans, T. P., & Schweik, C. M. A review and assessment of land-use change models: dynamics of space, time, and human choice. -61. 2002. Delaware, USA, USDA Forste Service.
Ref Type: Generic

Anyamba, A. & Tucker, C. J. (2005). Analysis of Sahelian vegetation dynamics using NOAA-AVHRR NDVI data from 1981-2003. *Journal of Arid Environments* **63**, 596-614.

Arbeitskreis Standortkartierung in der Arbeitsgemeinschaft Forsteinrichtung. (1980). *Forstliche Standortsaufnahme* Landwirtschaftsverl., Münster-Hiltrup.

Armstrong, S. J. (1985a). *Long-range Forecasting - From Crystal Ball to Computer*, 2 ed., pp. -688. John Wiley & Sons Inc, New York.

Armstrong, S. J. (1985b). Part II Forecasting Methods - Econometric Methods. In *Long-range Forecasting - From Crystal Ball to Computer*, ed. Armstrong, S. J., pp. 191-247. Wiley & Sons, New York.

Asrar, G., Kanemasu, E. T., Miller, G. P., & Weiser, R. L. (1986). Light Interception and Leaf Area Estimates from Measurements of Grass Canopy Reflectance. *Geoscience and Remote Sensing, IEEE Transactions on* **GE-24**, 76-82.

Bahrenberg, G. (1992). *Statistische Methoden in der Geographie 2. Multivariate Statistik* Teubner, Stuttgart.

Bahrenberg, G. (2003). *Statistische Methoden in der Geographie 2. Multivariate Statistik* Teubner, Stuttgart.

Bannari, A., Asalhi, H., & Teillet, P. M. Transformed difference vegetation index (TDVI) for vegetation cover mapping. 5, 3053-3055. 2002.
Ref Type: Conference Proceeding

Baumann, G. How to assess rangeland condition in semiarid ecosystems? The indicative value of vegetation in the High Atlas Mountains, Morocco. 2009. Unversity Cologne.
Ref Type: Thesis/Dissertation

Behnke, R. H. & Abel, N. (1996). Revisited: the overstocking controversy in semi-arid Africa. *World Animal Review* **87**, 4-27.

Behnke, R. H. & Scoones, I. (1993). Rethinking range ecology: Implications for rangeland management in Africa. In *Range Ecology at Disequilibrium - New Models of Natural Variability and Pastoral Adaption in African Savannas*, eds. Behnke, R., Scoones, I., & Kerven, C., pp. 1-30. Overseas Development Institute, London.

Behnke, R. H. (1995). *Range ecology at disequilibrium new models of natural variability and pastoral adaptation in African Savannas* Overseas Development Inst. [u.a.], London.

Bergkamp, G. (1998). A hierarchical view of the interactions of runoff and infiltration with vegetation and microtopography in semiarid shrublands. *CATENA* **33**, 201-220.

Berndtsson, R., Larson, M., Lindh, G., Malm, J., & Niemczynowicz, J. Climate-Induced Effects on the Water Balance--Preliminary Results from Studies in the Varpinge Experimental Research Basin. 437-449. 1989. Conference on Climate and Water. Volume I. September 11-15, Helsinki, Finland.
Ref Type: Conference Proceeding

Bester, F. V., Van Eck, J. A. J., Kölling, H., & Van Rooyen, B. (2003). The influence of stocking rate on the distribution of individual grass species in the sward. *Spotlight on Agriculture* **74**, 1-2.

Beven, K. J. (2003). *Rainfall-runoff modelling : the primer* Wiley, Chichester.

Bian, L. & Walsh, S. J. (1993). Scale Dependencies of Vegetation and Topography in a Mountainous Environment of Montana. *The Professional Geographer* **45**, 1-11.

Bollig, M. & Göbel, B. (1997). Risk, Uncertainty and Pastoralism: An introduction. *Nomadic Peoples* **1**, 5-21.

Bonan, G. B. (2002). *Ecological climatology : concepts and applications* Cambridge University Press, Cambridge [u.a.].

Booch, G., Maksimchuk, R., Engle, M., Young, B., Conallen, J., & Houston, K. (2007). *Object-oriented analysis and design with applications, third edition*, pp. -720. Addison-Wesley Professional.

Bork, E. W., West, N. E., & Walker, J. W. (1998). Cover components on long-term seasonal sheep grazing treatments in three-tip sagebrush steppe. *Journal of Range Management* **51**, 293-300.

Born, K., Christoph, M., Fink, A. H., Knippertz, P., Paeth, H., & Speth, P. (2009). Moroccan Climate in the Present and Future: Combined View from Observational Data and Regional

Climate Scenarios. In *Climatic Changes and Water Resources in the Middle East and in North Africa*, eds. Zereini, F. & Hötzl, H., pp. 29-45. Springer Verlag, Wien.

Born, K., Fink, A. H., & Paeth, H. (2008b). Dry and Wet Periods in the Northwestern Maghreb for Present Day and Future Climate Conditions. *Meteorologische Zeitschrift* **17**, 533-551.

Born, K., Fink, A. H., & Paeth, H. (2008a). Dry and Wet Periods in the Northwestern Maghreb for Present Day and Future Climate Conditions. *Meteorologische Zeitschrift* **17**, 533-551.

Bradley, B. A., Jacob, R. W., Hermance, J. F., & Mustard, J. F. (2007). A curve fitting procedure to derive inter-annual phenologies from time series of noisy satellite NDVI data. *Remote Sensing of Environment* **106**, 137-145.

Brown, J. H. (1999). Macroecology: progress and prospect. *Oikos* **87**, 3-14.

Brown, M. E. & Funk, C. C. (2008). Food Security Under Climate Change. *Science* **319**, 580-581.

Burrows, S. N., Gower, S. T., Clayton, M. K., Mackay, D. S., Ahl, D. E., Norman, J. M., & Diak, G. (2002). Applications of Geostatistics to Characterize Leaf Area Index (LAI) from Flux Tower to Landscape Scales Using a Cyclic Sampling Design. *Ecosystems* **5**, 667-679.

Busche, H. 2009.
Ref Type: Thesis/Dissertation

Carlson Toby N. & Ripley David A. (1997). On the Relation between NDVI, Fractional Vegetation Cover, and Leaf Area Index. *Remote Sensing of Environment* **62**, 241-252.

Carlson, T. N. & Ripley, D. A. (1997). On the Relation between NDVI, Fractional Vegetation Cover, and Leaf Area Index. *Remote Sensing of Environment* **62**, 241-252.

Cerda, A. (1999). Parent Material and Vegetation Affect Soil Erosion in Eastern Spain. *Soil Sci Soc Am J* **63**, 362-368.

Chen Jing M. & Cihlar Josef (1996). Retrieving Leaf area Index of Boreal Conifer Forests Using Landsat TM Images. *Remote Sensing of Environment* **55**, 153-162.

Chen, Z. M., Babiker, I. S., Chen, Z. X., Komaki, K., Mohamed, M. A. A., & Kato, K. (2004). Estimation of interannual variation in productivity of global vegetation using NDVI data. *International Journal of Remote Sensing* **25**, 3139-3159.

Chmielewski, F. M., Heyer, E., Hupfer, P., & Kuttler, W. (2005). *Witterung und Klima : eine EinfÃ¼hrung in die Meteorologie und Klimatologie* Teubner, Stuttgart [u.a.].

Colditz, R. R. Time Series Generation and Classification of MODIS Data for Land Cover Mapping. 1-334. 2007.
Ref Type: Thesis/Dissertation

Coleman, J. S. (2000). *Foundations of social theory* Belknap Press of Harvard Univ. Press, Cambridge, Mass. [u.a.].

Cramer, W., Bondeau, A., Woodward, F. I., Prentice, I. C., Betts, R. A., Brovkin, V., Cox, P. M., Fisher, V., Foley, J. A., Friend, A. D., Kucharik, C., Lomas, M. R., Ramankutty, N., Sitch, S., Smith, B., White, A., & Young-Molling, C. (2001). Global response of terrestrial ecosystem structure and function to CO_2 and climate change: results from six dynamic global vegetation models. *Global Change Biology* **7**, 357-373.

Cronshey, R., McCuen, R. H., Miller, N., Rawls, W., Robbins, S., & Woodward, D. Urban Hydrology for Small Watersheds - Technical Release 55. -164. 1986. United States Department of Agriculture, Natural Resources Conservation Service, Conservation Engineering Division.
Ref Type: Generic

Culmsee, H. Vegetation und Weidenutzung im Westlichen Hohen Atlas (Marokko). 1-244. 2004.
Ref Type: Thesis/Dissertation

Daren Harmel, R. & Smith, P. K. (2007). Consideration of measurement uncertainty in the evaluation of goodness-of-fit in hydrologic and water quality modeling. *Journal of Hydrology* **337**, 326-336.

Darfaoui, E. M. Livestock Watering Practices in the Moroccan Pre-Sahara: their Effects on Water and Nutrient Metabolism of Sheep in Different Body Conditions. 1-82. 1998. Logan, Utah, Utah State University.
Ref Type: Thesis/Dissertation

Daughtry, C. S. T., McMurtrey, J. E., Chappelle, E. W., Dulaney, W. P., Irons, J. R., & Satterwhite, M. B. (1995). Potential for Discriminating Crop Residues from Soil by Reflectance and Fluorescence. *Agron J* **87**, 165-171.

Davi, H., Soudani, K., Deckx, T., Dufrene, E., le Dantec, V., & Francois, C. (2006). Estimation of forest leaf area index from SPOT imagery using NDVI distribution over forest stands. *International Journal of Remote Sensing* **27**, 885-902.

de Jong, C., Cappy, S., Finckh, M., & Funk, D. (2008). A transdisciplinary analysis of water problems in the mountainous karst areas of Morocco. *Engineering Geology* **99**, 228-238.

Delcourt, H. R., Delcourt, P. A., & Webb III, T. (1982). Dynamic plant ecology: the spectrum of vegetational change in space and time. *Quaternary Science Reviews* **1**, 153-175.

Diekkrüger, B. (1996). SIMULAT - Ein Modellsystem zur Berechnung der Wasser und Stoffdynamik landwirtschaftlich genutzter Standorte. In *Sonderforschungsbereich 179. Wasser- und Stoffdynamik
in Agrarökosystemen. Abschlußbericht Band 1.* pp. 30-47.

Diekkrüger, B., Bormann, H., & Stephan, K. Quantifizierung von Fehlern und Unsicherheiten in der hydrologischen Modellierung. 2003.
Ref Type: Conference Proceeding

Diekkrüger, B., Bormann, H., & Stephan, K. Quantifizierung von Fehlern und Unsicherheiten in der hydrologischen Modellierung. -12. 2006. Dresdner Kompetenzzentrum Wasser/TU Dresden. DKW-Reihe.
Ref Type: Serial (Book,Monograph)

Dina, S. J. & Klikoff, L. G. (1973). Effect of Plant Moisture Stress on Carbohydrate and Nitrogen Content of Big Sagebrush. *Journal of Range Management* **26**, 207-209.

Diodato, N. (2006). Modelling net erosion responses to enviroclimatic changes recorded upon multisecular timescales. *Geomorphology* **80**, 164-177.

Diouf, A. & Lambin, E. F. (2001). Monitoring land-cover changes in semi-arid regions: remote sensing data and field observations in the Ferlo, Senegal. *Journal of Arid Environments* **48**, 129-148.

Dorn, R. I. & Oberlander, T. M. (1982). Rock varnish. *Progress in Physical Geography* **6**, 317-367.

Doudill, A. J. (1998). Soil water movement and nutrient cycling in semi-arid rangeland: vegetation change and system resilience. *Hydrological Processes* **12**, 443-459.

Draper, N. & Smith, H. (1981). *Applied Regression Analysis (2nd ed.)*, pp. -709. Wiley, New York.

du Plessis, W. P. (1999). Linear regression relationships between NDVI, vegetation and rainfall in Etosha National Park, Namibia. *Journal of Arid Environments* **42**, 235-260.

Easterling, W. E. P. K. A. P. B. K. M. B. L. E. S. M. H. A. K. J. M. J. F. S. J. S. F. N. T. Food, fibre and forest products. M.L.Parry, O. F. Canziani J. P. Palutikof P. J. van der Linden and C. E. Hanson Eds. 2007. Cambridge University Press, Cambridge, UK, 273-313. *Climate Change 2007: Impacts, Adaptation and Vulnerability. Contribution of Working Group II to the Fourth Assessment Report of the Intergovernmental Panel on Climate Change*. 10-2-0009.
Ref Type: Report

El, H., Harfi, A. E., Lang, Lang, J., Salomon, Salomon, J., Chellai, & Chellai, E. (2001). Cenozoic sedimentary dynamics of the Ouarzazate foreland basin (Central High Atlas Mountains, Morocco). *International Journal of Earth Sciences* **90**, 393-411.

Elbertzhagen, I. Vergleich von satellitengestützten Verfahren zur Bestimmung der Vegetationsperiode in Südmarokko. 2008.
Ref Type: Thesis/Dissertation

Ellis, J. E. (1994). Climate variability and complex ecosystem dynamics: implications for pastoral development. In *Living with uncertainty. New directions in pastoral development in Africa*, ed. Scoones, I., pp. 37-46. London.

Ellis, J. E. & Swift, D. M. (1988). Stability of African pastoral ecosystems: Alternate paradigms and implications for development. *Journal of Range Management* **41**, 450-459.

Emberger, L. (1939). Apercu général sur la végetation du Maroc. *Veröffentlichungen des Geobotanischen Instituts, Eidgenössische Technische Hochschule Rübel in Zürich* **14**, 40-157.

Farr, T. G., Rosen, P. A., Caro, E., Crippen, R., Duren, R., Hensley, S., Kobrick, M., Paller, M., Rodríguez, E., Roth, L., Seal, D., Shaffer, S., Shimada, J., Umland, J., Werner, M., Oskin, M., Burbank, D., & Alsdorf, D. The Shuttle Radar Topography Mission. -43.
Ref Type: Generic

Fensholt, R., Sandholt, I., & Rasmussen, M. S. (2004). Evluation of MODIS LAI, fAPAR and the relation between fAPAR and NDVI in a semi-arid environment using in situ measurements. *Remote Sensing of Environment* **91**, 490-507.

Fensholt, R., Sandholt, I., Rasmussen, M. S., Stisen, S., & Diouf, A. (2006). Evaluation of satellite based primary production modelling in the semi-arid Sahel. *Remote Sensing of Environment* **105**, 173-188.

Field, C. B., Randerson, J. T., & Malmström, C. M. (1995). Global Net Primary Production: Combining Ecology and Remote Sensing. *Remote Sensing of Environment* **51**, 74-88.

Finckh, M., Augustin, A., & Oldeland, J. The desertification paradox – decreasing degradability with increasing aridity in semiarid to arid rangelands. conference . 2009.
Ref Type: Abstract

Finckh, M. & Oldeland, J. Vegetation Monitoring and Evaluation of Scenarios in Semiarid Steppes of Southern Morocco. 48th IAVS Symposium. 2005a. Lissabon.
Ref Type: Conference Proceeding

Finckh, M. & Oldeland, J. Vegetation Monitoring and Evaluation of Scenarios in Semiarid Steppes of Southern Morocco. 48th IAVS Symposium. 2005b. Lissabon.
Ref Type: Conference Proceeding

Finckh, M. & Oldeland, J. Floristische und räumliche Dynamik von Vegetationseinheiten am Südrand des Hohen Atlas (Marokko). Wüstenränder multimedial. 2006. Bayreuth.
Ref Type: Conference Proceeding

Finckh, M. & Staudinger, M. Mikro- und makroskalige Ansätze zu einer Vegetationsgliederung des Drâa-Einzugsgebietes (Südmarokko). 14, 81-92. 2002. Hannover. Berichte der Reinhold-Tüxen-Gesellschaft.
Ref Type: Report

Finckh, M. & Staudinger, M. Spatial patterns and vegetation dynamics of degraded rangelands in the Drâa-Einzugsgebiet, Southern Morocco. 46th IAVS Symposium. 2003. Neapel.
Ref Type: Conference Proceeding

Fink, A., Reichert, B., Christoph, M., Kirscht, H., Schulz, O., Piecha, K., Brücher, T., Knippertz, P., Born, K., Oldeland, J., Finckh, M., Fritzsche, P., Poete, P., Klose, A., Busche, H., Cappy, S., Klose, S., Hoffmann, H., Osterhold, V., Bell, S., Haaken, K., Platt, S., Rademacher, C., Heidecke, C., Roth, A., & Schmidt, T. Impetus Atlas Morocco: Research results 2000-2007. 1-78. 2008. Köln, IMPETUS Project.
Ref Type: Report

Fisher, J. B., DeBiase, T. A., Qi, Y., Xu, M., & Goldstein, A. H. (2005). Evapotransipation models compared on a Sierra Nevada forest ecosystems. *Environmental Modelling & Software* **20**, 783-796.

Flynn, E. S., Dougherty, C. T., & Wendroth, O. (2008). Assessment of Pasture Biomass with the Normalized Difference Vegetation Index from Active Ground-Based Sensors. *Agron J* **100**, 114-121.

Foetzki, A. Wasserhaushalt und Wassernutzungseffizeinz von vier perennierenden Pflanzenarten im Vorland einer zentralasiatischen Flussoase. -189. 2002. 16-12-2002.
Ref Type: Thesis/Dissertation

Foody, G. M. (2003). Geographical weighting as a further refinement to regression modelling: An example focused on the NDVI-rainfall relationship. *Remote Sensing of Environment* **88**, 283-293.

Franklin, J. (1995). Predictive vegetation mapping: Geographic modelling of biospatial patterns in relation to environmental gradients. *Progress in Physical Geography* **19**, 474-499.

Gaile, G. L. & Willmott, C. J. (1984). *Spatial statistics and models* D. Reidel Pub. Co. ; Sold and distributed in the U.S.A. by Kluwer Boston Academic Publishers, Dordrecht; Boston; Hingham, MA, U.S.A.

Geerken, R. & Ilaiwi, M. (2004). Assessment of rangeland degradation and development of a strategy for rehabilitation. *Remote Sensing of Environment* **90**, 490-504.

Gentleman, W. M. (1974). Algorithm AS 75: Basic Procedures for Large, Sparse or Weighted Linear Least Problems. *Journal of the Royal Statistical Society.Series C (Applied Statistics)* **23**, 448-454.

Gibson, C. C., Ostrom, E., & Ahn, T. K. (2000). The concept of scale and the human dimensions of global change: a survey. *Ecological Economics* **32**, 217-239.

Giertz, S. Analyse der hydrologischen Prozesse in den sub-humiden Tropen Westafrikas unter besonderer Berücksichtigung der Landnutzung am Beispiel des Aguima-Einzugsgebietes in Benin. 1-267. 2004.
Ref Type: Thesis/Dissertation

Gillson, L. & Hoffman, M. T. (2007). Grazing and "Degradation": Response. *Science* **316**, 1565-1566.

Gottschalk, T. K., Huettmann, F., & Ehlers, M. (2005). Thirty years of analysing and modelling avian habitat relationships using satellite imagery data: a review. *International Journal of Remote Sensing* **26**, 2631-2656.

Griffiths, J. & Soliman.KH (1972). The Northern Desert (Sahara). In *World Survey of Climatology*, ed. Landsberg, H., pp. 75-131. Elsevier PUbl. Comp., Amsterdam, London, New York.

Griffiths, J. F. (1972). *Climates of Africa;* Elsevier Pub. Co., Amsterdam; New York.

Grimm, V., Berger, U., Bastiansen, F., Eliassen, S., Ginot, V., Giske, J., Goss-Custard, J., Grand, T., Heinz, S. K., Huse, G., Huth, A., Jepsen, J. U., Jï¿½rgensen, C., Mooij, W. M., Mï¿½ller, B., Pe'er, G., Piou, C., Railsback, S. F., Robbins, A. M., Robbins, M. M., Rossmanith, E., Rï¿½ger, N., Strand, E., Souissi, S., Stillman, R. A., Vabï¿½, R., Visser, U., & DeAngelis, D. L. (2006). A standard protocol for describing individual-based and agent-based models. *Ecological Modelling* **198**, 115-126.

Gruber, I. The impact of socio-economic development and climate change on livestock management in Benin. 1-262. 2008.
Ref Type: Thesis/Dissertation

Guevara, J. C., Cavagnaro, J. B., Estevez, O. R., Le Houérou, H. N., & Stasi, C. R. (1997). Productivity, management and development problems in the arid rangelands of the central Mendoza plains (Argentina). *Journal of Arid Environments* **35**, 575-600.

Guisan, A., Weiss, S. B., & Weiss, A. D. (1999). GLM versus CCA spatial modeling of plant species distribution. *Plant Ecology* **143**, 107-122.

Guisan, A. & Zimmermann, N. E. (2000). Predictive habitat distribution models in ecology. *Ecological Modelling* **135**, 147-186.

Heady, H. F. & Child, R. D. (1994). *Rangeland ecology and management* Westview Press, Boulder.

Hegarat-Mascle, S. L. (2006). Performance of change detection using remotely sensed data and evidential fusion: comparison of three cases of application. *International Journal of Remote Sensing* **27**, 3515.

Henriksen, H. J. r., Troldborg, L., Nyegaard, P., Sonnenborg, T. O., Refsgaard, J. C., & Madsen, B. (2003). Methodology for construction, calibration and validation of a national hydrological model for Denmark. *Journal of Hydrology* **280**, 52-71.

Hilker, T., Coops, N. C., Wulder, M. A., Black, T. A., & Guy, R. D. (2008). The use of remote sensing in light use efficiency based models of gross primary production: A review of current status and future requirements. *The Science of the Total Environment* **404**, 411-423.

Huete, A. (1988). A Soil-Adjusted Vegetation Index (SAVI). *Remote Sensing of Environment* **25**, 295-309.

Hulme, M. & Dessai, S. (2007). Climate prediction: a limit to adaptation? In *Global Environmental Change*.

Ilahiane, H. (1999). The Berber Agdal Institution: Indigenous Range Mangement in the Atlas Mountains. *Ethnology: An International Journal of Cultural and Social Anthropology* **38**, 21-45.

Illius, A. W. & O'Connor, T. G. (2000). Resource heterogeneity and ungulate population dynamics. *Oikos* **89**, 283-294.

Impetus. IMPETUS Final Report 2000-2003. -152. 2003.
Ref Type: Report

Impetus. Sechster Zwischenbericht - Zeitraum 01.01.2005 - 31.12.2005. -369. 2006.
Ref Type: Report

IPCC (2001). Summary for Policymakers. In *Sythesis Report* pp. 1-34.

IPCC. Good Practice Guidance for Land use, Land use change and Forestry. Penman, J. Gytarsky M. Hiraishi T. Krug T. Kruger D. Pipatti R. Buendia L. Miwa K. Ngara T. Tanabe K. Wagner F. 2003.
Ref Type: Report

IPCC Working Group1 (2001a). Observed Climate Variability and Change. In *The Scientific Basis* pp. 99-180.

IPCC Working Group1 (2001b). The Carbon Cycle and Atmospheric Carbon Dioxide. In *The Scientific Basis* pp. 183-237.

IPCC Working Group2 (2001a). Hydrology and Water Ressources. In *Climate Change 2001: Impacts, Adaptation and Vulnerability* pp. 191-233.

IPCC Working Group2 (2001b). Overview of Impacts, Adaptation, and Vulnerability to Climate Change. In *Climate Change 2001: Impacts, Adaptation and Vulnerability* pp. 77-102.

IPCC Working Group3 (2001). Technological and Economic Potential of Options to Enhance, Maintain, and Manage Biological Carbon Reservoirs and Geo-engineering. In *Climate Change 2001: Mitigation* pp. 301-343.

Iqbal, M. (1983a). *An Introduction to Solar Radiation* London.

Iqbal, M. (1983b). An Introduction to Solar Radiation Academic. *New York*.

Jacob, D., Van den Hurk, B. J. J. M., AndrÃ¦, U., Elgered, G., Fortelius, C., Graham, L. P., Jackson, S. D., Karstens, U., KÃ¶pken, C., Lindau, R., Podzun, R., Rockel, B., Rubel, F., Sass, B. H., Smith, R. N. B., & Yang, X. (2001). A comprehensive model inter-comparison study investigating the water budget during the BALTEX-PIDCAP period. *Meteorology and Atmospheric Physics* **77**, 19-43.

Jauffret, S. & Lavorel, S. (2003). Are plant functional types relevant to describe degradation in arid, southern Tunisian steppes? *Journal of Vegetation Science* **14**, 399-408.

Jeltsch, F., Moloney, K. A., Schurr, F. M., Köchy, M., & Schwager, M. (2008). The state of plant population modelling in light of environmental change. *Perspectives in Plant Ecology, Evolution and Systematics* **9**, 171-189.

Jensen, M. E. ed. (1990). *Evapotranspiration and Irrigation Water Requirements*.

Joly, F. (1954). *Les hamada sud-marocaines: R+®sultats de la Mission d'+®tude, 1951, de l'Institut scientifique ch+®rifien et du Centre de recherches sahariennes*.

Jorgensen, S. E. (1988). *Fundamentals of ecological modelling* Elsevier Science Pub. Co., Inc.,New York, NY.

Jörgensen, S. E. (1988). *Fundamentals of ecological modelling* Elsevier Science Pub. Co., Inc.,New York, NY.

Jörgensen, S. E. (2008). Overview of the model types available for development of ecological models. *Ecological Modelling* **215**, 3-9.

Jörgensen, S. E. & Bendoricchio, G. (2001). Preface, third edition., ed. Jörgensen, S. E., pp. ix-xi. Elsevier.

Justice, C., Belward, A., Morisette, J., Lewis, P., Privette, J., & Baret, F. (2000). Developments in the 'validation' of satellite sensor products for the study of the land surface. *International Journal of Remote Sensing* **21**, 3383-3390.

Kamotho, S., Strahm, W., & Wolfangel, C. The nature of drylands: diverse ecosystems, diverse solutions. Kamotho, S., Strahm, W., and Wolfangel, C. IUCN World Conservation Congress. 1-40. 2008. Barcelona.
Ref Type: Conference Proceeding

Karnieli, A. (2003). Natural vegetation phenology assessment by ground spectral measurements in two semi-arid environments. *International Journal of Biometeorology* **47**, 179-187.

Karnieli, A., Shachak, M., Tsoar, H., Zaady, E., Kaufman, Y., Danin, A., & Porter, W. (1996). The effect of microphytes on the spectral reflectance of vegetation in semiarid regions. *Remote Sensing of Environment* **57**, 88-96.

Kasperson, R. E., Kasperson, J. X., & Turner, B. L. Regions at risk comparisons of threatened environments. ... 1995.
Ref Type: Electronic Citation

Kemmerling, B. Sustainable range management - local strategies of a pastoral nomadic group in the High Atlas Mountains, Morocco. -127. 2008.
Ref Type: Thesis/Dissertation

Kendall, M. G. & O'Hagan, A. (1994). *Advanced theory of statistics 2B. Bayesian inference* Griffin, London.

Kennedy, W. The structural differentiation of Africa in the Pan African (+ 500 million years) tectonic episode. Inst Aft Geol Eighth Annu Rep Sci Results. 48-49. 1962.
Ref Type: Journal (Full)

Klose, A. Soil characteristics and soil erosion by water in a semi-arid catchment (Wadi Drâa, South Morocco) under the pressure of global change. 2009.
Ref Type: Thesis/Dissertation

Klose, S. Dissertation in preperation. 2011.
Ref Type: Thesis/Dissertation

Knapp, A. K. & Smith, M. D. (2001). Variation Among Biomes in Temporal Dynamics of Aboveground Primary Production. *Science* **291**, 481-484.

Knippertz, P., Christoph, M., & Speth, P. (2003). Long-term precipitation variability in Morocco and the link to the large-scale circulation in recent and future climates. *Meteorology and Atmospheric Physics* **83**, 67-88.

Knyazikhin, Y., Glassy, J., Privette, J. L., Tian, Y., Lotsch, A., Zhang, Y., Wang, Y., Morisette, J. T., Votava, P., Myneni, R. B., Nemani, R. R., & Running, S. W. MODIS Leaf Area Index (LAI) and Fraction of Photosynthetically Active Radiation Absorbed by Vegetation (FPAR) Product (MOD15) Algorithm Theoretical Basis Document. [Version 4.0], -126. 1999.
Ref Type: Generic

Kobayashi, H., Suzuki, R., & Kobayashi, S. (2007). Reflectance seasonality and its relation to the canopy leaf area index in an eastern Siberian larch forest: Multi-satellite data and radiative transfer analyses. *Remote Sensing of Environment* **106**, 238-252.

Kolb, K. J. & Sperry, J. S. (1999). Differences in drougt adaption between subspecies of sagebrush (Artemisia tridentata). *Ecology* **80**, 2373-2384.

Köppen, W. (1901). Versuch einer Klassifikation der Klimate: vorzugsweise nach ihren Beziehungen zur Pflanzenwelt. *Geographische Zeitschrift* -45.

Köppen, W. (1923). *Die Klimate der Erde: Grundriss der Klimakunde*, pp. -369. DeGruyter, Berlin.

Köppen, W. (1931). *Grundriss der Klimakunde: Klimate der Erde*, 2 ed., pp. -388. DeGruyter, Berlin.

Krause, P., Boyle, D. P., & Bäse, F. (2005). Comparison of different efficiency criteria for hydrological model assessment. *Advances in Geosciences* **5**, 89-97.

Kumar, D. N. & Maity, R. (2008). Bayesian dynamic modelling for nonstationary hydroclimatic time series forecasting along with uncertainty quantification. *Hydrological Processes* **22**, 3488-3499.

Lajtha, K. & Whitford, W. G. (1989). The effect of water and nitrogen amendments on photosynthesis, leaf demography, and resource-use efficiency in Larrea tridentata, a desert evergreen shrub. *Oecologia* **80**, 341-348.

Lambin, E. F. & Geist, H. J. LUCC: Global land-use and land-cover change: what have we learned so far? 27-30. 2001. Land.
Ref Type: Report

Lambin, E. F. & Geist, H. J. (2006). *Land-use and Land-Cover Change: Local Processes and Global Impacts* Springer, Berlin Heidelberg.

Lambin, E. F. & Strahler, A. H. (1994). Change-Vector Analysis in Multitemporal Space: A Tool To Detect and Categorize Land-Cover Change Processes Using High Temporal-resolution Satellite Data. *Remote Sensing of Environment* **48**, 231-244.

Lambin, E. F., Turner, B. L., Geist, H. J., Agbola, S. B., Angelsen, A., Bruce, J. W., Coomes, O. T., Dirzo, R., Fischer, G. n., Folke, C., George, P. S., Homewood, K., Imbernon, J., Leemans, R., Li, X., Moran, E. F., Mortimore, M., Ramakrishnan, P. S., Richards, J. F., Skï¿½nes, H., Steffen, W., Stone, G. D., Svedin, U., Veldkamp, T. A., Vogel, C., & Xu, J. (2001b). The causes of land-use and land-cover change: moving beyond the myths. *Global Environmental Change* **11**, 261-269.

Lambin, E. F., Turner, B. L., Geist, H. J., Agbola, S. B., Angelsen, A., Bruce, J. W., Coomes, O. T., Dirzo, R., Fischer, G. n., Folke, C., George, P. S., Homewood, K., Imbernon, J., Leemans, R., Li, X., Moran, E. F., Mortimore, M., Ramakrishnan, P. S., Richards, J. F., Skï¿½nes, H., Steffen, W., Stone, G. D., Svedin, U., Veldkamp, T. A., Vogel, C., & Xu, J. (2001a). The causes of land-use and land-cover change: moving beyond the myths. *Global Environmental Change* **11**, 261-269.

Larcher, W. (2000). Temperature stress and survival ability of Mediterranean sclerophyllous plants. *Plant Biosystems - An International Journal Dealing with all Aspects of Plant Biology: Official Journal of the Societa Botanica Italiana* **134**, 279-295.

Law Beverly E. (1995). Estimation of Leaf Area Index and Light Intercepted by Shrubs from Digital Videography. *Remote Sensing of Environment* **51**, 276-280.

Le Houérou, H. N. Browse in northern Africa. Le Houérou, H. N. International Symposium on Browse in Africa Addis Ababa, April 8-12, 1980. Browse in Africa: The current state of knowledge Chapter 5. 1980. Addis Ababa.
Ref Type: Conference Proceeding

le Houerou, H. N. (1980). The Rangelands of the Sahel. *Journal of Range Management* **33**, 41-45.

Le Houérou, H. N. (1984). Rain use efficiency: a unifying concept in arid-land ecology. *Journal of Arid Lands* **7**, 213-247.

Le Houérou, H. N. Eco-climatic and bio-geographic comparison between the rangelands of the iso-climatic Mediterranean arid zone of northern Africa and Near East. Omar, S. A. S., Razzaque, M. A., and Alsdirawi, F. Range Management in Arid Zones. Proceedings of the Second International Conference on Range Management in the Arabian Gulf , 25-40. 1995. Kuwait Institute for Scientific Research.
Ref Type: Conference Proceeding

Le Houérou, H. N. (1996). Climate change, drought and desertification. *Journal of Arid Environments* **34**, 133-185.

Le Houerou, H. N. (1997). Climate, flora and fauna changes in the Sahara over the past 500 million years. *Journal of Arid Environments* **37**, 619-647.

Le Houérou, H. N. (2001). Biogeography of the arid steppeland north of the Sahara. *Journal of Arid Environments* **48**, 103-128.

Le Houérou, H. N. (2004). An Agro-Bioclimatic Classification of Arid and Semiarid Lands in the Isoclimatic Mediterranean Zones. *Arid Land Research and Management* **18**, 301-346.

Legates, D. R. & McCabe, G. J., Jr. (1999). Evaluating the Use of "Goodness-of-Fit" Measures in Hydrologic and Hydroclimatic Model Validation. *Water Resour.Res.* **35**.

Leser, H. & Mosimann, T. (1997). *Landschaftsökologie : Ansatz, Modelle, Methodik, Anwendung* E. Ulmer, Stuttgart.

Levins, R. (1966). Strategy of Model Building in Population Biology. *American Scientist* **54**, 421-&.

Lieth, H. (1973). Primary Production: Terrestrial Ecosystems. *Human Ecology* **1**, 303-332.

Lillesand, T. M. (2006). *Remote sensing and image interpretation*.

Lovett, G., Cole, J., & Pace, M. (2006). Is Net Ecosystem Production Equal to Ecosystem Carbon Accumulation? *Ecosystems* **9**, 152-155.

Lupo, F., Reginster, I., & Lambin, E. F. (2001). Monitoring land-cover change in West Africa with SPOT Vegetation: impact of natural disasters in 1998-1999. *International Journal of Remote Sensing* **22**, 2633-2639.

Marques da Silva, J. R., Peca, J. O., Serrano, J. M., de Carvalho, M. J., & Palma, P. M. (2008). Evaluation of spatial and temporal variability of pasture based on topography and the quality of the rainy season. *Precision Agriculture* **9**, 209-229.

Maselli, F., Gilabert, M. A., & Conese, C. (1998). Integration of High and Low Resolution NDVI Data for Monitoring Vegetation in Mediterranean Environments. *Remote Sensing of Environment* **63**, 208-218.

Menz, G. Niederschlag und Biomasse in den Wechselfeuchten Tropen Ostafrikas: Neuere Methoden zur quantitativen Erfassung Klimaökologischer Raumparameter aus digitalen Satellitendaten (Meteosat und NOAA). 1996. University Bonn.
Ref Type: Thesis/Dissertation

Menz, G., Burkhardt, J., Goldbach, H., Porembski, S., Barthlott, W., Judex, M., Orthmann, B., Stadler, C., & Thamm, H. P. Functional relationships between spatio-temporal vegetation dynamics and the water cycle. Statusreport IMPETUS 2005 , 13. 2005.
Ref Type: Abstract

Michard, A. (2008). *Continental evolution : the geology of Morocco. Structure, Stratigraphy, and Tectonics of the Africa-Atlantic-Mediterranean Triple Junction*.

Middleton. & Thomas, D. (1997). *World atlas of desertification.. ed. 2* Arnold, Hodder Headline, PLC, London (United Kingdom).

Miller, R. Böden und Bodenerosion auf ausgewählten Standorten im Hohen Atlas/Südmarokko. 1-148. 2002. Gießen, Fachbereich Agrarwissenschaften und Umweltmanagement der Justus-Liebig-Universität Gießen.
Ref Type: Thesis/Dissertation

Miyazaki, S. (2004). Agrometeorological conditions of grassland vegetation in central Mongolia and their impact for leaf area growth. *Journal of Geophysical Research* **109**, D22106.

Monteith, J. L. (1965). Light Distribution and Photosynthesis in Field Crops. *Annals of Botany* **29**, 17-37.

Monteith, J. L. (1972). Solar radiation and productivity in tropical ecosystems. *Journal of Applied Ecology* **9**, 747-766.

Monteith, J. L. (1981). Evaporation and Surface Temperature. *Quarterly Journal of the Royal Meteorological Society* **107**, 1-27.

Moore, G. E. (1965). Cramming more components onto integrated circuits. *Proceedings of the IEEE* **86**, 82.

Moran, M. S., Jackson, R. D., Clarke, T. R., Cabot, F., Qi, J., Thome, K. J., & Markham, B. L. (1995). Reflectance Factor retrieval fron Landsat TM and SPOT HRV Data for Bright and Dark Targets. *Remote Sensing of Environment* **52**, 218-230.

Moriasi, D. N., Arnold, J. G., Van Liew, M. W., Bingner, R. L., Harmel, R. D., & Veith, T. L. (2007). Model evaluation guidelines for systematic quantification of accuracy in watershed simulations. *Transactions of the American Society of Agricultural and Biological Engineers* **50**, 885-900.

Muche, G., Schmiedel, U., & Finckh, M. BIOTABase - Ein vegetationsökologisches Datenbanksystem für Monitoring in Afrika. 48th IAVS Symposium. Abstracts 48th IAVS Symposium . 2005. Lissabon.
Ref Type: Conference Proceeding

Muhar, A. (2001). Three-dimensional modelling and visualisation of vegetation for landscape simulation. *Landscape and Urban Planning* **54**, 5-17.

Müller-Hohenstein, K. (1990). *Marokko: ein islamisches Entwicklungsland mit kolonialer Vergangenheit*.

Myneni, R. B. (1997). Estimation of global leaf area index and absorbed PAR using radiative transfer models. *IEEE transactions on geoscience and remote sensing [0196-2892]* **35**, 1380.

Myneni, R. B., Asrar, G., Tanré, D., & Choudhury, B. J. (1992). Remote Sensing of Solar Radiation Absorbed and Reflected by Vegetated Land Surfaces. *IEEE Transactions on Geoscience and Remote Sensing* **30**, 302-314.

Myneni, R. B., Maggion, S., Iaquinta, J., Privette, J. L., Cobron, N., Pinty, B., Kimes, D. S., Verstraete, M. M., & Williams, D. L. (1995a). Optical Remote Sensing of Vegetation: Modeling, Caveats, and Algorithms. *Remote Sensing of Environment* **51**, 169-188.

Myneni, R. B., Nemani, R. R., Shabanov, N. V., Knyazikhin, Y., Morisette, J. T., Privette, J. L., & Running, S. W. LAI and FPAR. ftp://ftp.iluci.org/Land_ESDR/LAI-FPAR_Myneni_whitepaper.pdf . 2006.
Ref Type: Electronic Citation

Myneni, R. B., Los, S. O., & Asrar, G. Potential Gross Primary Productivity of Terrestrial Vegetation from 1982 - 1990. *Geophys.Res.Lett.* **22**.

Myneni, R. B., Los, S. O., & Asrar, G. (1995b). Potential Gross Primary Productivity of Terrestrial Vegetation from 1982 - 1990. *Geophys.Res.Lett.* **22**.

Myneni, R. B., Los, S. O., & Asrar, G. (1995c). Potential Gross Primary Productivity of Terrestrial Vegetation from 1982 - 1990. *Geophys.Res.Lett.* **22**.

NASA. MODIS User Guide MOD13.
http://tbrs.arizona.edu/project/MODIS/UserGuide_doc.php , -93. 2006.
Ref Type: Electronic Citation

Nash, J. E. & Sutcliffe, J. V. (1970). River flow forecasting through conceptual models - Part 1 - A discussion of principles. *Journal of Hydrology* **10**, 282-290.

Neitsch, S. L., Arnold, J. G., Kiniry, J. R., & Williams, J. R. Soil and Water Assessment Tool - Theoretical Documentation - Version 2005. -494. 2005.
Ref Type: Report

Neitsch, S. L., Arnold, J. G., Kiniry, J. R., Williams, J. R., & King, K. W. Soil and Water Assessment Tool - Theoretical Documentation - Version 2000. -506. 2002. Texas, Texas Water Resources Institute.
Ref Type: Report

Niamir, M. Community Forestry: Herders' Decision-Making in Natural Resources Management in Arid and Semi-arid Africa. 1-133. 1989. Rom, FAO. Community Forestry Note.
Ref Type: Serial (Book,Monograph)

Nicholson, S. E. (2000). The nature of rainfall variability over Africa on time scales of decades to millenia. *Global and Planetary Change* **26**, 137-158.

Nicholson, S. E., Davenport, M. L., & Malo, A. R. (1990). A comparison of the vegetation response to rainfall in the Sahel and East Africa, using Normalized Differnece Vegetation Index from NOAA AVHRR. *Climatic Change* **17**, 209-241.

Nicholson, S. E., Tucker, C. J., & Ba, M. B. (1998). Desertification, Drought, and Surface Vegetation: An Example from the West African Sahel. *Bulletin of the American Meteorological Society* 815-829.

O'Brien, R. M. (2007). A caution regarding rules of thumb for variance inflation factors. *QUALITY & QUANTITY* **41**, 673-690.

O'Donnell, G. M., Czajkowski, K. P., Dubayah, R. O., & Lettenmaier, D. P. (2000). Macroscale hydrological modeling using remotely sensed inputs: Application to the Ohio River basin. *JOURNAL OF GEOPHYSICAL RESEARCH-ATMOSPHERES* **105**, 12499-12516.

O'Neill, R. V., Turner, S. J., Cullinan, V. I., Coffin, D. P., Cook, T., Conley, W., Brunt, J., Thomas, J. M., Conley, M. R., & Gosz, J. (1991). Multiple landscape scales: An intersite comparison. *Landscape Ecology* **5**, 137-144.

Oke, T. R. (2003). *Boundary layer climates*, 2 ed. Routledge, London.

Olsson, L. & Eklundh, L. (1994). Fourier Series for analysis of temporal sequences of satellite sensor imagery. *International Journal of Remote Sensing* **15**, 3735-3741.

Pachauri, R. K., Reisinger, A., & Intergovernmental Panel on Climate Change. (2007). *Climate change 2007 synthesis report* IPCC Secretariat, [Geneva, Switzerland].

Pachauri, R. K., Reisinger, A., & Intergovernmental Panel on Climate Change. Climate change 2007 synthesis report. IPCC . 2008.
Ref Type: Electronic Citation

Pachepsky, Y., Timlin, D. J., & Rawls, W. J. (2001). Soil Water Retention as Related to Topographic Variables. *Soil Sci Soc Am J* **65**, 1787-1795.

Paeth, H., Born, K., Podzun, R., & Jacob, D. (2005b). Regional dynamical downscaling over West Africa: model evaluation and comparison of wet and dry years. *Meteorologische Zeitschrift* **14**, 349-367.

Paeth, H., Born, K., Podzun, R., & Jacob, D. (2005a). Regional dynamical downscaling over West Africa: model evaluation and comparison of wet and dry years. *Meteorologische Zeitschrift* **14**, 349-367.

Paeth, H., Busche, H., & Diekkrüger, B. A dynamical-statistical weather generator for past and future climate. 1-40. 2006.

Ref Type: Unpublished Work

Paeth, H. & Hense, A. (2005). Mean versus extreme climate in the Mediterranean region and its sensitivity to future global warming conditions. *Meteorologische Zeitschrift* **14**, 329-347.

Pardo, A., Amato, M., & Chiarandï¿½, F. Q. (2000). Relationships between soil structure, root distribution and water uptake of chickpea (Cicer arietinum L.). Plant growth and water distribution. *European Journal of Agronomy* **13**, 39-45.

Patenaude, G., Milne, R., van Oijen, M., Rowland, C. S., & Hill, R. A. (2008). Integrating remote sensing datasets into ecological modelling: a Bayesian approach. *International Journal of Remote Sensing* **29**, 1295-1315.

Peng, C. (2000). From static biogeographical model to dynamic global vegetation model: a global perspective on modelling vegetation dynamics. *Ecological Modelling* **135**, 33-54.

Peters, R. H. (1991). *A critique for ecology* Cambridge University Press, Cambridge, England.

Pickup, G. (1995). A simple model for predicting herbage production from rainfall in rangelands and its calibration using remotely-sensed data. *Journal of Arid Environments* **30**, 227-245.

Pique, A. (1981). Northwestern Africa and the Avalonian Plate; relations during late Precambrian and late Paleozoic time. *Geolog* **9**, 319.

Pique, A. (2001). *Geology of Northwest Africa*.

Poesen, J., Nachtergaele, J., Verstraeten, G., & Valentin, C. (2003). Gully erosion and environmental change: importance and research needs. *CATENA* **50**, 91-133.

Potter, C. S. & Brooks, V. (1998). Global analysis of empirical relations between annual climate and seasonality of NDVI. *International Journal of Remote Sensing* **19**, 2921-2948.

Potter, C. S. & Klooster, S. A. (1999). Dynamic global vegetation modelling for prediction of plant functional types and biogenic trace gas fluxes. *Global Ecology and Biogeography* **8**, 473-488.

Powell, N. Co-Management in Non-Equilibrium Systems: Cases from Namibian Rangelands. 7-230. 1998. Uppsala, Swedish University of Agricultural Sciences.
Ref Type: Thesis/Dissertation

Prince, S. D. A model of regional primary production for use with coarse resolution satellite data. International Journal of Remote Sensing 12[6], 1313-1330. 1991a.
Ref Type: Magazine Article

Prince, S. D. Satellite remote sensing of primary production: comparison of results for Sahelian grasslands 1981-1988. International Journal of Remote Sensing 12[6], 1301-1311. 1991b.
Ref Type: Magazine Article

Prince, S. D., Kerr, Y. H., Goutorbe, J.-P., Lebel, T., Tinga, A., Bessemoulin, P., Brouwer, J., Dolman, A. J., Engman, E. T., Gash, J. H. C., Hoepffner, M., Kabat, P., Monteny, B., Said, F., Sellers, P., & Wallace, J. (1995). Geographical, Biological and Remote Sensing Aspects of

the Hydrologic Atmospheric Pilot Experiment in the Sahen (HAPEX-Sahel). *Remote Sensing of Environment* **51**, 215-234.

Prince, S. D., Wessels, K. J., Tucker, C. J., & Nicholson, S. E. (2007). Desertification in the Sahel: a reinterpretation of a reinterpretation. *Global Change Biology* **13**, 1308-1313.

Prince, S. D. & Goward, S. N. (1995). Global Primary Production: A Remote Sensing Approach. *Journal of Biogeography* **22**, 815-835.

Puigdefabregas, J., Sole, A., Gutierrez, L., del Barrio, G., & Boer, M. (1999). Scales and processes of water and sediment redistribution in drylands: results from the Rambla Honda field site in Southeast Spain. *Earth-Science Reviews* **48**, 39-70.

Purevdorj, Ts., Tateishi, R., Ishiyama, T., & Honda, Y. (1998). Relationships between percent vegetation cover and vegetation indices. *Int.J.Rem.Sens.* **19**, 3519-3535.

Qi J., Kerr Y.H., Moran M.S., Weltz M., Huete A.R., Sorooshian S., & Bryant R. (2000). Leaf Area Index Estimates Using Remotely Sensed Data and BRDF Models in a Semiarid Region. *Remote Sensing of Environment* **73**, 18-30.

Quattrochi, D. A. & Goodchild, M. F. (1997). *Scale in remote sensing and GIS* Lewis Publishers, Boca Raton, Fla.

Rallison, R. E. & Miller, N. (1981). Past, Present, and Future SCS Runoff Procedure. In *Rainfall Runoff Relationship*, ed. Singh, V. P., pp. 353-364. Water Resources Publication, Littleton , Colorado.

Rauh, W. (1952). *Vegetationsstudien im Hohen Atlas und dessen Vorland*.

Refsgaard, J. C. (1997). Parameterisation, calibration and validation of distributed hydrological models. *Journal of Hydrology* **198**, 69-97.

Remsberg, E. E. B. P. P. M. T. (1994). An assessment of satellite temperature distributions used to derive the net diabatic transport for zonally averaged models of the middle atmosphere. *Journal of geophysical research-atmospheres* **99**, 23001-23017.

Richards, C. A. & Wadleigh, C. H. (1952). Soil water and plant growth. *Soil Physical Conditions and Plant Growth* 73-251.

Richters, J. (2005a). Biomass production and seasonal ecologic behaviour based on a remote sensing modelling approach. In *Atlas of Cultural and Environmental Change in Arid Africa*, eds. Bubenzer, O., Bolten, A., & Darius, F., pp. 86. Heinrich-Barth-Institut, Köln.

Richters, J. Entwicklung eines fernerkundungsgestützten Modells zur Erfassung von pflanzlicher Biomasse in NW-Namibia. -258. 2005b.
Ref Type: Thesis/Dissertation

Rosegrant, M. W., Cai, X., & Cline, S. A. World water and food to 2025. -388. 2002. Washington, USA, International Food Policy Research Institute.
Ref Type: Generic

Rousseeuw, P. J. (1984). Least Median of Squares Regression. *Journal of the American Statistical Association* **79**, 871-880.

Running, S. W., Nemani, R. R., Glassy, J., & Thornton, P. E. MODIS Daily Photosythesis (PSN) and Annual Net Primary Production (NPP) Product (MOD17) Algorithm Theoretical Basis Document. [Version 3.0], -59. 1999.
Ref Type: Generic

Runyon, J., Waring, R. H., Goward, S. N., & Welles, J. M. (1994). Environemental limits on net primary production and light-use efficiency across the Oregon transect. *Ecological Applications* **4**, 226-237.

Sabbe, H. & Veroustraete, F. Estimation of Net Primary and Net Ecosystem Productivity of European terrestrial ecosystems by means of the C-Fix model and NOAA/AVHRR data. http://vegetation.cnes.fr/vgtprep/vgt2000/veroustraete.html . 2000.
Ref Type: Electronic Citation

Sander, H. & Becker, T. (2002). Klimatologie des Kaokolandes. In *Interdisziplin¨are Perspektiven zu Kultur- und Landschaftswandel im ariden und semiariden Nordwest Namibia.*, eds. Bollig, M., Brunotte, B., & BeckerT., Selbstverlag Geographie Uni Köln, Cologne.

Sandford, S. (1983). *Management of Pastoral Development in the third World* WILEY, CHICHESTER.

Sandford, S. (1994). Improving the efficiency of opportunism: new directions for pastoral development. In *Living with uncertainty. New directions in pastoral development in Africa*, ed. Scoones, I., pp. 174-182. London.

Scanlon, T. M., Albertson, J. D., Caylor, K. K., & Williams, C. A. (2002). Determining land surface fractional cover from NDVI and rainfall time series for a savanna ecosystem. *Remote.Sensing.of Environment* **82**, 376-388.

Schaefer, M. & Tischler, W. (1983). *Ökologie : mit englisch-deutschem Register* Fischer, Stuttgart.

Scheffer, F., Schachtschabel, P., Blume, H.-P., Brümmer, G., Hartge, K.-H., Schwertmann, U., Fischer, W. R., Renger, M., & Strebel, O. (1989). *Lehrbuch der Bodenkunde*, 12 ed., pp. 1-491. Ferdinand Enke Verlag, Stuttgart.

Schimel, D. S. (1995). Terrestrial ecosystems and the carbon cycle. *Global Change Biology* **1**, 77-91.

Scholes, R., Hassan, R. M., Ash, N., & Millennium Ecosystem Assessment (Program) (2005). *Ecosystems and human well-being : findings of the Condition and Trends Working Group of the Millennium Ecosystem Assessment* Island Press, Washington, D.C.

Scholz, F. Nomadismus. Theorie und Wandel einer sozio-ökologischen Kulturweise. Erdkundliches Wissen[118]. 1995. Stuttgart.
Ref Type: Serial (Book,Monograph)

Schönwiese, C. D. (1997). Anthropogene und natürliche Signale im Klimageschehen. *Naturwissenschaften* **84**, 65-73.

Schultz, P. A. (1995b). Global analysis of the relationships among a vegetation index, precipitation and land surface temperature. *International Journal of Remote Sensing* **16**, 2755.

Schultz, P. A. (1995a). Global analysis of the relationships among a vegetation index, precipitation and land surface temperature. *International Journal of Remote Sensing* **16**, 2755.

Schultz, P. A. & Halpert, M. S. (1993). Global correlation of temperature, NDVI and precipitation. *Advances in Space Research* **13**, 277-280.

Schulz, O. Analyse schneehydrologischer Prozesse und Schneekartierung im Einzugsgebiet des Oued M'Goun, Zentraler Hoher Atlas (Marokko). -160. 2006.
Ref Type: Thesis/Dissertation

Schulz, O., Busche, H., & Benbouziane, A. (2008a). 2.6 Decadal Precipitation Variances and Reservoir lnflow in the Semi-Arid Upper Draa Basin (South - Eastern Morocco). In *Climatic Changes and Water Resources in the Middle East and North Africa*, ed. Fathi Zereini, H. H., pp. 165. Springer.

Schulz, O., Busche, H., & Benbouziane, A. (2008b). Decadal Precipitation Variances and Reservoir lnflow in the Semi-Arid Upper Draa Basin (South - Eastern Morocco). In *Climatic Changes and Water Resources in the Middle East and North Africa*, ed. Fathi Zereini, H. H., pp. 165. Springer.

Scoones, I. (1993). Why are there so many animals? Cattle population dynamics in the communal areas of Zimbabwe. In *Range Ecology at Disequilibrium - New Models of Natural Variability and Pastoral Adaption in African Savannas*, eds. Behnke, R., Scoones, I., & Kerven, C., pp. 62-76. Overseas Development Institute, London.

Seaquist, J. W., Olsson, L., & Ardö, J. (2003). A remote sensing-based primary production model for grassland biomes. *Ecological Modelling* **169**, 131-155.

Seaquist, J. W., Olsson, L., Ardös, J., & Eklundh, L. (2006). Broad-scale increase in NPP quantified for the African Sahel, 1982-1999. *International Journal of Remote Sensing* **27**, 5115-5122.

Sellers, P. J., Meeson, B. W., Hall, F. G., Asrar, G., Murphy, R. E., Schiffer, R. A., Bretherton, F. P., Dickinson, R. E., Ellingson, R. G., Field, C. B., Huemmrich, K. F., Justice, C. O., Melack, J. M., Roulet, N. T., Schimel, D. S., & Try, P. D. (1995). Remote-Sensing of the Land-Surface for Studies of Global Change - Models, Algorithms, Experiments. *Remote Sensing of Environment* **51**, 3-26.

Sellers, P. & Schimel, D. (1993). Remote sensing of the land biosphere and biogeochemistry in the EOS era: science priorities, methods and implementation--EOS land biosphere and biogeochemical cycles panels. *Global and Planetary Change* **7**, 279-297.

Shinoda, M. (1995). Seasonal phase lag between rainfall and vegetation activity in tropical Africa as revealed by NOAA satellite data. *International Journal of Climatology* **15**, 639-656.

Snyman, H. A. (1998). Dynamics and sustainable utilization of rangeland ecosystems in arid and semi-arid climates of southern Africa. *Journal of Arid Environments* **39**, 645-666.

Snyman, H. A. (2005). Rangeland degradation in a semi-arid South Africa--I: influence on seasonal root distribution, root/shoot ratios and water-use efficiency. *Journal of Arid Environments* **60**, 457-481.

Strahler, A., Muchoney, D., Borak, J., Friedl, M., Gopal, S., Lambin, E., & Moody, A. MODIS Land Cover Product Algorithm Theoretical Basis Document (ATBD) - MODIS Land Cover and Land-Cover Change. [Version 5.0], -66. 1999a.
Ref Type: Generic

Strahler, A. H., Lucht, W., Barker Schaaf, C., Tsang, T., Gao, F., Li, X., Muller, J. P., Lewis, P., Barnsley, M. J., Strugnell, N., Hu, B., Hyman, A., d´Entremot, R. P., Chen, L., Liu, Y., McIver, D., Liang, S., Disney, M., Hobson, P., Dunderdale, M., & Roberts, G. MODIS BRDF/Albedo Product: Algorithm Theoretical Basis Document. [Version 5.0], -53. 1999b.
Ref Type: Generic

Strengers, B., Leemans, R., Eickhout, B., de Vries, B., & Bouwman, L. The land use projections in the IPCC SRES scenarios as simulated by the IMAGE 2.2 model. 2001.
Ref Type: Conference Proceeding

Swift, L. W. (1973). Estimating solar radiation on mountain slopes. *Agricultural meteorology* **12**, 36.

Swift, L. W. (1976). Algorithm for Solar Radiation on Mountain Slopes. *Water Resources Research* **12**.

Tian, Y., Dickinson, R. E., Zhou, L., Zeng, X., , D. Y., Myneni, R. B., Knyazikhin, Y., Zhang, X., Friedl, M., Yu, H., Wu, W., & Shaikh, M. (2004). Comparison of seasonal and spatial variations of leaf area index and fraction of absorbed photosynthetically active radiation from Moderate Resolution Imaging Spectroradiometer (MODIS) and Common Land Model. *Journal of Geophysical Research* **109**.

Todd, S. W. (2006). Gradients in vegetation cover, structure and species richness of Nama-Karoo shrublands in relation to distance from livestock watering points. *Journal of Applied Ecology* **43**, 293-304.

Tucker, C. J. (1979). Red an Photographic Infrared Linear Combinations for Monitoring Vegetation. *Remote Sensing of Environment* **8**, 127-150.

Tucker, C. J., Justice, C. O., & Prince, S. D. (1986). Monitoring the Grasslands of the Sahel 1984-1985. *International Journal of Remote Sensing* **7**, 1571-1581.

Turner, D. P., Cohen, W. B., Kennedy, R. E., Fassnacht, K. S., & Briggs, J. M. (1999). Relationships between Leaf Area Index and Landsat TM Spectral Vegetation Indices across Three Temperate Zone Sites. *Remote Sensing and Environment* **70**, 52-68.

Van den Poel, D. & Larivière, B. (2004). Customer attrition analysis for financial services using proportional hazard models. *European Journal of Operational Research* **157**, 196-217.

Veroustraete, F., Sabbe, H., & Eerens, H. (2002). Estimation of carbon mass fluxees over Europe using the C-fix model and Euroflux data. *Remote Sensing of Environment* **83**, 376-399.

Verstraeten, W. W., Veroustraete, F., & Feyen, J. (2006). On temperature and water limitation of net ecosystem productivity: Implementation in the C-Fix model. *Ecological Modelling* **199**, 4-22.

Verstraeten, W. W., Veroustraete, F., Heyns, W., Van Roey, T., & Feyen, J. (2008). On uncertainties in carbon flux modelling and remotely sensed data assimilation: The Brasschaat pixel case. *Advances in Space Research* **41**, 20-35.

von Wehrden, H. & Wesche, K. Relationships between climate, productivity and vegetation in southern Mongolian drylands. Basic and Applied Dryland Research . 2007.
Ref Type: Abstract

Wagenseil, H. & Samimi, C. (2006). Assessing spatio-temporal variations in plant phenology using Fourier analysis on NDVI time series: results from a dry savanna environment in Namibia. *International Journal of Remote Sensing* **27**, 3455-3471.

Watson, R. T., Noble, I. R., Bolin, B., Ravindranath, N. H., Verardo, D. J., & Dokken, D. J. IPCC Special Report: Land use, land-use change and forestry. Summary for policymakers. -30. 2000. Cambridge, UK, Cambridge University Press.
Ref Type: Report

Weber, B. Untersuchungen zum Bodenwasserhaushalt und Modellierung der Bodenwasserflüsse entlang eines Höhen- und Ariditätsgradienten (SE Marokko). -251. 2004.
Ref Type: Thesis/Dissertation

Weber, G. E., Moloney, K., & Jeltsch, F. (2000). Simulated long-term vegetation response to alternative stocking strategies in savanna rangelands. *Plant Ecology* **150**, 77-96.

Weischet, W. & Endlicher, W. (2000). *Regionale Klimatologie Teil 2: Die Alte Welt: Europa - Afrika - Asien*.

White Michael A., Asner Gregory P., Nemani Ramakrishna R., Privette Jeff L., & Running Steven W. (2000). Measuring Fractional Cover and Leaf Area Index in Arid Ecosystems: Digital Camera, Radiation Transmittance, and Laser Altimetry Methods. *Remote Sensing of Environment* **74**, 45-57.

White, M. A., Thornton, P. E., & Running, S. W. (1997c). A continental phenology model for monitoring vegetation responses to interannual climatic variability. *Global Biogeochemical Cycles* **11**, 217-234.

White, M. A., Thornton, P. E., & Running, S. W. (1997b). A continental phenology model for monitoring vegetation responses to interannual climatic variability. *Global Biogeochemical Cycles* **11**, 217-234.

White, M. A., Thornton, P. E., & Running, S. W. (1997a). A continental phenology model for monitoring vegetation responses to interannual climatic variability. *Global Biogeochemical Cycles* **11**, 217-234.

Wierenga, P. J. (1987). Variation of soil and vegetation with distance along a transect in the Chihuahuan Desert. *Journal of Arid Environments* **13**, 53.

Williams, J. R., Jones, C. D., & Dyke, P. T. (1995). The EPIC model. In *Computer models of watershed hydrology* pp. 909-1000. Water resources Publications.

Willmott, C. J. (1981). On the validation of models. *Physical Geography* **2**, 184.

Wissel, C. (1992). Aims and Limits of Ecological Modeling Exemplified by Island Theory. *Ecological Modelling* **63**, 1-12.

Wisskirchen, K. Aufbau einer operationellen NPP Modellierung am DFD. 103-109. 2003. DFD.
Ref Type: Conference Proceeding

Woodcook C. & Strahler, A. H. (1987). The factor of scale in remote sensing. *Remote Sensing of Environment* **21**, 311.

Xie, H., Tian, Y. Q., Granillo, J. A., & Keller, G. R. (2007). Suitable remote sensing method and data for mapping and measuring active crop fields. *International Journal of Remote Sensing* **28**, 395-411.

Xiong, X. (2005). Terra MODIS on-orbit spatial characterization and performance. *IEEE Transactions on Geoscience and Remote Sensing* **43**, 355.

Zhang, X., Friedl, M. A., Schaaf, C. B., Strahler, A. H., Hodges, J. C. F., Gao, F., Reed, B. C., & Huete, A. (2003). Monitoring vegetation phenology using MODIS. *Remote Sensing of Environment* **84**, 471-475.

Zhang, X., Friedl, M. A., & Schaaf, C. B. (2006). Global vegetation phenology from Moderate Resolution Imaging Spectroradiometer (MODIS): Evaluation of global patterns and comparison with in situ measurements. *Journal of Geophysical Research - Biogeosciences* **111**.